Investigating the impact of zoledronate on the healthspan of mice.

The University Of Sheffield.

Jeremy Richards: 180242199.

Department of Oncology and Metabolism.

Supervisors: Professor Ilaria Bellantuono,

Doctor Kasia Whysall,

and Professor Eugene McCloskey.

Thesis submitted for the degree of doctorate of philosophy.

Submitted September 2022.

Acknowledgements.

I'd like to express my enormous gratitude to Ilaria Bellantuono for supervising this PhD project. I would like to thank her for the enormous amount of time, effort and resources that has gone into advising me on this project. I would like to also offer my gratitude to my secondary supervisors Eugene McCloskey and Kasia Whysall for their invaluable advice and outside perspective on this project during many online meetings.

I would like to thank Zhengqi Chen for demonstrating protein extraction, western blotting and tissue culture. Thanks to Caroline Fry for giving me further advice on mesenchymal stem cell culture. I would like to say a huge thank you to Alex Rayson for assisting with the healthspan assays, the tissue dissections and for providing a variety of technical support throughout my project. I'd also like to thank Mark Kinch for assisting with mouse dissections throughout the project. Thanks to Carl Wright and Mark Ariaans for performing the blood collection during the mouse studies. Thanks to Claudia Tulotta for demonstrating bone marrow collection. A big thank you to the BSU staff for taking excellent care of the mice during my animal experiments, particularly to Tom Heywood and Carol Pentland. Thanks to Amy Spencer for advising on statistical analysis for the healthspan experiment.

I'd like to thank my numerous flatmates I have had during my PhD: Steven, Priya, Johnno, Alexander, Patty, Johanna, Valentine, Luciano, Fernando, Megan, Katerina, Jamie, Clara, Haodong, Luisa, Ludo, Tzuhao, Manami, Sriti, Clisman, Patrick, Becca, James and Azeer. Being able to come home and just have a chat with people going through a similar postgraduate experience to me has made this PhD journey a real joy. I was very lucky to have known you all.

I'd like to say a big thank you to my Mum, Dad and Sister back in Dorset. Thanks for offering me a place of rest and sanctuary during the holidays. I hope I've made you all proud.

"Tibia or not tibia, that is the question!" - A humerus osteology joke

Summary-

Zoledronate is a bisphosphonate given once yearly to treat osteoporosis. Older people taking bisphosphonates appear to have all around better survival, a large percentage of this improvement in survival appears to be mediated through non-skeletal effects. For example, previous studies have shown improved survival from infection and cardiac arrythmia. Previous work from our research group has demonstrated that zoledronate works as a geroprotector in Mesenchymal Stem Cells and *Drosophila*. These studies demonstrated that ZOL's ability to work as a geroprotector were mediated through the mTOR pathway, a major longevity pathway. Whether zoledronate can also promote healthy ageing in more advanced model organisms such as mice remains to be determined.

During this project, AKT was used as a marker of mTOR inhibition in mouse tissues in order to determine an appropriate interval of administration of zoledronate in mice. Surprisingly, p-AKT inhibition was achieved at 3 days post-injection in the largest number of mouse tissues in response to zoledronate treatment. This suggested that a twice weekly treatment regimen of zoledronate treatment would be optimal to consistently inhibit mTOR signalling in mice. Following on from this, 12-month-old mice were administered zoledronate twice weekly until they reached 23 months of age. From 18 months of age, mice were assessed for muscular strength, frailty, survival, weight gain, metabolic function, neuromuscular and cognitive function. Zoledronate treatment was able to improve frailty in mice, but not the other parameters of mouse healthspan. Future experiments should examine the effects of mTOR markers in older mice. In addition, future experiments should compare the kinetics by which ZOL inhibits mTOR in mice and humans.

Contents page-

List of Figures-

List of Tables-

List of abbreviations-

AEBSF- 4-(2-aminoethyl) benzenesulfonyl fluoride hydrochloride

AKT – Protein Kinase B.

AUC – Area Under the Curve

BCA – Bicinchoninic Acid Solution

BPs - Bisphosphonates

BSA – Bovine Serum Albumin

CDK – Cyclin Dependent Kinase

DOC - Deoxycholic acid sodium salt

DI – Discrimination Index

DMEM – Dulbecco's Modified Eagle Medium

DMSO – Dimethyl-sulfoxide

EDTA - Ethylene-diamine-tetra-acetic acid

FBS – Foetal Bovine Serum

FI – Frailty Index

FOH – Farnesol

FOXO3A – Forkhead box 3A

GAPDH - Glyceraldehyde 3-phosphate dehydrogenase

GGOH - Geranylgeraniol

GH – Grid Hanging

GSK3β - Glycogen Synthase Kinase-3 Beta

GTT -Glucose Tolerance Test

HCl – Hydrochloric Acid

HSC – Hematopoietic Stem Cells

hMSC – Human Mesenchymal Stem Cells

IGEPAL - (Octylphenoxy poly(ethyleneoxy)ethanol)

ITT - Insulin Tolerance Test

LC3 – Microtubule-associated protein 1A/1B-light chain 3

LDS - Lithium Dodecyl Sulphate

LTM – Long Term Memory

MEFs – Mouse Embryonic Fibroblasts

MNC – Bone Marrow Mononuclear Cells

MSC – Mesenchymal Stem Cell

mTOR – Mammalian Target of Rapamycin

n-BP – Nitrogen containing Bisphosphonate

NOR – Novel Object Recognition

P70S6K - Ribosomal protein S6 kinase beta-1

PAGE – Polyacrylamide Gel Electrophoresis

PBS – Phosphate Buffered Saline

PME – Post-mortem Examination

PVDF - Polyvinylidene Fluoride

RAPTOR- Regulatory Associated Protein of mTOR

RICTOR- Rapamycin Insensitive Companion of mTOR

ROS – Reactive Oxygen Species

RT- Room Temperature

RV- Reference Value

S6 – Ribosomal protein S6

SASP – Senescence Associated Secretory Phenotype

SDS – Sodium Dodecyl Sulphate.

STM – Short Term Memory

TBS – Tris-Buffered Saline

TBST – Tris-Buffered Saline with Tween-20.

TRIS - Tris(hydroxymethyl)aminomethane

ULK1 – Unc-51 Like Autophagy Activating Kinase 1

ZOL – Zoledronate

Chapter 1- Background

1.1 Ageing related diseases and the ageing population-

Ageing is associated with an increased incidence of diseases that can impact the quality of life of older people. There are many examples of such diseases: these can impact the neurological, cardiac and musculoskeletal systems of older people. In the musculoskeletal system, three common examples of these age-related diseases include sarcopenia, osteoporosis and osteoarthritis (Grote *et al.* 2019). Age is also associated with increased incidence of cancers, cardiovascular diseases and neurological diseases such as Alzheimer's (Driver *et al.* 2008*;* Hofman *et al.* 1991; Bhatnagar *et al.* 2015; White *et al.* 2014). In addition to this older people are at increased risk of developing and dying from infectious disease, as discussed extensively by others (Schneider *et al.* 1983; Yoshikawa 2000). This was particularly notable during the recent COVID pandemic, age was a major risk factor for severity and mortality of the disease (Ferguson *et al.* 2020; Chen *et al.* 2020).

Having any one of these conditions would seriously effect quality of life, but older people often have multiple chronic health conditions at once. This is known as multimorbidity which currently affects over half of adults over the age of 65 in the UK (Barnett *et al.* 2012). This is projected to rise to 67% of the population of adults over the age of 65 by 2035 in the UK (Kingston *et al.* 2018). A major driving force of this is an increasingly ageing population in the western world. Projections indicate that by 2041, 35% of adults in the UK will be of pension age (Leeson *et al.* 2013). Globally, the picture is similar. By 2041, the number of people over 65 is projected to rise from 461 million in 2004 to 2 billion by 2041 (Clegg *et al.* 2013). In terms of age-related musculoskeletal diseases, 21% of persons over the age of 85 have sarcopenia (Dodds *et al.* 2017). Approximately, 17% of women and 9% of men who are aged 50 or older are at risk of osteoarthritis (French *et al.* 2016). Furthermore, 10% of postmenopausal women and 8% of men over the age of 60 are at risk of developing osteoporosis (Tian *et al.* 2017). In order to reduce the incidence and severity of these diseases, it is necessary to better understand the cellular changes that occur with ageing that the diseases share.

1.2 The geroscience hypothesis-

The geroscience hypothesis states that interventions targeting features of the biology of ageing can prevent the onset of multiple age-related diseases (Sierra and Kohanski 2021). This is because ageing is a major risk factor for multiple-age related diseases and the biological mechanisms of ageing are targetable. Therefore, decelerating the biological mechanisms of ageing reduces the risk of developing age-related diseases. Geroprotectors are a class of drug that act through decelerating the ageing process to promote healthy ageing of the overall organism. It is the hope of ageing research that by better understanding the biological processes of ageing that it may be possible to reduce the likelihood of developing these diseases (Figure 1.1). This should result in an increased healthspan, the period of life in which people are disease free. This in turn should improve the health, independence and psychological well-being of older people.

There have been a variety of processes associated with cellular ageing identified in the literature that are believed to contribute to the ageing of cells. These are commonly referred to as the hallmarks of ageing (López-Otín *et al.* 2013). These include the accumulation of damage to the genome, mitochondrial dysfunction, altered nutrient sensing, altered intercellular signalling, epigenetic changes, loss of proteostasis, loss of stem cell function, loss of telomeres and cellular senescence (for overview see Figure 1.2). How each hallmark contributes to ageing shall be elaborated upon in the subsequent section.

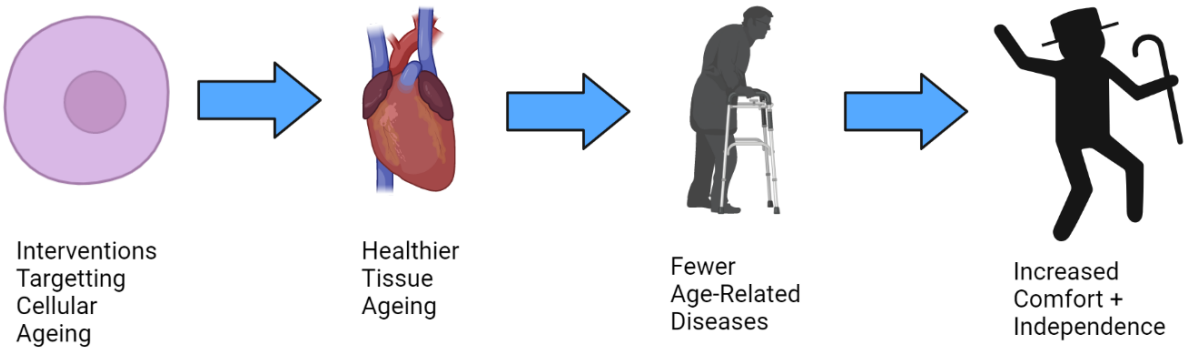

Figure 1.1 - How interventions targeting biological ageing processes can benefit older people. Created with bio-render.

1.3 The hallmarks of ageing-

One example of a hallmark of ageing is that DNA damage increases with age. Accumulating levels of DNA damage have been observed in both mammalian cells and tissues with age (Jeyapalan *et al.* 2007; Sedelnikova *et al.* 2002; Wang *et al.* 2009). The importance of DNA damage in the ageing process have been further illustrated in genetic studies in mice. Such studies have shown that mutated mice with deficient DNA repair proteins exhibit accelerated ageing syndromes (Murga *et al.* 2009; Vermeij *et al.* 2016; Yousefzadeh *et al.* 2020).

Telomeres can be located on the end of chromosomes. These consist of repeated sequences of DNA (TTAGGG) and a t loop that protects the ends of the telomeres during DNA repair (Griffith *et al.* 1999). This t loop is in turn maintained by a complex of proteins known as the shelterin complex (De Lange 2005). The enzyme telomerase replenishes telomeres with additional TTAGGG repeats (Bodnar *et al.* 1998), but telomerase is not expressed in most mammalian somatic cells. During cell divisions these slowly erode in length, eventually to the point in which a state of cell cycle arrest is achieved (Harley *et al.* 1990). This is known as replicative senescence. Telomere attrition has been observed in ageing tissues in mammals in certain specific tissues (Daniali *et al.* 2013; Nakamura *et al.* 2002; Smith *et al.* 2011). In addition, mice lacking telomerase exhibit a shorter lifespan (Rudolph *et al.* 1999; Armanios *et al.* 2009). These studies implicate the importance of telomeres shortening with ageing.

Cellular senescence is a process by which cells enter a state of stable cell cycle arrest in response to a variety of different stressful stimuli (Hayflick and Moorhead 1961; Harley *et al.* 1990; Chang *et al.* 1999; Toussaint *et al.* 2000; Serrano *et al.* 1997; Van Nguyen *et al.* 2007; Bai *et al.* 2020). For example, this can be due to replicative senescence, in which telomere attrition results in a cessation of cellular division (Bodnar *et al.* 1990). Increased levels of senescent cells have been implicated in the development of a variety of ageing related diseases in mice such as sarcopenia, osteoporosis and cardiovascular disease (Xu *et al.* 2018; Farr *et al.* 2017; Childs *et al.* 2016). Promisingly, selective clearance of these senescent cells has even been demonstrated to prevent certain age-related diseases in mice (Baker *et al.* 2011; Farr *et al.* 2017; Jeon *et al.* 2017; Roos *et al.* 2016; Xu *et al.* 2018).

Senescent cells exhibit altered secretomes, this is known as the senescence associated secretory phenotype (SASP). The SASP is made up of a combination of interleukins, cytokines and MMPs (matrix metalloproteases). Examples of components released by the SASP include TNF-α, IL-6 and IL-8 (Coppé et al. 2008; Acosta *et al.* 2008). This SASP is an important driver of cellular and tissue ageing. This is due to the process of paracrine senescence. Paracrine senescence is a process by which SASP components induce senescence in neighbouring cells (Acosta *et al.* 2013). One-way in which paracrine senescence is achieved is via CXCR2 signalling when SASP components bind to the surface of neighbouring cells (Acosta *et al.* 2008). In addition, paracrine senescence can also be induced via ROS release to neighbouring cells (Nelson *et al.* 2012).

Another hallmark of ageing is that of dysfunctional proteostasis. Proteostasis is the processes by which cells maintain homeostasis of the proteome. Proteostasis is achieved through several different mechanisms. One of which is autophagy, this is a process by which organelles and proteins are degraded via the action of digestive enzymes in the lysosome. Autophagy has been implicated in the ageing process because of the impact of multiple autophagy inducers on increasing the lifespan of mice (Eisenberg *et al.* 2009; Harrison *et al.* 2009; O'Rourke *et al.* 2013; Mason *et al.* 2018). Another mechanism by which proteostasis is associated with ageing is through a loss of function of the proteasomal system. This was implicated in the ageing process in a study in which transgenic mice with lowered levels of proteasomal activity had diminished lifespans (Tomaru *et al.* 2012). Further evidence supporting this notion was found on a study on *C. elegans*. This study found that EGF treatment increased the lifespan of *C. elegans* that corresponded to increased proteasomal activity (Liu *et al.* 2011). Proteostasis is also maintained through the actions of chaperone proteins that prevent misfolding of proteins. Studies have shown that model organisms overexpressing chaperone proteins have increased lifespan (Morrow *et al.* 2004; Walker and Lithgow 2003). This suggests that chaperone proteins also have an important role to play in ageing.

Another hallmark of ageing is that of mitochondrial dysfunction. In the 1970s, it was proposed that mitochondrial dysfunction creates free radicals such as reactive oxygen species (ROS) that drives ageing (Harman 1972). ROS are capable of

damaging DNA, proteins and accelerating telomere attrition (Cui *et al.* 2012; Von Zglinicki 2002). However, ROS also have a role to play in normal cell function (Finkel 2011). The importance of mitochondrial dysfunction is also illustrated by studies on long lived organisms. These studies have shown that some longer-lived organisms have a greater resistance to oxidative stress and lower ROS production (Lambert *et al.* 2007; Ogburn *et al.* 2001; Ungvari *et al.* 2011). The importance of mitochondrial dysfunction was demonstrated more recently during a study on the mitophagy inducer Urolithin A (Ryu *et al.* 2016). Mitophagy is the process by which autophagy degrades mitochondria. This study was able to show that the drug treatment increased the lifespan of *C. elegans,* further implicating mitochondrial dysfunction in the ageing process.

A feature of ageing is a decreased regenerative capacity of tissues. A driving factor for this is the decreased function of stem cells. Stem cells are a group of cells that are capable of self-renewal and differentiation into multiple different cell types. Ageing is associated with changes in the stem cell population, for example an altered differentiation into other cell types. A notable example of this is the ability of hemopoietic stem cells (HSCs) to produce lymphoid compared to myeloid cells with age (Pang *et al.* 2011). The importance of stem cell ageing was also illustrated in transplantation studies that have illustrated how transferring stem cells from young animals to aged mice increases their lifespan (Lavasani *et al.* 2012; Guderyon *et al.* 2020).

Ageing is associated with genomic damage, both of telomeric and non-telomeric regions. In addition to this there are epigenetic changes that occur within genomes that are observed in ageing. These include changes in DNA methylation, changes to histones, remodelling of heterochromatin and changes in transcription (Maleszewska *et al.* 2016; Smith-Vikos and Slack 2012; Tsurumi and Li 2012). Interventions targeting epigenetic mechanisms have been shown to increases the lifespan of model organisms, implicating their importance in the ageing process (Boulias *et al.* 2012; Jin *et al.* 2011; Liu *et al.* 2013).

Interventions targeting nutrient sensing pathways such as caloric restriction, have long been demonstrated to improve the lifespan of a diverse range of model organisms (McCay and Cromwell 1935; Klass 1977; Turturro *et al.* 1999; Colman *et*

al. 2014). In addition to this, the importance of specific nutrient sensing pathways has been implicated in longevity. An example of this is the insulin and IGF-1 signalling pathway (IIS). This pathway has been implicated in increasing lifespan in mutation studies on IGF-R in *Drosophila, C. elegans* and mice (Kenyon *et al.* 1993; Tatar *et al.* 2001; Holzenberger *et al.* 2003). This pathway is also upstream of AKT/ mTOR signalling. The nutrient sensitive mTOR pathway also has a strong relationship to cellular ageing, which is discussed further in the next section.

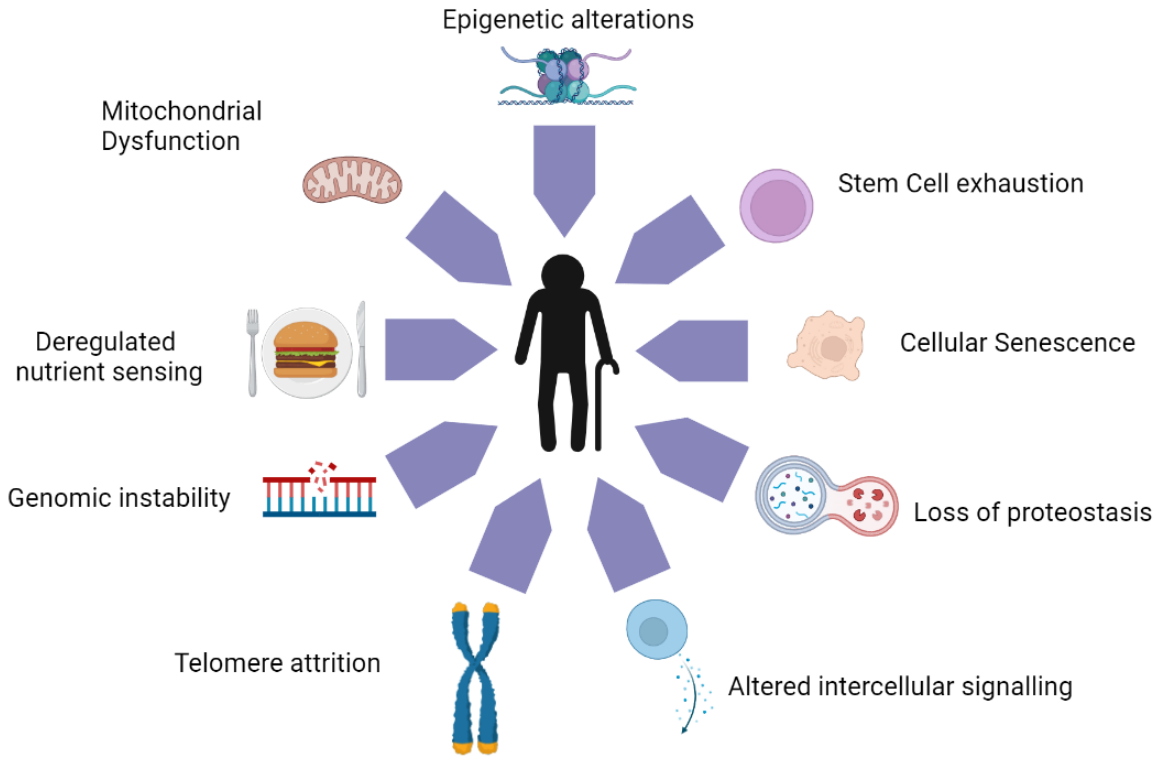

Figure 1.2 – The hallmarks of ageing. Adapted from "The Hallmarks of Ageing" (López-Otín *et al.* 2013). Created with Bio-Render.

1.4 mTOR signalling and Ageing-

The mTOR pathway has been linked to ageing due to roles in regulating multiple hallmarks of ageing such as regulating autophagy, repair of DNA damage and nutrient sensing. For one to understand how mTOR signalling works, it is first important to understand the roles of the two different mTOR protein complexes: mTORC1 and mTORC2. These two complexes differ in their composition as well as in their downstream targets and cellular functions. Both complexes contain similar

components: such as an mTOR complex and DEPTOR. However, both mTORC1 and mTORC2 contain additional proteins that are unique to each complex. For example, RAPTOR (Regulatory Associated Protein of mTOR) is unique to mTORC1 and RICTOR (Rapamycin Insensitive Companion of mTOR) is unique to mTORC2. There are many important markers of mTOR activation. One of which is the activity of the mTOR protein complex itself. This complex contains 2549 amino acids and has several different domains. One of which is the negative regulatory domain (NRD), which contains several phosphorylation sites that are required for mTOR activation: one of which is Ser2448 (Li et al. 2014). In addition to mTOR, there are downstream markers that can be assessed to measure levels of mTORC1 and mTORC2 signalling (see Figure 1.3 for overview of mTORC1 and mTORC2 signalling).

The mTORC1 complex is involved in regulating the cell cycle, autophagy and protein translation (Wang *et al.* 2001; Smith and Proud 2008; Rabanal-Ruiz *et al.* 2017). Activation of mTORC1 can be achieved by amino acids, glucose and growth factors (Dash *et al.* 2006; Iiboshi *et al.* 1999; Sengupta *et al.* 2010). The mTORC1 complex interacts with a variety of downstream proteins to regulate biological processes inside cells. In terms of mTORC1 signalling, P70S6K is one downstream protein of mTORC1 signalling (Bahrami *et al.* 2014). This protein in turn regulates ribosomal protein S6, this protein is involved in translation of proteins at ribosomes. On a similar note, mTORC1 signalling is also responsible for the activation of 4EPB1. This protein is also responsible for the regulation of protein translation (Qin and Zhang 2016). In addition, 4EPB1 can regulate another feature of cellular ageing, that of the senescent associated secretory phenotype (Herranz *et al.* 2015; Laberge *et al.* 2015). The importance of the senescence associated secretory phenotype is discussed further in section 1.3. Another example of a protein regulated by mTORC1 signalling is ULK1 (inhibition of mTORC1 activates ULK1). This protein is responsible for the formation of the autophagosome (Chan *et al.* 2007; Kim *et al.* 2011). Defective autophagy is another feature of cellular ageing that is regulated by mTOR signalling.

Meanwhile, mTORC2 regulates cytoskeletal maintenance, glucose homeostasis and proliferation (Elstrom *et al.* 2004; Jacinto *et al.* 2004; Rosner *et al.* 2009). Similarly, it

is believed to be primary regulated upstream by growth factors (Fu and Hall 2020). Other upstream activators of mTORC2 signalling have yet to be definitively identified in the literature. A marker of downstream activation of mTORC2 would be the serine/ threonine kinase protein AKT (also known as protein Kinase B) (Sarbassov et al. 2005; Hresko and Mueckler 2005). AKT is a serine/threonine protein kinase that regulates cell functions such as glucose metabolism, survival, cytoskeletal and proliferation. AKT in turn can regulate the activity of other proteins downstream such as FOXOs, GLUT4 and GSK3β (Cong *et al.* 1997; Manning and Toker 2017). It also appears that mTORC2 may also play a minor role in the regulation of autophagy (Arias *et al.* 2015). Other markers of mTORC2 signalling include the cell signalling proteins SGK1 and PKC (Alessi et al. 2009; Szwed et al. 2021).

Interestingly, geroprotectors such as rapamycin work by inhibiting mTOR signalling. Rapamycin has been shown to increase the lifespan of a variety of model organisms such as in *Drosophila* and mice (Harrison *et al.* 2009; Miller *et al.* 2014; Strong *et al.* 2020; Bjedov *et al.* 2010). In addition to this mTOR inhibitors such as rapamycin have been demonstrated to improve healthy ageing in model organisms such as mice in terms of improvement in healthspan parameters (Bitto *et al.* 2016; Ham *et al.* 2020; Zhang *et al.* 2014). Due to the numerous ways in which the mTOR pathway interacts with the ageing process, developing drug therapies that exploit this pathway is vital to improving the healthspan of older people.

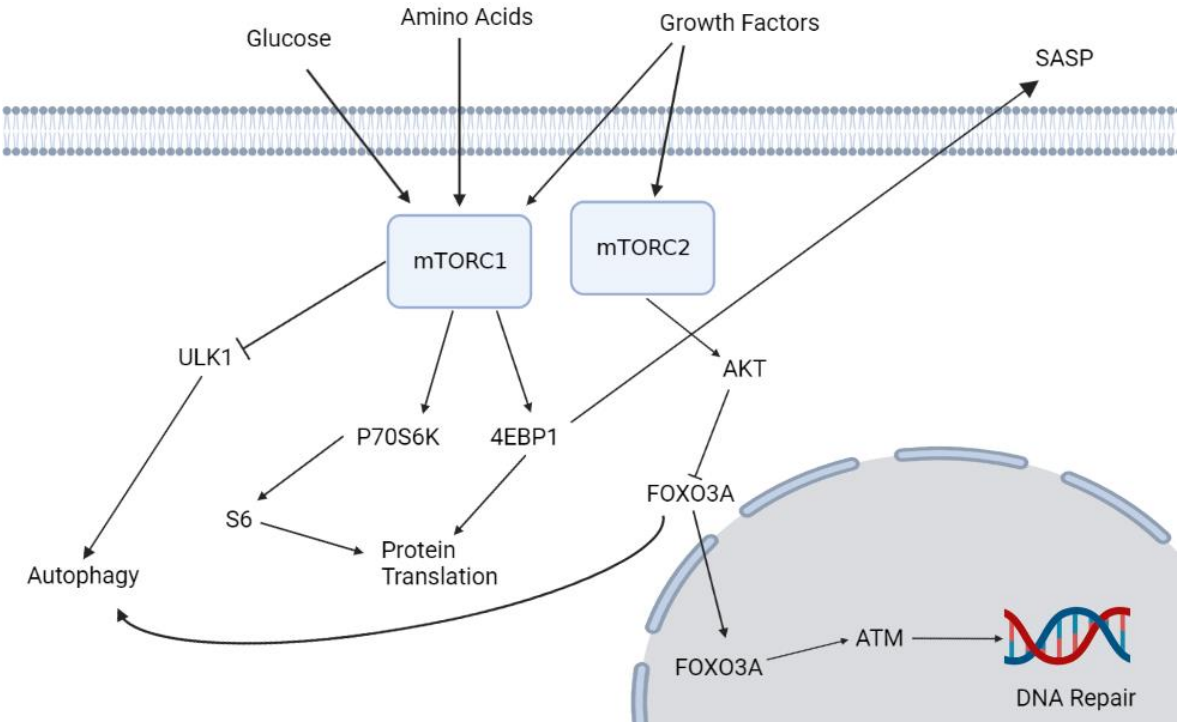

Figure 1.3 – Diagrammatic overview of mTORC1 and mTORC2 signalling. Created with Bio-Render.

1.5 Zoledronate-

Zoledronate (ZOL) is a nitrogen containing bisphosphonate (n-BP) used to treat osteoporosis. These nitrogen containing bisphosphonates are used to treat diseases of the bone by limiting the ability of osteoclasts to resorb bone (Alakangas *et al.* 2002; Carano *et al.* 1990). This limitation of bone resorption in turn leads to reduced levels of marker of bone resorption, greater bone density and reduced risk of fracture. This has been illustrated during clinical trials, as has been extensively reviewed by others (Dhillon 2016; Zhang *et al.* 2012). Mechanistically: nitrogen containing bisphosphonates such as ZOL block the mevalonate pathway by inhibiting the farnesyl diphosphate synthase (FPPS) enzyme (Dunford *et al.* 2001). The mevalonate pathway is an important pathway responsible for the prenylation of proteins and to produce steroids (Goldstein and Brown 1990; Buhaescu and Izzedine 2007). In the context of reducing bone resorption, this inhibition of the mevalonate pathway is important as a loss of protein prenylation is detrimental to the formation and survival of osteoclasts (Coxon *et al.* 2000).

1.6 The development of bisphosphonates-

Bisphosphonates (BPs) are analogues of inorganic pyrophosphates. The key difference in their chemical structure is that BPs have a P-C-P group instead of a P-O-P group (see Figure 1.4). Initially, bisphosphonates were used as water softeners due to their affinity for calcium and their ability to prevent calcium carbonate precipitation (Russell 2011). However, their potential for medical use was first demonstrated during a search for new drugs that could influence bone formation and resorption.

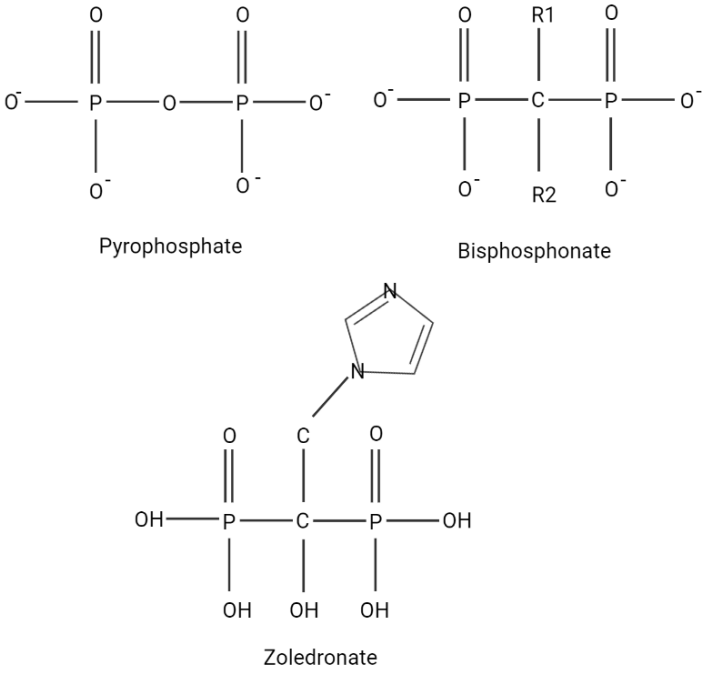

Figure 1.4 - Chemical structure of bisphosphonates and pyrophosphates.

In the 1960s, there was a search for compounds that could influence the calcification of bone. Initially, a pyrophosphate was found in the urine of patients that could inhibit the formation of the bone component hydroxyapatite *in vitro* (Fleisch *et al.* 1962). However, the authors also previously found that pyrophosphates were degraded by alkaline phosphatases (Fleisch and Newman 1961). Due to the presence of alkaline phosphatase in the bone, this would make pyrophosphates unsuitable as drug treatments for bone disorders. Due to these findings, an alternative was sought to these naturally occurring compounds that had similar chemical properties but would not be degraded by alkaline phosphatases.

Bisphosphonates were later trialled as an alternative to pyrophosphates due to their similar chemical structure (Figure 1.4). In 1969 bisphosphonates were found to be capable of limiting bone resorption *in vitro* (Fleisch *et al.* 1969). This was then later backed up by work in rats that indicated that bisphosphonates could reduce bone loss in rats that had immobilisation induced osteoporosis (Michael *et al.* 1971). This would form the foundation for future work for bisphosphonates as treatments for osteoporosis. Two such bisphosphonates were used in this study, these were called EDHP and Cl2MDP, these would be later known as clodronate and etidronate.

Bisphosphates can be split roughly into two types: nitrogen and non-nitrogen containing bisphosphonates. Both classes of bisphosphonate treat diseases of the bone by inhabiting the action of osteoclasts to resorb bone. Although the two different types of bisphosphonate achieve this through very different mechanisms. The non-nitrogen containing bisphosphonates were the first class of bisphosphonates to be developed. Examples of these non-nitrogen containing bisphosphonates are the previously mentioned etidronate and clodronate. These function as ATP analogues. Mechanistically they reduce the action of osteoclasts by being converted into a cytotoxic analogue of ATP that induces apoptosis of osteoclasts (Frith *et al.* 2001; Lehenkari *et al.* 2002). Later, nitrogen containing bisphosphonates were developed. Examples of these include risedronate, pamidronate, alendronate, ibandronate and zoledronate. Nitrogen containing bisphosphonates have a slightly different mechanism of action. These work by inhibiting the actions of the FPPS enzyme that is a part of the mevalonate pathway (Dunford *et al.* 2001). The mevalonate pathway is responsible for the prenylation of proteins and formation of cholesterol. Protein prenylation is a post translation modification. This prenylation is necessary for the formation of proteins such as RAS, RAB and Coenzyme Q10 (Luckman *et al.* 1998; Goldstein and Brown 1990; Ghirlanda *et al.* 1993; Zhang and Casey 1996). For an overview of the mevalonate pathway, please see the figure below (Figure 1.5).

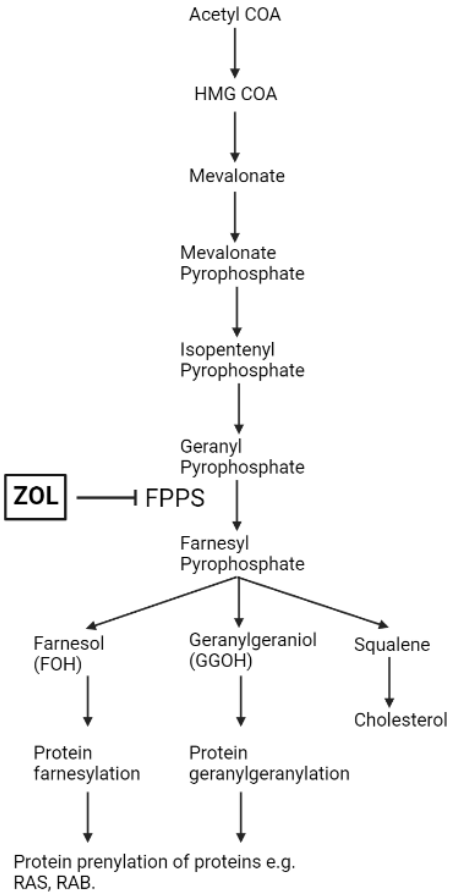

Figure 1.5 Overview of the mevalonate pathway. Adapted from Misra *et al.* 2016. Created with Bio-Render.

1.7 The clinical development of Zoledronate-

Zoledronate is a particularly potent inhibitor of FPPS compared to other bisphosphonates. During one study ZOL was found to have an IC50 value for FPPS that was more than 10 times lower than other clinically used bisphosphonates such as alendronate, pamidronate and risedronate (Dunford *et al.* 2001). Bisphosphonates tend to accumulate preferentially in the bone. This has been made apparent in studies that use radioactive labelling of bisphosphonates (Weiss *et al.* 2008; Nikzad *et al.* 2013; Yousefnia *et al.* 2015). ZOL also has a higher affinity for hydroxyapatite (which is component of the bone) compared to other bisphosphonates (Nancollas *et al.* 2006). This is important for understanding why zoledronate acts on the bone, why it remains present in the bone for such a long period of time and why its clinical outcomes are so enduring (Dhilion 2016; Colón-Emeric *et al.* 2010; Weiss *et al.* 2007).

During clinical trials, it became apparent that ZOL was capable of having beneficial effects on the bone for a considerable period of time after infusion. During one such trial it was discovered that giving ZOL yearly was just as effective as giving it every three months at improving bone mineral density and in lowering markers of bone resorption (Reid *et al.* 2002). Further information on the duration of ZOL's effectiveness on improving bone mineral density was revealed more recently (Grey *et al.* 2017). In this trial on osteopenia, it was demonstrated that ZOL was effective at improving bone mineral density for up to 5 years and that this effect was dose dependent (increasing strength of effect from 1 mg to 5 mg).

During the Health Outcomes and Reduced Incidence with Zoledronic acid Once Yearly Pivotal Fracture Trial (HORIZON) trial, postmenopausal women were given a single dose of 5 mg ZOL. The incidence of bone fractures was then assessed following the administration of the drug (Lyles *et al.* 2007). ZOL treatment was found to reduce bone fractures by 35%. Reducing the number of hip fractures is important for older people as hip fractures are linked to higher risk of death for older people and higher risk of subsequent fractures (Colón-Emeric *et al.* 2003; Richmond *et al.* 2003). ZOL is also effective in reducing bone turnover markers and reducing the number of fractures in older women with osteopenia (Reid *et al.* 2018).

After the success of these clinical trials, ZOL is now used for the treatment of osteoporosis. For treatment and prevention of osteoporosis, it is administered yearly via an infusion (Dhillon 2016). As mentioned earlier, this is due to the ability of ZOL treatment to increase bone density and lower fracture risk in osteoporosis patients (Black *et al.* 2007). In addition to this, ZOL has other medical applications in other bone related diseases. ZOL is also administered to prevent skeletal related events (SREs) in cancer patients (Kohno *et al.* 2005; Lipton *et al.* 2003; Rosen *et al.* 2004). These SREs occur when a cancer metastasises and spreads to the bone. ZOL is used to reduce the fracture risk, improve bone density and reduce pain during these SREs. ZOL is also given to reduce pain caused by these SREs (Kohno *et al.* 2005; Saad *et al.* 2004). Although, ZOL is administered more frequently to treat SREs than during osteoporosis treatment (every three to four weeks). Zoledronate is also used to treat other diseases that involve abnormal bone remodelling such as Paget's disease (Reid *et al.* 2005; Ralston *et al.* 2019). Overall, the ZOL is currently used to

treat skeletal diseases, although emerging research suggests it may confer additional non-skeletal benefits to older people.

1.8 Side effects of zoledronate treatment-

Like with any other drug treatment, zoledronate has been known to demonstrate some side effects. Common examples of side effects of zoledronate treatment include fever, muscle pain and flu-like symptoms (Black *et al.* 2007; Lee *et al.* 2012). This is known as the acute phase response. Fortunately, these side effects are short in duration and typically last for around several days (Reid *et al.* 2010). There are also rarer side effects of zoledronate treatment that have been documented in the literature, a notable example of which is osteonecrosis of the jaw (ONJ). The incidence of this side effect is far less frequent ~ 1< in 7000 (Grbic et al. 2008). This incidence is increased in the case of cancer treatment (~8.4%), as ZOL is administered on a more regular basis (monthly) compared to osteoporosis (Kajizono et al. 2015). Fortunately, the incidence of ONJ can be greatly reduced through maintenance of a good standard of dental health (Vandone et al. 2011; Ripamonti et al. 2009). There have also been rare incidences of atypical femur fracture in response to prolonged use of bisphosphonates, including ZOL (Schleicher *et al.* 2014; Meier *et al.* 2012; Edwards *et al.* 2012). Like with any other potential medical intervention, one must weigh these side effects against any potential benefits of the treatment. In the case of zoledronate the limited duration, preventability and low incidence of these side effects must be weighed against the many potential benefits outlined in this chapter.

1.9 Evidence that bisphosphonates can improve survival and non-skeletal health in patients-

Despite zoledronate's notoriety as a drug for treating disorders of the bone, evidence in the literature has slowly emerged to indicate that zoledronate may confer non-skeletal benefits to the health of older people (for overview see Figure 1.6). Many clinical studies have shown that bisphosphonate treatment can improve the overall survival of patients with diseases of the bone, as has been extensively reviewed by

others (Center *et al.* 2020). In addition to improving general survival, bisphosphonates may also confer increased resilience in older people following admission to intensive care. One such study looked at whether bisphosphonates changed the outcomes from admission to the intensive care unit (ICU) (Lee *et al.* 2016). Over 7000 patients in Australia were included as a part of this study. The patients who took BPs were older than the control group (average age of 68 years old for BP vs 56 years old for non-BP group). Despite this, they had improved a 59% increased rate of in-hospital mortality following a visit to the ICU. Supporting this notion, anther nitrogen containing bisphosphonate has been found to have similar effect. For example, the nitrogen containing bisphosphonate pamidronate improved survival following a visit to a respiratory care unit (RCU) (Schulman *et al.* 2016). It was unclear in these studies as to whether this increased resilience was due to increased bone strength or other non-skeletal factors.

A clue as to how ZOL confers an increase in survival in older people was found during analyses of the HORIZON trial. During initial analysis of this trial, overall risk of death was found to be reduced by 28% in patients given ZOL once yearly via an infusion (Lyles *et al.* 2007). Another analysis of the HORIZON trial found evidence that ZOL's ability to confer a benefit to survival could be due to non-skeletal effects. A blinded retrospective analysis of the HORIZON study found that only 8% of the reduction in mortality was due to a reduction in fractures and that the other 92% of reduction in mortality was not (Colón-Emeric *et al.* 2010). This implied that ZOL was acting through other mechanisms to reduce mortality. This study also showed that older patients had a reduced risk of death from cardiac arrythmias and risk of death from infection. However, there was no changed in the incidence of either cardiac arrythmias or infection in this study. The implies ZOL is improving the resilience of older people to these diseases. This study was important for laying the groundwork for future investigations into how ZOL may confer non-skeletal benefits into promoting the survival of older people.

Further work in the literature was able to support the notion that n-BPs can improve the immune function of older people. A more recent study found a weak association between reduced incidence of pneumonia infections and ZOL treatment in post-menopausal women (p=0.09) (Reid *et al.* 2021). Another study on nitrogen

containing bisphosphonates demonstrated a similar effect. A study on a separate population of older patients taking nitrogen containing bisphosphates showed that they had a significantly reduced incidence and mortality from pneumonia (Sing *et al.* 2020). Other recent studies have also examined the impact of BPs on COVID. One such study found that zoledronate treatment (but not other BPs) resulted in a decreased likelihood of incidence of COVID (Blanch-Rubio *et al.* 2020). A limitation to this study is that it only looked at incidence, not at survival or severity of the disease. These findings of that study were somewhat contradicted by a more recent study indicating that bisphosphonates have no effect on COVID survival, incidence or severity (Degli Esposti *et al.* 2021). However, this study looked at all bisphosphonates collectively and did not distinguish between individual bisphosphonates. The authors did acknowledge that it was impossible to rule out that ZOL could have had a different effect to the other BPs in a similar fashion to the 2020 study. Unfortunately, they were unable to perform a similar analysis as there were insufficient numbers of ZOL patients in their study to analyse ZOL patients individually. In addition to the improvement in survival from pneumonia, analysis of the HORIZON trial indicated reduced death from cardiac arrhythmias (Colón-Emeric *et al.* 2010). Supporting this notion, some studies have shown reduced risk of cardiovascular events in older patients given bisphosphonates (Reid *et al.* 2020; Sing *et al.* 2018; Wolfe *et al.* 2013). However, this is contradicted by meta-analyses on bisphosphonates that show no change in the incidence of cardiac events and cardiac mortality (Kim *et al.* 2015; Kranenburg *et al.* 2016). One possible explanation for this is disparity is that there may be a beneficial effect of certain bisphosphonates such as ZOL on cardiac function, but not for all bisphosphonates. The exact extent to which any enhancement of immune and cardiac function by ZOL plays in promoting the survival of older people remains unknown.

As well as improving immune function and cardiac function in older people, it is also possible that ZOL could reduce the incidence of other non-skeletal age-related diseases. As mentioned previously in section 1.4, ZOL can prevent the development of SREs in cancer. However, there is also evidence to suggest that ZOL treatment lowers the total rate of cancer incidence and risk of a fatal stroke in older women (Reid *et al.* 2020). Supporting this notion, some studies have indicated that postmenopausal women taking bisphosphonates had reduced incidences of

endometrial cancer and colon cancer (Pazianas *et al.* 2012; Newcomb *et al.* 2015). In addition, one trial showed that postmenopausal women taking ZOL had improved survival from breast cancer (Coleman *et al.* 2014). Contradicting this, other studies have found no effect of bisphosphonates in lowering incidence of breast cancer in postmenopausal women (Hue *et al.* 2014). One possible explanation for this is that ZOL's improvement in survival, but not incidence of breast cancer could be due to increased bone strength and/ or reduced bone metastasises. Indeed, there is also evidence to suggest that BPs can reduce the incidence of skeletal metastasises during breast cancer (Kremer *et al.* 2014; Powles *et al.* 2006). Another study found that bisphosphonate prescription was associated with increased risk of gastrointestinal cancers (Green *et al.* 2010). The authors did acknowledge that the patients receiving bisphosphonates were slightly older than the control group, which may partially explain this outcome. Overall, there is some evidence to suggest that ZOL's effects on improving survival in certain cancers, although this may be mediated partly by its effects on the skeleton.

In addition to increased risk of cancer, ageing is also associated with increased risk of developing other diseases such as type 2 diabetes. There is some evidence from retrospective clinical studies to suggest that patients taking nitrogen containing bisphosphonates had a reduced risk of developing diabetes (Vestergaard 2011; Chan *et al.* 2015; Toulis *et al.* 2015). This adds to the body of evidence that suggests that ZOL may have beneficial non-skeletal effects on older people. There is also some evidence to indicate zoledronate may impact muscle function in patients. Recently, there was one study in China that indicated that zoledronate improved muscle mass in osteoporosis patients compared to untreated patients (Huang *et al.* 2021). It is difficult to determine whether this was due to ZOL's effect on bone or through another mechanism, but this study does offer an initial hint at zoledronate's may improve muscle function. This study should be criticized for its small sample size and lack of variety in muscular parameters examined. Further studies are required to replicate this finding before drawing any definitive conclusions. Another recent study contradicted these findings and claimed that older patients taking zoledronate had impaired muscle and memory function (Bahsi *et al.* 2020). A major limitation to this conclusion was that they did not have a control group of older patients that were not treated with zoledronate. It only looked at patients who had

taken zoledronate over the course of several years. It is therefore difficult to conclude if these changes in this study were as a result of the drug treatment or due to age-related changes. Contradicting the finding that ZOL lowers memory function in older patients, another study found that bisphosphonate treatment reduced the likelihood of developing dementia in people over the age of 50 (Chang et al. 2014). Overall, it currently remains unclear whether ZOL treatment can improve neurological function in older people.

The effects of n-BPs on diseases of non-skeletal tissues are a little counterintuitive. Pharmacokinetically the bulk of zoledronate stays in the bone in animal models (Weiss *et al.* 2008; Nikzad *et al.* 2013; Yousefnia *et al.* 2015). The concentration of ZOL in the bone is over 10-1000 times higher in bone than other non-skeletal tissues (depending on tissue type). Evidence regarding zoledronate's distribution in human tissues is lacking in the literature at present, which certainly does highlight a limit in our understanding as to zoledronate's presence in these tissues in patients. Collectively, the clinical studies cited in this chapter imply that zoledronate could be working in an extra-skeletal fashion to promote healthy ageing and survival of older people. Crucially it has also yet to be determined whether zoledronate promotes survival through its effects on the bone or on other tissue types. Although, there has been some emerging evidence in the last decade that indicates that zoledronate may be targeting mechanisms of ageing in cells that could explain these non-skeletal effects.

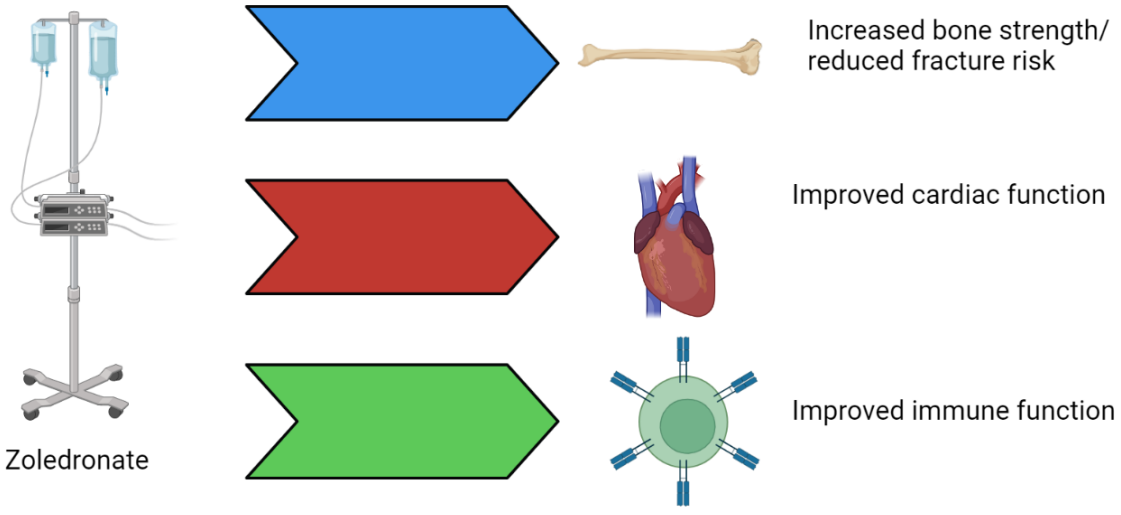

Figure 1.6 - Mechanisms by which ZOL has been shown to improve survival in older patients. Created with Bio-Render.

1.10 Evidence supporting ZOL's ability to act as a geroprotector-

ZOL was first shown to be a geroprotector in a mesenchymal stem cell model in 2016 (Misra *et al.* 2016). This was first indicated by a reduction in features of one hallmark of ageing: that of cellular senescence. Human Mesenchymal Stem Cells (hMSCs) treated with zoledronate took longer to reach a state of replicative senescence and retained their spindle shaped morphology for longer compared to PBS treated control cells. Furthermore, Zoledronate treatment resulted in a reduction in protein markers associated with senescence: p16 and p21. Both p16 and p21 are markers of senescence as they are cyclin dependent kinase (CDK) inhibitors (Chkhotua *et al.* 2003; McConnell *et al.* 1998; Stein *et al.* 1999). This means that one would expect to see more of these proteins when the cells have stopped dividing. The study then went on to look at another hallmark of ageing, that of increased DNA damage. Zoledronate was also able to reduce the amount of DNA damage in later passage hMSCs in terms of a reduction in the DNA damage marker γ-H2AX. This marker binds to sites of DNA damage and recruits DNA repair proteins (Fernandez-Capetillo *et al.* 2002; Rogaku *et al.* 1998). ZOL's also was able to demonstrate a reduction in DNA damage during a comet assay in late passage hMSCs, further supporting this conclusion.

ZOL's reduction of DNA damage was also intriguing in the context of cellular ageing due to the signalling mechanism by which it was achieved. It was found that various downstream markers of mTOR signalling were impacted by ZOL treatment by hMSCs, including FOXO3A. The authors were then able to implicate FOXO3A in ZOL's reduction of DNA damage through gene silencing (siRNA) of FOXO3A. They were also able to offer a hint of zoledronate's potential for combatting cellular ageing *in vivo* through a reduction in DNA damage on the bone marrow and cortical bone of irradiated mice. This study was important as it demonstrated that ZOL inhibited the mTOR pathway, which is central to many ageing processes (section 1.4). This work was also important because it demonstrated that ZOL was influencing features of cellular ageing and that ZOL increased DNA repair in mice.

This work was later supported by a study that demonstrated how ZOL treatment increased longevity and the healthy ageing of *Drosophila* (Chen *et al.* 2021). Zoledronate treatment (in the drinking water) at both 1 µM and 10 µM was able to

improve the survival of both male and female wDah *Drosophila* when treatment began at mid-life (40 days). This was also the case for when zoledronate was given from birth for male flies, but not for female flies. Although, the effect of giving ZOL from birth in improving the survival of flies was quite small compared to when treatment began at mid-life. In terms of improving healthy ageing parameters in *Drosophila*, Zoledronate treatment beginning at 40 days of age was able to improve the climbing ability of flies at middle age (56 days old), but not at older age (when >63 days). Zoledronate treatment starting at birth or from mid-life was also able to improve another feature of *Drosophila* ageing, that of gut permeability. However, this only reached statistical significance when ZOL treatment started at birth.

ZOL treatment was able to increase the survival of *Drosophila* treated with H_2O_2, an inducer of oxidative stress. The signalling molecule FOXO, was implicated in this increase in survival by ZOL through treatment of flies heterozygous for FOXO with ZOL and H_2O_2. Overall, this work on *Drosophila* was important in showing that zoledronate could improve the healthspan of a model organism. It was also important because *Drosophila* lack mineralized bone, the component that ZOL has affinity for in mammalian systems. Instead, they have chitin exoskeletons (Moussian *et al.* 2005). This implicated non-skeletal effects of ZOL on the improvement in lifespan and healthspan in this study. While certain hallmarks of ageing have been identified as being impacted by ZOL treatment in these studies, it is possible that other hallmarks of ageing could also be impacted. In subsequent sections of this chapter, the potential for ZOL to impact these hallmarks of ageing will be examined.

1.11 Evidence that ZOL may impact the other hallmarks of ageing-

1.11.1 Nutrient Sensing-

Zoledronate has been demonstrated to inhibit multiple downstream markers of the mTOR pathway in hMSCs such as p-AKT, p-P70S6K and p-mTOR (Misra *et al.* 2016). Zoledronate has also been demonstrated to inhibit markers of the mTOR pathway in other cell systems. In the breast cancer cell line MDA-MB-468 ZOL was capable of inhibiting the mTOR markers p-AKT and p-mTOR (Lan *et al.* 2013). Additional evidence has indicated that ZOL promotes the production of miRNAs

involved in regulating AKT and mTOR signalling in the MCF7 breast cancer cell line (Fanale *et al.* 2016). Zoledronate was also able to inhibit markers of the mTOR pathway in Osteosarcoma cells (Li and Li 2019). The nitrogen containing bisphosphonates alendronate and pamidronate were also able to inhibit the mTOR pathway in myeloma and breast cancer cells respectively (Tang *et al.* 2010; Tsubaki *et al.* 2015). These studies in cancer cell models should be criticized for their excessive/ non-physiological concentration used to observe this inhibition of the mTOR pathway, which was used in the range of 10-200 µM. However, collectively they do support the notion that ZOL can inhibit the mTOR pathway in multiple different cell types. Furthermore, Zoledronate treatment was also found to inhibit AKT signalling in *Drosophila* (Chen *et al.* 2021). Whether ZOL is also capable of inhibiting the mTOR pathway in more advanced animal models (such as in mice), remains to be determined. The mTOR pathway also interacts with other hallmarks of ageing (Figure 1.7), which are discussed further in later sections.

Another way nitrogen containing BPs could impact ageing through nutrient sensing pathways is by lowering levels of circulating IGF-1. This has found to be the case with zoledronate in osteoporotic patients (Perifanis *et al.* 2007). This was also found to the case in response to the n-BP pamidronate in rats that had been treated with growth hormone (Kapitola *et al.* 2001). The mechanisms behind this decrease remain unclear. However, this suggests that ZOL could be having an impact on more than one nutrient sensitive ageing associated pathway.

1.11.2 Genomic instability-

Zoledronate has been demonstrated to reduce DNA damage through mTOR inhibition in hMSCs (Misra *et al.* 2016). ZOL was also found to upregulate the DNA repair protein ATM in hMSCs. Zoledronate also limited DNA damage following irradiation of mice in the same study. Furthermore, zoledronate treatment was able to reduce levels of DNA damage in *Drosophila* (Chen *et al.* 2021). In addition to this there is evidence that zoledronate can reduce levels of DNA damage in a cancer model. Skin cells derived from Neurofibromatosis patients were found to have reduced levels of DNA damage when treated with zoledronate (Combemale *et al.* 2022).

However, there is some contradictory evidence in the literature to suggest that zoledronate can induce DNA damage in certain circumstances. Zoledronate treatment was sufficient to increase levels of the DNA damage marker y-H2AX in osteosarcoma cells and keratinocytes (Iguchi *et al.* 2007; Ohnuki *et al.* 2012). However, in both instances the cells were treated with 100 µM Zoledronate. This dose is rather a lot higher than that which would be reached physiologically and is sufficient to induce apoptosis in certain cell types (Iguchi *et al.* 2007; Lan *et al.* 2013). Other than the previously mentioned mTOR-FOXO3-ATM induced DNA damage response (Misra *et al.* 2016), there could be other mechanisms by which ZOL could trigger a DNA repair response. Mice that had been genetically engineered to have lower levels of mTOR signalling exhibited increased expression of the DNA repair proteins MGMT and NDRG1 (Dominick *et al.* 2017). It is possible that ZOL could also increase the expression of these proteins also due to its inhibition of the mTOR pathway. Although, that has yet to be determined.

1.11.3 Telomere attrition-

Zoledronate's impact on telomere attrition remains unclear. Studies on nitrogen containing BPs in prostate and cancer cells indicated that nitrogen containing BP treatment reduced telomerase expression (Dalle Carbonare *et al.* 2005; Valenti *et al.* 2005). It was suggested by the authors that this might be a mechanism by which BPs reduce levels of cell viability in cancer cell lines. It is difficult to compare this in an ageing context as cancer cells express elevated levels of telomerase to begin with in order to maintain their continuing proliferation (Shay *et al.* 2001). Another study looked at telomere length in leukocytes in post-menopausal women who had been receiving nitrogen containing bisphosphonates (Kalyan *et al.* 2014). This study found that there was no difference in telomere length in response to zoledronate treatment. This supports the notion that a reduction in telomeres by n-BPs may be unique to cancer. Either way, it is also possible that the impact of zoledronate on the other hallmarks of ageing might outweigh any potential impact on telomerase expression.

1.11.4 Autophagy / Proteostasis-

As mentioned previously zoledronate can inhibit the mTOR pathway. A notable example of a cytoprotective effect of mTOR inhibition is that of increased autophagy (Jung *et al* 2010; Dunlop *et al.* 2014; Arias *et al.* 2015). This can be through activation of ULK or through the activity of FOXOs. Due to zoledronate's inhibition of the mTOR pathway, it is also possible that zoledronate could induce autophagy. Indeed, some evidence in the literature exists to suggest that zoledronate can induce autophagy in a couple of different cancer cell models (Ge *et al.* 2014; Lu *et al.* 2016). However, a major limitation to these studies again was that zoledronate was applied at excessive concentrations that would be unlikely to be reached *in vivo* (>10 µM). This induction in autophagy seen in these cell models could be due to cell death caused by a cytotoxic dose the drug was administered at (Denton and Kumar 2019; Iguchi *et al.* 2007)**.**

Another way in which ZOL could target proteostasis is through the proteasomal system. There is also some evidence to indicate that ZOL increases the production of miRNAs involved in ubiquitin mediated proteostasis in MCF-7 breast cancer cells (Fanale *et al.* 2016). Although, the effects of ZOL or other BPs on proteasomal activity have yet to be substantiated by other studies. An alternative mechanism by which zoledronate could improve proteostasis with age is by increasing levels of chaperone proteins that prevent protein aggregates. There are a couple of examples in the literature that suggests that n-BPs could induce increased expression of heat shock proteins, an example of chaperone proteins. One such study demonstrated how zoledronate could increase levels of the transcription factor HSF-1 in osteosarcoma cells (Lamoureux *et al.* 2014). This transcription factor is responsible for transcription of a variety of heat shock protein genes involved in protein folding. Similarly, a study on osteoblast like cells indicated that the nitrogen containing bisphosphonates risedronate and alendronate increased levels of heat shock protein 90 expression (Romanello *et al.* 2006). It is possible that ZOL could also help alleviate cellular ageing through the prevention of protein aggregation.

1.11.5 Mitochondrial dysfunction-

If ZOL can improve autophagy (as discussed in section 1.11.4), it could also aid in the clearance of defective mitochondria via mitophagy. In addition to this, zoledronate's ability to influence FOXO3A could also improve mitochondrial dysfunction. Increased activity of FOXO3A was one of the markers of zoledronate treatment in hMSCs (Misra *et al.* 2016). Some studies have indicated that increased activation of FOXO3A can improve features of mitochondrial dysfunction (Kops et al. 2002; Celestini et al. 2018).

However, there is some evidence that nitrogen containing BPs could have a negative impact on mitochondrial function. Since the mevalonate pathway is responsible for the formation of prenylated proteins, it is also responsible for the production of prenylated proteins required for the mitochondrial respiratory chain such as Coenzyme Q10. A study found that n-BP receiving osteoporotic patients had reduced levels of coenzyme Q10 in their circulation (Kalyan *et al.* 2014). The work in this study should be criticised for the relatively low number of control patients (n=17). There are a variety of mechanisms by which zoledronate could be influencing the healthy ageing of mitochondria. It has also been suggested that mTOR inhibitors reduce DNA damage by lowering the levels of ROS by increasing expression of superoxide dismutase and other antioxidants (Kofman *et al.* 2012; Calap-Quintana *et al.* 2015). In addition to this, FOXO3A activation can also increase antioxidant activity (Kops *et al.* 2002). Given that ZOL inhibits mTOR and activates FOXO3A it is possible that is could also enhance the antioxidant activity of cells.

1.11.6 Cellular Senescence-

An indication that zoledronate was able to combat several features of cellular senescence was demonstrated in hMSCs (Misra *et al.* 2016). This was indicated by a reduction in features associated with cellular senescence present in late passage primary hMSCs. Cells treated with zoledronate took longer to reach a state of replicative senescence and retained their spindle shaped morphology for longer compared to PBS treated control cells. Zoledronate treatment resulted in a reduction in protein markers associated with cellular senescence: that of the cell cycle arrest proteins p16 and p21. Although, it is unclear whether this reduction in markers of senescence was due to prevention of a state of cellular senescence being reached

(senostatic) or selective cell death of senescent cells (senolytic). Although, judging by the senostatic effects of drugs that target similar pathways such as rapamycin (Laberge *et al.* 2015; Herranz *et al.* 2015), this would seem to be the more likely mechanism. Supporting this notion, an experiment conducted in *Drosophila* suggested that ZOL had a preventative effect on limiting cellular damage to promote survival (Chen *et al.* 2021). This was done by comparing the survival of *Drosophila* treated with H_2O_2 at 11 days of age; an agent that induces oxidative stress and reduces lifespan. Survival of flies was improved when ZOL was given prior to H_2O_2 but not when given simultaneously with H_2O_2. This suggests that ZOL is having a preventative rather than a curative effect on cellular damage to promote longevity in *Drosophila*. Although a limitation to this argument is that it was unclear during this study whether a reduction in cellular senescence itself was a cause of the increased survival. Conversely, the n-BP pamidronate can induce senescence in oral keratinocytes. This was shown by increased levels of the cellular senescence markers p16 and senescence associated β-galactosidase (Kim *et al.* 2011). Although, this may be due to rare side effect of BPs specific to the mouth such as osteonecrosis of the jaw (ONJ). In addition, the drug was administered at a high, non-physiological concentration that may also explain these findings (50 μM).

1.11.7 Intercellular communication-

ZOL may also impact this hallmark of ageing. This is because DNA damage is a key driver of the SASP (Rodier *et al.* 2009). Since ZOL has already been shown to reduce DNA damage in hMSCs (Misra *et al.* 2016), it is also possible it could alleviate the SASP. The SASP can also be induced by mitochondrial dysfunction (Wiley *et al.* 2016). If zoledronate can impact mitochondrial dysfunction (section 1.11.5), it could also alleviate the SASP through this mechanism. Another key driver of the SASP is that of NF-kB signalling (Chien *et al.* 2011). It has been demonstrated that zoledronate can lower levels of active NF-kB in cancer and myeloid cells (Schech *et al.* 2013; Wolf *et al.* 2006). In addition to this, drugs that target similar pathways to ZOL such as rapamycin have been shown to be capable of reducing the SASP (Laberge *et al.* 2015; Herranz *et al.* 2015). Given that ZOL can also inhibit mTOR markers (Misra *et al.* 2016), it is also possible that ZOL could have a similar effect on the SASP of older cells. ZOL's impact on the release of inflammatory factors from immune cells may contradict this hypothesis. ZOL can induce an acute

phase response that typically lasts for less than 48 hours. This results in the release of pro-inflammatory cytokines from immune cells (Anastasilakis *et al.* 2012; Welton *et al.* 2013). This suggests that ZOL may also drive a pro-inflammatory environment in the short-term following administration due to the acute phase response. Whether the impact of the acute phase response would outweigh any long-term anti-inflammatory impact on the SASP in the remains unknown.

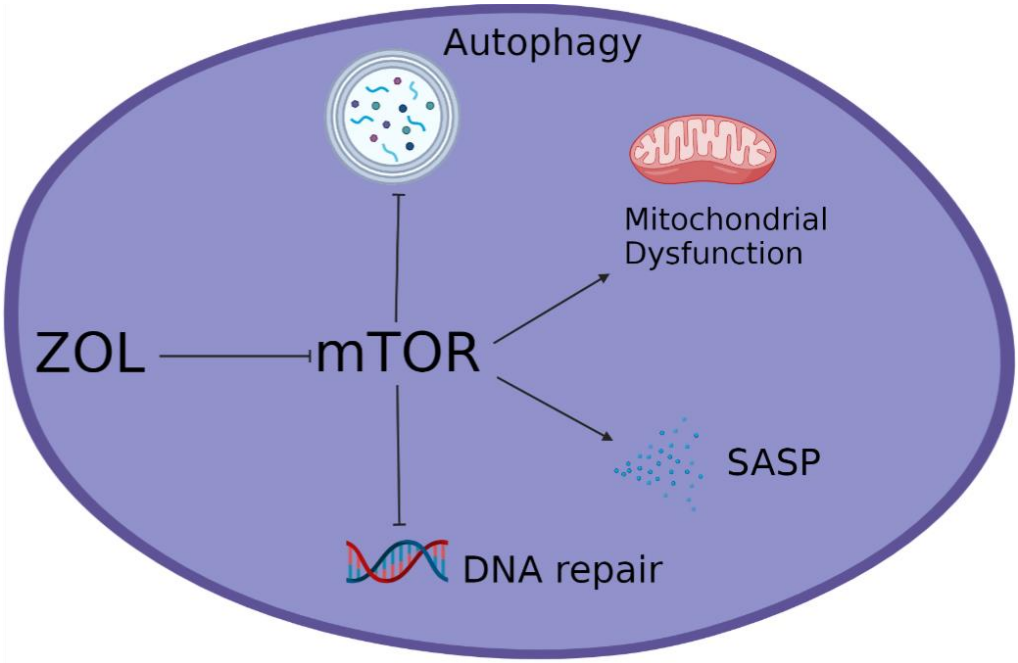

Figure 1.7 - The potential impact of ZOL's inhibition of mTOR on features of the hallmarks of ageing. Created with Bio-Render.

1.11.8 Stem Cell Dysfunction-

Zoledronate can seemingly alleviate some features of stem cell dysfunction. In hMSCs, cells treated with zoledronate were able to proliferate for longer before reaching a state of replicative senescence (Misra *et al.* 2016). In addition to this zoledronate treated hMSCs had a higher number of clonogenic cells compared to control treated cells when assessed via CFU-F, CFU-O and CFU-A. These experiments indicated that zoledronate increased the ability of hMSCs in later passage cells to differentiate *in vitro*. These also had lower levels of the DNA damage marker γ-H2AX. This experiment suggested that ZOL treatment increased

the resistance of stem cells to DNA damage, another hallmark of ageing. This was further demonstrated *in vivo* through the irradiation of mice. Mesenchymal progenitor cells from irradiated mice had higher numbers of CFU-F cells compared to irradiated control mice. In addition, more recent work showed that ZOL treatment was able to prevent age related changes to intestinal stem cells in *Drosophila* (Chen *et al.* 2021). ZOL treated flies had lower numbers of intestinal stem cells compared to control flies at old age (60 days). However, other work in the literature has contradicted these findings. One such study indicated that zoledronate could reduce proliferation and induce apoptosis of hMSCs (Ebert *et al.* 2009). However, this work did use much higher concentrations of zoledronate of 25-50 μM. Again, it is unlikely that such a concentration would be reached physiologically.

1.11.9 Epigenetic alterations-

Another way in which ZOL could target a hallmark of ageing is via epigenetic changes. An example of an ageing intervention that targets epigenetic changes with age is that of HDAC inhibitors to reduce histone deacetylation. This has been used in mice to improve memory with age (Peleg *et al.* 2010). The n-BP ibandronate has been shown to be an effective HDAC inhibitor in cancer cell lines (Karlic *et al.* 2015). It is possible that other n-BPs such as ZOL could be used to improve the memory of older organisms through a similar mechanism. Another way in which ZOL maybe influencing epigenetic ageing of cells is through increasing levels of certain miRNAs that promote longevity (Fanale *et al.* 2016). In this study it was shown that ZOL can alter levels of miRNAs that regulate AKT and mTOR signalling *in vitro* in breast cancer cells. Whether this is also the case in an ageing context remains unclear.

Another mechanism by which ZOL could be influencing epigenetic mechanism is by increasing levels of KDM6A. KDM6A demethylates H3k27me3. Knocking out KDM6A has a negative impact on the self-renewal of bone marrow cells from aged mice (Tian *et al.* 2021). In addition to this, overexpression of a KDM6A/B ortholog increased lifespan in *C. elegans* (Labbadia and Morimoto 2015). ZOL may have epigenetic effects on ageing through increasing levels of KDM6A and KDM6B. One study showed that zoledronate increased levels of KDM6A and KDM6B in macrophages (Yang *et al.* 2020). The exact mechanisms by which n-BP achieves these epigenetic changes in these prior studies currently remains unknown.

1.12 The pipeline for developing interventions that target hallmarks of ageing-

During this chapter, it is hoped that the potential of ZOL to impact the hallmarks of ageing has been illustrated. The end goal of ageing interventions is to treat a root cause of ageing to improve the health of older people. This usually begins with experiments to identify compounds or other interventions that impact the hallmarks of ageing in the context of cultured cells. Once successfully identified, this then leads to these interventions being tested in model organisms. In model organisms such interventions tend to look at two distinct outcomes. One of which is an improvement in lifespan: how long an organism lives in response to an intervention. The other is an improvement in healthspan: how long an organism remains free of disease/ remains in good health. Usually this begins with an invertebrate model such as *Drosophila* or *C. elegans*. The next step is to test the intervention in a mammalian system such as in mice. Finally, such interventions can then start to be tested in patients during clinical trials.

The efficacy of ZOL in improving the healthy ageing of cells and *Drosophila* has been demonstrated (Misra *et al.* 2016; Chen *et al.* 2020). The next step will be to assess with ZOL improves the healthy ageing of mice. A recently proposed pipeline for standardised testing of ageing interventions should be used to assess healthy ageing in mice (Bellantuono *et al.* 2020). This study focussed on determining whether zoledronate can improve the healthy ageing of mice using this pipeline for assessing healthy ageing. If successful, the hope of this research is that this intervention could then be tested in a clinical trial on patients to improve healthy ageing in the older population.

Hypotheses-

1) Zoledronate can inhibit mTOR in mouse tissues.

2) Zoledronate can improve the healthspan of mice.

Objectives-

1) To detect if ZOL is capable of inhibiting mTOR in mouse tissues and how regularly to give the drug by western blotting for p-AKT as a marker.
2) To determine if ZOL improves the healthspan of mice by giving ZOL to older mice and assessing their healthspan parameters.

Chapter 2- Materials and Methods

2.1 Mouse Experiments-

Animal experiments were performed according to protocols outlined in the project licence (PCF1D350B) and personal licence granted by the home office. Female C57BL/6J mice were purchased from Charles River (Charles River, Wilmington, Massachusetts, USA). Mice were kept at 21 °C and on a 12-h:12-h light: dark cycle. C57BL/6J mice were used as this is the strain that was recommended by the toolbox on measuring mice healthspan paper (Bellantuono *et al.* 2020). C57BL/6J mice were chosen as the preferred strain of mouse in the toolbox paper because they have been widely used in previous studies on mouse healthspan. Using the same strain of mouse helps ensure that studies that use the toolbox are standardised and makes it easier to compare the effectiveness of ZOL with other healthspan interventions in the field. In addition to this, C57Bl/6J are widely available to order from vendors and their widespread use means that their housing, maintenance, age-related changes and health-related conditions are well understood.

During the mouse experiments, mice were culled at the end of the experiment or if they reached a humane end point as set out in the project licence. These humane endpoints included rapid weight loss (>20%), widespread piloerection, dermatitis covering more than 10% of the body, abnormally hunched posture, loss of physical activity or appetite that cannot be reversed by mild veterinary intervention. Mice were examined throughout these experiments for signs of these of humane endpoints or for any other indication of ill health. Furthermore, mice were weighed twice weekly as part of the healthspan experiment (see Figure 4.3) and to ensure animal welfare. After the culling, mice underwent a post-mortem examination and had their tissues collected for further study. Any signs of tumours or other organ abnormalities were noted. Tissues were either flash frozen or stored in paraffin for future histological analysis.

2.2 Drug treatments-

Zoledronate was prepared by dissolving zoledronate powder 1.45 mg/ml powder in Phosphate Buffered Saline (PBS) to create a 5 mM concentration solution. This solution was diluted further in PBS to create a 25 µg/ml solution for mouse intraperitoneal injections. During the time course experiments, 10-week-old C57BL/6J mice were injected intraperitoneally with 125 µg/ kg zoledronate (thanks to Hal Ebetino for providing Zoledronate powder) or with an equivalent amount of PBS. During the healthy ageing study, C57BL/6J mice were injected intraperitoneally with 125 µg/ kg zoledronate or with an equivalent amount of PBS twice a week starting at 12 months of age for the duration of the healthspan pipeline.

For *in vitro* experiments, the 5 mM ZOL solution was further diluted in Dulbecco's Modified Eagle Medium (DMEM) media containing 10% Foetal Bovine Serum (FBS, Thermofisher, Waltham, Massachusetts, USA) to reach the required concentrations. As a control treatment, cells were given an equal amount of PBS. Clinical Zoledronate solution was ordered from the Northern General hospital pharmacy (Tillomed laboratories, Luton, UK). This stock solution was at 0.8 mg/ml and diluted further in media to reach the desired concentration.

Farnesol (FOH) (MCL, Sigma, Burlington, Massachusetts, USA) and geranylgeraniol (GGOH) (Sigma) were diluted to 7.33 mg/ml and 9.58 mg/ml respectively in 100% ethanol. This resulted in the creation of 33mM FOH and GGOH solutions. These were then further diluted in the DMEM media to reach a concentration of 33 µM. This concentration was sufficient to reverse inhibition of the mevalonate pathway in a previous study (Misra *et al.* 2016). An equivalent amount of ethanol was used as a control for FOH and GGOH. Media was not replenished after drug treatment unless otherwise stated.

2.3 Tissue collection-

2.3.1 Culling and timing of tissue collections-

During most of the time course experiments, mice were culled via cervical dislocation, were dissected and had their tissues flash frozen in liquid nitrogen for further analysis at the end of the experiment. However, if blood was collected from the mice a different culling method was used. In order to collect the mouse blood,

mice were culled via cardiac puncture under anaesthesia (5% isoflurane (Zoetis, Parsippany, New Jersey, USA) and 2 L/ minute oxygen). A 25g needle containing a small volume (approximately 100 µl) of heparin (Wockhardt, Mumbai, Maharashtra, India) was used to collect the blood.

If mice were subjected to dietary manipulation prior to tissue collection, food was withdrawal food overnight for 16 hours followed by subsequent refeeding of each mouse for 45 minutes. For the time course experiments, tissues were collected at Day 1, Day 3, Day 7 or Day 24 post-injection. A time point of Day 3 was used as it took three days for p-AKT inhibition to be achieved by ZOL in a previous study on hMSCs *in vitro* (Misra *et al.* 2016). Time points of Day 7 and Day 24 post-injection were selected to see if ZOL maintained p-AKT inhibition in the longer term following a single dose of the drug. A time point of time Day 1 post-injection was also selected in case ZOL's impact on p-AKT in mouse tissues was shorter in duration than that observed in hMSCs (Misra *et al.* 2016). There were three mice per group for the first set of time course experiments (Figures 3.2-3.7). This number was used as this group size was sufficient to inhibit p-AKT in hMSCs and *Drosophila*. During the next set of time course experiments a larger group size was used (n=6). This group size was decided using power calculations using the data from the previous ZOL time course experiments to work out the group size needed to reliably detect a significant change. Power calculations used a power of 80% and an alpha of 0.05.

2.3.2 Bone marrow collection-

Femurs were placed in DMEM media containing 10% FBS. These femurs were then cut at the end with a scalpel and placed in PCR tubes. These PCR tubes had the end cut off and were placed inside an eppendorf. The femurs were centrifuged at 2012 g for 3 minutes to pellet the bone marrow. The flushed femur was then flash frozen for further analysis. This pellet was then resuspended in 100 ml of lysis buffer, incubated for 15 minutes and spun at 9477 g for 10 minutes to collect the protein lysate.

2.3.3 Collection of Blood from mice-

The mouse blood (approximately 0.5-1 ml) was drawn up and then placed in a 15 ml tube. Blood was diluted 1:4 in PBS. 5 ml of Ficoll (GE Healthcare, Chicago, Illinois, USA) was then added. These were then spun at 300 g for 30 minutes at RT with the

break switched off. The mononuclear layer was extracted with a pasteur pipette and diluted in 20 ml of PBS. This was then spun at 150 g for 10 minutes, the pellet was resuspended in 1 ml of PBS and transferred to an eppendorf tube. Cells were counted by diluting them 1:5 in 2% acetic acid (glacial acetic acid and distilled water). Cells were counted in a Fuchs Rosenthal Haemocytometer (VWR International, Radnor, Pennsylvania, USA). Cells were then spun at 735 g in a microcentrifuge, had their supernatant removed and then the pellet was flash frozen in LN.

2.3.4 Choice of AKT as a biomarker in time course experiments-

AKT was used as the primary marker for ZOL's activity in mouse tissues. As mentioned earlier, AKT is a serine/threonine protein kinase. In terms of its cellular function, it regulates glucose metabolism, survival, cytoskeletal and proliferation. It is also important in the context of ageing as other AKT inhibitors can induce autophagy, thus alleviating a hallmark of ageing (Cheng *et al.* 2022). This study also demonstrated that AKT inhibition can increase the lifespan of *Drosophila,* further illustrating the importance of AKT signalling in ageing. AKT has also been shown to be a marker that is robustly inhibited by ZOL during previous studies on hMSCs and *Drosophila* (Misra *et al.* 2016; Chen *et al.* 2020). Some of the downstream signalling molecules of AKT signalling also have a role to play in cellular ageing. For example, the inhibition of AKT causes increased activation of FOXO transcription factors. These in turn can alleviate features of cellular ageing through activation of autophagy and through increased antioxidant production (Kops *et al.* 2002; Warr *et al.* 2013). Furthermore, interventions that increase activation of FOXOs have been shown to increase lifespan in model organisms (Chen *et al.* 2019; Demontis and Perrimon 2010; Lin *et al.* 1997). Another protein downstream of AKT signalling is GSK3β. This protein was implicated in the development of cellular senescence and the SASP in a recent study in which GSK3β was knocked out in podocytes (Fang *et al.* 2022). This resulted in a reduction in the SASP and cellular senescence in podocytes *in vitro*. Collectively, these studies suggest that downstream molecules of AKT signalling have an important role to play in cellular ageing.

2.4 Human Mesenchymal Stem Cells (hMSCs) culturing-

2.4.1 Establishment of hMSCs lines-

MSCs were obtained from bone marrow donors. These donors were young and healthy patients (2-15 years old) who were undergoing an osteotomy at Sheffield Children's hospital. Criteria for exclusion as a donor included having a bone marrow abnormality, metabolic defect or cancer. Informed written parental consent was obtained in full compliance with local ethics committee requirements (NHS ethical approval #19/SW/0195). Initial culturing of hMSCs from bone marrow was performed by Caroline Fry and Zhengqi Chen. This was done by collecting bone marrow in DMEM media containing 10% FBS, 0.01% penicillin/streptomycin (Sigma) and 0.1% heparin. Bone marrow mononuclear cells (BMC) were collecting by centrifugation at 800 g for 20 minutes in lymphocyte separation medium (1.077g/L, PAA Laboratories, Somerset, UK). The interphase layer was then collected and 18 ml of PBS was added for every 2 ml of BMCs. The cells were then centrifuged again at 800 g for 10 minutes. Cells were resuspended in 2 ml of PBS and then counted with 5% acetic acid in a Fuchs Rosenthal Haemocytometer. Following this, another 18 ml of PBS was added and the cells were centrifuged again at 800 g for 5 minutes. The pellet was resuspended in DMEM media containing 10% FBS, plated at 8000 cells per cm^2 in a T25 flask (Thermofisher) and left in an incubator at 37^0C at 5% CO2. The media was replenished 24 hours later to remove non-adherent cells. Once cells reached 90% confluency, they were replated as described in section 2.4.4.

2.4.2 Defrosting hMSCs-

Cryovials of hMSCs were stored at $–200^0$C in liquid nitrogen. Cryovials of cells were initially defrosted in a water bath at 37^0C. The defrosted cells were then transferred into 10 ml of DMEM media (Gibco, Paisley, UK) containing 10% FBS. The cells were then centrifuged at 693 g for 5 minutes. After this, the pellet was resuspended in DMEM media (containing 10% FBS) and seeded into a T75 flask. The cells were then placed in an incubator at 37^0C, 5% CO_2. After 24 hours since the cells had been defrosted, the media was replenished.

2.4.3 Maintenance of hMSC cultures-

The cells were cultured in DMEM media containing 10% FBS. Cells were cultured in an incubator at 37^0C at 5% CO2. Flasks were replenished with fresh media twice weekly. Cells were examined regularly to check confluency.

2.4.4 Cell passaging-

Once cells reached 90% confluency, the cells were split and seeded into new flasks. Initially the media was removed and then the flask was washed with PBS. Following this, trypsin-EDTA (Thermofisher) containing 0.05 % Trypsin, 0.53 mM Ethylene-diamine-tetra-acetic acid (EDTA) was added to the cells. The cells were then placed in the incubator for 3-4 minutes. Once the cells detached, the trypsin was inactivated through the addition of DMEM media containing 10% FBS. The cells were then subjected to centrifugation at 693 g for 5 minutes. Following this, the supernatant was removed and the pellet was gently resuspended in DMEM media containing 10% FBS. A cell count was performed using trypan blue (Sigma) and a Fuchs Rosenthal Haemocytometer. 5000 cells per cm^2 were then seeded into a new T75 flask (Thermofisher) or T25 flask. Newly seeded flasks were then placed in an incubator for further culturing 37^0C at 5% CO2.

2.4.5 Freezing of cells-

As described in 2.6.5, flasks had their media removed, were washed with PBS and trypsinized. After this, the cells were resuspended in a freezing mixture consisting of 10% DMSO (Thermofisher) in FBS. The cells were then moved to a cryovial and placed in a freezer -80^0C. The next day, the cells were then transferred to liquid nitrogen for long term storage at –200^0C in liquid nitrogen.

2.5 Protein Extraction-

2.5.1 Extraction of protein from bone marrow, brain, heart, intestine, kidney, flushed femur, pancreas, skeletal muscle, spleen and tibia mouse tissues-

Following tissue dissection and flash freezing, extraction of the protein lysates from the mouse tissues was performed. To begin with, lysis buffer was prepared by fully defrosting mammalian cell lysis buffer (MCL) (Sigma). This buffer consists of 0.5% Sodium Dodecyl Sulphate, 750 mM Sodium Chloride, 2.5 % Deoxycholic acid sodium salt (DOC), 5% IGEPAL (Octylphenoxy poly(ethyleneoxy)ethanol) and Tris

buffer (5 mM EDTA, 250 mM Tris-HCl, pH 7.5). Phosphatase inhibitor (Sigma) was added to the MCL, this inhibitor cocktail contains Calyculin A, (–)-p-Bromolevamisole oxalate and Cantharidin. This was added at 1% of total volume of the MCL. Protease inhibitor was also added to the MCL. The protease inhibitor cocktail consists of 4-(2-aminoethyl) benzenesulfonyl fluoride hydrochloride (AEBSF) (104 mM), Aprotinin (80 µM), and Bestatin (4 mM), E-64 (1.4 mM), Leupeptin (2 mM) and Pepstatin A (1.5 mM). The protease inhibitor (Sigma) was added at 2% of total volume of the MCL.

Collected tissues were placed on dry ice. They were placed on scales and weighed. This was done in order to determine the volume of lysis buffer required to add to successfully lyse the tissues (1 mg of tissue per 30 µl of lysis buffer). After weighing, tissues were kept on dry ice. A mortar and pestle were cooled by pouring liquid nitrogen onto them. The tissue was then placed into the cooled mortar and pestle. Then the tissue was crushed using the mortar and pestle. Once the tissue had reached the state of a fine powder it was transferred to a 50 ml falcon tube along with the liquid nitrogen. These tubes were then placed on ice. Once the liquid nitrogen had evaporated, lysis buffer was added according to the tissue weight. The samples were then sonicated for 10 seconds. This sonication was repeated another two times for 10 seconds for each sample. Following this, the samples were left to incubate for 15 minutes at 4°C on a shaker. Next, the samples were subjected to centrifugation at 9477 g for 10 minutes in a microcentrifuge. Lastly, the supernatant was then removed and stored in the freezer at –20°C.

2.5.2 Protein extraction of blood cells-

In the instance of the peripheral blood cells were collected as described in 2.3.3 and lysis buffer was prepared as described in section 2.5.1. In addition, it was also necessary to also add 0.025 Units/µL Benzonase Nuclease (Sigma) to remove DNA contamination at 0.1% of total volume of the lysis buffer. Sample buffer (see section 2.7) was then added to the lysis buffer at a ratio of 1:4. This loading buffer was then added to the entire pellet. The samples were then boiled for five minutes at 97^0C and the samples were then ready for loading during subsequent western blot analysis. The rest of the steps of the western blotting protocol for p-AKT and total AKT were followed in the same fashion as outlined in section 2.7.1.

2.5.3 Protein extraction of cultured hMSCs-

Cells were trypsinised as described in section 2.4.4. The pellet was then resuspended in PBS and a cell count performed. Following this the cells were centrifuged at 693 g for 3 minutes in a microcentrifuge. Following removal of the supernatant, the cell pellet was re-suspended in mammalian cell lysis buffer (also containing 1% Protease and 2% Phosphatase inhibitor). The volume of lysis buffer added corresponded to the number of cells (500 µl of buffer per 3 million cells). The cells were then placed on a shaker at 4^0C for 15 minutes to incubate. Then the lysate was subjected to centrifugation at 9477 g at 4^0C for 10 minutes in a microcentrifuge. The supernatant was then taken off and stored in a freezer at -20^0C for future use.

2.6 Bicinchoninic acid (BCA) assay

In order to quantify the concentration of protein present in the lysates a Bicinchoninic acid assay (BCA) was performed. This was required to load consistent amounts of protein (40 µg) for the western blot assay. To begin with a Bovine Serum Albumin (BSA) calibration curve was created from a series of BSA: Lysis buffer standards (0-2000 µg/mL). These standards contained either 0 µg/mL, 250 µg/mL, 500 µg/mL, 750 µg/mL, 1000 µg/mL, 1250 µg/mL, 1500 µg/mL or 2000 µg/mL BSA/ lysis buffer. 10 µl of each protein standard was loaded in triplicate to a 96 well plate. Following this, protein samples of interest were diluted 1:10 in lysis buffer (5 µl protein sample and 45 µl lysis buffer) and 10 µl of each diluted protein sample was also loaded onto the 96 well plate in triplicate.

Next, a 1:50 copper sulphate (Sigma)/ BCA was prepared. 200 µl of the copper sulphate/ BCA solution was then added to each sample in the 96 well plate for half an hour at room temperature (RT). Addition of the Copper Sulphate/ BCA solution resulted in a purple colour change in the presence of amino acid residues due to the reduction of Cu^{2+} ions to Cu^{+1}. This colour changes were measured with a Spectramax M5e (Molecular devices, Wokingham, UK) plate reader to determine protein concentration. Readings were made at 560nm with Softmax pro 7 software (Molecular devices, San Jose, California, USA).

2.7 Western Blotting of hMSCs and mouse tissues-

Running buffer was prepared containing 2.5 mM Tris, 19.2 mM glycine, 0.01% SDS (Bio-Rad, Hercules, California, USA). Sample buffer was prepared by diluting mercapthoethanol (Sigma) 1:10 in 4X laemmli buffer (Bio-Rad). The laemmli buffer consists of 1% Lithium Dodecyl Sulphate (LDS), 10% glycerol, 0.005% Bromophenol Blue and 62.5 mM Tris-HCl at pH 6.8. Tris Buffered Saline with Tween-20 (TBST) was prepared by adding 0.1% Tween-20 in Tris Buffered Saline (TBS) (160g NaCl, 60g Tris Base, pH 7.5 HCl dissolved in deionised water).

Following this, protein ladder (Precision Plus Protein™ All Blue Prestained Protein Standard, Bio-Rad, Hempstead, UK) and protein lysates were defrosted on ice. Once lysates had been defrosted, these were then added to the sample buffer (1:4 Sample buffer: Protein lysate sample). These were then boiled for five minutes at 97^0C. 40 µg of protein lysate and 5 µl of the protein ladder were then loaded onto a 4–15% Criterion™ TGX™ Precast Midi Protein Gel (Bio-Rad). This was run for 1 hour on ice at 180V in running buffer. Once the run had been completed, a transfer cassette was then assembled using Trans-Blot Turbo Midi 0.2 µm PVDF Transfer Pack (Bio-Rad). From bottom to top this transfer cassette consisted of one stack of filter paper, a 0.2 µm PVDF membrane, one gel and one additional transfer stack of filter paper. Semi dry transfer of the protein from the gel to the membrane was then performed using a turbo-blot transfer machine (Bio-Rad) at 2.5 A, 25 V for 7 minutes.

Once the transfer had been completed, the membrane was placed in blocking solution for 1 hour at RT on a shaker. This blocking solution was either 5% BSA (Sigma) or 1-5% dry milk powder dissolved in TBST depending on the antibody (see Table 2.1). Following this, the membranes were incubated with primary antibody overnight at 4°C. For a full list of antibodies used during western blotting, please see Table 2.1. After the primary antibody incubation, the membranes were washed in 1X TBST for 5 minutes three times. The membrane was then incubated with secondary antibodies for 1 hour at RT. The membranes were then washed a further three times in 1X TBST (5 minutes per wash). Imaging of membranes was performed using the ChemiDoc MP imaging system (Bio-Rad) and Image Lab 6.0 software (Bio-Rad). Following this, western blot images were quantified in Image Lab 6.0 software.

Table 2.1- Table of blocking solutions and antibodies used during western blotting.

Antibody	Concentration in blocking solution	Blocking Solution	Antibody Incubation Time	Company	Product Number
p-AKT	1: 1000 for tissues, 1:500 for hMSCs	5% BSA	Overnight at 4°C	Cell Signalling, Danvers, MA, USA.	#4060
Total AKT	1: 1000	5% BSA	Overnight at 4°C	Cell Signalling	#9272
p-P70S6K	1: 500	5% BSA	Overnight at 4°C	Cell Signalling	#9205
Total P70S6K	1: 1000	5% BSA	Overnight at 4°C	Cell Signalling	#9202
p-S6	1: 2000	5% BSA	Overnight at 4°C	Cell Signalling	#5364
Total S6	1: 2000	5% BSA	Overnight at 4°C	Cell Signalling	#2217
p-mTOR	1: 500	5% BSA	Overnight at 4°C	Cell Signalling	#2976
Total mTOR	1: 250	5% BSA	Overnight at 4°C	Cell Signalling	#2983
GAPDH	1: 2500	5% Dry Milk Powder	1 hour at RT	Cell Signalling	#12004168
Goat Anti-Rabbit	1: 2500	5% Dry Milk Powder	1 hour at RT	Cell Signalling	#12004161

2.8 Assessment of mouse healthspan-

2.8.1 Timing of assays and experimental design-

For all healthspan assays, baseline health measurements were made at 10 months prior to the start of the intervention. Drug intervention with ZOL or PBS began at 12 months of age. The next set of healthspan measurements to test the efficacy of the treatments were taken at 18 months for all assays. The final measurements were taken at 22 months for most assays (for frailty the final measurement occurred at 23 months). Some assays had measurements taken between 18 and 22 months (see Figure 4.1 for further details on this). These assays were performed in 18–23-month-old mice to see what the effects of the drug were in older mice. Some of the assays required a greater gap between them than others to minimise stress to the animals, for example the glucose tolerance test. The timings of these assays are based off a standardised toolbox for assessing the healthy ageing of mice (Bellantuono *et al.* 2020).

Cages of mice were randomly assigned PBS or ZOL treatment using a random number generator. A limitation to this approach is that the mice were assigned to the cages upon arrival by the animal house staff prior to this, so there was no way of telling if the assignment of individual mice to their cages was random. There were 19 mice per treatment group at the start of the experiment, this was slightly lower than the recommended amount in the toolbox for assessing healthy ageing in mice paper (n=20 per group) (Bellantuono *et al.* 2020). This was due to the animal vendors having an insufficient supply of aged mice in the months leading up to the start of the experiment. The aim was to try and get as close to the recommended 20 mice per group as possible given the limited aged mouse availability. In the toolbox paper, power calculations were used using data from multiple healthspan studies/ interventions to work out how many mice would be required. This involved the use of power calculations with a power of 80% and an alpha of 0.05. The aim of these calculations was to work out how many mice were needed to detect significant changes across multiple different healthspan assays.

2.8.2 Open field-

Individual mice were then placed in the novel object arena and their movements tracked with a Ethovision software (Noldus, Wageningen, Netherlands) and tracking camera (Basler, Ahrensburg, Germany). The mice were trained in the empty arena to habituate them to the arena and measure levels of stress prior to the novel object recognition test. The software measured the amount of time the mice spent in each part of the arena and how far they moved as measurements of stress. An average score for each of these open field parameters was then calculated for each treatment group for each time point for further analysis.

2.8.3 Novel Object Recognition-

The mice were individually placed in the novel object arena that contained two identical objects. They were left in the arena for 10 minutes each and Ethovision software measured their movement within the arena. Then 60 minutes after the baseline measurement was performed, the mouse was placed back in the arena and one novel object was introduced. The ethovision software recorded this mouse for a further 10 minutes with the novel object. This was used to measure short-term memory (STM) during the novel object recognition. As part of the long-term memory (LTM) test, the mice were re-introduced into the novel object arena the next day. They underwent a new session in the arena with another novel object (a different object to the short-term memory novel object) and one familiar object from the previous day.

The ethovision XT software was then used to calculate how long the mouse spent exploring the novel object compared to the old object. A discrimination index was calculated which determines how long the mouse spends exploring the novel object vs the original object. A score of 0 means no preference for either object, a score of >0.2 indicates that the animal prefers to explore the novel object. The discrimination index (DI) was calculated as follows:

Discrimination Index = (Exploration time novel object – Exploration time training object)/ (Exploration time novel object + Exploration time training object)

2.8.4 Grid Hanging-

Mice were weighed at the start of this procedure. Mice were placed in the grid hanging apparatus and this was inverted so the mice were hanging upside down. The mice were then timed to measure how long it took for them to let go of the apparatus once inverted. If a mouse took longer than seven minutes, the measurement stopped and was recorded as seven minutes. This was repeated three times for each mouse on each time point (1 hour gap minimum between repeats). This was then used to calculate an average time to fall and an average time to fall for each treatment group for each time point.

2.8.5 Rotarod-

Mice were weighed at the start of the procedure. Mice were placed on the rotarod apparatus (Ugo Basile, Gemonio, Italy). The speed started at 4 rpm and was accelerated to 40 rpm. The time taken for the mouse to fall off the rotarod apparatus was measured and recorded. If the mouse took longer than 5 minutes, the mouse was taken off and labelled as 5 minutes. This was repeated three times and the average time taken to fall off was recorded. This was then used to calculate an average time to fall for each treatment group for each time point.

2.8.6 Frailty Index -

Mice were weighed at the start of the procedure. Mice were assessed for a variety of frailty phenotypes. There were 29 criteria in total (see Table 2.2 for full list). Mice can either score a 0, a 0.5 or a 1 for each criterion of the frailty index. A score of 0 for indicates the absence of that frailty phenotype. A score of 0.5 indicates that individual frailty criteria has been partially reached. A score of 1 indicates that the individual frailty criteria has been fully reached. These measurements were used to create an overall frailty score. An overall score was calculated by taking the sum of the frailty scores for all the different frailty criteria and dividing by the number of criteria in the frailty index (n=29). The higher the overall frailty score, the frailer the mouse.

Table 2.2 – List of criteria of the frailty index. Adapted from Whitehead *et al.* 2014.

Category	Name of Assay	Description	Severity guide
Integument	Alopecia	Loss of fur.	0= no hair loss 0.5= <25% hair loss 1= >25% hair loss
	Loss of fur colour	Loss of black fur colour. Becomes grey or brown with age.	0= Fully black fur colour 0.5= Small patches of brown or grey 1= Widespread grey/ brown fur across body
	Dermatitis	Prescence of skin lesions.	0= No dermatitis 0.5= Singular focal dermatitis lesion 1= Multiple or widespread lesions
	Loss of Whiskers	Reduced number of whiskers with age.	0= Full whiskers 0.5= Partial loss of whiskers 1= Full loss of whiskers
	Coat Condition	Coat loses its sleek, shiny appearance and becomes more ruffled.	0= Sleek, shiny coat 0.5= Slightly ruffled coat 1= Matted coat/ lack of grooming
Physical / Musculoskeletal	Tumours	Increased incidence of tumours in older mice.	0= No visible tumours 0.5= One visible tumour <1 cm in size 1= One tumour >1 cm or multiple small tumours
	Distended abdomen	Excess fluid beneath rib cage indicates that abdomen is distended.	0= No distended abdomen 0.5= Slight bulge below ribcage 1= Clear bulge below ribcage
	Kyphosis	Curvature of the spine with age.	0= No kyphosis 0.5= Slight curvature of the spine 1= Clear curvature of the spine
	Tail Stiffening	Tail loses flexibility with age.	0= No tail stiffening 0.5= Tail responsive, but does not curl 1= Tail totally unresponsive
	Gait Disorders	Any hobbling or unusual movement.	0= No gait disorders 0.5= Abnormal gait 1= Abnormal gait and impaired movement

	Tremor	Increased likelihood of tremor and loss of climbing ability.	0= No tremor 0.5= Slight tremor 1= Major tremor, loss of climbing ability
	Body Condition	Bone may become indetectable due to fat or too prominent with age.	0= Bone not prominent, but can still be felt 0.5= Bone slightly prominent or difficult to feel 1= Bone not felt or bones clearly prominent
Auditory	Vestibular Disturbance	When mouse is slowly lowered towards surface it may spin or twist.	0= No disturbance 0.5= Slight twist or spinning when lowered 1= Severe twisting and spinning when lowered
	Hearing Loss	Loss of hearing with age.	0= No hearing loss 0.5= Partial response to auditory stimuli 1= No response to auditory stimuli
Ocular + Nasal	Cataracts	Increased likelihood of cataracts with age (opaque patch in eye).	0= No cataracts 0.5= Small white spot 1= Fully opaque lens
	Corneal Opacity	Increased likelihood of corneal opacity with age.	0= No corneal opacity 0.5= Small amounts of white spots and clouding in cornea 1= Widespread white spots and clouding in cornea
	Eye discharge	Increased chance of discharge or swelling of eyes with age.	0= No ocular swelling or secretion 0.5= Slight swelling or secretion 1= Noticeable swelling or secretion
	Micro-phthalmia	Sunken/ shrunken eyes with age.	0= Eyes are normal size 0.5= One or both eyes slightly smaller and/ or sunken 1= One or both eyes very smaller and/ or sunken
	Vision Loss	Lower mouse gently to surface, test if it reaches out to surface with forelimbs.	0= Reaches >8 cm from table surface 0.5= Partial vison loss, reaches 2-8 cm from table surface 1= Reaches <2 cm away from table surface
	Menace Reflex	Whether a mouse responds to an object being	0= Full menace reflex 0.5= Responds some of the time to object 1= No menace reflex

		moved slowly towards its eye.	
	Nasal Discharge	Increased discharge from the nose with age.	0= No nasal discharge 0.5= Small amount of nasal discharge 1= Obvious discharge, both nostrils
Digestive	Malocclusions	Examine for overgrown or uneven looking teeth.	0= Normal looking teeth 0.5= Teeth uneven 1= Teeth overgrown and uneven
	Rectal Prolapse	Check to see if rectum is visible beneath tail.	0= No rectal prolapse 0.5= Small rectal prolapse visible 1= Clearly visible rectal prolapse
	Vaginal Prolapse	Check to see if tissue is visible.	0= No vaginal prolapse 0.5= Small vaginal prolapse visible 1= Clearly visible vaginal prolapse
	Diarrhoea	Examine mice and cage for signs of diarrhoea.	0= No diarrhoea visible 0.5= Faeces or bedding near rectum 1= Faeces, blood and bedding near rectum. Faecal smearing in cage
Respiratory	Breathing Rate	Check mice for any change in breathing rate and depth.	0= Breathing rate normal 0.5= Small change in breathing rate and depth 1= Obvious change in breathing rate, gasping
Discomfort	Grimace Scale	Examine face for signs of discomfort e.g., cheek bulge.	0= No signs of grimacing 0.5= 1-2 signs of grimacing 1= >3 signs of grimacing
	Piloerection	If hairs are sticking up and if so, in which parts of the body.	0= No piloerection 0.5= Piloerection at base of neck 1= Widespread piloerection
	Weight	Compare weights to reference values from age and sex matched adults.	0= Weight does not differ from reference value (RV) 0.25= >1 Standard deviation from RV 0.5= > 2 Standard deviation from RV 0.75= > 3 Standard deviation from RV 1= > 4 Standard deviation from RV

2.8.7 Glucose tolerance test -

Food was removed overnight for 16 hours prior to the start of the assay. A glucose solution was prepared comprising of 30% Glucose (Sigma), 0.9% NaCl (Sigma) in distilled water. This solution was passed through a sterile filter (0.2 µm) prior to administration. Mice were weighed at the start of the assay. EMLA cream (Aspen, Umhlanga, South Africa) was applied to the tail of each mouse to minimise discomfort prior to blood sampling. A small nick using a scalpel was made on the mouse's tail and a blood glucose reading was made using a AlphaTrak 2 Glucometer (Zoetis). This was done to create a baseline measurement prior to glucose injection.

Mice were then injected with Glucose Solution (1 g/kg glucose). After the glucose had been injected, further blood glucose readings were made at different intervals post injection. These were made at 15, 30-, 45-, 60- and 120-minutes post injection. This was used to produce graphs of blood glucose over time for each mouse. This was then averaged for each treatment group for each time point. The area under the curve (AUC) was then calculated for each mouse's blood glucose response over time. This was then used to calculate an average AUC for each treatment group for each time point to determine glucose tolerance.

2.8.8 Insulin tolerance test -

Food was removed for 3 hours prior to the start of the assay. An insulin solution was prepared comprising of Humuluin-R (Lilly, Indianapolis, Indiana, USA) and 0.9% NaCl in distilled water. This solution was passed through a sterile filter (0.2 µm) prior to administration. Mice were weighed at the start of the assay. EMLA cream (Aspen, Umhlanga, South Africa) was applied to the tail of each mouse to minimise discomfort prior to blood sampling. A small nick using a scalpel was made on the mouse's tail and a blood glucose reading was made using a AlphaTrak 2 Glucometer (Zoetis). This was done to create a baseline measurement prior to glucose injection.

Mice were then injected with Insulin Solution (0.75 U/kg insulin). After the insulin had been injected, further blood glucose readings were made at different intervals post injection. These were made at 15, 30-, 45-, 60- and 120-minutes post injection. This was used to produce graphs of blood glucose over time for each mouse and treatment group. The area under the curve (AUC) was then calculated for each mouse's blood glucose response over time. This was then used to calculate an

average AUC for each treatment group for each time point to determine insulin sensitivity.

2.9 Statistical Analysis-

Data was input into GraphPad Prism 9.0 software. Data on graphs is displayed as the mean +/- the standard deviation. In the case of the frailty and grid hang data, data was analysed through a mixed effects model using R Studio Software (PBC, Boston, Massachusetts USA). This was only possible for assays containing more than 3 time points at ages greater than 10 months. Otherwise, statistical significance was determined by an unpaired T-test if there were two conditions or one-way ANOVA with Bonferroni's post-hoc test if there were more than two conditions analysed. Differences between two proportions of a population was calculated with a two-proportion Z test. A statistical significance level of $p < 0.05$ was considered significant.

Chapter 3 - Investigating the activity of Zoledronate in mouse tissues.

3.1 Introduction-

ZOL has been shown previously in the literature to reduce several markers of mTOR signalling *in vitro* in hMSCs after three days of treatment. These markers included p-mTOR, p-AKT and p-P70S6K (Misra *et al.* 2016). This study also showed how inhibition of this pathway by ZOL was reversed with the addition of FOH and GGOH. This implicated blockage of the mevalonate pathway by ZOL in its ability to inhibit mTOR signalling. In addition, treatment of MSCs with the PI3K inhibitor LY294002 resulted in inhibition of p-AKT, translocation of FOXO3A into the nucleus and reduction in DNA damage in a similar fashion to ZOL. In comparison, rapamycin treatment did not achieve any of these during this study. This suggests that ZOL's ability to act as a geroprotector is facilitated through inhibition of mTORC2 signalling. Therefore, measuring inhibition of the mTORC2 marker p-AKT is an important way of measuring ZOL's activity. ZOL was also found to inhibit p-AKT in *Drosophila* in a later study (Chen *et al.* 2021). Similarly, this inhibition of mTOR was reversed with FOH and GGOH, again implicating the mevalonate pathway in the inhibition of mTOR by ZOL. Inhibition of mTOR markers by ZOL has also been observed in a couple of cancer cells *in vitro* such as in breast cancer and osteosarcoma cells (Li and Li 2019; Lan *et al.* 2013). Whether ZOL is also found to reduce any of these markers *in vivo* in mice is currently unknown and should be established prior to conducting further work assessing the healthy ageing of mice.

In order to address the question as to whether zoledronate improves the healthy ageing of mice, one must first determine if ZOL is active in mice and in which mouse tissues it is active in. In addition to this it is important to determine how regularly ZOL is needed to be administered in order to inhibit mTOR signalling. P-AKT was selected as a marker for detecting zoledronate's activity in mice in this study. This is due to the robustness of detecting inhibition of p-AKT as a marker of mTOR inhibition by ZOL in hMSCs and in *Drosophila* (Misra *et al.* 2016; Chen *et al.* 2021). In addition, a recent study has shown that an AKT specific inhibitor can promote the lifespan of *Drosophila* (Cheng *et al.* 2022). This further highlights the importance of AKT signalling in ageing. In order to determine the dosage interval of ZOL treatment, mice were injected with ZOL or PBS. Tissues were then collected at different time

points per group post injection and levels of p-AKT/ total AKT was then assessed via western blot.

A dose of 125 µg/ kg ZOL was used because this dose has previously been sufficient to reduce DNA damage in response to irradiation in the bone of C57BL/6J mice (Misra *et al.* 2016). This dose was used during the remainder of these ZOL time course experiments. An IP injection of zoledronate was used to administer the drug. This is also because previous work on prevention of DNA damage following irradiation in the bone of mice in response to ZOL treatment used an IP injection to administer the drug (Misra *et al.* 2016). In addition to this, a study on macrophages compared the effects of IP vs SC and IV injection on protein prenylation on macrophages in mice. They found IP injection to be the most effective injection method for reducing protein prenylation by ZOL in macrophages (Ali *et al.* 2015).

3.2 Effect of zoledronate on p-AKT in tissues of non-fasted mice-

In order to test what impact zoledronate had on mTOR signalling in mouse tissues, 10-week-old C57BL/6J mice were injected with 125 µg/ kg zoledronate or with an equivalent amount of PBS. Mouse tissues were collected at Day 1, 3, 7 or 24 post injection (see Figure 3.1). Tissues were flash frozen and then had their protein content extracted. These protein lysates were then subjected to western blot analysis of p-AKT and the housekeeper protein GAPDH. Treatment of mice with ZOL resulted in a significant reduction in p-AKT in the spleen at day 7 and muscle at day 1 in *ad libitum* fed mice. However, there was no change in the other tissues (the brain or the heart) examined during this experiment (Figures 3.2-3.5). There was notable variation between mice in the same treatment group across multiple tissues and treatment intervals.

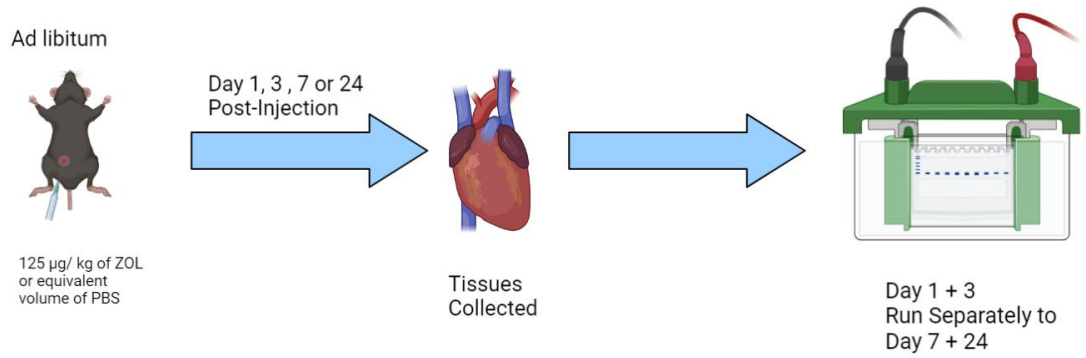

Figure 3.1 – Diagrammatic representation of ZOL time course experiment without fasting. Created with bio-render.com.

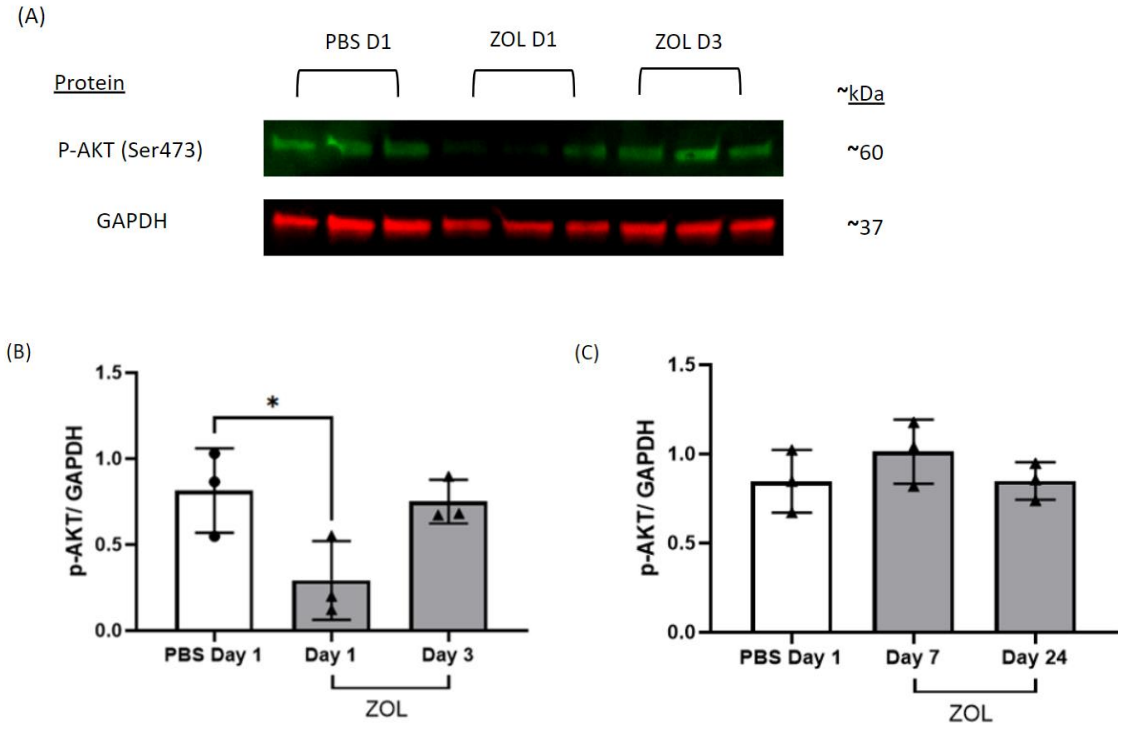

Figure 3.2- Zoledronate reduces p-AKT expression at day 1 in skeletal muscle of non-fasted mice.

A) Example Western blot of p-AKT and GAPDH expression of non-fasted mice in response to ZOL (muscle). B) Quantification of p-AKT/GAPDH in the muscle at Day 1 and Day 3. C) Quantification of p-AKT/GAPDH in the muscle at Day 7 and Day 24. Data is shown as the mean +/- the standard deviation. Data were analysed through one way ANOVA and Tukey's multiple comparison post-hoc test. PBS = Control Mice, ZOL = Zoledronate treated mice (n=3 per treatment group).

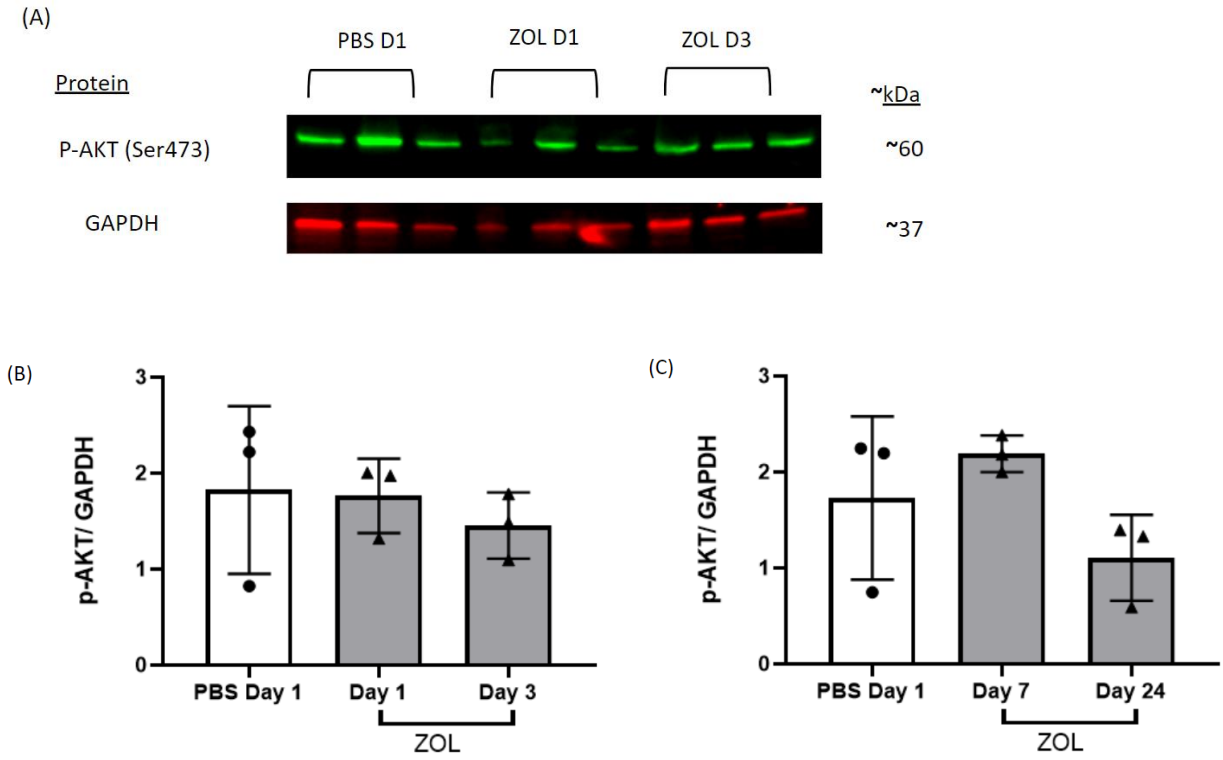

Figure 3.3- Zoledronate does not change p-AKT expression in the heart of non-fasted mice.

A) Example Western blot of p-AKT and GAPDH expression in the heart of non-fasted mice. B) Quantification of p-AKT/GAPDH in the heart at Day 1 and Day 3. C) Quantification of p-AKT/GAPDH in the heart at Day 7 and Day 24. Data is shown as the mean +/- the standard deviation. Data were analysed through one way ANOVA and Tukey's multiple comparison post-hoc test. PBS = Control Mice, ZOL = Zoledronate treated mice (n=3 per treatment group).

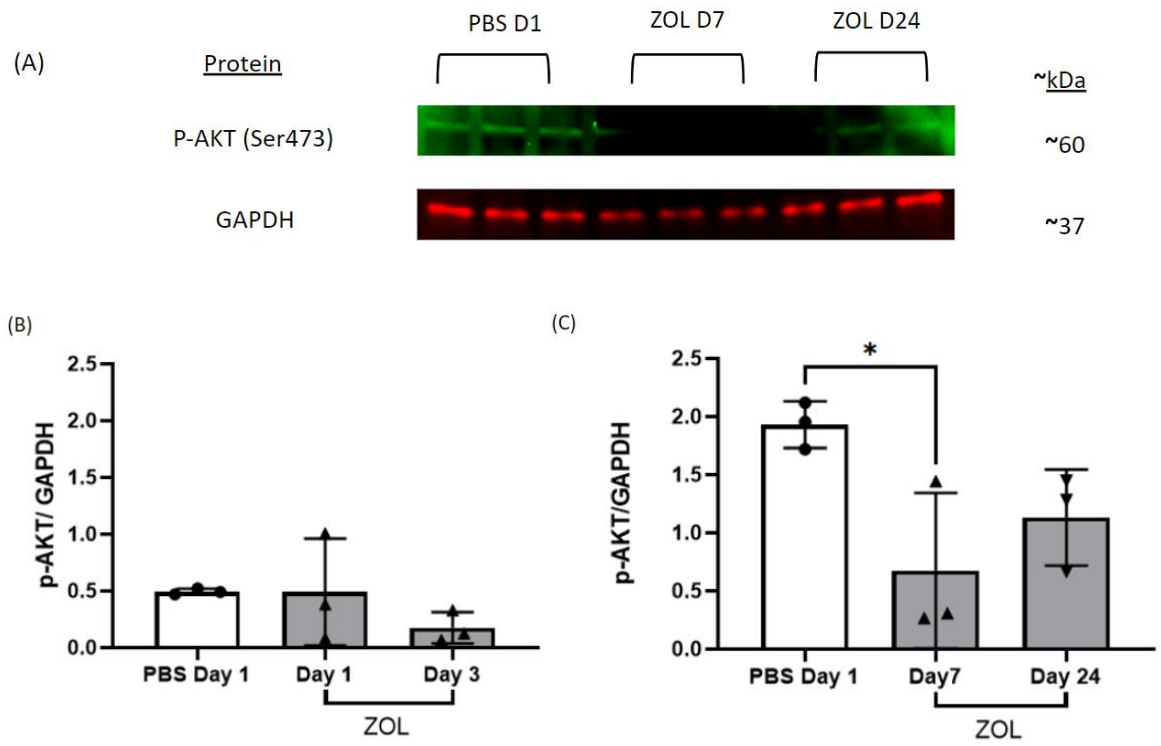

Figure 3.4- Zoledronate reduces p-AKT expression at day 7 in response to ZOL in the spleen of non-fasted mice.

A) Example Western blot of p-AKT and GAPDH expression in the spleen of non-fasted mice. B) Quantification of p-AKT/GAPDH expression in the spleen at Day 1 and Day 3. C) Quantification of p-AKT/GAPDH in the spleen at Day 7 and Day 24. Data is shown as the mean +/- the standard deviation. Data were analysed through one way ANOVA and Tukey's multiple comparison post-hoc test. PBS = Control Mice, ZOL = Zoledronate treated mice (n=3 per treatment group).

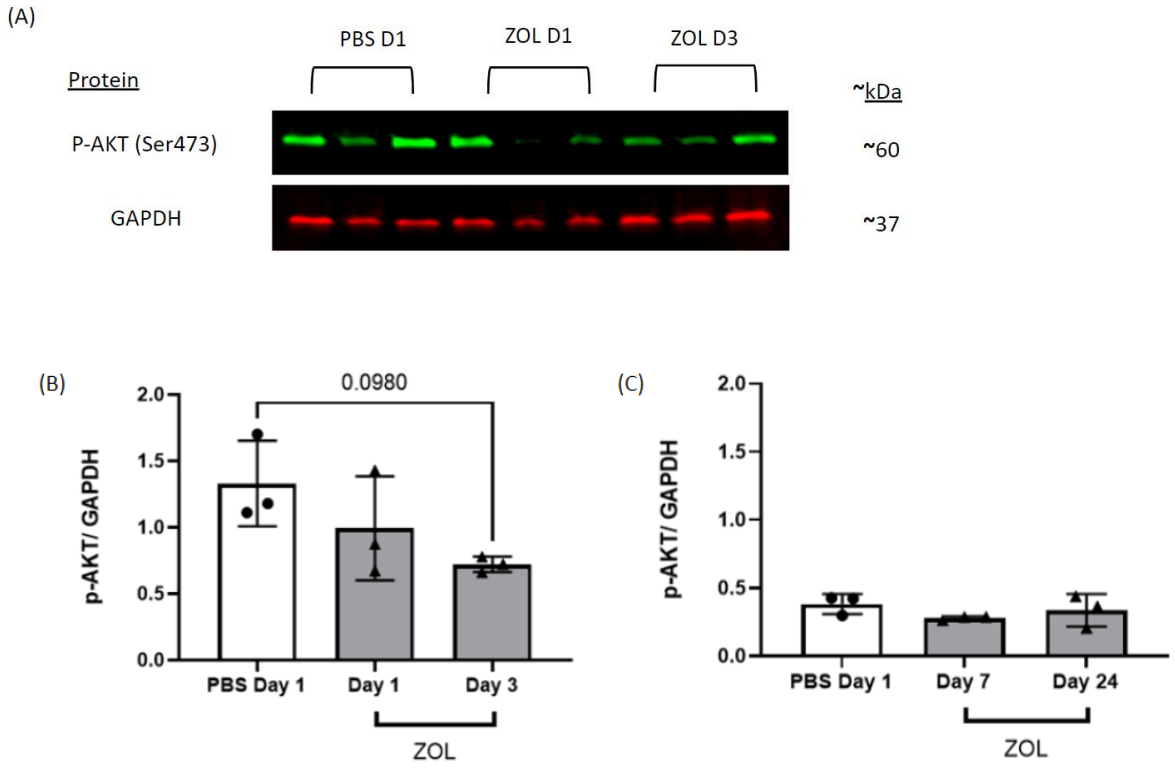

Figure 3.5- Zoledronate does not change in p-AKT expression in the brain of non-fasted mice at the time points examined.

A) Example Western blot of p-AKT and GAPDH expression in the brain of non-fasted mice. B) Quantification of p-AKT/GAPDH in the brain at Day 1 and Day 3. C) Quantification of p-AKT/GAPDH in the brain at Day 7 and Day 24. Data is shown as the mean +/- the standard deviation. Data were analysed through one way ANOVA and Tukey's multiple comparison post-hoc test. PBS = Control Mice, ZOL = Zoledronate treated mice (n=3 per treatment group).

3.3 Effect of overnight fasting on AKT signalling in the muscle-

Due to the difficulty in detecting changes in p-AKT in the prior experiment, it was decided that further optimisation of the experimental design was required. Due to the nutrient sensitivity of p-AKT signalling (Sharma *et al.* 2012), it is possible that the a*d libitum* feeding regimen could create inconsistent feeding times prior to tissue collection that could be contributing to the variation in responses to ZOL. Other work in the literature has indicated that withdrawal of food for 16 hours followed by 45 minutes of refeeding prior to sacrifice is a more suitable method for measuring changes of mTOR markers in mice (Baar *et al.* 2016; Lamming *et al.* 2012). This approach allows for mice to feed at a consistent time prior to sacrifice. It was decided that this optimisation of mouse feeding times prior to tissue collection would be compared to *ad libitum* feeding prior to tissue collection. The aim of this experiment was to determine if this standardised feeding approach would lead to reduced variability in p-AKT and allow for more easily detectable changes in p-AKT in response to ZOL.

During this experiment, 10-week-old mice were treated with 125 µg/ kg zoledronate or with an equivalent amount of PBS. Mice from both treatment groups were then split into two further groups: *ad libitum* fed and fasted-refed mice from the optimised feeding regiment. Fasted-refed mice had food withdrawn overnight for 16 hours prior to tissue collection, they were then refed for 45 minutes prior to tissue collection. Skeletal muscle tissue was collected at Day 1 or Day 3 post injection. For overview of experiment, see Figure 3.6. There were no significant changes in p-AKT at Day 1 for either fasted or non-fasted mice (Figure 3.7), contradicting the findings of the previous experiment (Figure 3.2). This experiment revealed a significant reduction in p-AKT at day 3 in response to zoledronate compared to PBS in the fasted mice, which was not observable in the non-fasted mice (Figure 3.7). This reduction was not observed during the previous experiment in which mice were fed *ad libitum* (Figure 3.2). This experiment also revealed a tendency for mice with standardised feeding to have higher overall levels of p-AKT in the control mice compared to the *ad libitum* fed mice. Having a higher level of p-AKT to begin with should make changes easier to detect. This fasting-refeeding optimisation approach would be used in future experiments due to the higher levels of p-AKT seen in fasted-refed mice and the

work in the literature that showed its robustness for measuring changes in mTOR markers (Baar *et al.* 2016; Lamming *et al.* 2012).

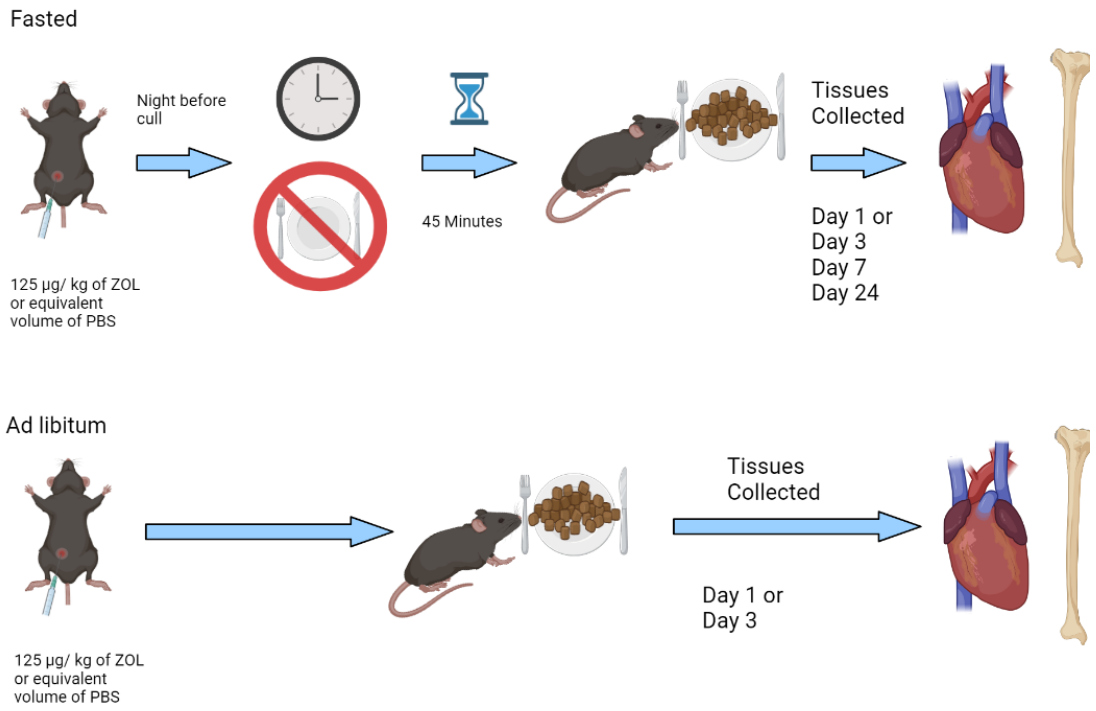

Figure 3.6 – Diagrammatic representation of the standardised feeding experiment. Created with Bio-Render.

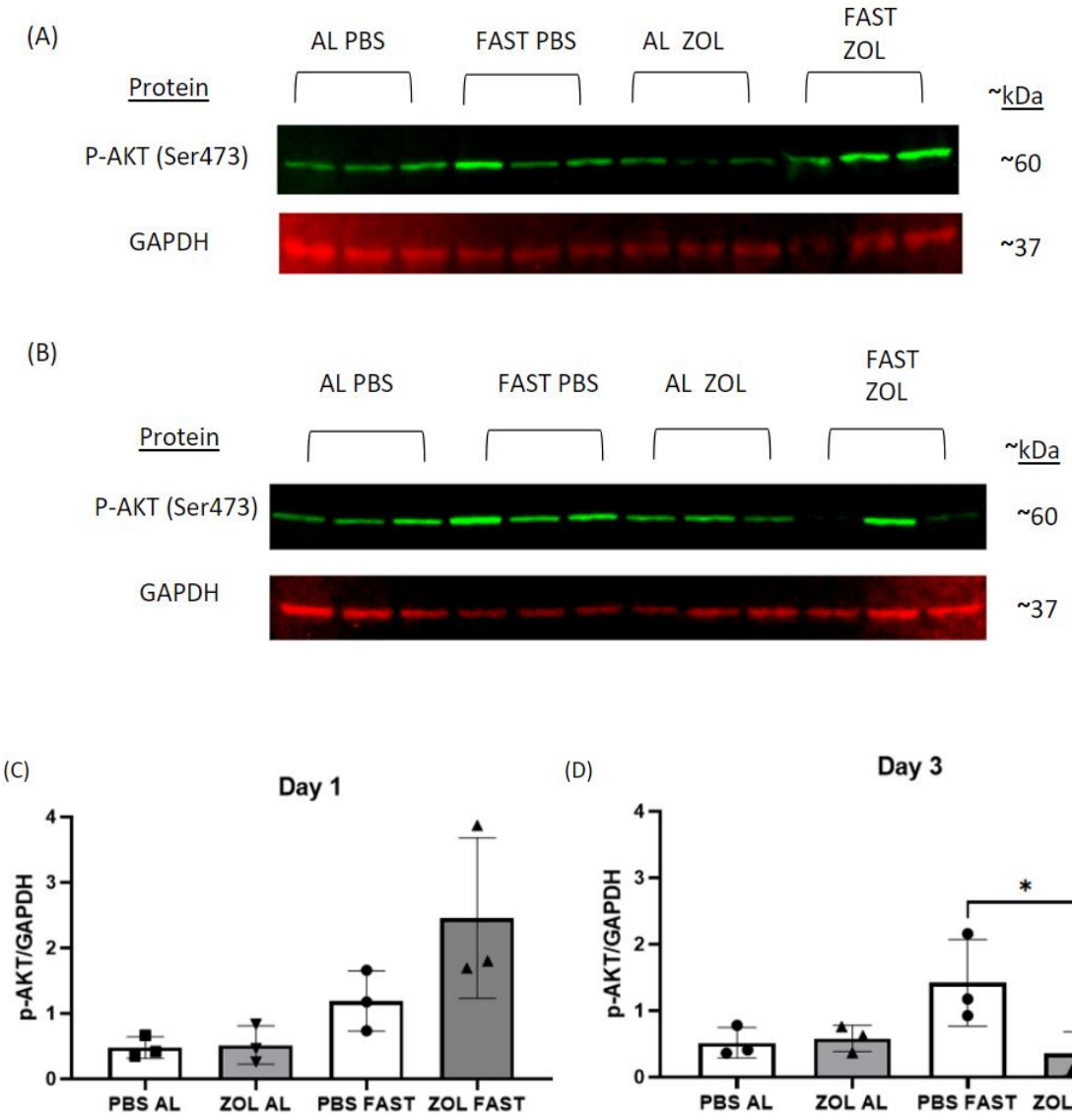

Figure 3.7- Fasting of mice allows for detection of previously undetected changes in p-AKT in skeletal muscle in response to ZOL.

A) Day 1 Western blot of p-AKT and GAPDH for both fasted and non-fasted mice. B) Day 3 Western blot of p-AKT and GAPDH for both fasted and non-fasted mice. C) Quantification of p-AKT/GAPDH for Day 1. D) Quantification of p-AKT/GAPDH for Day 3. Data is shown as the mean +/- the standard deviation. Data were analysed through one way ANOVA and Bonferroni's multiple comparison post-hoc test. PBS = Control Mice, ZOL = Zoledronate treated mice (n=6 per treatment group).

3.4 Zoledronate time course experiment when feeding is standardised-

It was decided to repeat the time course experiment from 3.2, but this time using the standardised feeding regimen from section 3.3 to detect changes in p-AKT. Blotting of total AKT was also performed to create a ratio of p-AKT/ total AKT to further reduce any variation caused by differing levels of total AKT between mice. This may have contributed to the inability to consistently detect changes in p-AKT in the skeletal muscle at Day 1 in *ad libitum* mice (Figures 3.2 and 3.7). In addition to this, a greater number of mice was used per group (6 mice per group) to increase the statistical power and to therefore improve the ability to detect changes in p-AKT.

During this time course experiment, 10-week-old mice were again treated with 125 µg/ kg zoledronate or with an equivalent amount of PBS. Mice were again fasted overnight for 16 hours on the day before sacrifice and then refed for 45 minutes prior to collection of tissues. Mice had their tissues collection at Day 1, 3, 7 or 24 post injection. See timeline figure for a visual representation of the experiment (Figure 3.8). A greater variety of tissues were examined in this experiment such as the brain, gut, heart, kidney, pancreas, spleen, skeletal muscle, tibia, flushed femur and bone marrow. Bone marrow was also flushed from mouse femurs to compare which compartment of the bone was exhibiting the greatest change in response to ZOL treatment. Upon analysis, it was confirmed there was a drop in the ratio of p-AKT/ Total AKT in the kidney, pancreas, skeletal muscle, spleen, and tibia at day 3 post-injection (Figures 3.9, 3.12, 3.16, 3.17 and 3.18). There was a significant drop in the ratio of p-AKT/ Total AKT in the heart at day 7 post injection (Figure 3.14). There was also a significant increase in the ratio of p-AKT/ Total AKT in the kidney post-injection at day 7 (Figure 3.16). There was a significant decrease in the ratio of p-AKT/ total AKT in the brain at Day 24 post injection (Figure 3.13).

In order to verify these findings, this experiment was repeated using the same number of mice, injection dose and feeding regimen (Figures 3.9-3.18). This time tissues were collected at day 3 and day 7 post injection. This was done as these time points had the greatest numbers of significant results during the previous experiment. Upon repeating this experiment, there was a significant drop in p-AKT/ Total AKT in the kidney, spleen, skeletal muscle, tibia as was observed during the

previous experiment (Figures 3.9, 3.12, 3.16 and 3.18). There was no significant reduction in p-AKT/ total AKT in the pancreas during the second experiment, unlike during the first experiment (Figure 3.17). On a similar note, there was a significant drop in p-AKT/ Total AKT in the heart after 7 days (Figure 3.14). As previously, this there was a significant increase in the ratio of p-AKT/ total AKT in the second experiment in the kidney (Figure 3.16). This experiment was mostly able to reproduce the findings of the first experiment. Overall, the greatest number of tissues showed a decrease in p-AKT was at Day 3 post injection.

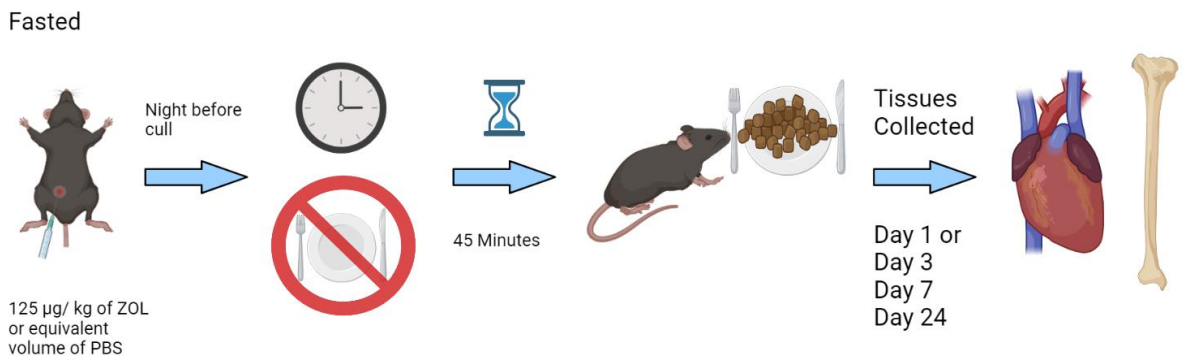

Figure 3.8 – Diagrammatic representation of fasting-refeeding ZOL time course experiments. Created with bio-render.com.

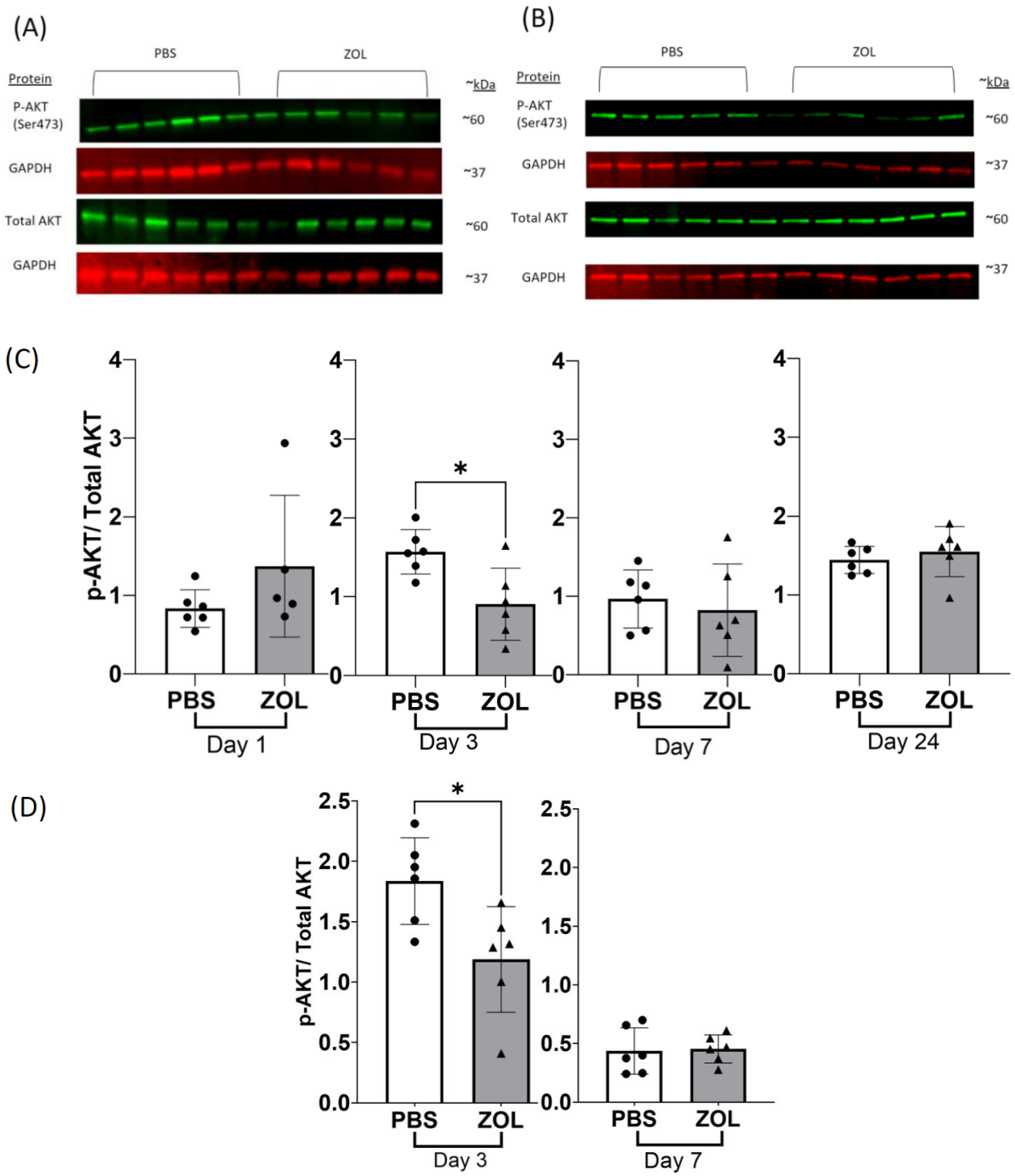

Figure 3.9- Zoledronate reduces p-AKT expression at Day 3 post injection in the tibia.

Western blotting assessing the expression of p-AKT/ Total AKT in the tibia at Day 1, Day 3, Day 7 and Day 24 post injection. A) Example Western Blot of tibia tissue for GAPDH, p-AKT and Total AKT expression in experiment 1. B) Example Western Blot of tibia for GAPDH, p-AKT and Total AKT expression in experiment 2. C) Fasting time course tissue experiment 1 quantifications (Day 1, Day 3, Day 7 and Day 24 Post injection). D) Fasting time course experiment 2 (Day 3 and Day 7). Data is shown as the mean +/- the standard deviation. Data were analysed through an unpaired T-Test. PBS = Control Mice, ZOL = Zoledronate treated mice (n=6 per treatment group).

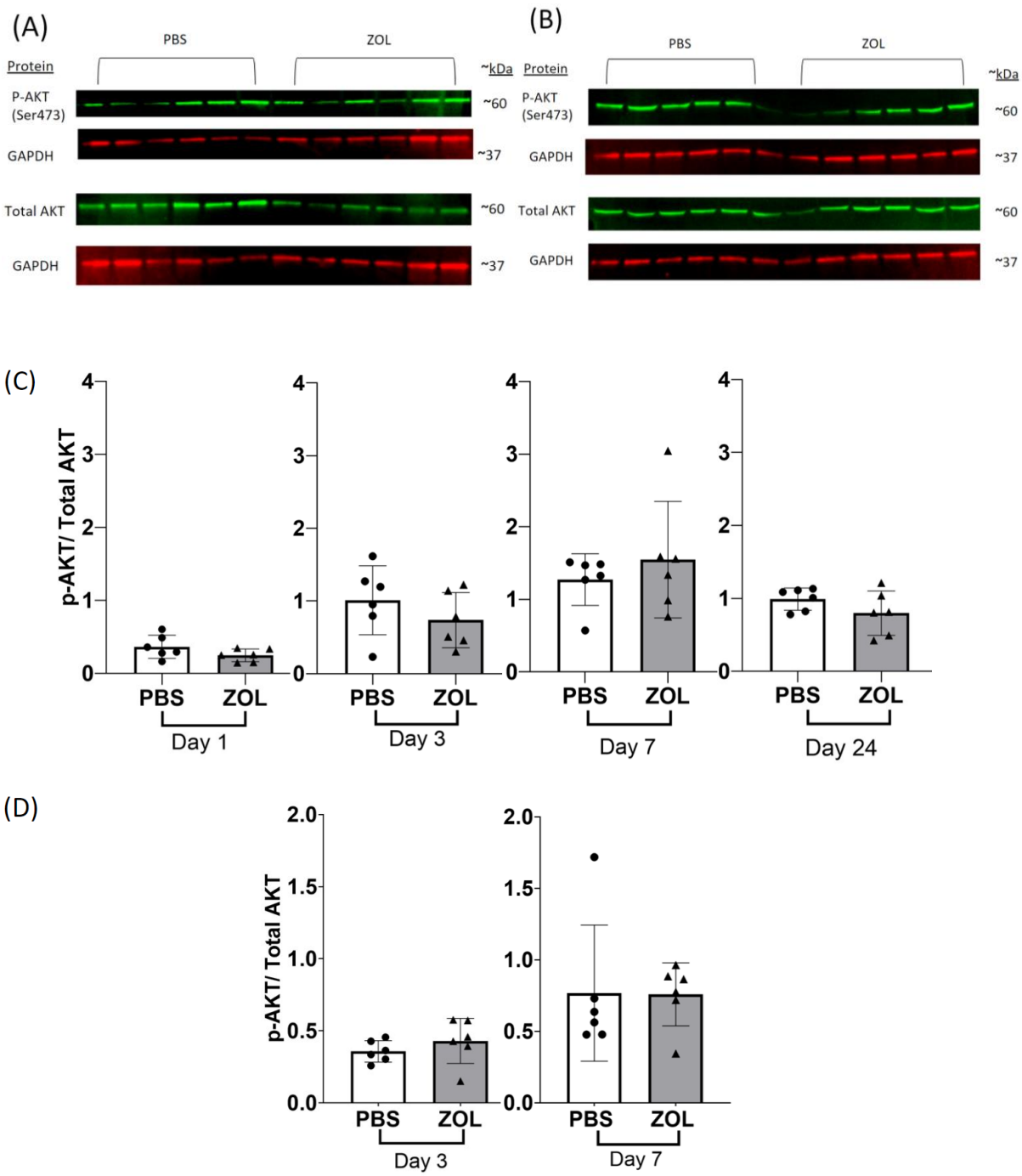

Figure 3.10- Zoledronate has no impact on p-AKT in bone marrow at the time points examined.

Western blotting assessing the expression of p-AKT/ Total AKT in the bone marrow at Day 1, Day 3, Day 7 and Day 24 post injection. A) Example Western Blot of bone marrow tissue for GAPDH, p-AKT and Total AKT expression in experiment 1. B) Example Western Blot of bone marrow tissue for GAPDH, p-AKT and Total AKT expression in experiment 2. C) Fasting time course experiment 1 quantifications (Day 1, Day 3, Day 7 and Day 24 Post injection). D) Fasting time course experiment 2 quantifications (Day 3 and Day 7). Data is shown as the mean +/- the standard deviation. Data were analysed through an unpaired T-Test. PBS = Control Mice, ZOL = Zoledronate treated mice (n=6 per treatment group).

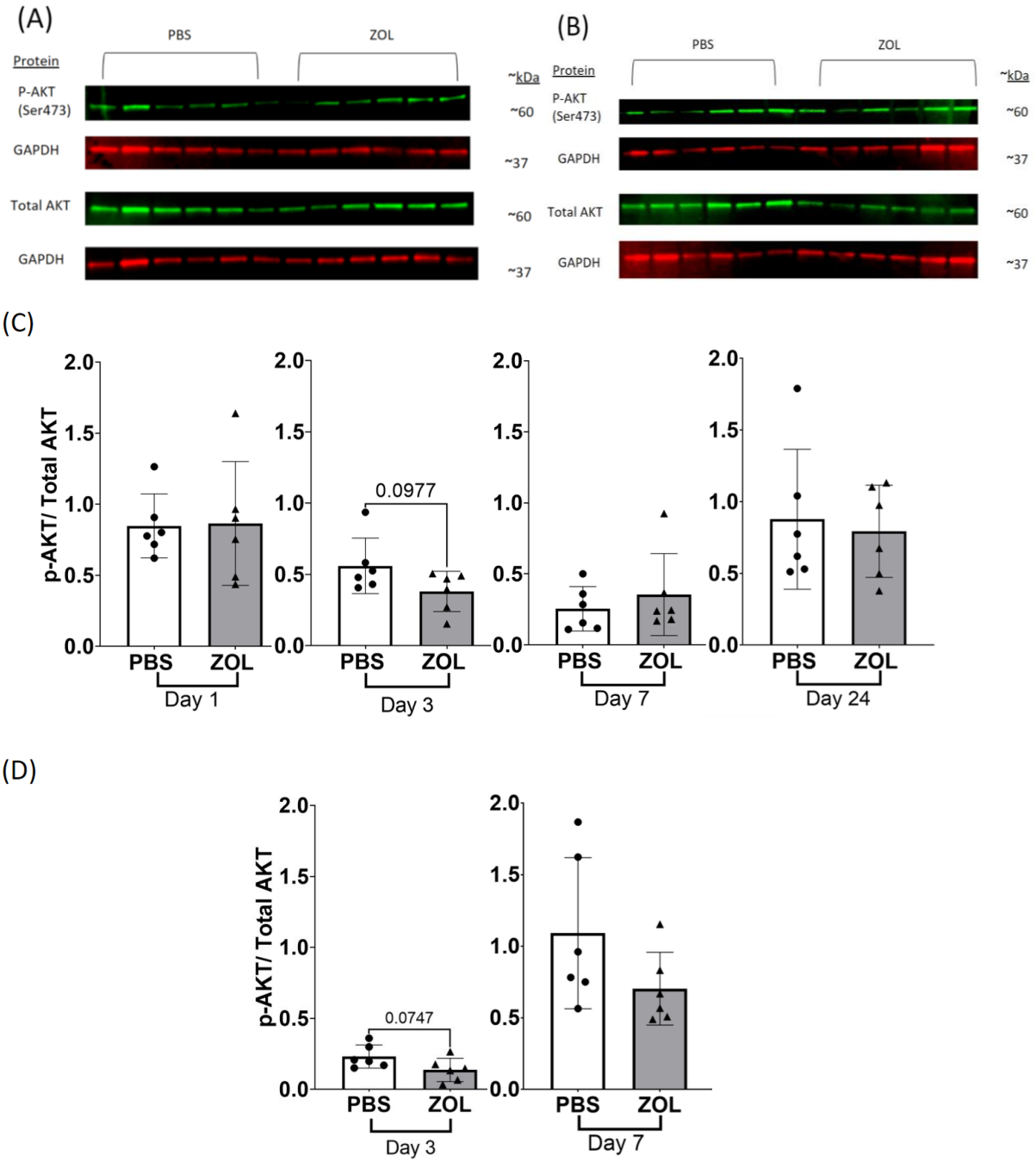

Figure 3.11- Zoledronate does not reduce p-AKT expression at Day 3 post injection in the flushed femur.

Western blotting assessing the expression of p-AKT/ Total AKT in the flushed femur Day 1, Day 3, Day 7 and Day 24 post injection. A) Example Western Blot of flushed femur tissue for GAPDH, p-AKT and Total AKT expression in experiment 1. B) Example Western Blot of flushed femur tissue for GAPDH, p-AKT and Total AKT expression in experiment 2. C) Fasting time course experiment 1 quantifications (Day 1, Day 3, Day 7 and Day 24 Post injection). D) Fasting time course experiment 2 quantifications (Day 3 and Day 7). Data is shown as the mean +/- the standard deviation. Data were analysed through an unpaired T-Test. PBS = Control Mice, ZOL = Zoledronate treated mice (n=6 per treatment group).

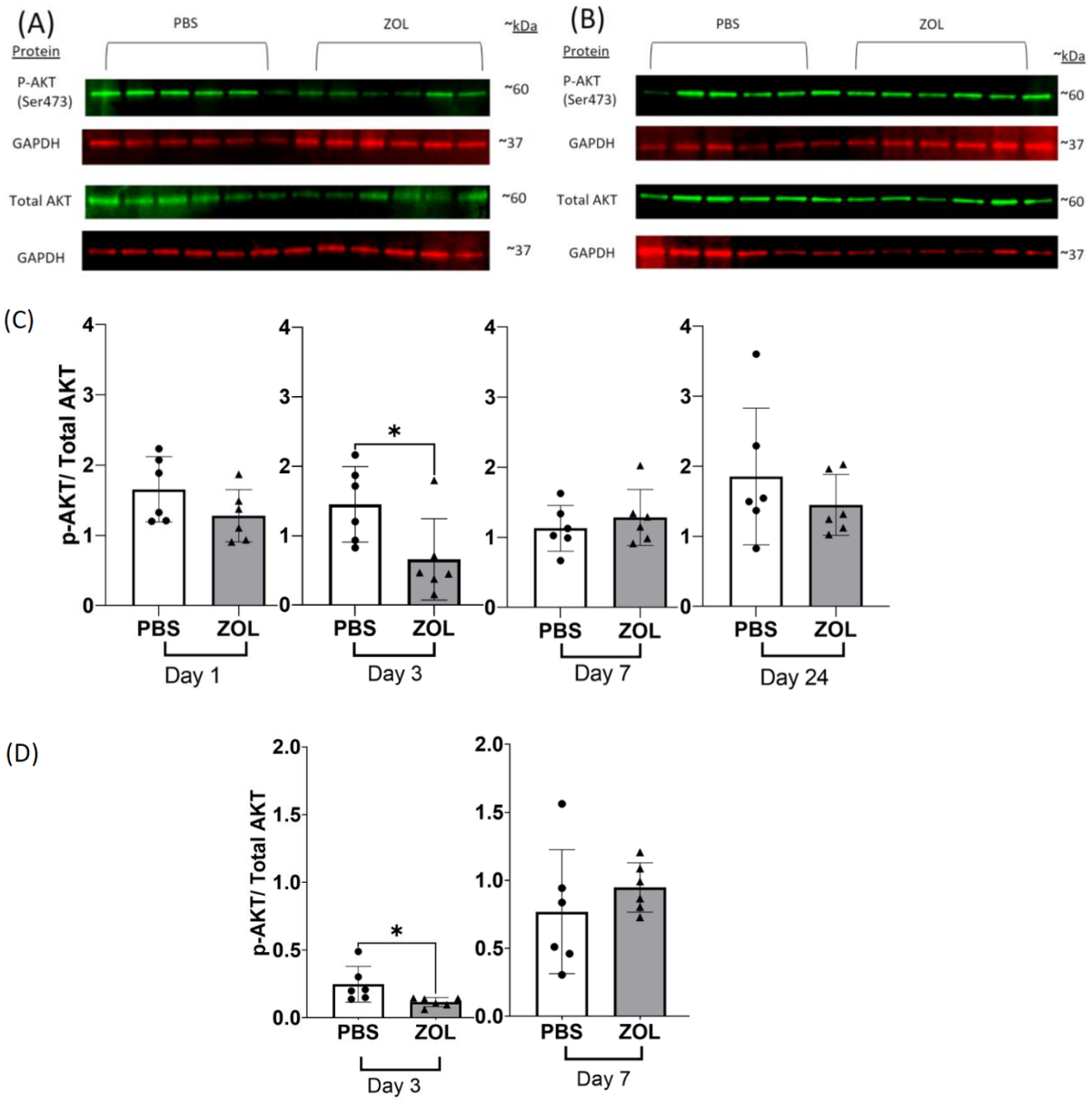

Figure 3.12- Zoledronate reduces the expression of p-AKT in skeletal muscle 3 days post injection.

Western blotting assessing the expression of p-AKT/ Total AKT in the muscle Day 1, Day 3, Day 7 and Day 24 post injection. A) Example Western Blot of muscle tissue for GAPDH, p-AKT and Total AKT expression in experiment 1. B) Example Western Blot of muscle tissue for GAPDH, p-AKT and Total AKT expression in experiment 2. C) Fasting time course experiment 1 quantifications (Day 1, Day 3, Day 7 and Day 24 Post injection). D) Fasting time course experiment 2 (Day 3 and Day 7). Data is shown as the mean +/- the standard deviation. Data were analysed through an unpaired T-Test. PBS = Control Mice, ZOL = Zoledronate treated mice (n=6 per treatment group).

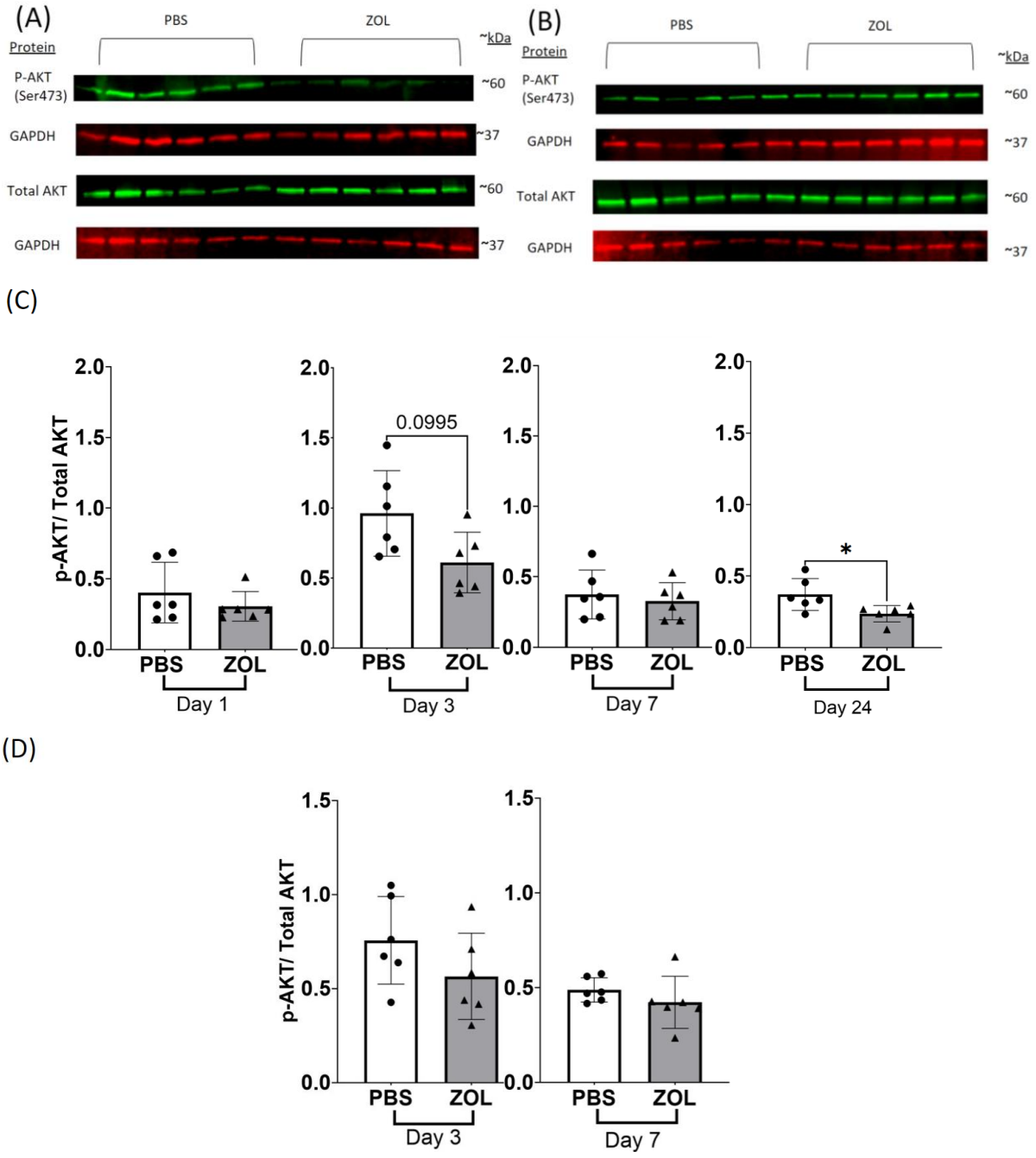

Figure 3.13- Zoledronate reduces the expression of p-AKT in the brain 24 days post injection.

Western blotting assessing the expression of p-AKT/ Total AKT in the brain Day 1, Day 3, Day 7 and Day 24 post injection. A) Example Western Blot of brain tissue for GAPDH, p-AKT and Total AKT expression in experiment 1. B) Example Western Blot of brain tissue for GAPDH, p-AKT and Total AKT expression in experiment 2. C) Fasting time course experiment 1 quantifications (Day 1, Day 3, Day 7 and Day 24 Post injection). D) Fasting time course experiment 2 quantifications (Day 3 and Day 7). Data is shown as the mean +/- the standard deviation. Data were analysed through an unpaired T-Test. PBS = Control Mice, ZOL = Zoledronate treated mice (n=6 per treatment group).

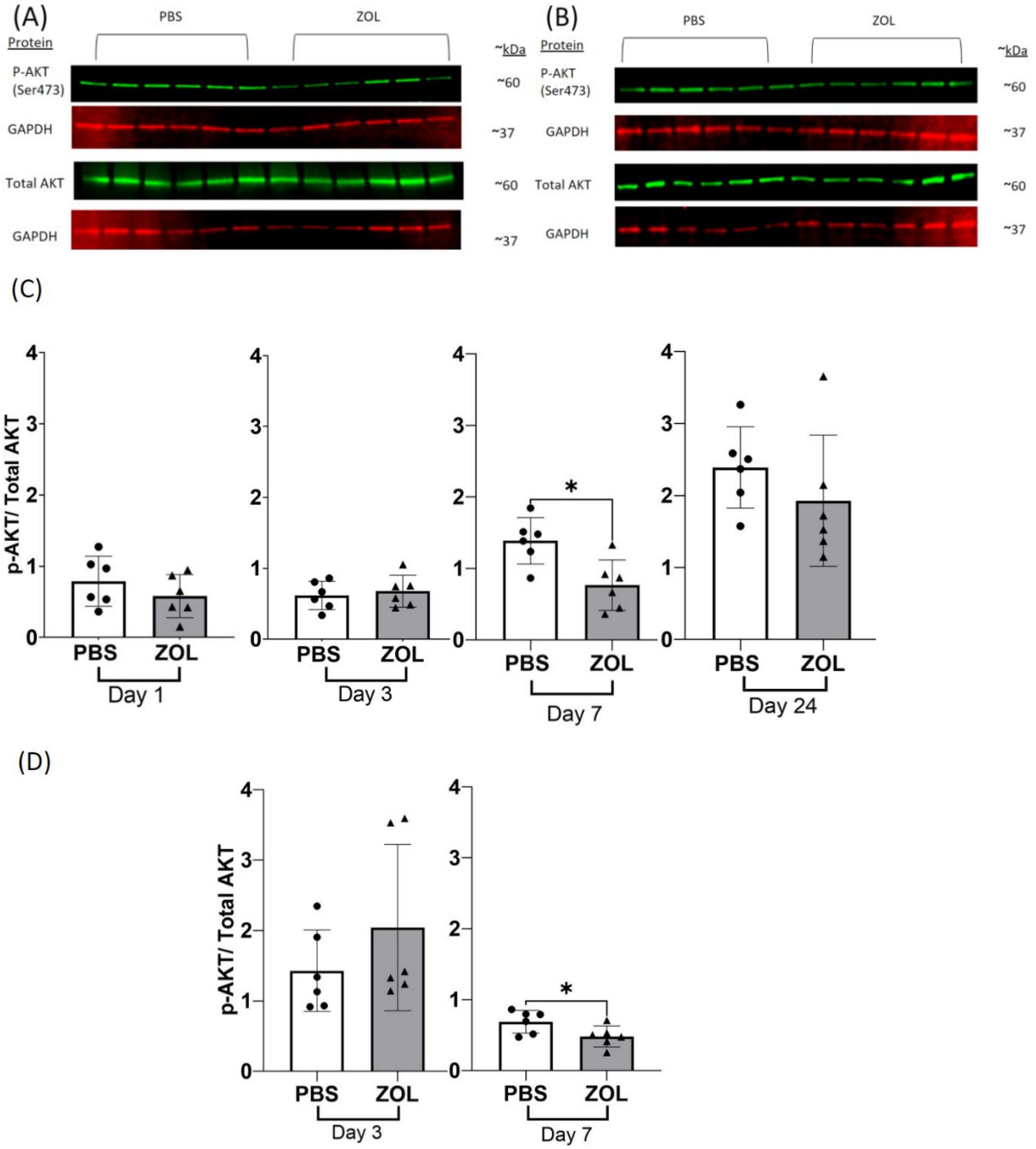

Figure 3.14- Zoledronate reduces the expression of p-AKT in heart 7 days post injection.

Western blotting assessing the expression of p-AKT/ Total AKT in the heart Day 1, Day 3, Day 7 and Day 24 post injection. A) Example Western Blot of heart tissue for GAPDH, p-AKT and Total AKT expression in experiment 1. B) Example Western Blot of heart tissue for GAPDH, p-AKT and Total AKT expression in experiment 2. C) Fasting time course experiment 1 quantifications (Day 1, Day 3, Day 7 and Day 24 Post injection). D) Fasting time course experiment 2 quantification (Day 3 and Day 7). Data is shown as the mean +/- the standard deviation. Data were analysed through an unpaired T-Test. PBS = Control Mice, ZOL = Zoledronate treated mice (n=6 per treatment group).

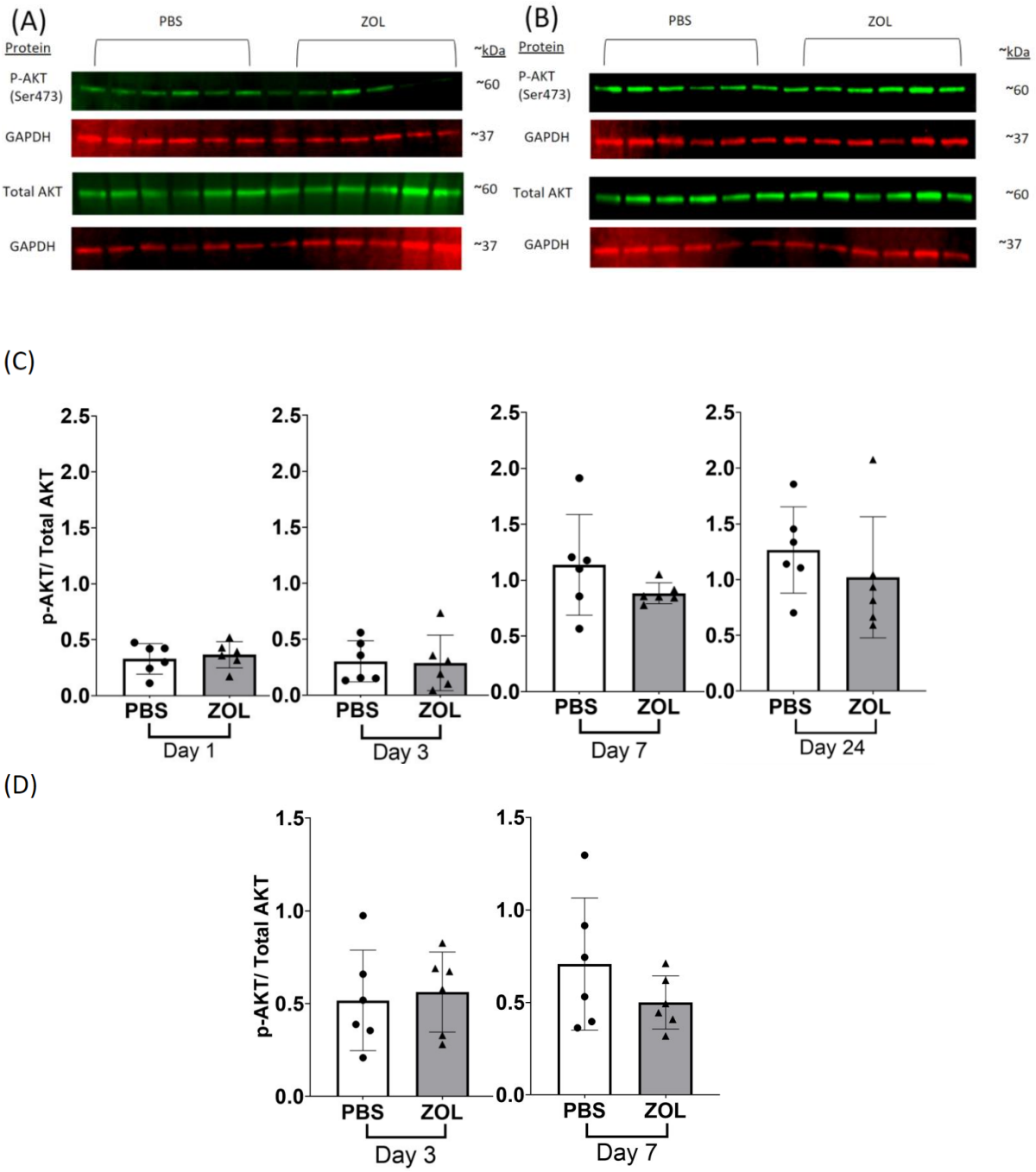

Figure 3.15- Zoledronate has no impact on the expression of p-AKT in the intestine at the time points examined.

Western blotting assessing the expression of p-AKT/ Total AKT in the intestine Day 1, Day 3, Day 7 and Day 24 post injection. A) Example Western Blot of intestine tissue for GAPDH, p-AKT and Total AKT expression in experiment 1. B) Example Western Blot of intestine tissue for GAPDH, p-AKT and Total AKT expression in experiment 2. C) Fasting time course experiment 1 quantifications (Day 1, Day 3, Day 7 and Day 24 Post injection). D) Fasting time course experiment 2 quantifications (Day 3 and Day 7). Data is shown as the mean +/- the standard deviation. Data were analysed through an unpaired T-Test. PBS = Control Mice, ZOL = Zoledronate treated mice (n=6 per treatment group).

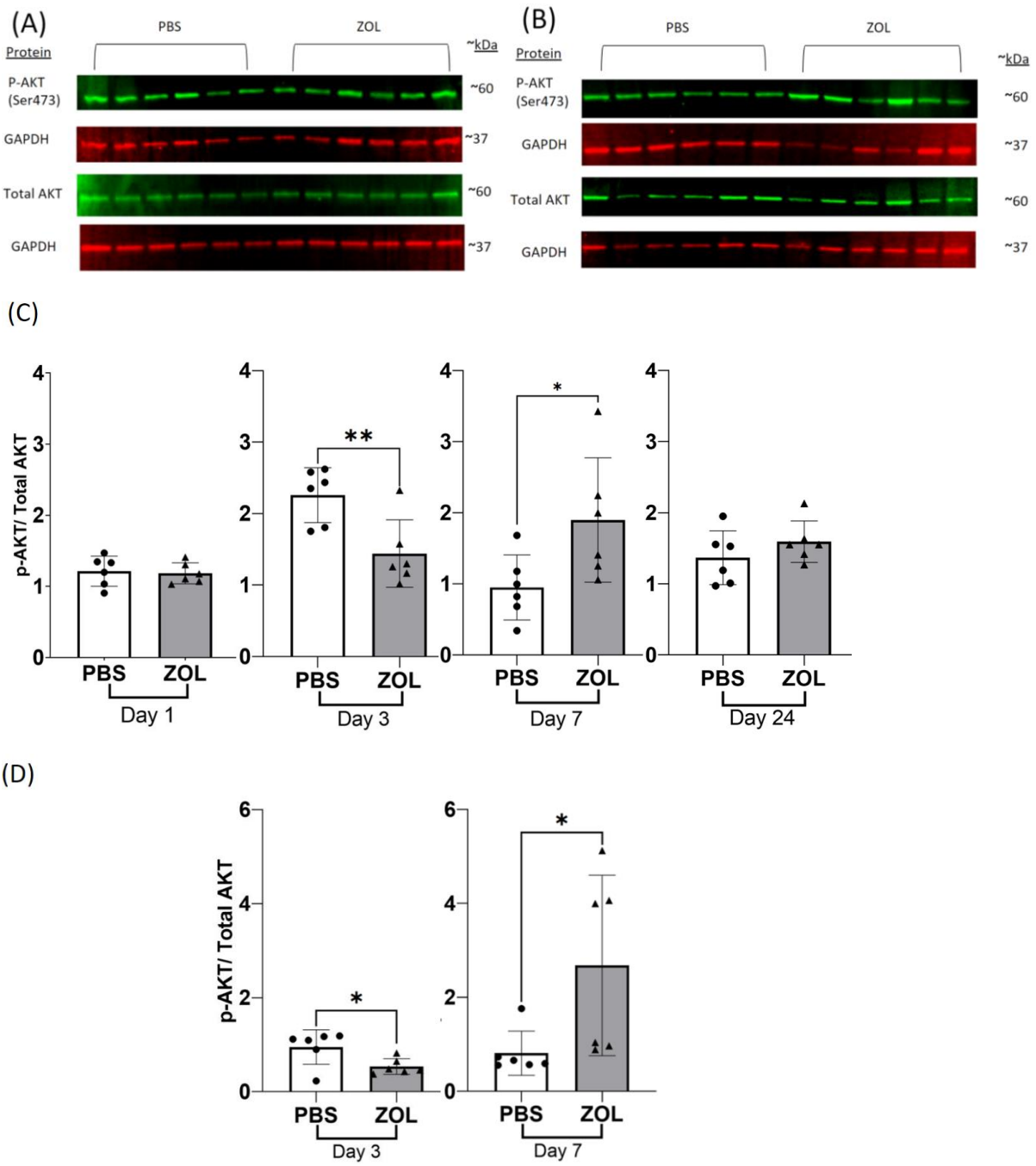

Figure 3.16- Zoledronate increases the expression of p-AKT at Day 7 and reduces the expression of p-AKT in the kidney at 3 days post injection.

Western blotting assessing the expression of p-AKT/ Total AKT in the kidney Day 1, Day 3, Day 7 and Day 24 post injection. A) Example Western Blot of kidney tissue for GAPDH, p-AKT and Total AKT expression in experiment 1. B) Example Western Blot of kidney tissue for GAPDH, p-AKT and Total AKT expression in experiment 2. C) Fasting time course experiment 1 quantification (Day 1, Day 3, Day 7 and Day 24 Post injection). D) Fasting time course experiment 2 quantification (Day 3 and Day 7). Data is shown as the mean +/- the standard deviation. Data were analysed through an unpaired T-Test. PBS = Control Mice, ZOL = Zoledronate treated mice (n=6 per treatment group).

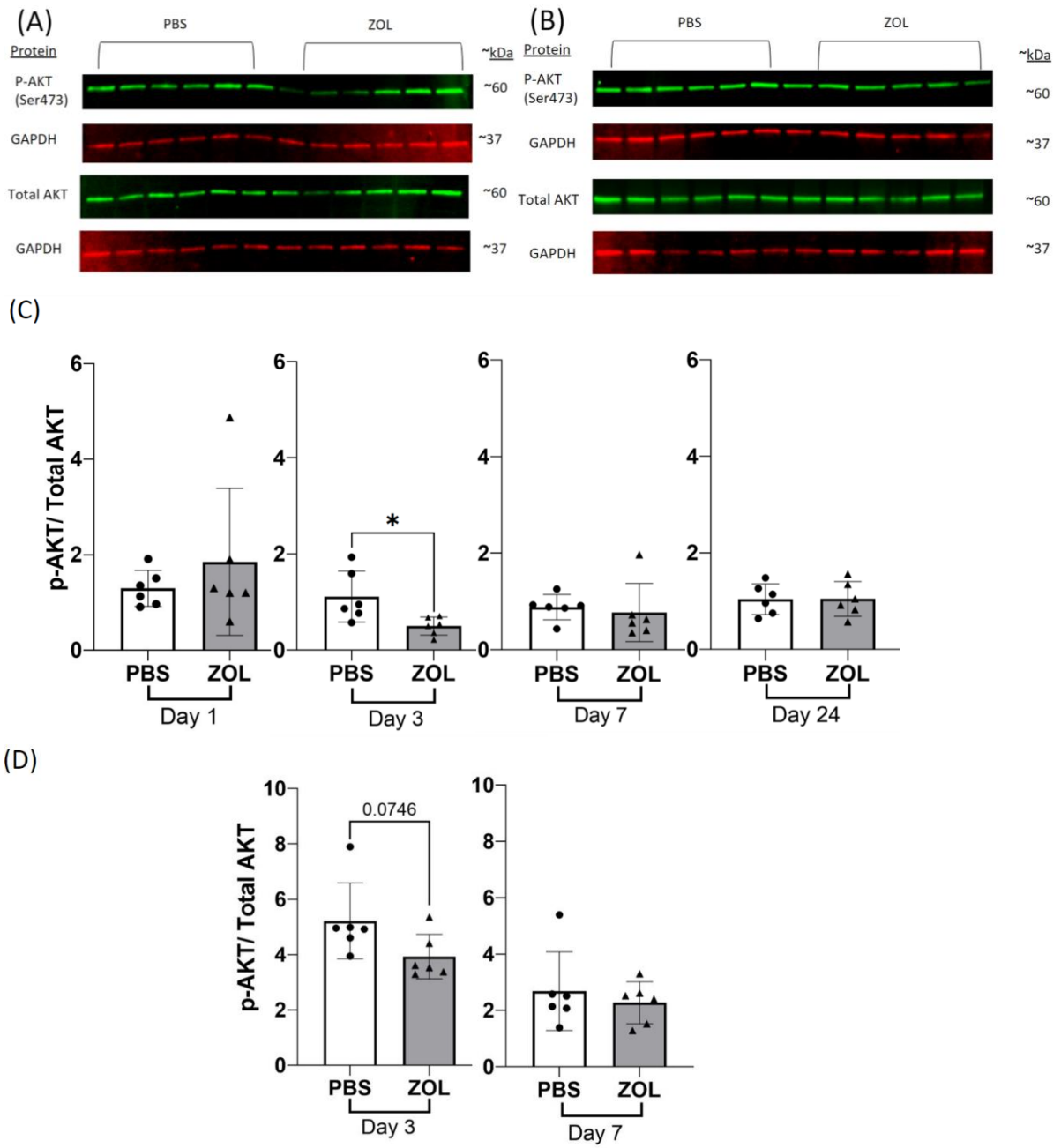

Figure 3.17- Zoledronate decreases the expression of p-AKT at Day 3 post-injection in the pancreas.

Western blotting assessing the expression of p-AKT/ Total AKT in the pancreas Day 1, Day 3, Day 7 and Day 24 post injection. A) Example Western Blot of pancreas tissue for GAPDH, p-AKT and Total AKT expression in experiment 1. B) Example Western Blot of pancreas tissue for GAPDH, p-AKT and Total AKT expression in experiment 2. C) Fasting time course experiment 1 quantifications (Day 1, Day 3, Day 7 and Day 24 Post injection). D) Fasting time course experiment 2 quantifications (Day 3 and Day 7). Data were analysed through an unpaired T-Test. PBS = Control Mice, ZOL = Zoledronate treated mice (n=6 per treatment group).

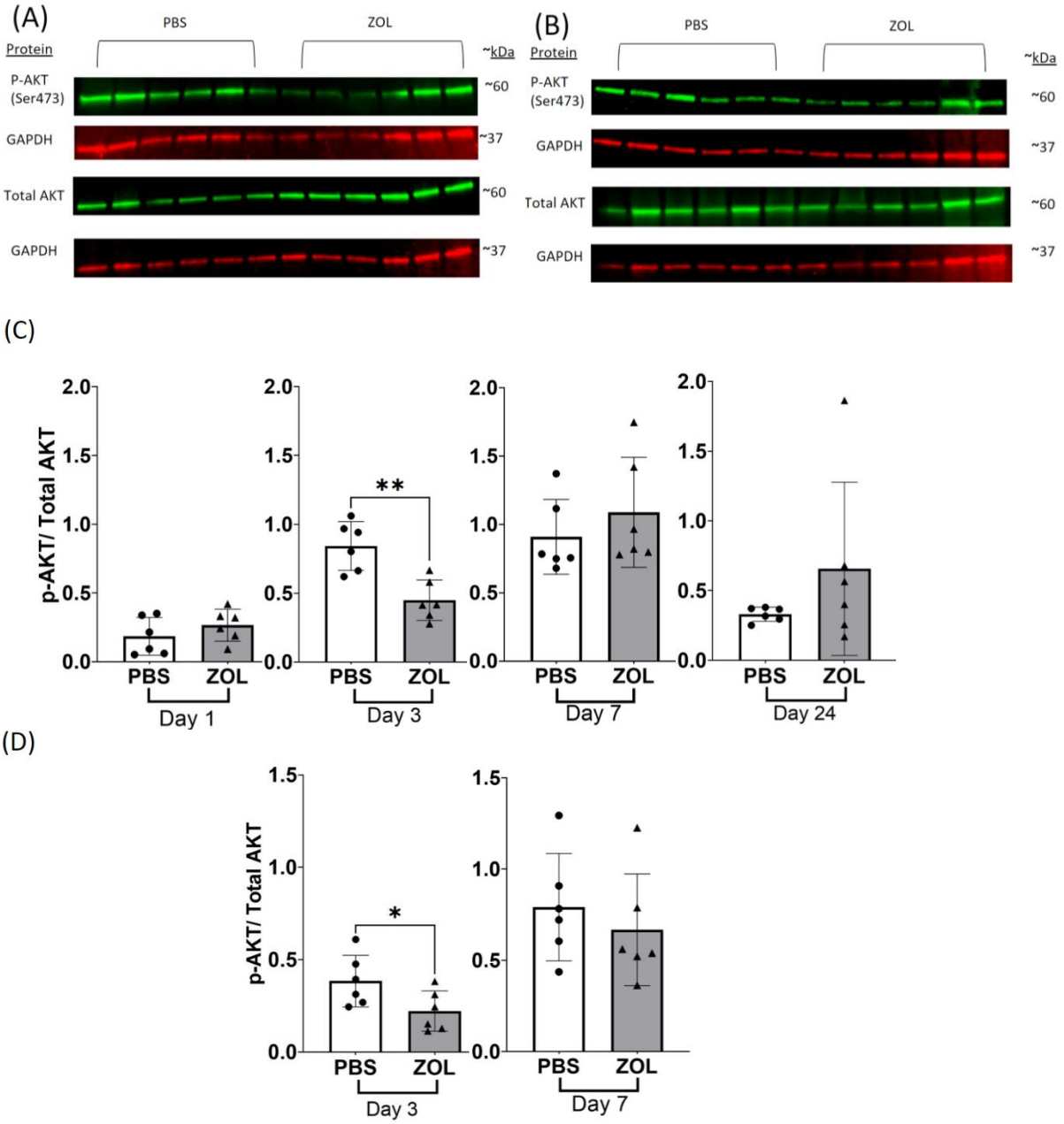

Figure 3.18- Zoledronate decreases the expression of p-AKT at Day 3 post-injection in the spleen.

Western blotting assessing the expression of p-AKT/ Total AKT in the spleen Day 1, Day 3, Day 7 and Day 24 post injection. A) Example Western Blot of spleen tissue for GAPDH, p-AKT and Total AKT expression in experiment 1. B) Example Western Blot of spleen tissue for GAPDH, p-AKT and Total AKT expression in experiment 2. C) Fasting time course experiment 1 quantifications (Day 1, Day 3, Day 7 and Day 24 Post injection). D) Fasting time course experiment 2 quantifications (Day 3 and Day 7). Data is shown as the mean +/- the standard deviation. Data were analysed through an unpaired T-Test. PBS = Control Mice, ZOL = Zoledronate treated mice (n=6 per treatment group).

3.5 Optimisation of peripheral blood cell western blot-

In order to determine whether zoledronate was active in blood cells, it was first necessary to optimise the western blotting protocol for this tissue type. This was due to the small number of blood cells available from each mouse and the requirement of a different method of protein extraction used to obtain lysates from the blood. This involved directly adding the lysis buffer to the cell pellet prior to loading (see section 2.5.2). Initial attempts to blot peripheral blood cells from mice were largely unsuccessful, as signal for both total AKT and GAPDH was extremely weak (Figure 3.19A). In addition to this there were notable smears on the blot, this suggested possible DNA contamination. Cell counts during the peripheral blood cell extraction indicated that there were around 100,000 blood cells extracted per mouse. This was in part due to the low volume of blood that it was possible to extract using the cardiac puncture method described in section 2.3.1. So initially, optimisation focussed on whether there were sufficient cells loaded to detect the markers of interest. To test this varying numbers of hMSCs (from 32,500, 65,000, 125,000, 250,000 and 500,000 hMSCs) were loaded onto a western blot for total AKT and GAPDH. All numbers of hMSCs (32,500-500,000) were sufficient to generate a signal for GAPDH and total AKT (Figure 3.19B). This suggested that 100,000 cells would be sufficient to generate a signal for total AKT and GAPDH.

One of the issues identified in the first blot of the peripheral blood cells was that of visible DNA contamination (Figure 3.19A). In order to resolve this, a DNase was applied 1:10,000 to the lysis buffer (following the manufacturer's instructions) to reduce the DNA contamination. The peripheral blood cell protein extracts were split in two to blot for p-AKT and total AKT. This was deemed as an appropriate risk to take as the previous figure (Figure 3.19B) indicated that a cell number of 32,500 hMSCs was sufficient to produce a measurable signal for both total AKT and GAPDH. Adding the DNase to the peripheral blood cell protein lysates resulted in blots that had acceptable signal strength for p-AKT, total AKT and GAPDH (Figure 3.19C). It also greatly reduced the amount of DNA contamination visible on the blot. Doubling the concentration of DNase did not improve the signal strength nor did it reduce the levels of DNA contamination any further (Figure 3.19D).

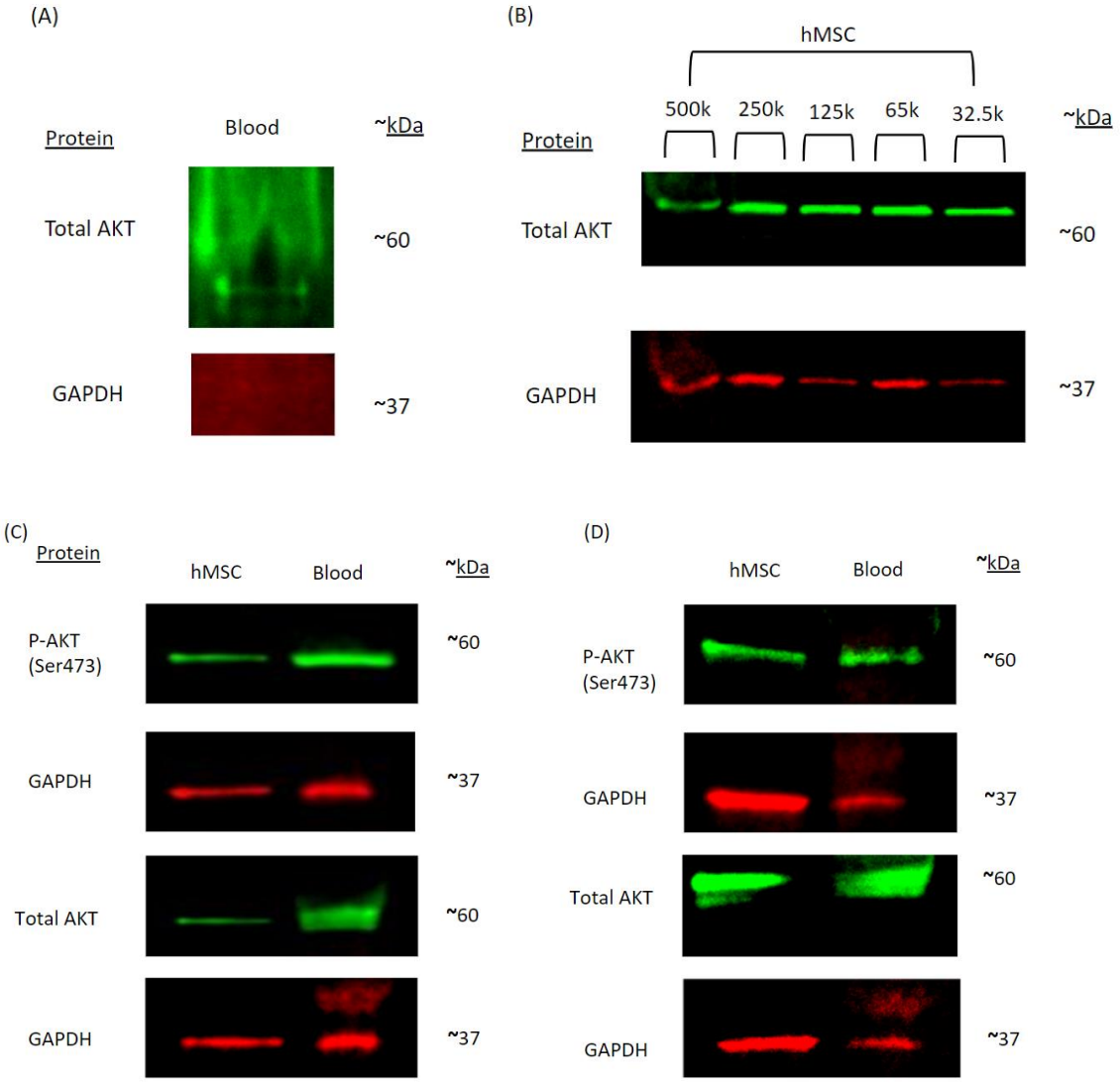

Figure 3.19 – Optimisation of blood western blot.

A) WB of blood for total AKT. B) WB of different numbers of hMSCs to ensure cell number was sufficient. C) Western blot of p-AKT and total AKT blood with DNase. D) Western blot of p-AKT and total AKT in the blood with 2X DNase.

3.6 Zoledronate's impact on peripheral blood cells –

During experiment 2 of the fasting time course experiment, peripheral blood cells were collected as described in section 2.5 from 10-week-old mice. Protein extraction was performed using the optimised peripheral blood cell protein extraction protocol (as used in Figure 3.19C). These cells were blotted for p-AKT, total AKT and GAPDH as per the other cell types. This experiment was only performed for Day 3 and Day 7 during the second experiment. This was due to the need to optimise the blood extraction protocol and because of the technical challenges with collecting peripheral blood cells from mice. Analysis of the western blot data indicated that there was no change in the ratio of p-AKT/ total AKT at either Day 3 or Day 7 (Figure 3.20).

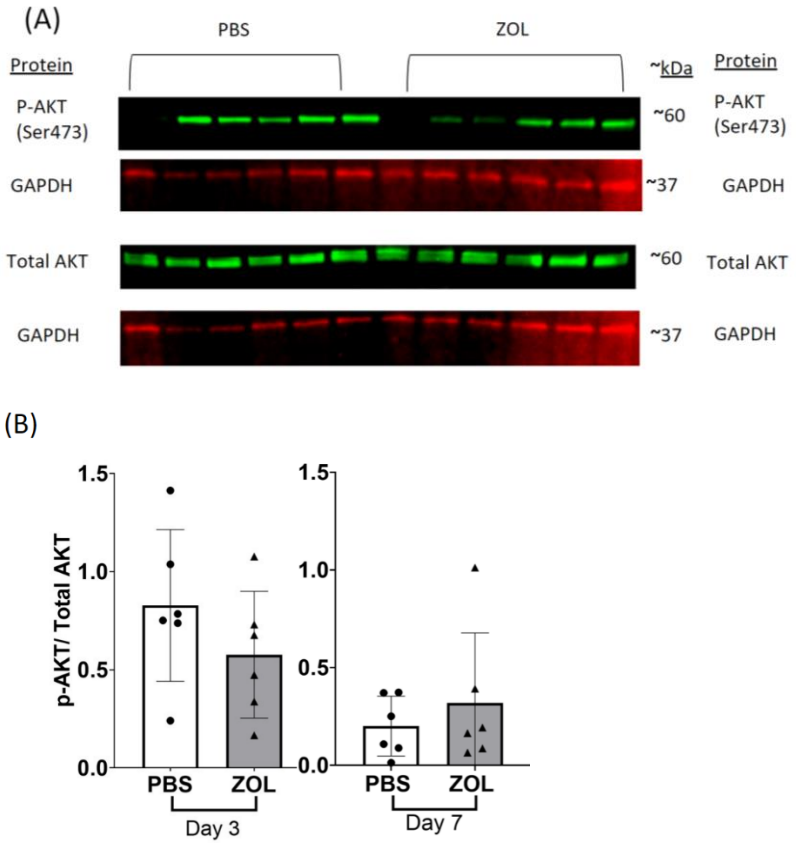

Figure 3.20- Zoledronate treatment does not impact p-AKT expression at the time points examined in extracted peripheral blood cells.

Western blotting of p-AKT/ Total AKT ratio after Day 3 and Day 7. A) Example Western Blot of GAPDH, p-AKT and Total AKT expression in the peripheral blood cells. B) Fasting time course peripheral blood cells quantification (Day 3 and Day 7 post injection). Data is shown as the mean +/- the standard deviation. Data were analysed through an unpaired T-Test. PBS = Control Mice, ZOL = Zoledronate treated mice (n=6 per treatment group).

3.7 Discussion-

Previous studies have shown that zoledronate can inhibit p-AKT in hMSCs and *Drosophila* (Misra *et al.* 2016; Chen *et al.* 2021). The work conducted in this chapter has built upon this prior work and has shown that that zoledronate can inhibit AKT signalling pathway in mouse tissues. Time course experiments on fasted mice found that zoledronate can inhibit the AKT pathway in mouse tissues in the muscle, tibia, kidney, pancreas, spleen, heart and brain in fasted-refed mice (Figures 3.9, 3.12, 3.13, 3.14, 3.16, 3.17 and 3.18). This work was also able to establish a treatment regimen of ZOL treatment that inhibits p-AKT in the highest number of mouse tissues: that of Day 3 post injection. Treatment of mice at this interval shall be conducted for healthspan work conducted later in this investigation. Repeating the experiment at Days 3 and 7 was able to mostly reproduce the results from the first experiment. These short-term effects on p-AKT are surprising given the long-term effects seen in terms of improved patient survival following a yearly infusion (Colón-Emeric *et al.* 2010). One explanation for this disparity could be due to mice having quicker rates of bone turnover than humans (Dresner Pollak *et al.* 1996; Melton *et al.* 1997; Shahnazari *et al.* 2012; Wishart *et al.* 1995). If ZOL gets released from the bone more quickly in mice and is deposited sooner in non-skeletal tissues, then this may partially explain why the effect on p-AKT is shorter in duration. This may become less of an issue in older mice, as the bone turnover rate decreases with age in mice (Shahnazari *et al.* 2012). Another explanation for the disparity could be that the downstream gero-protective effects of mTOR inhibition could be more long lasting than the initial inhibition of p-AKT. This is supported by a recent study that demonstrated that a short-term treatment of rapamycin early in life was capable of increasing lifespan in mice and *Drosophila* long after cessation of treatment (Aiello *et al.* 2022).

ZOL's activity in the bone at Day 3 (Figure 3.9) is unsurprising given that n-BPs preferentially accumulate in the bone. Previous studies on radioactively labelled ZOL indicate that it is present in the bone of dogs, mice and rats for at least a week (Weiss *et al.* 2008; Yousefnia *et al.* 2015; Nikzad *et al.* 2013). In addition to this, nitrogen containing bisphosphonates are retained in the bone of mice for over a month (Mönkkönen *et al.* 1990; Masarachia *et al.* 1996). This suggests that despite ZOL's presence in the bone, there is only a short-term effect on the p-AKT signalling

pathway. Another possibility is that negative feedback mechanisms could temporarily restore levels of these mTOR markers. This is supported by recent work in the literature that showed a transient return to baseline of p-P70S6K after initial inhibition by deprivation of arginine or leucine Mouse Embryonic Fibroblasts (MEFs) (Buel *et al.* 2022).

Another possibility is that this is a tissue specific response to treatment with an mTOR inhibitor. Supporting this notion, previous work on inhibition of mTOR markers in mouse tissues found tissue specific variation in responses to rapamycin (Arriola Apelo *et al.* 2016). p-AKT and p-S6 were only inhibited in skeletal muscle when given daily, not when given every five days in mouse skeletal muscle. Interestingly, adipose tissue behaved differently to skeletal muscle. There was no change in p-AKT with either treatment interval, but p-S6 was reduced at both treatment intervals (Arriola Apelo *et al.* 2016). This study supports the idea that mTOR inhibition by drug treatment varies from tissue to tissue regardless of how regularly the drug is administered. This could explain why some of the tissues didn't respond to ZOL in terms of changes to p-AKT and why there is no long-term inhibition of p-AKT in the bone. It's also worth considering that there is a great deal of variation in the expression of levels of mTOR markers including AKT between different mouse tissues (Baar *et al.* 2016). This may impact the ability to detect changes in mTOR markers in some mouse tissues.

The work conducted in this chapter was important for emphasising that ZOL is also active in non-skeletal as well as skeletal mouse tissues. This is consistent with some of the studies conducted previously in the literature. As mentioned previously, ZOL treatment has been shown to reduce mortality from cardiac arrythmias and pneumonia (Colón-Emeric *et al.* 2010). This led to speculation that ZOL was also active in promoting survival through non skeletal effects. Previous work in the literature has also indicated that zoledronate is present in non-skeletal tissues in mammalian systems such as dogs, rats and mice (Weiss *et al.* 2008; Nikzad *et al.* 2013; Yousefnia *et al.* 2015). Although these analyses have indicated that the gap in concentration of the drug is 10-1000 lower than that found in the bone (depending on the tissue). Despite this major gap in concentration, p-AKT was inhibited in some non-skeletal tissues during the study conducted in this chapter. These included the

skeletal muscle, kidney, heart, pancreas, spleen and brain. Therefore, it may be possible to hypothesise that ZOL is capable of inhibiting p-AKT at low concentrations.

An explanation for the effect of zoledronate in the muscle (Figure 3.12) could be due to its proximity to the bone. ZOL's activity on p-AKT in muscle tissue may also explain why a recent study indicated that ZOL can improve muscle function in osteoporotic patients (Huang *et al.* 2021). If this inhibition of p-AKT in the muscle could be achieved continuously, then it may have very promising implications for improving healthy muscular ageing. The finding that ZOL can inhibit p-AKT in the brain of mice (Figure 3.13) is also interesting as it may mean that ZOL could improve the neurological function of older mice. It is also interesting in the context of previous work in the literature had indicated that the concentration of ZOL in the brain is extremely low (Weiss *et al.* 2008; Yousefnia *et al.* 2015). Despite this, one study has shown that bisphosphonate treatment has been shown to reduce the likelihood of developing dementia in people over the age of 50 (Chang *et al.* 2014). Therefore, it is possible that ZOL is active at low concentrations in the brain and that this is still sufficient to promote healthy neurological ageing.

ZOL was able to inhibit p-AKT in the pancreas during the first experiment, although during the second experiment there was no significant change (Figure 3.17). Given the importance of the pancreas for the synthesis of insulin, this may mean that ZOL could confer metabolic benefits to older people. This may relate to previous findings in the literature that n-BPs lower the incidence of type 2 diabetes in post-menopausal women (Vestergaard 2011; Chan *et al.* 2015; Toulis *et al.* 2015). Similarly, ZOL demonstrated an ability to inhibit p-AKT in the spleen (Figure 3.18). ZOL's activity in the spleen may relate to previous findings that showed that ZOL can improve survival and reduce incidence of certain infectious diseases in patients (Colón-Emeric *et al.* 2010; Reid *et al.* 2021; Blanch-Rubio *et al.* 2020). Again, the concentration of ZOL in the pancreas and spleen are much lower than in the skeletal system in mice, rats and dogs (Weiss *et al.* 2008; Yousefnia *et al.* 2015). Despite this, the drug remains active on p-AKT in these tissues in mice.

ZOL's inactivity in terms of p-AKT activity in the blood is somewhat surprising (Figure 3.20). Previous work in the literature has indicated that ZOL is present in the blood

during the first week following treatment in mammals including mice (Weiss *et al.* 2008; Chen *et al.* 2007; Nikzad *et al.* 2013). One explanation for the lack of p-AKT change is that peripheral blood cells may not respond to the drug the same way as other tissues. ZOL might be present in the blood, but not be active on p-AKT signalling. Another possibility is that the effect on p-AKT is too small to be detected with 6 mice and a larger population of mice would be required to detect any changes. Since zoledronate accumulates in the bone, it could be impacting the formation of specific cell types in the blood which are then carried around the rest of the body. Another line of thought is that ZOL could be carried around the body in a subset of cells found in the blood such as macrophages. A couple of studies have indicated that n-BPs are internalised by macrophages in a similar fashion to osteoclasts (Thompson *et al.* 2006; Junankar *et al.* 2015; Ali *et al.* 2015). One of these studies indicated that macrophages facilitated the transport of n-BPs to tumours (Junankar *et al.* 2015). In addition to this, one paper in mice indicated that ZOL treatment increased the amount of unprenylated protein in macrophages, suggesting that the drug is active in macrophages (Munoz *et al.* 2021). Despite this, macrophages have yet to be demonstrated to be depositing these n-BPs in non-cancerous tissues.

The kidney contains one of the highest concentrations of ZOL outside of the skeleton in mammalian studies during the first week of treatment (Weiss *et al.* 2008; Nikzad *et al.* 2013; Yousefnia *et al.* 2015). This is because approximately 40% of a ZOL infusion is excreted mostly through urination within 24 hours (Chen *et al.* 2002; Weiss *et al.* 2007) and needs to pass through the kidney. In addition to this kidney cells have been shown to respond to the ZOL in terms of inhibition of the mevalonate pathway through reduced FPPS activity *in vitro* (Lühe *et al.* 2008). Therefore, it is unsurprising that the drug is active reducing p-AKT at Day 3 post injection in the kidney. However, what was more surprising was that there was a consistent increase in p-AKT in response to zoledronate in the kidney at Day 7 post injection (Figure 3.16). This is different to the other tissues, in which the only significant changes showed a decrease in p-AKT/ Total AKT. Again, one possibility is that the result is due to a tissue specific response.

Of note, there was also some diversity in how quickly these tissues responded to zoledronate. One exception to this is the kidney (as mentioned above). Another

exception to this appears to be in the heart (Figure 3.14). Previous work has indicated that ZOL reduces mortality from cardiac arrythmias, suggesting ZOL has an impact on the heart (Colón-Emeric *et al.* 2010). The work in this chapter provides additional evidence that ZOL is active in the heart. As to why ZOL takes longer to become active in the heart remains unclear as there is ample evidence in the literature to suggest ZOL is present in the heart for at least a week in mice (Nikzad *et al.* 2013; Yousefnia *et al.* 2015).

Whether the short duration of ZOL's on p-AKT in mouse tissues is due to clearance of the drug or whether it is due to ZOL only being able to inhibit p-AKT for three days at a time when given repeatedly remains unknown. It is also interesting to compare the duration of ZOL's ability to inhibit markers in mouse tissues to rapamycin. After injection of rapamycin, it can induce inhibition of a different downstream mTOR marker (p-S6) for up to 5 Days in mouse tissues (Arriola Apelo *et al.* 2016; Rensing *et al.* 2015). This is slightly longer in duration than ZOL's ability to inhibit p-AKT in mouse tissues. This may imply that ZOL is a less potent inhibitor of mTOR than rapamycin in mice, although it would be necessary to measure levels of p-S6 in response to ZOL in mouse tissues to substantiate this.

There were a couple of major limitations to this study. One such limitation was that only p-AKT was examined as a marker of ZOL's activity. Other markers of mTOR activity such as p-P70S6K and p-mTOR have been shown to be inhibited in hMSCs by ZOL (Misra *et al.* 2016). In addition to this, inhibition of the mevalonate pathway by ZOL was not directly assessed in mouse tissues this time around. A previous study on hMSCs demonstrated that zoledronate was active in inhibiting the mevalonate pathway by measuring levels of unprenylated RAP1A (Misra *et al.* 2016). Unfortunately, it was not possible to use this antibody to measure levels of protein prenylation/ mevalonate pathway inhibition in this study on mouse tissues as production of the antibody had been discontinued (Rap 1A, sc-1482, Santa Cruz). No new antibody was available for measuring protein prenylation. A limitation to this approach of using unprenylated RAP1A to measure mevalonate pathway inhibition is that there are several hundred different proteins that are prenylated and this approach only measures changes to one (Sebti 2005).

Another limitation of this work is that zoledronate's activity was assessed in young mice rather than in old mice. This is important as the ZOL healthspan study shall be conducted on older mice. This could be important as levels of mTOR markers change with age in mouse tissues (Baar *et al.* 2016). This may affect which tissues exhibit mTOR markers inhibition by ZOL. A further flaw with this work was that there were the large gaps between Days 3, 7 and 24. Previous work in the literature has shown that a transient return to baseline and activation of mTOR markers can occur in MEFs following mTOR inhibition by deprivation of arginine and leucine (Buel *et al.* 2022). This was followed by a subsequent return of inhibition of the mTOR markers p-AKT and p-P70S6K. In order to ensure there are no further reductions in mTOR markers at later time points, it may be advisable to look at other time points such as Day 5, 10 and 14. While further work is still needed to build on these findings to better understand mTOR inhibition by ZOL in mouse tissues, it has been possible to determine that ZOL is active on p-AKT in mouse tissues. In addition, a ZOL treatment interval has also been determined to best inhibit p-AKT in the greatest number of mouse tissues.

Chapter 4- The effect of Zoledronate on the healthspan of mice

4.1 Introduction-

Previous work has indicated that ZOL can improve features of ageing in hMSCs (Misra *et al.* 2016). This included a reduction in markers of senescence, younger looking cell morphology, reduced levels of DNA damage and an increased time to reach replicative senescence. A further study was able to indicate that ZOL could increase the lifespan of *Drosophila* (Chen *et al.* 2021). In addition to this, this study also found that ZOL was able to improve features of healthspan in *Drosophila*. This was demonstrated through increased climbing ability and improved intestinal function. Given that ZOL improves features of healthy ageing in cells and flies, it is now pertinent to ask whether ZOL can improve the healthy ageing of mice.

In the above-mentioned studies, there was a decrease in p-AKT in response to ZOL in hMSCs and *Drosophila*. Other work in the literature has indicated that the AKT inhibitor GSK690693 was capable of increasing lifespan and intestinal function with age in *Drosophila* (Cheng *et al.* 2022). Given the importance of p-AKT inhibition in improving in improving features of ageing in flies, it is also possible that p-AKT inhibition could confer benefits to the healthy ageing and survival of more advanced model organisms such as in mice. During the previous chapter, a dosage interval of injecting ZOL twice weekly was determined to be sufficient in inhibiting p-AKT in a variety of tissues (Figures 3.8-3.20). Since zoledronate inhibits p-AKT signalling in mice, it is possible to hypothesis that zoledronate treatment at this treatment interval could improve the healthy ageing of mice. In addition to this, ZOL can inhibit other markers associated with mTOR signalling as p-P70S6K and p-mTOR in hMSCs (Misra *et al.* 2016). Given that mTOR inhibitors such as rapamycin can improve the lifespan and healthspan of mice (Harrison *et al.* 2009; Bitto *et al.* 2016), it also is possible that ZOL could confer similar benefits to ageing mice. In order to determine if this is the case, a protocol agreed upon by a panel of international experts to measure mouse healthspan was used (Bellantuono *et al.* 2020). These included looking at novel object recognition, rotarod, grid hanging, glucose tolerance, insulin tolerance and frailty index.

4.2 Design of mouse healthspan experiment-

The mice in this chapter were first tested for a baseline level of health prior to the start of the intervention. This was done by performing all the healthspan assays at 10 months of age, prior to the intervention starting at 12 months (middle age). Taking these measurements at 10 months first was important for assessing changes that occur in healthy compared to aged mice during these assays. In addition, there is evidence to suggest that starting the ZOL intervention during middle age is important for maximising the benefits of the drug treatment. During a prior study, starting ZOL treatment in female *Drosophila* in middle age had a greater impact in terms of lifespan increase than if treatment began at birth (Chen *et al.* 2021). In addition to this, retrospective studies on post-menopausal women taking ZOL (treatment starting at middle-age) demonstrated that they had reduced mortality from cardiac arrhythmias and pneumonia (Colón-Emeric *et al.* 2010). Together these studies suggest that starting ZOL treatment at middle age in female organisms should confer maximal benefits to survival and healthspan. Due to this, treatment of female mice with ZOL began at middle age during this mouse healthspan study.

The zoledronate treatment regimen began when the mice were 12 months of age and continued throughout the rest of the study. Mice were injected twice a week with 125 µg/kg of zoledronate or with an equivalent volume of PBS, as during the previous chapter on p-AKT activity in mouse tissues (Figures 3.2-3.20). The next set of healthspan measurements were taken 6 months after the treatment regimen began, when the mice reached old age at 18 months (see Figure 4.1 for overview of experiment). Frailty index and grid hanging tests were performed monthly from 18 months of age until the end of the experiment. Rotarod was performed at months 10,18, 20 and 22. The remaining assays were performed once at 18 and once at 22 months. This pipeline for the timings of these assays is consistent with a toolbox developed for assessing the healthy ageing of mice (Bellantuono *et al.* 2020).

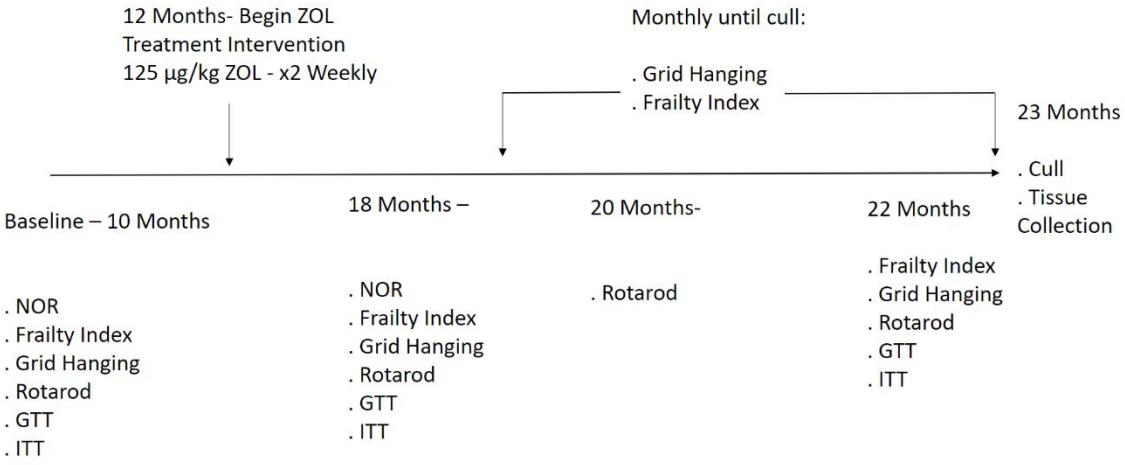

Figure 4.1- A schematic representation of the experimental plan to test the effects of Zoledronate on the healthspan of mice. Detailing months in which assays are performed and information on drug treatment.

4.3 ZOL has no effect on weight gain of older mice-

Mice were weighed twice weekly as part of their injection regimen as part of this experiment. The average weights of the two treatment groups were recorded and the average weight over time was plotted below (Figure 4.2A). There was no significant difference between the average weights of the two treatments at any of the major time points in which healthy ageing assays were conducted (Figure 4.2B). From this analysis, ZOL appears to make no difference to weight gain with age.

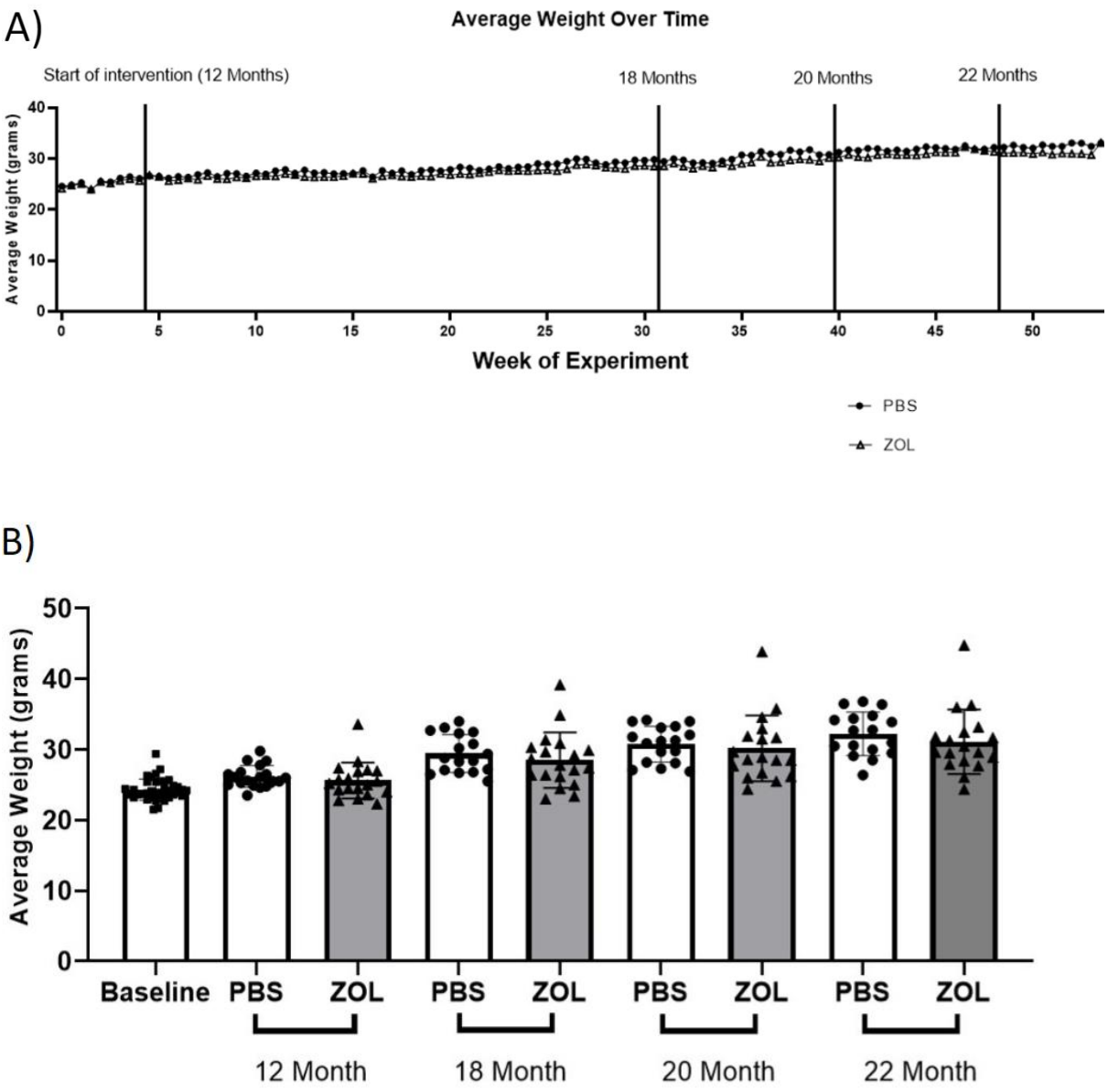

Figure 4.2–- Zoledronate has no effect on weight gain of older mice.

A) Average weight over time for PBS and ZOL mice over time. B) PBS vs ZOL weights by month. Data in B) is shown as the mean +/- the standard deviation. Significance assessed by an unpaired one-way ANOVA with Bonferroni's post-hoc test. PBS = Control Mice, ZOL = Zoledronate treated mice (n=15-19 per treatment group, depending on mouse survival).

4.4 ZOL treatment delays the onset of frailty in mice-

In order to determine if mouse frailty is improved in response to zoledronate, a frailty index was used to assess levels of mouse frailty. This consists of a series of frailty criteria such as loss of fur colour, kyphosis and hearing loss. For the full list of the 29 mouse frailty criteria assessed, please see Table 2.2. Together the sum of these 29 measurements were used to create a frailty score by dividing by the total number of measurements. Mice were tested at 10 months of age (baseline), 18 months, 19 months, 20 months, 21 months, 22 months and 23 months. Both PBS and ZOL mice had a significantly higher frailty score with age (Figure 4.3). Crucially, Zoledronate treatment was able to significantly lower the frailty score overall compared to PBS mice.

A)

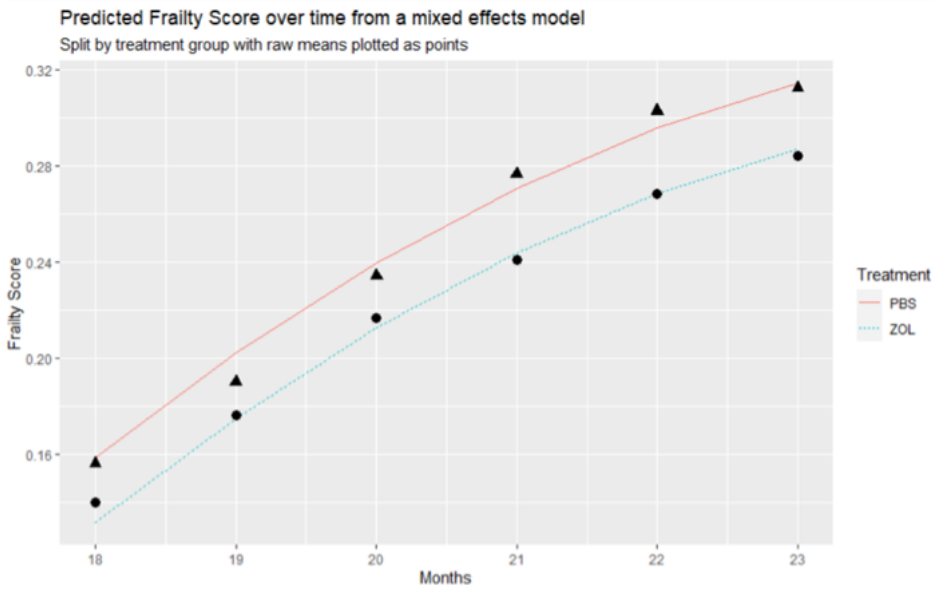

B)

```
Fixed effects:
               Estimate Std. Error         df t value Pr(>|t|)
(Intercept)  -1.702e+00  3.375e-01  1.733e+02  -5.042 1.15e-06 ***
Baseline.10M  7.900e-01  2.510e-01  3.200e+01   3.148 0.003550 **
TreatmentZOL -2.714e-02  1.098e-02  3.200e+01  -2.473 0.018895 *
Months        1.579e-01  3.308e-02  1.730e+02   4.773 3.85e-06 ***
Months_sq    -3.092e-03  8.063e-04  1.730e+02  -3.835 0.000176 ***
---
Signif. codes:  0 ‘***’ 0.001 ‘**’ 0.01 ‘*’ 0.05 ‘.’ 0.1 ‘ ’ 1
```

Figure 4.3- ZOL treatment delays the onset of frailty in mice.

A) A graph from a mixed effects model of frailty index scores with age for PBS and ZOL mice. B) Statistical analysis output of linear mixed effect model. Data analysed through a linear mixed effects using R, taking into consideration changes with age relative to baseline and overall differences between treatments. PBS = Control Mice, ZOL = Zoledronate treated mice (n=14-19 per treatment group, depending on mouse survival).

4.5 ZOL does not impact muscular function with age-

In order to examine muscular function with age in response to ZOL, a grid hanging test was performed. Mice were tested at the ages of 10 months (baseline), 18 months, 19 months, 20 months, 21 months and 22 months. Mice were placed on the grid hanging apparatus and the apparatus was inverted. The time in when it took the mice to fall was measured. There was no significant change in how long it took for mice to fall with age during the grid hanging test (Figure 4.4). Overall, there was also no effect of ZOL treatment on performance during the grid hang test.

A)

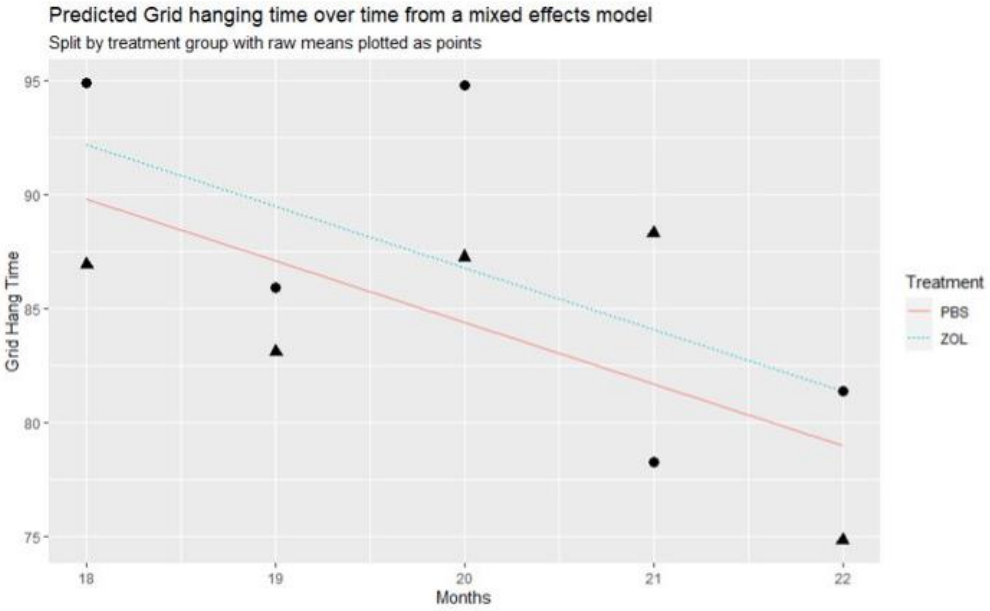

B)

```
Fixed effects:
             Estimate Std. Error        df t value Pr(>|t|)
(Intercept)  89.83837   44.06882 170.40581   2.039  0.04304 *
Baseline.10M  0.18564    0.06044  32.00000   3.072  0.00432 **
TreatmentZOL  2.40947   11.81963  32.00000   0.204  0.83976
Months       -2.70095    2.01455 139.00000  -1.341  0.18220
---
Signif. codes:  0 ‘***’ 0.001 ‘**’ 0.01 ‘*’ 0.05 ‘.’ 0.1 ‘ ’ 1
```

Figure 4.4- ZOL treatment does not impact muscular function with age.

A) A graph from a linear mixed effects model of grid hanging scores with age for PBS and ZOL mice. B) Statistical analysis output of mixed effect model from R indicating changes with age and treatment. Data analysed through a linear mixed effects model using R, taking into consideration changes with age relative to baseline and overall differences between treatments. PBS = Control Mice, ZOL = Zoledronate treated mice (n=14-19 per treatment group, depending on mouse survival).

4.6 ZOL treatment does not significantly change neuromuscular function by 22 months-

Rotarod was performed in order to assess neuromuscular function with age in response to ZOL treatment. The time taken for the mice to fall off the mice apparatus was measured as a way of measuring neuromuscular function. This assay was performed at 10 months of age (baseline), 18 months, 20 months and 22 months. There was a significant reduction in how long the mice spent one the rotarod with age in the PBS mice at 20 months compared to baseline (Figure 4.5). However, this did not reach statistical significance at the other two time points examined (18 and 22 months). Furthermore, there was no significant change in the ZOL mice's time to fall off the rotarod compared to baseline at any time point. There was no significant effect of ZOL on performance on the rotarod test by 22 months (p=0.071).

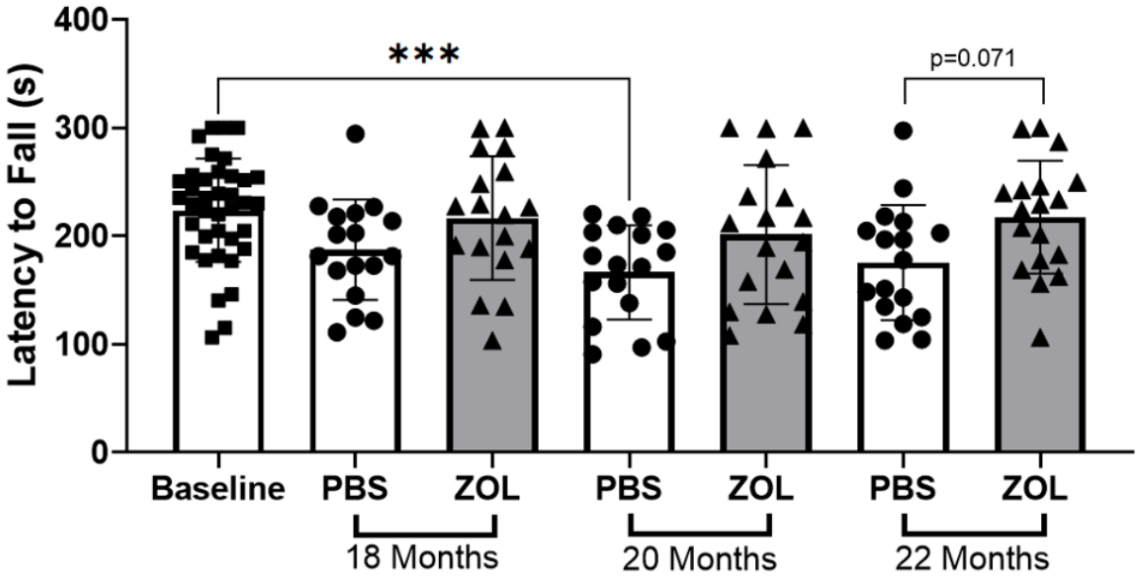

Figure 4.5- ZOL treatment does not significantly change neuromuscular function by 22 months.

Graph of Rotarod Assay Latency to fall by month and treatment. Data Analysed through one-way ANOVA and Bonferroni's post hoc test. PBS = Control Mice, ZOL = Zoledronate treated mice (n=15-19 per treatment group, depending on mouse survival).

4.7 ZOL treatment does not impact glucose tolerance-

Mice had their metabolic function examined by performing a glucose tolerance test (GTT). Mice were fasted overnight, injected with glucose and had their blood glucose levels assessed over the course of two hours. This created a series of blood glucose curves which was used to calculate the area under the curve (AUC) for each time point of the assay for both treatment groups. Mice were tested at the ages of 10 months of age (baseline), 18 months and 22 months. There was a significant reduction in the AUC of the mice for both treatment groups with age compared to baseline for both treatment groups (Figure 4.6B). This suggests that the mice became more sensitive to glucose with age. There was no change in the AUC when comparing PBS and ZOL mice at any time point, suggesting that ZOL treatment had no impact on glucose sensitivity.

4.8 ZOL treatment increases insulin resistance at 18 months-

Mice had their metabolic function examined by performing an insulin tolerance test (ITT). This assay is performed in a similar fashion to that of the GTT test. Mice were fasted for three hours prior to the start of the assay and had their blood glucose measured at different points after injection with insulin. Mice were tested at the ages of 10 months of age (baseline), 18 months and 22 months. There was a significant reduction in the AUC when comparing 18-month PBS mice to baseline (Figure 4.7B). However, there was no change with age in the 22-month-old PBS mice. This suggests that insulin sensitivity does change temporarily with age in C57BL/6J mice. ZOL treated mice had a significantly higher AUC at 18 months, compared to PBS mice. However, there was no difference between PBS and ZOL mice at 22 months. This suggests that ZOL increases insulin resistance temporarily in older mice.

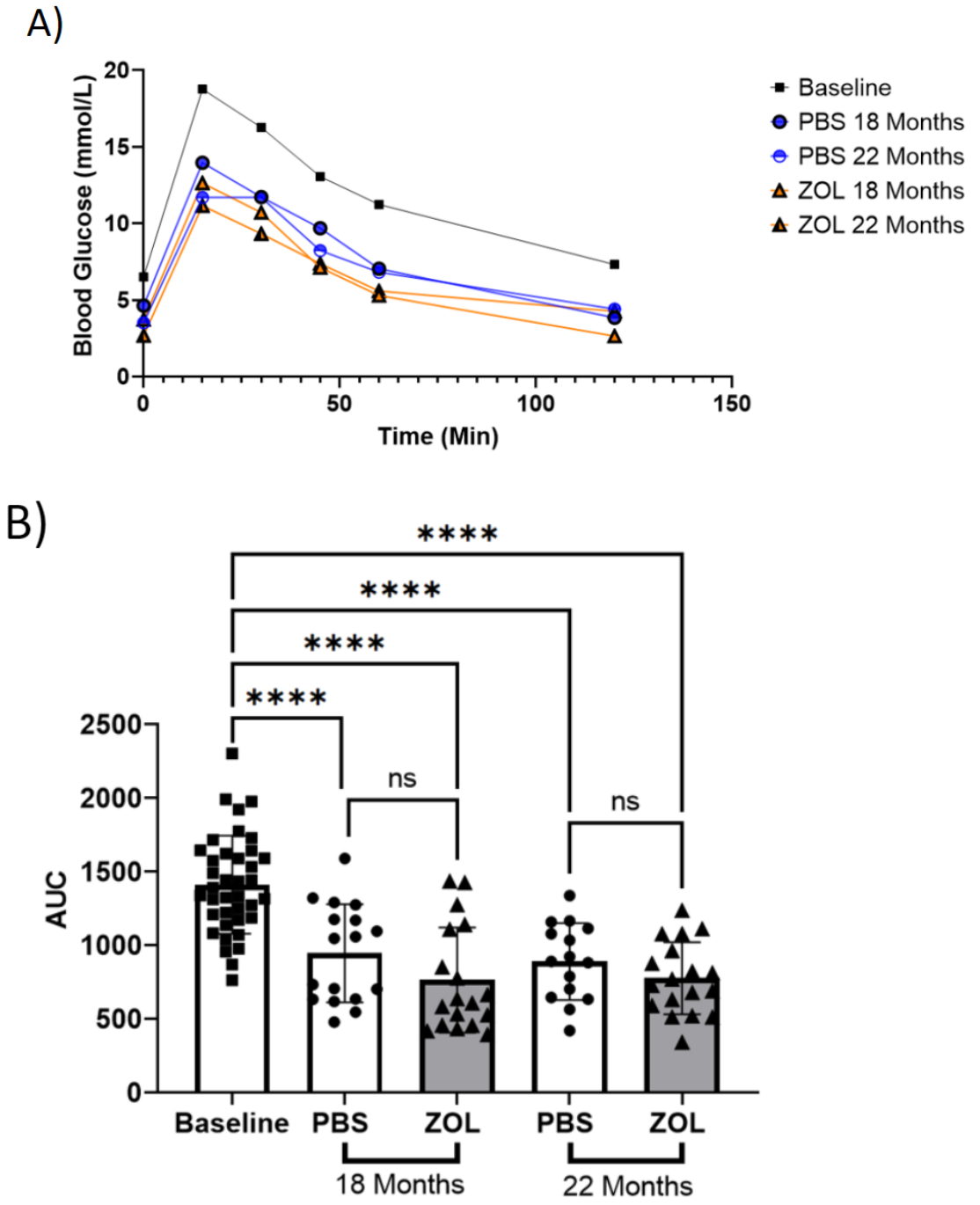

Figure 4.6- ZOL treatment does not impact glucose tolerance.

A) GTT Graphs of blood glucose data for all mice. B) Area Under the Curve of GTT assay for all mice during the different months of the assay. Data were analysed through one-way ANOVA and Bonferroni's post-hoc test. PBS = Control Mice, ZOL = Zoledronate treated mice (n=15-19 per treatment group, depending on mouse survival).

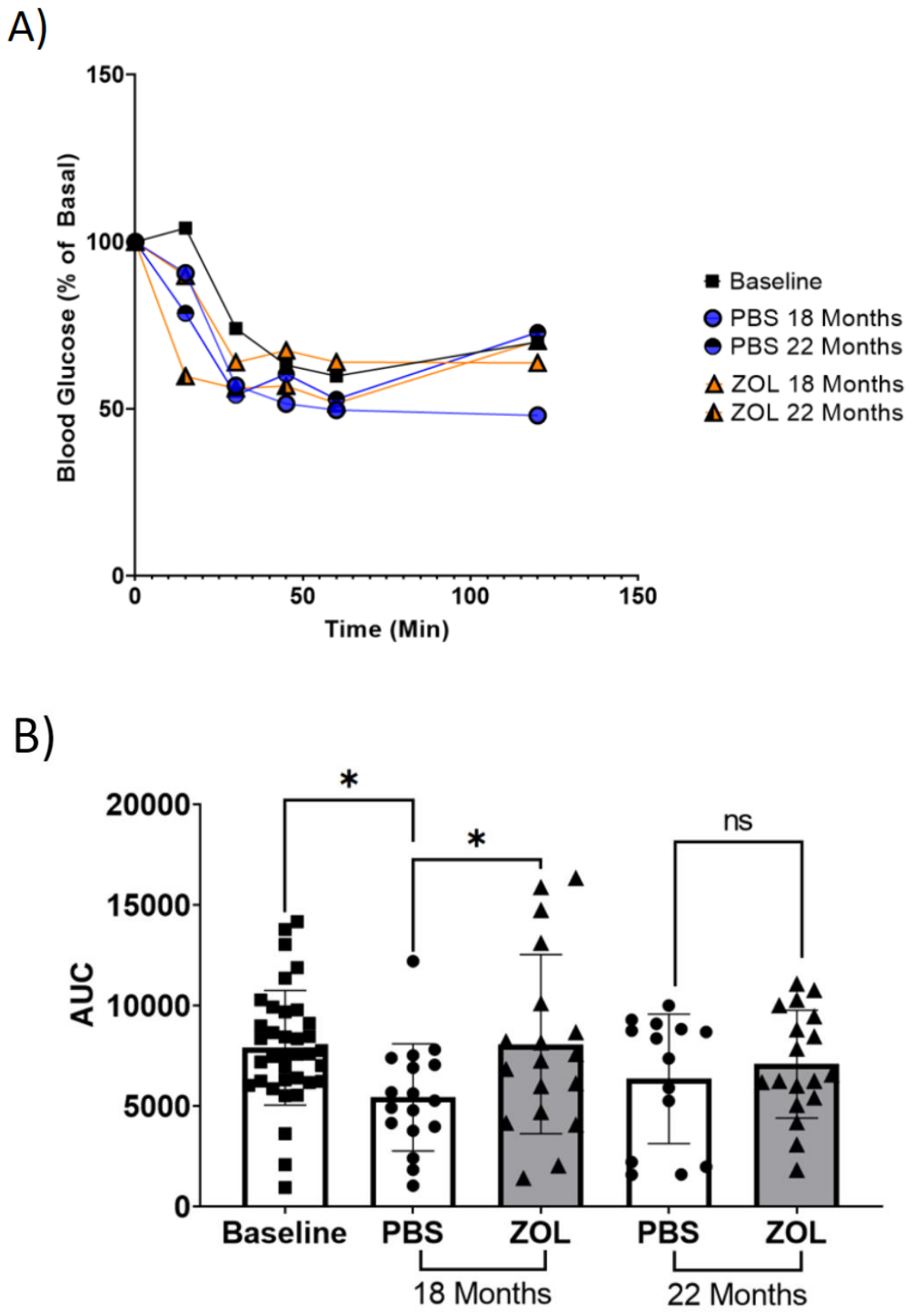

Figure 4.7- ZOL treatment increases insulin resistance at 18 months.

A) ITT Graphs for the all the mice B) AUC of ITT assay for all mice treatments and months. Data is shown as the mean +/- the standard deviation of the AUC. Data were analysed through one way ANOVA with Bonferroni's multiple comparison post-hoc test. PBS = Control Mice, ZOL = Zoledronate treated mice (n=15-19 per treatment group, depending on mouse survival).

4.9 ZOL has no effect on performance in the open field test-

Prior to assessment of neurological function by novel object recognition, levels of mouse stress were assessed via the open field (OF) test. The willingness of the mouse to move and its overall ability to move can also affect the outcome of this test. In order to determine stress levels, the mice were placed in an empty novel object arena. Various stress parameters were then measured such as time spent in the corner of the arena and total distance moved. Mice were tested at the ages of 10 months of age (baseline), 18 months and 22 months. ZOL treated mice spent longer in corners of the open field arena with age (Figure 4.8A). However, the PBS mice did not spend significantly longer in corners with age ($p=0.079$). There was no difference between PBS and ZOL mice in terms of time spent in corners at 18 months of age. There was a significant increase in vision loss with age at 18 months and 22 months compared to baseline for both treatment groups (Figure 4.8B). There was also no significant difference between PBS and ZOL mice for either time point in terms of vision loss. There was no difference with age in the total distance moved during the open field test for either treatment condition (Figure 4.8C). ZOL treatment also made no difference to distance moved during the open field test. Overall, ZOL treatment did not have much impact on performance during the open field test.

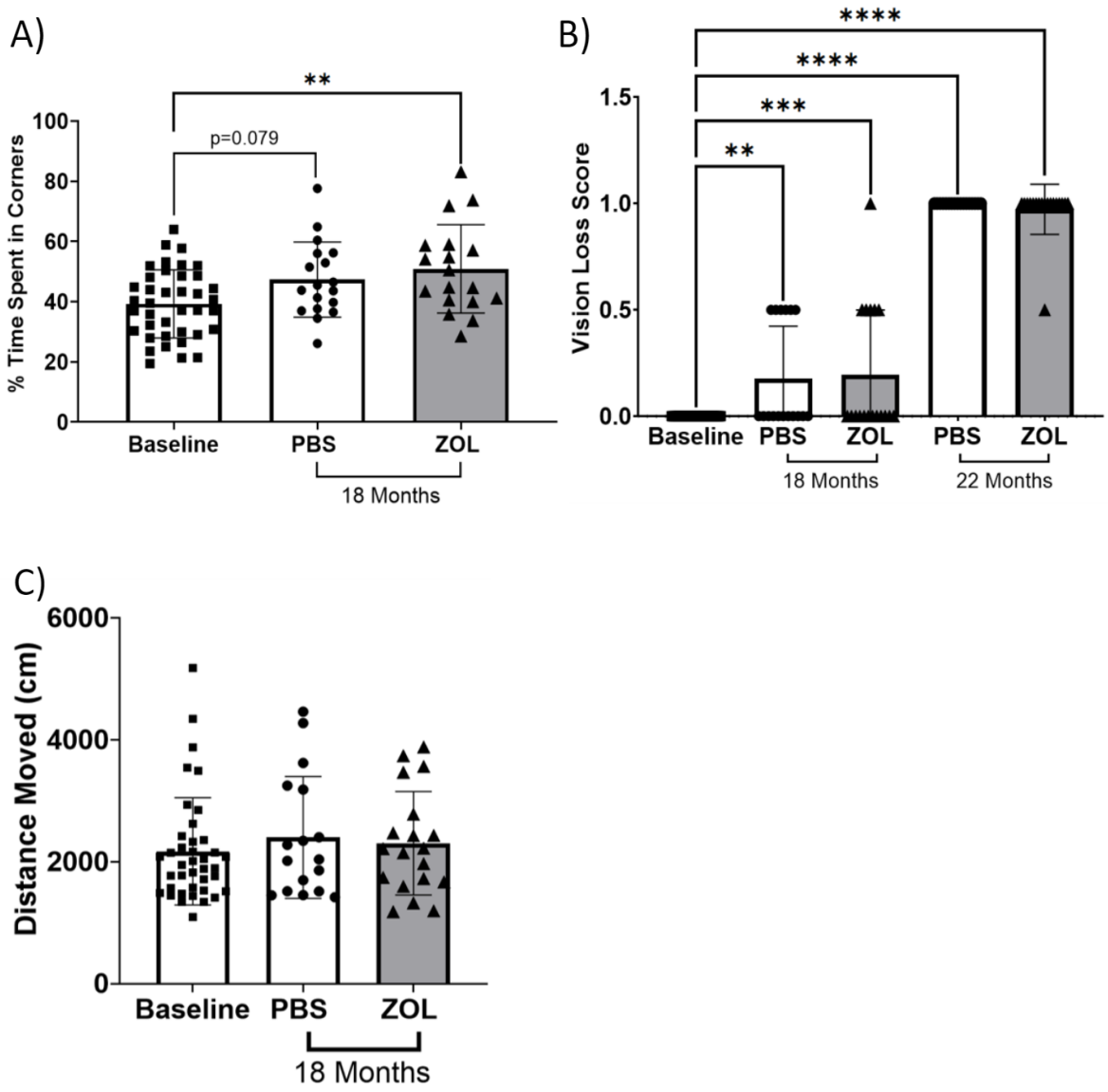

Figure 4.8- ZOL treatment does not impact stress during the open field test.

A) Percentage time spent in corners by month for PBS and ZOL mice. B) Vision loss scores during frailty assay at 18 and 22 months. C) Distanced moved during OF test. Data is shown as the mean +/- the standard deviation. Data were analysed through one way ANOVA with Bonferroni's multiple comparison post-hoc test. PBS = Control Mice, ZOL = Zoledronate treated mice (n=17-19 per treatment group, depending on mouse survival).

4.10 ZOL treatment does not impact to cognitive function-

In order to determine cognitive ability of the mice with age is influenced by ZOL treatment, novel object recognition was performed. This involves placing two identical objects in an arena and then replacing one of the identical objects with a new distinct object. Whether the mice prefer the new object is then used to calculate a discrimination index. This was either done an hour later (short-term memory) or a day later (long-term memory) after training. Mice were tested at baseline (10 months) and at 18 months of age. One ZOL mouse was fully blind at 18 months (Figure 4.8B) and was excluded from further novel object recognition analysis. Blindness was tested using the vision loss test from the frailty index (Table 2.2). This involved slowly lowering the mice towards the table surface and recording at what distance the mouse reached out to the surface of the table.

There was no significant change with age when comparing 18 months and baseline PBS mice for the short-term memory (STM) test's discrimination index (Figure 4.9A). There was no significant difference when comparing the discrimination index of the PBS and ZOL mice at 18 months of age during the STM test. There was no significant difference in the discrimination index with age for either for the PBS or ZOL mice in the long-term memory (LTM) test (Figure 4.9B). In addition to this there was no significant difference in the discrimination index of the mice when comparing the PBS or the ZOL mice at 18 months. It was not possible to repeat this experiment at 22 months as originally planned, as almost all the mice were entirely blind by 22 months (Figure 4.8B). Overall, ZOL treatment does not impact cognition during the NOR test in older mice.

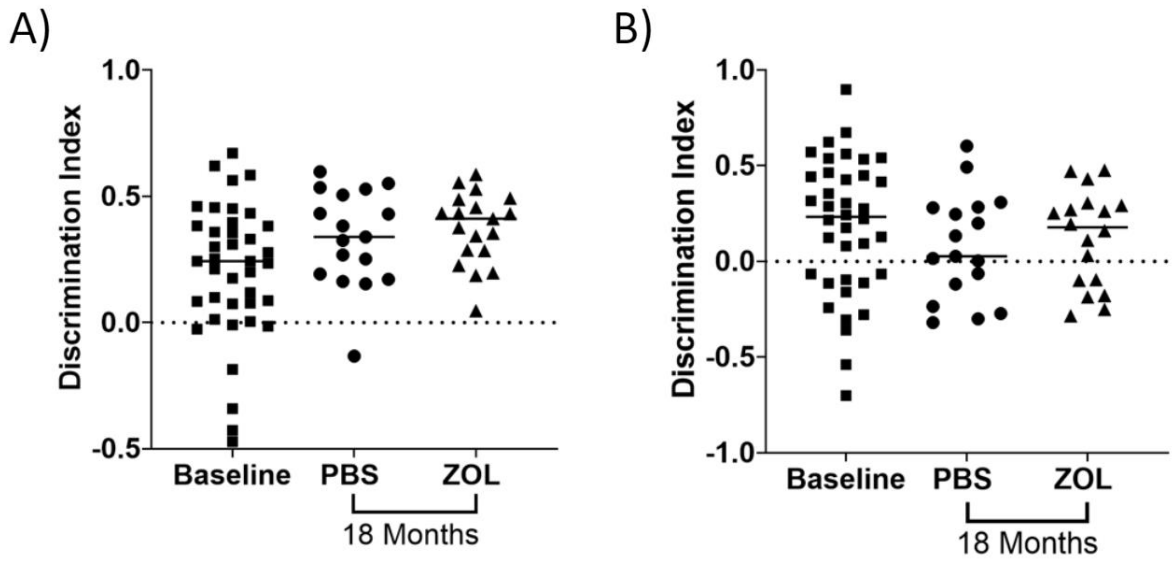

Figure 4.9- ZOL treatment does not impact cognitive function.

A) Discrimination index of the short-term memory test during novel object recognition test for all mice by month and treatment. B) Discrimination index of the long-term memory test during novel object recognition test for all mice by month and treatment. Data is shown as the mean +/- the standard deviation. Data were analysed through one way ANOVA with Bonferroni's multiple comparison post-hoc test. PBS = Control Mice, ZOL = Zoledronate treated mice (n=17-19 per treatment group, depending on mouse survival).

4.11 ZOL does not significantly change mortality in older mice-

Throughout the duration of the experiment, mice were monitored for signs of severe illness that would constitute grounds for euthanasia under our project licence. For a list of these humane endpoints, please see section 2.3.1. When this point was reached the mice were culled, a post-mortem examination was performed, and tissues were then collected for analysis in future investigations. During the post-mortem examination, mice were examined for any abnormalities in the appearance of their organs or visible tumours. There was no significant change in survival in response to ZOL treatment (p=0.094) (Figure 4.10A). There was no significant difference in terms of the proportion of mice that had a tumour present during the post-mortem examinations between the PBS and ZOL groups of mice (Figure 4.10B).

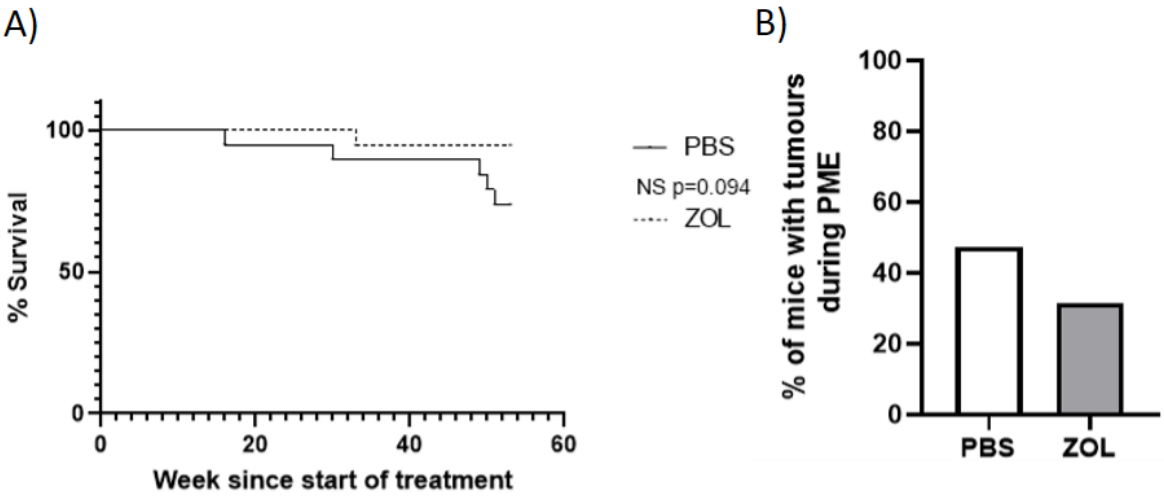

Figure 4.10- ZOL does not significantly change mortality in older mice.

A) Humane end point curve. B) Observable tumour incidence during post-mortem examination. 19 mice per treatment group were given PBS or ZOL. PBS = Control Mice, ZOL = Zoledronate treated mice. When a humane end point was reached date of survival was noted. Difference between two humane end point curves assessed via Log-rank (Mantel–Cox) test. Tumour incidence significance determined with a two-proportion Z test.

4.12 Discussion-

ZOL treated mice scored lower overall on the frailty index, suggesting that ZOL lowers frailty in older mice (Figure 4.3). This study was the first to demonstrate that an mTOR inhibitor can reduce frailty in older mice. There was a steady increase in the frailty index for both treatment groups by month, which only began to level off at 23 months in the PBS mice. This monthly increase in the frailty index in control C57BL/6J mice after 18 months is consistent with previous studies (Keller *et al.* 2019; Rockwood *et al.* 2017; Richardson *et al.* 2021). The work conducted in this study was able to verify that the mouse frailty index is an effective means of assessing changes with age in mice.

The inability of ZOL to improve features of muscular ageing during the grid hanging assay is surprising (Figures 4.4), given ZOL's activity in the muscle on p-AKT signalling in mice (Figure 3.12). This is also surprising given how ZOL, can improve the muscle function of mice in other contexts. For example, ZOL treatment was able to improve the muscle function of mice given chemotherapy in terms of grip strength and whole muscle contractility (Hain *et al.* 2020). ZOL was also able to improve the ability of *Drosophila* to climb with age (Chen *et al.* 2021). In addition to this, evidence in the literature suggests that ZOL can have a small effect on improving muscle mass in osteoporosis following a yearly infusion (Huang *et al.* 2021). Despite this, ZOL has no overall effect on performance during the grid hanging test (Figure 4.4). There was no significant change in performance in the grid hang assay for either of the treatment groups with age. This contradicts the findings of previous studies in the literature that indicate that grid hanging performance is lower in older C57BL/6J mice compared to young C57BL/6J mice (Shang *et al.* 2020; Ahn *et al.* 2017). The inability to detect changes in the grid hanging test might be because the changes with age that occur in this assay by 22 months are too small to detect in female mice. Drugs such as rapamycin that target similar pathways to ZOL have been shown to improve time to fall on the grid hanging test at 30 months of age compared to vehicle treated mice (Ham *et al.* 2020). This may suggest that later time points are required to detect changes in response to drug interventions involving the mTOR pathway in terms of grid hanging time.

ZOL did not significantly improve performance on the rotarod test by 22 months (p=0.071) (Figure 4.5). An explanation as to why ZOL did not improve rotarod significantly is that the mice's performance had not deteriorated sufficiently by 22 months compared to 18 months (as during the grid hanging test). Another explanation for this lack of change with age could be because of the gender of the mice. A previous study has shown that performance on the rotarod test deteriorates significantly with age in male C57BL/6J mice, but not in female C57BL/6J mice (Fischer *et al.* 2016). However, this change was only detectable after 28 months of age. This suggests that repeating this experiment in male mice and assessing them at 28 months may be optimal for ensuring the mice's performance on the rotarod has deteriorated sufficiently. Ensuring that the performance on the rotarod has deteriorated sufficiently with age may make it easier to measure the impact of any geroprotector intervention (such as ZOL) has on rotarod in future studies. Previous studies in the literature have shown that the mTOR inhibitors rapamycin and everolimus can improve the ability of mice to perform on the rotarod (Bitto *et al.* 2016; Zhang *et al.* 2013). However, in both studies this effect was seen after 24 months of age. In addition, treatment began later during the mice's lifespan in both these studies (18-21 months). So, it is difficult to make a direct comparison to this investigation. Although taken together, these studies support the notion that mTOR inhibition may have a positive effect on rotarod/ neuromuscular ability with age in mice.

During the GTT assay, mice showed increased glucose sensitivity with age (Figure 4.6). This was demonstrated by a significant decrease in the AUC for both the older ZOL and the older PBS mice when compared to baseline. While this may seem counterintuitive, there is some precedent in the literature for this. Studies on GTT in mice have shown a decrease in the AUC/ increase in glucose sensitivity with age (Leiter *et al.* 1988; Oh *et al.* 2016; Marmentini *et al.* 2021). Mechanistically this is believed to be caused by reduced insulin clearance in the liver of mice at older age (Marmentini *et al.* 2021). The consequence of this is that glucose is believed to be cleared more quickly from the blood with age in mice. ZOL treatment made no difference to glucose sensitivity compared to PBS treated mice during the GTT assay at any of the time points examined. Previous work on other mTOR inhibitors such as rapamycin has shown that daily administration of rapamycin reduces

glucose tolerance in mice (Arriola Apelo *et al.* 2012; Lamming *et al.* 2013). A potential reason for the difference in response between ZOL and rapamycin maybe due to ZOL being administered less frequently than rapamycin. This is supported by the observation that weekly administration of rapamycin does not impact glucose tolerance (Arriola Apelo *et al.* 2016). ZOL's inability to influence glucose metabolism is surprising given its activity in the pancreas (Figure 3.17). In addition to this, some studies have suggested that patients taking n-BPs have a reduced risk of developing diabetes (Vestergaard 2011; Chan *et al.* 2015; Toulis *et al.* 2015). This makes ZOL's lack of an effect on GTT even more surprising. Overall, ZOL's inability to influence glucose sensitivity is surprising given the effect other drugs targeting similar pathways have on glucose homeostasis.

During the ITT, there was a significant reduction in the AUC under the curve for the PBS mice compared to the baseline (Figure 4.7). However, by 22 months there was no change in the AUC compared to baseline. This suggests that insulin sensitivity improves in a transient fashion with age. Alternatively, the change with age was too small to be consistently detected at older age. This seems more likely, as previous studies in the literature found no significant change with age in insulin sensitivity in mice (Ehrhardt *et al.* 2019; Lamming *et al.* 2013; Marmentini *et al.* 2021). There was a significant increase in the AUC when comparing 18-month-old ZOL and PBS mice. However, at 22 months there was no change when comparing ZOL and the PBS mice. This suggests that ZOL treatment increases insulin resistance at 18 months, but this is only temporary. Drugs targeting similar pathways have also been shown to induce insulin resistance when given daily to mice (Lamming *et al.* 2012; Arriola Apelo *et al.* 2016). A flaw with these studies is that these studies were conducted on young mice (2 months old), so it is unknown what long term effect rapamycin has on insulin resistance on older mice. One reason for the transient nature of this induction of insulin resistance might be the differing levels of expression of mTOR markers in mouse tissues with age in older mice (Baar *et al.* 2015). This could be important as insulin resistance by rapamycin is dependent on mTORC2 inhibition (Deblon *et al.* 2012; Lamming *et al.* 2012). While inhibition of p-AKT in younger mice by ZOL has been established (Figures 3.2-3.20), it is currently unknown what extent this inhibition is maintained in older mice. It is possible that if levels of mTOR markers change with age, that this could affect the ability of mTOR inhibitors to inhibit

mTORC2 and induce insulin resistance. This might explain why the induction of insulin resistance was seen at 18 months and not 22 months. Overall, the healthspan experiment provided further evidence that mTORC2 inhibition may have a role to play in the induction of insulin resistance in mice. However, there was little metabolic change overall in response to ZOL treatment (across both GTT and ITT).

During the open field test, there was no significant change in how long mice spent in the corners of the novel object recognition arena with age in the PBS mice at 18 months compared to baseline (Figure 4.8A). However, there was a significant increase in how long the ZOL mice spent in corners of the novel object recognition arena with age. Previous studies in the literature have indicated that old mice spend longer in corners with age during the open field test (Benice *et al.* 2006; Shoji and Miyakawa 2019). This would indicate the ZOL mice became more stressed with age during this assay. Alternatively, this could also have been influenced by any changes to the mouse's physical ability to move or willingness to move. Another explanation for this increase in time spent in corners might have been due to the increase in partial blindness in the mice at 18 months (Figure 4.8B). This blindness score originated from the frailty index. At 18 months most of the mice had no vision loss during the frailty index, but some of the mice experienced partial vision loss (a vision loss score of 0.5). These mice could still see but were short sighted. This might explain why mice prefer to stay in corners at 18 months of with age. ZOL treatment made no difference when compared to PBS treatment in terms of time spent in corners at 18 months. Similarly, rapamycin also has no effect on time spent in corners during the open field test in younger mice (Cleary *et al.* 2008; Cambiaghi *et al.* 2013). This suggests that mTOR inhibition makes no difference to performance during the open field test. One ZOL mouse had total vision loss/ a vision loss score of 1 at 18 months (Figure 4.8B). This blind mouse was excluded from the novel object recognition analysis as a result. By 22 months almost all the mice were fully blind, so it was not possible to perform either the OF or NOR assay at this time point, as would have been consistent with originally proposed pipeline (Bellantuono *et al.* 2020).

There was no change in distanced moved during the open field test with age when comparing 18- month-old mice to baseline (Figure 4.8C). This suggests that ageing

makes no difference to the stress of the mice in terms of distance moved during the open field test. This contradicts the findings of previous studies that have shown a reduction in distance moved during the open field test with age in mice (Benice *et al.* 2006; Shoji and Miyakawa 2019). A possible explanation for this could have been due to differences in levels of physical fitness in the cohorts of mice. This could have been due to differences in mouse housing or food pellet composition during our study. There was also no significant change when comparing PBS and ZOL mice at 18 months in terms of distance moved. This is also consistent with previous work on mTOR inhibitors such as rapamycin that show no effect on distance moved during the open field test (Cleary *et al.* 2008; Cambiaghi *et al.* 2013).

In terms of neurological function, there was no significant change with age in the STM test (Figure 4.9A). This agrees with previous findings in the literature that show that STM does not change with age in mice (Wimmer *et al.* 2012; Fahlström and Ulfhake 2011). There was also no significant difference when comparing PBS and ZOL mice during the STM test at 18 months. There was no change in LTM with age for either the PBS or ZOL mice (Figure 4.9B). This contradicts previous studies that have shown that LTM decreases with age during NOR (Wimmer *et al.* 2012; Fahlström and Ulfhake 2011). An explanation for this disparity could be that the older mice in these studies in the literature were older than 20 months (Wimmer *et al.* 2012; Fahlström and Ulfhake 2011). The authors did not mention if a vision loss test was performed on these older mice, so it is unclear if this could have impacted their results. Therefore, a limitation to the NOR conducted in this chapter is that the mice were only examined at one time point following treatment (18 months old) for the neurological tests. This was due to almost all the mice becoming fully blind by the originally proposed final time point for NOR (22 months) (Figure 4.8B). Repeating the experiment, but performing NOR monthly on mice that are not fully blind from 18-21 months be optimal for measuring any changes in response to drug treatment. This may increase the chances of detecting a change in response to ZOL treatment if this experiment was to be repeated. ZOL's inability to impact cognitive function is surprising given that a previous study that showed that ZOL treatment lowered the risk of people over the age of 50 from developing dementia (Chang *et al.* 2014). It is also surprising given the impact of ZOL on p-AKT in the brain (Figure 3.13). Currently, there is a lack of research on the effects of other mTOR inhibitors such as

rapamycin on NOR in mice. Overall, ZOL treatment made no different to cognitive function during the NOR test.

There was no impact on ZOL on mouse weight gain compared to PBS mice (Figure 4.2). This is surprising as drugs that target similar pathways such as rapamycin have been shown in studies to have a modest effect on decreasing weight with age in older female mice (Bitto *et al.* 2016; Miller *et al.* 2014; Strong *et al.* 2020). The mice steadily gained weight throughout their lives, but this began to level off at around 20 months. This is consistent with weight gain in ageing female C57BL/6J mice found in the literature (Fisher *et al.* 2016; Fahlström and Ulfhake 2011; Turturro *et al.* 1999).

ZOL did not significantly alter the likelihood of a mouse getting seriously ill and reaching a humane endpoint (p=0.094) (Figure 4.10A). This inability to detect a significant change may be due to limitations in how long the experiment was conducted for. It may have been possible to detect a statistically significant improvement in survival in mice if they had been kept to an older age. Previous studies on ZOL have indicated that it may have a beneficial impact on survival in model organisms and in clinical studies. A notable example of this would be how ZOL treatment improved the survival of *Drosophila* (Chen *et al.* 2021). This is also consistent with previous findings in the literature on patients. For example, older institutionalised patients taking bisphosphonates were found to have 27% reduced risk of death overall (Sambrook *et al.* 2010). Another study demonstrated that ZOL can improve the survival of older patients who had a fractured hip, independent of further fracture reduction (Colón-Emeric *et al.* 2010). The 73.7% survival of the 23-month-old PBS mice by the end of the experiment was roughly consistent with previous studies in the literature on female C57BL/6J mice survival with age (Rowlatt *et al.* 1976; Turturro *et al.* 1999).

Interestingly, only one ZOL mouse reached a humane endpoint. Given the very small number of total mice who reached a humane endpoint in this study (n=6), it is difficult to draw too many conclusions from this. It would be very interesting to test how long this effect on survival is maintained for by keeping the mice alive for longer. It is difficult to determine whether any potential changes in survival in response to ZOL are due to increased bone strength, improved immune function (see section 1.9) or

inhibition of mTOR (or a combination of the three). The exact mechanisms by which ZOL confers a benefit to survival in mammals remain unknown.

The inability of ZOL to significantly lower the incidence of tumours during the post-mortem examination was surprising (Figure 4.10B). Especially given how, a retrospective study on patients found that ZOL reduces the incidence of cancer in older female patients (Reid *et al.* 2020). Once again, it is possible that the mice were not kept alive long enough for a change to be measured. Another possibility was that some tumours may not have been visible during the post-mortem examination. Future histological studies on the tissues collected during this experiment may be more able to more accurately detect any difference in tumour incidence between the two groups of mice. This tumour incidence was roughly equal to that of previous studies on aged female C57BL/6J control mice culled at 22-24 months (Rowlatt *et al.* 1976; Nakamura *et al.* 1992).

A flaw with this study is that only female mice were examined for changes in healthy ageing. Female mice were selected for this study because of the benefits to survival in response to ZOL treatment starting at middle age in female *Drosophila* and in patients (Chen *et al.* 2021; Colón-Emeric *et al.* 2010). This could be an issue as there were differences in survival between *Drosophila* receiving ZOL treatment (Chen *et al.* 2021). Female *Drosophila* had a slightly stronger improvement in lifespan in response to ZOL treatment starting at mid-life than male *Drosophila* (Chen *et al.* 2021). There are also gender differences in how mice respond to other mTOR inhibitors such as rapamycin in terms of lifespan increase (Harrison *et al.* 2009; Miller *et al.* 2014; Strong *et al.* 2020). Female mice responded more positively to rapamycin in terms of percentage increase in survival during these studies. Lastly, genetic knockouts of mTORC2 had a detrimental effect on the lifespan of male but not female mice (Lamming *et al.* 2014). Overall, these studies suggest that ZOL may have a different effect on the lifespan of male mice.

A limitation to this investigation was that it was not possible to determine if p-AKT was inhibited in the mouse tissues by the end of the healthspan experiment. This would have provided some evidence that a marker of mTOR signalling was inhibited by the end of the experiment in mouse tissues. It is also possible that different doses or treatment intervals of ZOL may confer more beneficial effects on healthspan.

There is some *in vitro* evidence that supports the notion that repeated doses of zoledronate at lower doses may be more beneficial in inhibiting mTOR. One paper on osteoblasts indicated that treating cells with zoledronate twice weekly for two weeks resulted in a reduction in p-S6/ total S6 when at 1 nM and increased the ratio of p-S6/ total S6 when at 1 µM (Gao *et al.* 2018). This suggests that lower doses of ZOL may be beneficial for inhibiting mTORC1 when given repeatedly. However, it is important to better understand the mechanisms by which ZOL inhibits the mTOR pathway (both mTORC1 and mTORC2) at different concentrations, before recommending any future healthspan studies using different doses of ZOL in mice.

There is evidence collected during this investigation to support the notion that 3 Days post injection is the best time interval for inhibiting p-AKT (Figures 3.2-3.30). However, it is currently unknown whether this inhibition was maintained in response to multiple injections over the course of the healthspan experiment. From a mechanistic standpoint the FPPS enzyme should remain consistently inhibited since p-AKT inhibition is due to mevalonate pathway inhibition (Misra *et al.* 2016). However, given that p-AKT increases in the kidney at Day 7 post injection (Figure 3.16), it is possible that there may be a feedback mechanism that increases p-AKT. It would be advisable to eliminate the possibility of repeated doses of ZOL activating rather than inhibiting mTOR markers. This will be addressed in future experiments in a later chapter.

Overall, this chapter was able to determine that ZOL can modestly improve some features of healthy ageing in mice by 23 months of age. However, this was limited by the fact that the mice had to be culled by 23 months and couldn't be assessed at later age. An example of this would have been mouse survival (Figure 4.10A), as this did not significantly change in response to ZOL (p=0.094). This may also have influenced rotarod, which also did not significantly change by the end of the experiment (p=0.071) (Figure 4.5). Unfortunately, it was not possible to complete the healthspan pipeline up until 24 months as recommended by others (Bellantuono *et al.* 2020) due to time restrictions for the completion of this degree. Going back to the *in vitro* model that first demonstrated that ZOL could act as a geroprotector (Misra *et al.* 2016) may offer some additional insights into the outcome of this healthspan experiment.

Chapter 5 - Effect of zoledronate on mTOR pathway in hMSCs *in vitro*.

5.1 Introduction-

Given the modest impact of ZOL treatment on healthspan in chapter 4, it was decided to examine the mechanisms by which ZOL can inhibit mTOR in a bit more detail. ZOL's inability to substantially improve healthspan in mice could have been due to preferential inhibition of mTORC2 compared to mTORC1. Given the importance of inhibiting mTORC1 signalling in promoting longevity (Selman *et al.* 2009; Zhang *et al.* 2017), it was important to look at ZOL's impact on mTORC1 signalling more thoroughly. Another possibility was that prolonged exposure to an mTOR inhibitor such as ZOL may have different effects on mTOR markers compared to a short-term exposure. Some studies have shown that prolonged mTOR inhibition by stimuli such as deprivation of specific amino acids can trigger feedback mechanisms through long term hyperactivation of mTOR markers following initial inhibition (Buel *et al.* 2022; Moloughney *et al.* 2016). In order to start to answer some of these questions, it was decided to return to the *in vitro* model that first demonstrated that ZOL could work as a geroprotector (hMSCs).

As described in a previous section (Section 1.10), mTOR signalling is split into two signalling complexes: mTORC1 and mTORC2. Both complexes contain similar components: such as an mTOR complex and DEPTOR. However, both mTORC1 and mTORC2 contain additional proteins that are unique to each complex such as RICTOR (Rapamycin Insensitive Companion of mTOR) and RAPTOR (Regulatory Associated Protein of mTOR). There are many important markers of mTOR activation. One of which is the activity of the mTOR protein complex itself. This complex contains 2549 amino acids and has several different domains. One of which is the negative regulatory domain (NRD), which contains several phosphorylation sites that are required for mTOR activation: one of which is Ser2448 (Li *et al.* 2014). In addition to mTOR, there are downstream markers that can be assessed to measure levels of mTORC1 and mTORC2 signalling. One example of such a downstream marker is that of AKT. AKT is a serine/threonine protein kinase that regulates cell functions such as glucose metabolism, survival, cytoskeletal and proliferation. AKT is activated by phosphorylation at Ser473 by mTORC2 (Sarbassov

et al. 2005). P70S6K is an enzyme responsible for activation of ribosomal protein S6 and is a marker of mTORC1 activation. This is because mTORC1 phosphorylates P70S6K at Thr389, which is part of P70S6K's linker domain (Bahrami et al. 2014). Ribosomal protein S6 is activated by P70S6K and is involved in translation of proteins at ribosomes.

Firstly, the work in this chapter sought to verify that ZOL can inhibit markers of mTOR signalling. Secondly, the experiments conducted during this chapter sought to reveal insights into the mechanisms of ZOL's inhibition of mTOR. This included improving gaps in our understanding of how long mTOR inhibition is achieved by ZOL in hMSCs. This is important given the short duration of p-AKT inhibition observed in mouse tissues in a previous chapter (Figures 3.2-3.20). This raises the question as to whether this effect is unique to mice or can also be seen in hMSCs. It is also currently unknown at what range of concentrations mTOR inhibition by ZOL is achieved. This is important for understanding the mouse tissue results in chapter 3. Radioactive labelling studies of ZOL study on mice, dogs and rats has uncovered a similar disparity in concentration of the drug between skeletal and non-skeletal mouse tissues (Weiss *et al.* 2008; Nikzad *et al.* 2013; Yousefnia *et al.* 2015). Previous studies have indicated that other nitrogen containing bisphosphonates are found at relatively low concentrations in mice in non-skeletal mouse tissues (Mönkkönen *et al.* 1990; Masarachia *et al.* 1996). Despite this, ZOL can achieve inhibition of p-AKT in these non-skeletal tissues. During the ZOL healthspan experiment in mice, the drug was given repeatedly, as opposed to once during the ZOL tissue time course experiments in chapter 3. Therefore, it is also important to begin to better understand whether repeated doses of ZOL treatment are capable of inhibiting mTOR markers.

5.2 Donor gender has no effect on ZOL's ability to inhibit p-AKT at 1 µM-

During the ZOL time course and healthspan experiments, female mice were treated with ZOL. In addition to this, analysis of the improvement of non-skeletal survival by ZOL focussed on post-menopausal women (Colón-Emeric *et al.* 2010). Furthermore, ZOL treatment beginning at midlife has a greater impact on *Drosophila* lifespan extension that on male *Drosophila* (Chen *et al.* 2021). During the experiments conducted in this chapter, hMSCs were grown from donors of different genders. To determine if donor gender was having any effect on ZOL's ability to inhibit p-AKT, a comparison by donor gender in the reduction in p-AKT was performed. These were all from cells treated at 1 µM for three days across the different experiments conducted in this chapter. Upon completion of the analysis, the average reduction in p-AKT per donor in response to 1 µM for three days was unaffected by donor gender (Figure 5.1).

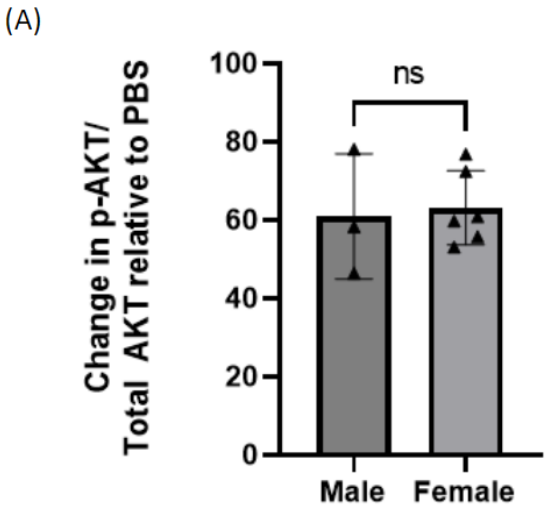

Figure 5.1- Donor gender has no effect on ZOL's ability to inhibit p-AKT at 1 µM.

A) Quantification of reduction in p-AKT/ Total AKT ratio by gender. Data is shown as the mean +/- the standard deviation. Data were analysed through an unpaired T-test. PBS = Control hMSCs, ZOL = Zoledronate treated hMSCs (n=3-6 per treatment group).

5.3 Zoledronate can reduce p-AKT signalling when frozen and so can ZOL that is used clinically in patients-

The ZOL solution used in these experiments was originally in powder form and was of a different formulation to the ZOL that is used clinically. Consequently, it was prudent to ensure that both formulations of ZOL were effective at inhibiting p-AKT. In addition, ZOL was prepared fresh from powder during the *in vitro* experiments. In comparison, a large bulk solution of ZOL was prepared from the powder and was frozen in aliquots to ensure reproducibility between injections during the healthspan experiment. This experiment also sought to verify that freezing the ZOL solution did not impact p-AKT inhibition in the hMSC model prior to the start of the injection regimen in the healthspan experiment.

Cells were either treated with zoledronate at 1 µM freshly prepared from powder, 1 µM frozen ZOL solution that had been prepared from powder or 1 µM ZOL solution used clinically in patients. All three zoledronate treatments showed reduced p-AKT/ Total AKT compared to the PBS control (Figure 5.2). There was no significant difference between ZOL treatments in terms of the reduction in the p-AKT/ total AKT ratio compared to the control. This indicates that the ZOL solution used in patients and the bulk frozen solution can inhibit p-AKT.

During the mouse healthspan experiment (chapter 4), the bulk frozen ZOL solution was used throughout for injections. Towards the end of the healthspan experiment, spare aliquots of this ZOL solution were used to treat hMSCs from for three days at 1 µM. This was done when the mice were 20 months old (10 months after the solution was formulated). This was to check that 10 months of freezing had not impaired the ability of the bulk ZOL solution to inhibit p-AKT. This experiment was able to demonstrate that the ZOL solution used throughout the healthspan experiment was still effective at inhibiting p-AKT in hMSCs after 10 months of freezing (Figure 5.3).

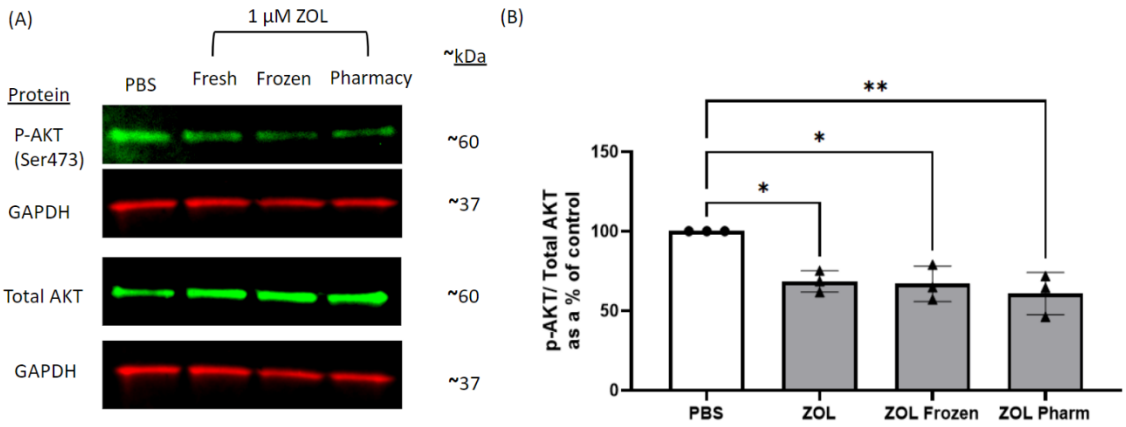

Figure 5.2- Zoledronate can reduce p-AKT signalling when frozen and so can ZOL that is used clinically in patients.

A) Example western blot for the expression of p-AKT, total AKT and GAPDH. B) Quantification of p-AKT/ Total AKT ratio. Data is shown as the mean +/- the standard deviation. Data were analysed through one way ANOVA and Tukey's multiple comparison post-hoc test. PBS = Control hMSCs, ZOL = Zoledronate treated hMSCs (n=3 per treatment group).

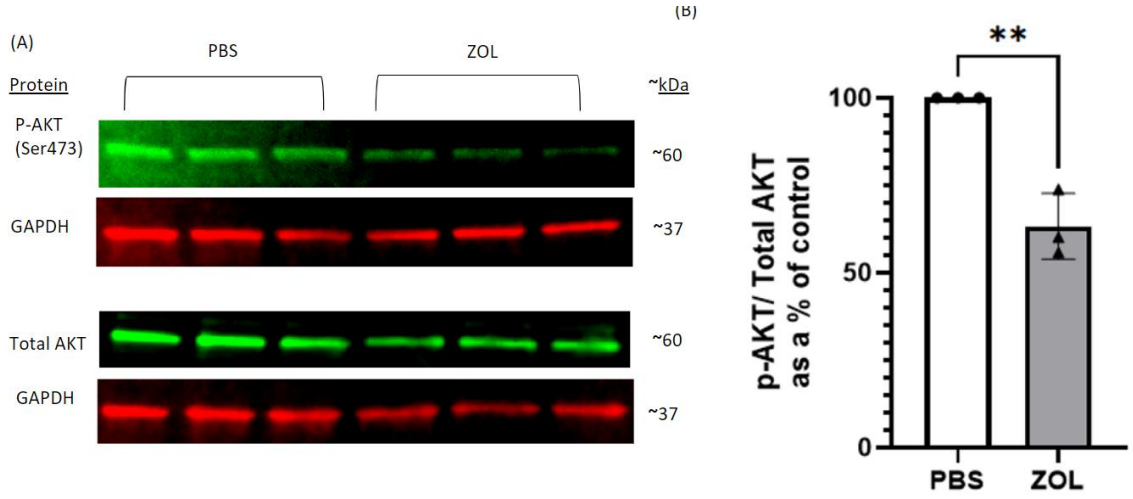

Figure 5.3- Zoledronate solution used in healthspan experiment can inhibit p-AKT in hMSCs 10 months after freezing of solution.

A) Example western blot of p-AKT, total AKT and GAPDH expression. B) Quantification of p-AKT/ Total AKT ratio. Data is shown as the mean +/- the standard deviation. Data were analysed through an unpaired T-test. PBS = Control hMSCs, ZOL = Zoledronate treated hMSCs (n=3 per treatment group).

5.4 Zoledronate can inhibit p-AKT in human Mesenchymal Stem Cells (hMSCs) at a broad variety of concentrations-

ZOL can inhibit p-AKT in a broad variety of non-skeletal mouse tissues (Figures 3.2-3.20). This was surprising as previous work in the literature on radioactively labelled ZOL indicated that ZOL is present in non-skeletal mammalian tissues at concentrations 10-1000 times lower than the bone (Weiss *et al.* 2008; Yousefnia *et al.* 2015; Nikzad *et al.* 2013). In hMSCs, ZOL was able to inhibit mTOR signalling at 1 µM ZOL after 72 hours (Misra *et al.* 2016). However, the impact of other concentrations of ZOL on p-AKT markers was not examined. This could be important as a previous study demonstrated that ZOL can activate the mTOR marker p-S6 at high concentrations of ZOL and inhibit it at 1 nM in osteoblasts (Gao *et al.* 2018). In order to examine this, hMSCs were treated with varying concentrations of ZOL (1 pM- 10 µM) for 72 hours. As a control cell were treated with an equivalent volume of PBS. The inhibition of p-AKT/ total AKT was maintained in response to zoledronate compared to PBS at all concentrations examined (Figure 5.4). There was no significant difference in p-AKT inhibition between doses of ZOL run on the same blot.

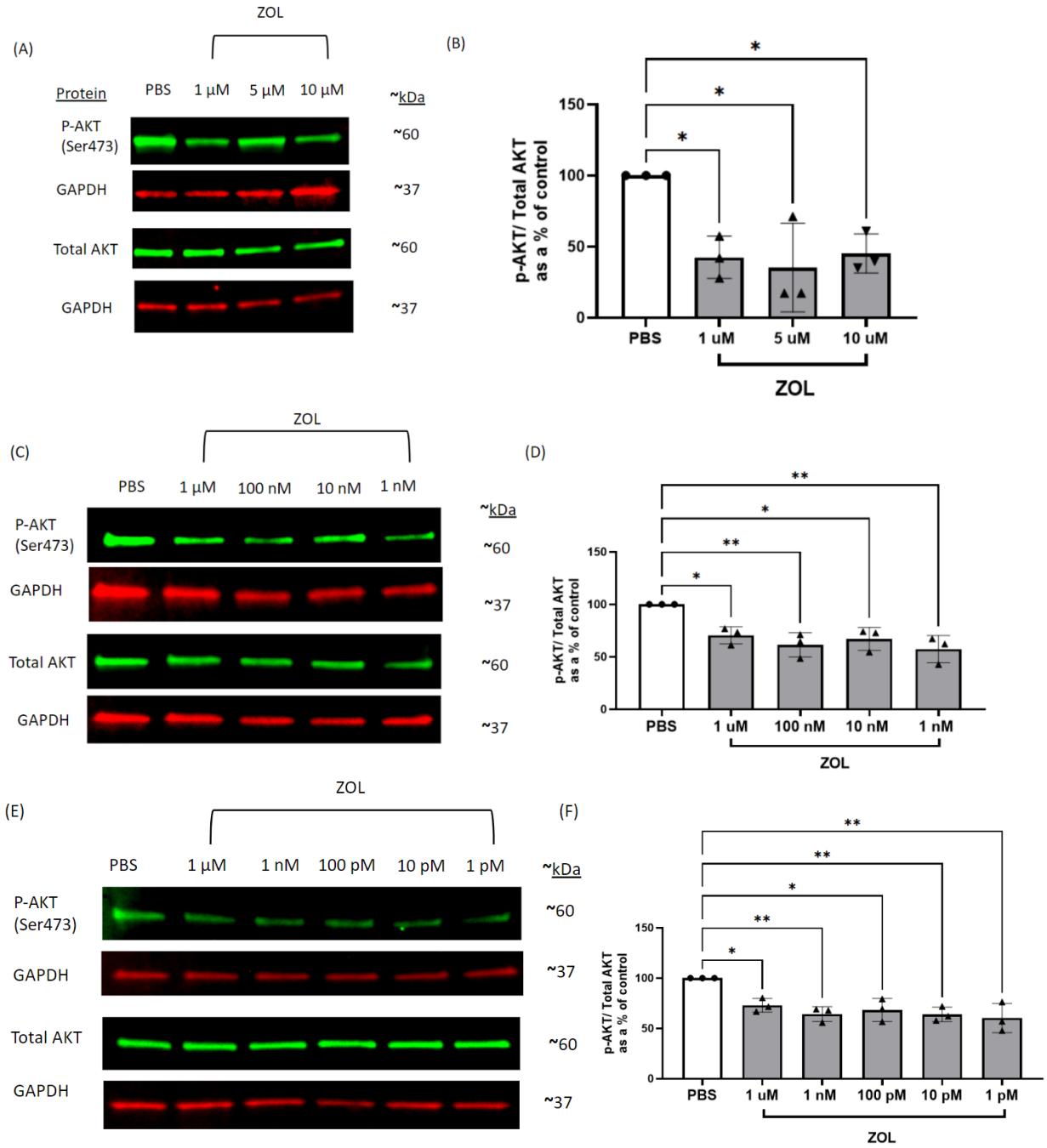

Figure 5.4- Zoledronate can inhibit p-AKT in human Mesenchymal Stem Cells (hMSCs) at a broad variety of concentrations.

A) Example western blot of p-AKT, Total AKT and GAPDH expression in response to ZOL at 1-10 µM concentration. B) Quantification of p-AKT/ Total AKT ratio at µM concentration. C) Example blot of p-AKT/ Total AKT expression in response to ZOL at 100-1 nM concentration. D) Quantification of p-AKT/ Total AKT ratio at nM concentration. E) Example blot of p-AKT/ Total AKT expression in response to ZOL at 100pM-pM concentration. F) Quantification of p-AKT/ Total AKT ratio at pM concentration. Data is shown as the mean +/- the standard deviation. Data were analysed through one-way ANOVA and Tukey's multiple comparison post-hoc test. PBS = Control hMSCs, ZOL = Zoledronate treated hMSCs (n=3 per treatment group).

5.5 Inhibition of p-AKT by ZOL is mediated by the mevalonate pathway-

A previous study was able to demonstrate that the mevalonate pathway was involved in the inhibition of p-AKT by ZOL at 1 µM in hMSCs (Misra *et al.* 2016). This was done by treating cells with downstream products of the mevalonate pathway: FOH and GGOH in addition to ZOL. During this previous study, treating hMSCs with FOH and GGOH reversed the inhibition of p-AKT by ZOL. This implicated the mevalonate pathway in ZOL's inhibition of p-AKT. In order to verify this finding, this experiment would be repeated in hMSCs. In addition to this, cells would be treated with 1 µM or 1 nM ZOL, to determine if the mevalonate pathway was responsible for the inhibition of p-AKT at both concentrations.

There was a significant drop in the ratio of p-AKT/ Total AKT in response to zoledronate at both 1 µM and 1 nM concentrations (Figure 5.5). Crucially the addition of the downstream metabolites (FOH and GGOH) in combination with zoledronate treatment reversed this inhibition of p-AKT. Treatment of cells with ethanol and ZOL at these two concentrations failed to reverse the inhibition. Since ethanol was used to dissolve the FOH and GGOH, this would implicate the mevalonate pathway in the inhibition of p-AKT signalling at both 1 µM and 1 nM concentrations.

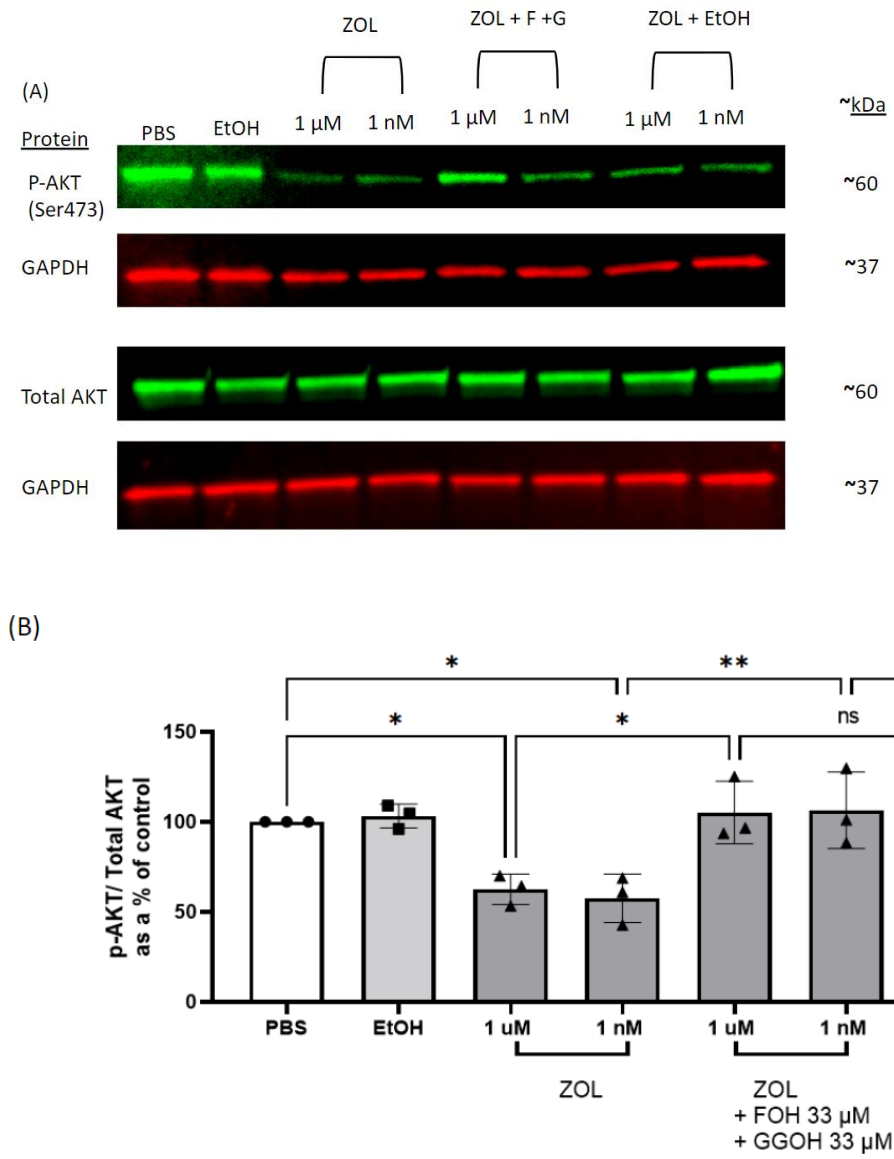

Figure 5.5- Inhibition of p-AKT by ZOL is mediated by the mevalonate pathway.

A) Example western blot of the expression of p-AKT, total AKT and GAPDH. B) Quantification of p-AKT/ Total AKT ratio. Data is shown as the mean +/- the standard deviation. Data were analysed through one way ANOVA and Bonferroni multiple comparison post-hoc test. PBS = Control hMSCs, ZOL = Zoledronate treated hMSCs (n=3 per treatment group).

5.6 Zoledronate lowers levels of mTOR markers at concentrations of 1 µM-1 pM-

During a previous experiment, ZOL treatment was able to inhibit the downstream mTORC2 marker p-AKT at concentrations as low as 1 pM (Figure 5.4). A previous study had found that 1 µM ZOL reduces levels of the following mTOR markers in hMSCs after 72 hours: p-P70S6K (Thr421/Ser424), p-AKT (Ser473) and p-mTOR (Ser2448) (Misra *et al.* 2016). It was unclear if ZOL had a similar effect on other markers of overall mTOR and mTORC1 activity at lower concentrations. To this end, hMSCs were again treated with varying concentrations of ZOL for 72 hours and several markers of mTOR activity were assessed. This time the following mTOR markers were examined via western blot: p-AKT, p-P70S6K and p-S6 and p-mTOR. In addition, the total amount of each of these markers was assessed: total AKT, total P70S6K, total S6 and total mTOR. The markers p-S6 and p-P70S6K are markers of mTORC1 activity. Meanwhile, p-mTOR corresponds to overall levels of mTOR signalling that are reduced by zoledronate. Inhibition of p-AKT was again examined to verify the findings from the previous experiment.

Inhibition of p-AKT signalling was again observed at concentrations of 1 µM, 1 nM and 1 pM ZOL (Figure 5.6B), verifying the findings of the previous experiment. Inhibition of p-mTOR was also achieved at concentrations 1 µM, 1 nM and 1 pM ZOL in hMSCs (Figure 5.6C). There was a significant reduction in the phosphorylation of p-P70S6K at 1 nM, but not at the other concentrations examined (Figure 5.6D). Similarly there was a significant reduction in the phosphorylation of p-S6 at 1 µM and 1 nM, but no significant change in response to 1 pM ZOL (Figure 5.6E). This inability to reach significance at certain concentrations of ZOL might be attributed to the larger variation observed in the reduction of p-S6 and p-P70S6K.

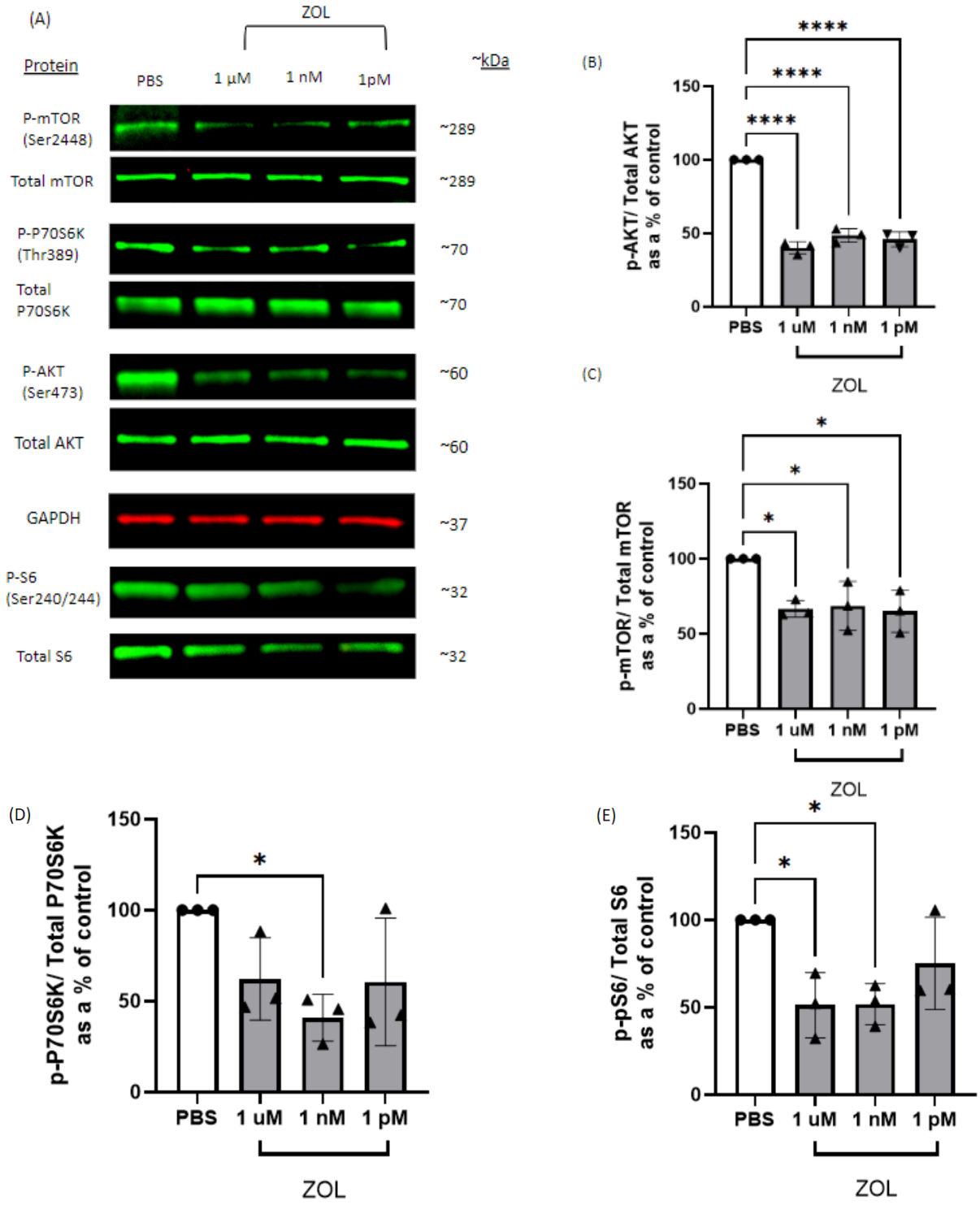

Figure 5.6- Zoledronate lowers levels of mTOR markers at concentrations of 1 µM-1 pM.

A) Example western blots of the expression of p-mTOR, total mTOR, p-P70S6K, total P70S6K, p-AKT, total AKT, p-S6 total S6 and GAPDH. B) Quantification of p-AKT/ Total AKT ratio. C) Quantification of p-mTOR/ Total mTOR ratio. D) Quantification of p-P70S6K/ Total P70S6K ratio. E) Quantification of p-S6/ Total S6 ratio. Data is shown as the mean +/- the standard deviation. Data were analysed through one way ANOVA and Tukey's multiple comparison post-hoc test. PBS = Control hMSCs, ZOL = Zoledronate treated hMSCs (n=3 per treatment group).

5.7 Washing off zoledronate results in a short duration of inhibition of markers of mTOR signalling-

During the time course experiments in mice, the effect of ZOL on p-AKT inhibition was short in duration following a single injection and was absent by day Day 7 in most tissues (Figures 3.2-3.20). In order to determine if ZOL treated hMSCs exhibited a similar duration of mTOR inhibition, hMSCs were treated with ZOL for three days at 1 μM as previously discussed in this chapter. Afterwards, cells were rinsed twice with PBS and had fresh medium applied to them (without ZOL). These were then cultured for either 1, 3, 5 or 7 days after the washing off and then western blotting of the same mTOR markers as in Figure 5.6 was performed. An additional treatment condition of three days of ZOL treatment and no washing off was also collected. For an overview of the experiment, please see Figure 5.7.

When cells were treated with 1 μM ZOL for three days and no washing off was attempted, there was a reduction in p-AKT (Figure 5.8B). There was also a significant reduction in p-mTOR and p-S6 prior to washing off (Figure 5.8C and Figure 5.8E). There was no significant reduction in p-P70S6K prior to washing off the drug (Figure 5.8D). There was a significant reduction in p-AKT in response to ZOL after 1 Day of washing off the drug and a significant increase in p-AKT at Day 7 after washing off the drug (Figure 5.8B). However, there was no other change in p-AKT at the other time points. Similarly, there was a significant reduction in p-mTOR in response to ZOL after 1 Day of washing off the drug and a significant increase in p-mTOR at Day 7 after washing off the drug (Figure 5.8C). Again, there was no change in p-mTOR at the other time points examined. There was no significant change in p-P70S6K after washing off ZOL at any of the time points examined (Figure 5.8D). There was an increase in p-S6 in response to ZOL after washing off at Day 5, but there was no other significant change at the other time points examined (Figure 5.8E).

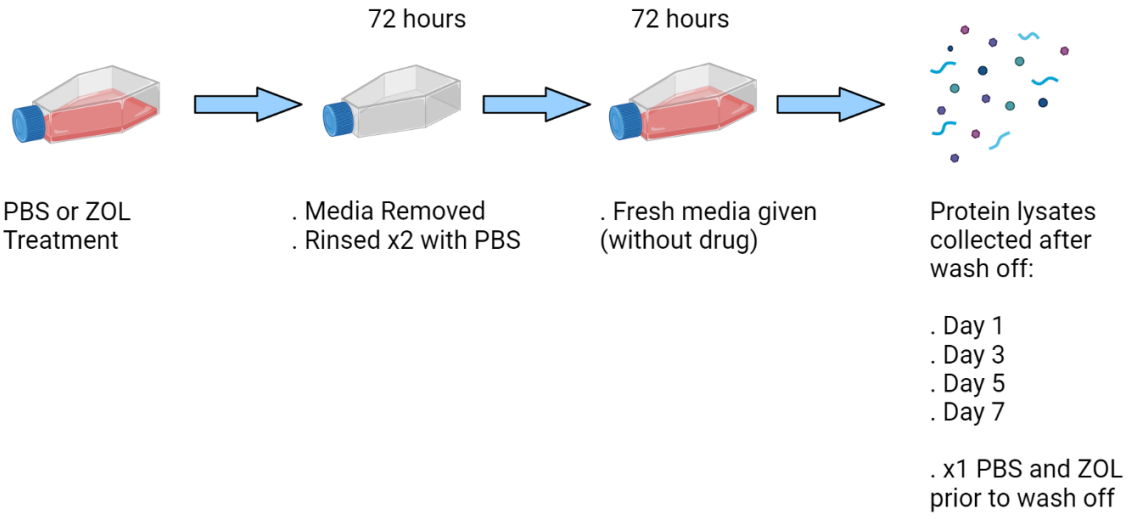

Figure 5.7 - Diagrammatic representation of washing off ZOL experiment. Created with Bio-Render.com.

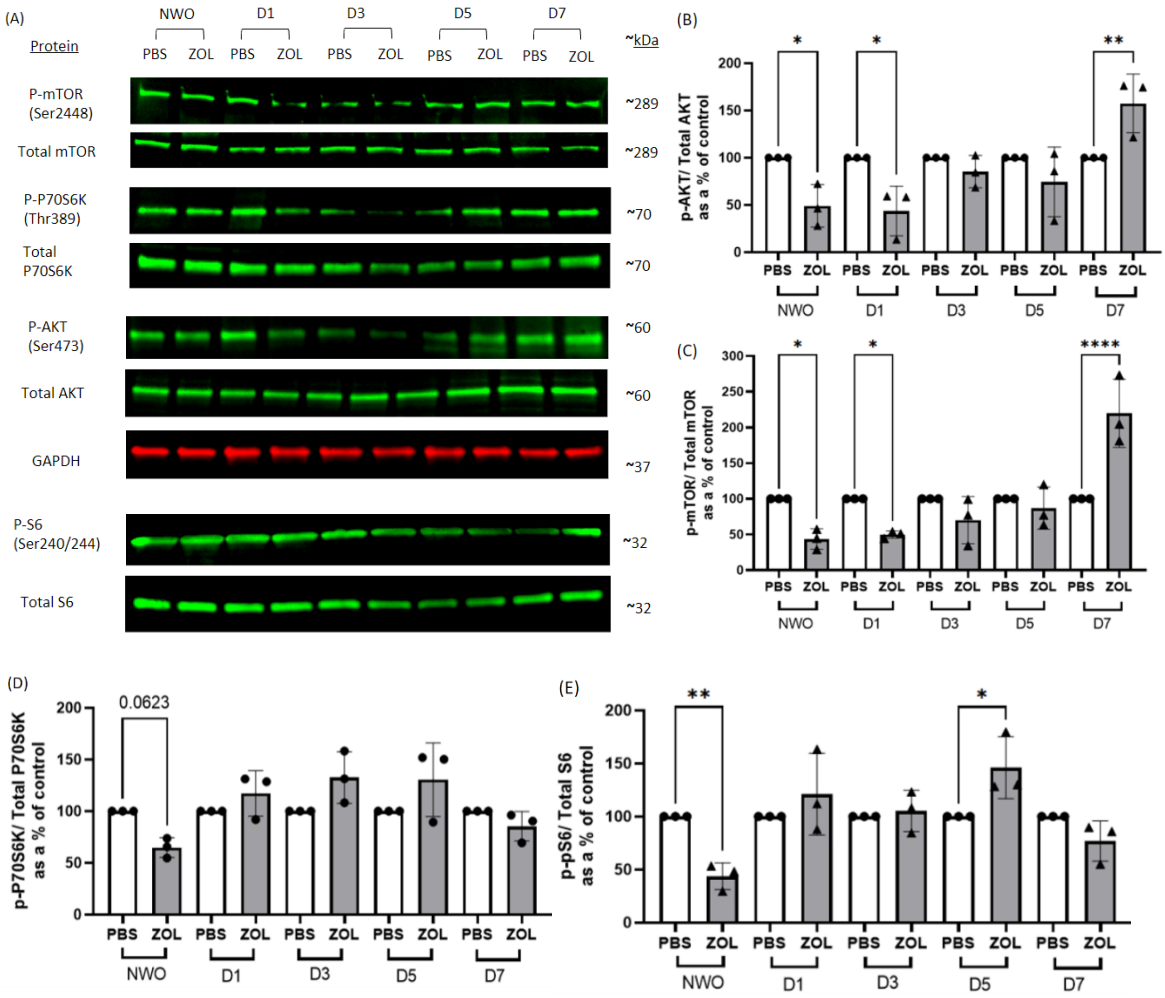

Figure 5.8- Washing off zoledronate results in a short duration of inhibition of markers of mTOR signalling.

A) Example western blots of the expression of p-mTOR, total mTOR, p-P70S6K, total P70S6K, p-AKT, total AKT, p-S6, total S6 and GAPDH. B) Quantification of p-AKT/ Total AKT ratio. C) Quantification of p-mTOR/ Total mTOR ratio. D) Quantification of p-P70S6K/ Total P70S6K ratio. E) Quantification of p-S6/ Total S6 ratio. Data is shown as the mean +/- the standard deviation. Data were analysed through one way ANOVA and Bonferroni's multiple comparison post-hoc test. PBS = Control hMSCs, ZOL = Zoledronate treated hMSCs (n=3 per treatment group). NWO= No Wash Off, D1= Day 1, D3 = Day 3, D5 = Day 5 and D7 = Day 7.

5.8 Repeated doses of ZOL have differing effects on various markers of mTOR inhibition-

In order to determine if the effects of ZOL on inhibiting markers of mTOR markers was maintained when given repeatedly, hMSCs were given a fresh dose of 1 µM ZOL every three days for 12 days. Protein extraction was performed on cells treated for 3, 6, 9 or 12 days with ZOL or PBS (see Figure 5.9 for overview). Since mice were given ZOL twice weekly as part of the healthspan experiment, it was important to gain some insight into what impact repeated doses of ZOL had on the mTOR markers. Repeated doses of ZOL were sufficient to reduce the p-AKT at all time points examined: after Day 3, 6, 9 and 12 of ZOL treatment (Figure 5.10B). Similarly, the p-mTOR was also reduced by repeated doses of ZOL at Day 3, 6, 9 and 12 (Figure 5.10C). Meanwhile, p-P70S6K was reduced at Day 3 but was unchanged at the other time points (Figure 5.10D). Similarly, p-S6 was reduced at Day 3 but was unchanged at the other time points (Figure 5.10E).

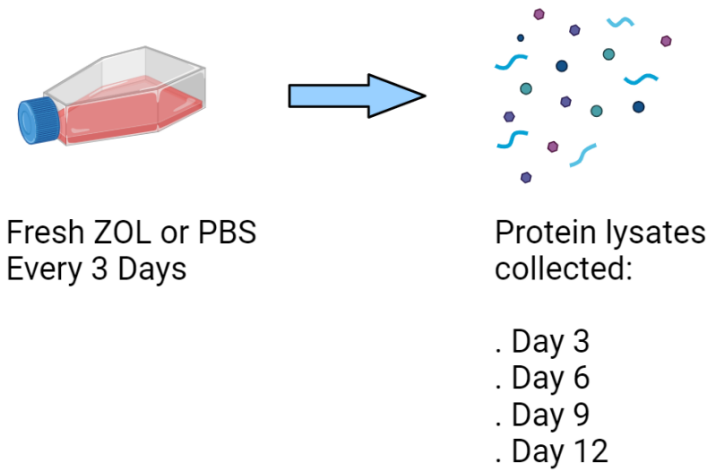

Figure 5.9 - Diagrammatic representation of repeated ZOL dose experiment. Created with Bio-Render.com.

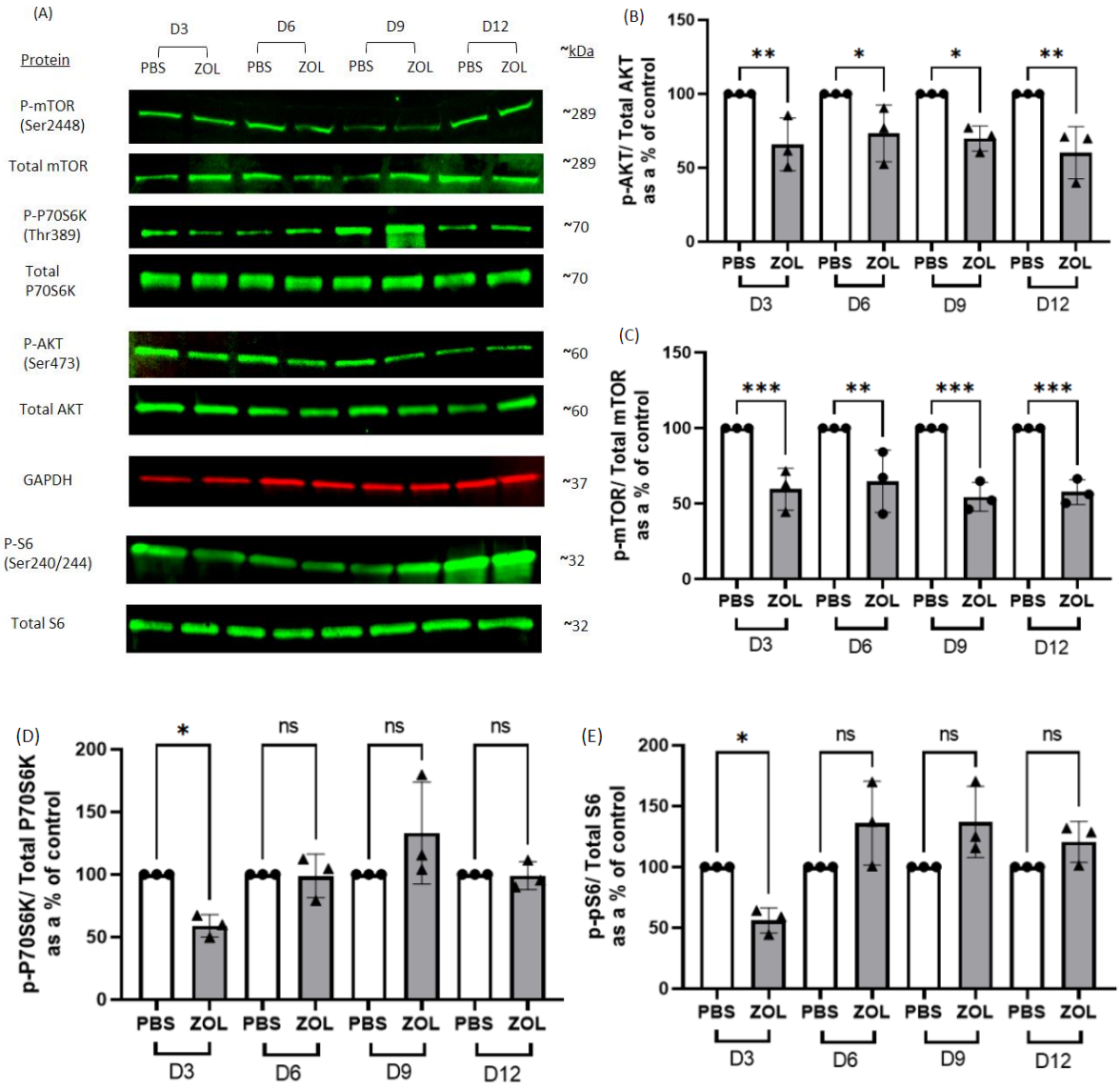

Figure 5.10- Repeated doses of ZOL having differing effects on various markers of mTOR inhibition.

A) Example western blots of the expression of p-mTOR, total mTOR, p-P70S6K, total P70S6K, p-AKT, total AKT, p-S6, total S6 and GAPDH. B) Quantification of p-AKT/ Total AKT ratio. C) Quantification of p-mTOR/ Total mTOR ratio. D) Quantification of p-P70S6K/ Total P70S6K ratio. E) Quantification of p-S6/ Total S6 ratio. Data is shown as the mean +/- the standard deviation. Data were analysed through one way ANOVA and Bonferroni's multiple comparison post-hoc test. PBS = Control hMSCs, ZOL = Zoledronate treated hMSCs (n=3 per treatment group). D3 = Day 3, D6 = Day 6, D9= Day 9 and D12 = Day 12.

5.9 Discussion-

Given the modest effects of ZOL treatment on mouse healthspan in the previous chapter, the work conducted in this chapter sought to shed further light on the mechanisms of mTOR inhibition by ZOL. Firstly, this involved checking that the ZOL solution used during the healthspan experiment was capable of inhibiting p-AKT in hMSCs. Indeed, prior to the injection regimen and 10 months after freezing, the ZOL solution was still capable of inhibiting the p-AKT pathway in hMSCs (Figure 5.2). This suggests that the ZOL solution throughout the healthspan experiment should have been capable of inhibiting p-AKT in the mice. Western blotting of the mouse tissues collected at the end of the experiment will be necessary to verify this though. This experiment was also able to demonstrate that the ZOL used in patients clinically has a similar inhibitory effect at 1 µM on p-AKT signalling as the solution derived from the ZOL in powder form (Figure 5.2). This supports the notion that the ZOL given to patients should have a similar effect on p-AKT to the ZOL powder that was used during these experiments.

ZOL inhibited p-AKT at a broad variety of different concentrations in hMSCs in this study (Figure 5.4). A connection could be drawn between this consistent drop in p-AKT/ Total AKT in cells and the effects zoledronate has on non-skeletal tissues (see Figures 3.2-3.19). Studies in mammalian systems (mice, rats and dogs) in the literature have indicated that radioactively labelled zoledronate is present in these tissues at far lower concentrations than in the bone (Weiss *et al.* 2008; Nikzad *et al.* 2013; Yousefnia *et al.* 2015). The concentration of ZOL in these tissues was found to be 10-1000 times lower depending on tissue type. Interestingly, there is still some activity in some of these tissues in response to ZOL in terms of p-AKT reduction (for example in the heart). The effects of ZOL on p-AKT signalling at low concentrations may explain why it ZOL is capable of inhibiting p-AKT in these non-skeletal tissues.

This study was also able to verify the previous finding in the literature that ZOL treatment at 1 µM was due to the mevalonate pathway in hMSCs (Figure 5.5) (Misra *et al.* 2016). Crucially, it was also able to demonstrate that the inhibition of ZOL at a lower concentration of 1 nM was also dependent on the mevalonate pathway. There is some evidence in the literature that indicates that ZOL can inhibit the FPPS enzyme at nM concentrations, which supports these findings (Dunford *et al.* 2001; Ali

et al. 2015). However, the reduction at picomolar concentrations is particularly surprising given the lack of evidence in the literature to support its activity on FPPS at these levels. Although, if ZOL can have a physiological effect at pM concentrations it may explain why some of the effects of ZOL are so long lasting following a yearly infusion of the drug. For example, the slow release of ZOL from the bone following a yearly infusion could lead to the drug being deposited in other tissues at these lower concentrations. This may also explain improvements in survival from cardiac arrythmias and infections seen in clinical studies which are indicative of a non-skeletal effect following a yearly administration of (Sing *et al.* 2020; Colón-Emeric *et al.* 2010). If this resulted in repeated doses of the drug being delivered to non-skeletal tissues, this may explain the discrepancies between the short duration of p-AKT inhibition in mouse tissues following a single dose (Figure 3.2-3.20) and the long-term impact on survival in patients. Although this is somewhat contradicted by the lack of inhibition at Day 24 post injection in the time course experiments (Figures 3.2-3.20). One explanation for this could be the drug could be swiftly cleared from non-skeletal tissues following deposition of the drug caused by release from the bone. This would be consistent with the short duration of mTOR inhibition when a single dose of ZOL is washed off from hMSCs (Figure 5.8).

The experiment on four different markers of mTOR signalling (Figure 5.6) was able to demonstrate that ZOL was capable of inhibiting p-AKT at concentrations of 1 µM, 1 nM and 1 pM. It was also able to demonstrate that p-mTOR was also inhibited at concentrations of 1 µM, 1 nM and 1 pM. This suggests that overall levels of p-mTOR and mTORC2 signalling are inhibited by ZOL at a broad variety of concentrations of 1 µM, 1 nM and 1 pM. However, the mTORC1 activity markers showed a weaker response. Inhibition of p-S6 was significantly reduced at concentrations of 1 µM and 1 nM. Meanwhile, significant inhibition of p-P70S6K was only achieved at doses of 1 nM ZOL. There was no significant inhibition of p-P70S6K at the other concentrations of ZOL examined. Interestingly there was a significant drop in p-P70S6K after three days of ZOL 1 µM treatment during the repeated ZOL dose experiment (Figure 5.10). Therefore, this experiment was somewhat able to verify previous findings that ZOL can inhibit p-P70S6K at doses of 1 µM when given for three days to hMSCs (Misra *et al.* 2016). However, this effect was not quite as consistent as had been previously reported.

One possible explanation for this is that ZOL's effect on p-P70S6K is too weak to be reliably detected with three MSC donors per experiment. Differences in how hMSCs from individual donors respond to ZOL may explain why this did not reach significance in this experiment. In future, it may be advisable to use more than three donors to detect p-P70S6K inhibition at 1 µM by ZOL in hMSCs. Another factor that could have impacted the drug's ability to inhibit p-P70S6K in hMSCs is the time of day in which the drug was administered. An example of this is the sensitivity of the mTORC1 marker p-S6 to circadian rhythms in culture in cultured cancer cells (Zhang *et al.* 2018). The inability to reliably detect changes in p-P70S6K could also be due to the density at which the cells were seeded or collected. The phosphorylation of P70S6K is lowered by increased cell density (Trajkovic et al. 2019; Leontiva et al. 2014). If the cells had been seeded or collected at a higher density in this study than previously, this may explain the lack of inhibition of p-P70S6K at 1 µM (Misra *et al.* 2016). Differences in these factors might explain why it was more difficult to detect inhibition in mTORC1 markers in response to ZOL.

There also appeared to be a difference in how mTORC1 markers responded to ZOL during the subsequent experiment. For example, there appeared to be a difference in the way in which the mTORC1 markers responded to zoledronate compared to p-AKT and p-mTOR in the washing off experiment (Figure 5.8). Inhibition of the mTOR markers p-P70S6K and p-S6 lasted only for the first few days and inhibition was no longer present after washing off. In contrast, inhibition of p-AKT and p-mTOR lasted for slightly longer during this experiment (up to Day 1 after washing off). This implies the effect of ZOL on p-AKT and p-mTOR might be slightly more potent than that of on mTORC1 markers. On a similar note, repeated doses of ZOL given every three days consistently inhibit p-AKT and p-mTOR for up to 12 days of treatment (Figure 5.10). Meanwhile, both p-S6 and p-P70S6K were only inhibited at Day 3 of treatment. This suggests that again mTORC1 markers are impacted differently to p-AKT and p-mTOR by ZOL. Inhibition of mTORC1 by ZOL would appear to be more temporary. This contrasts with rapamycin that can maintain inhibition of p-S6 for up to 7 Days in mouse brains following administration of the drug (Rensing *et al.* 2015). On a related note, mice fed rapamycin continuously throughout their lives had reduced levels of p-S6 in their visceral fat pads when harvested at 750-880 days of age (Harrison *et al.* 2009). Similarly, daily administration of rapamycin inhibits p-S6

in skeletal muscle and adipose tissue (Arriola Apelo *et al.* 2016). During these studies, continuous treatment of mice with rapamycin resulted in inhibition of p-S6. This contradicts with what is seen in hMSCs when treated continuously with ZOL every three days (Figure 5.10). This supports the idea that ZOL and rapamycin have a different mechanism in how they achieve mTORC1 inhibition.

Another possibility is that a lower doses of ZOL may have a different effect on mTORC1 inhibition when given repeatedly. A study on osteoblasts found that there was an increase in p-S6 when ZOL was given every three days at 1 µM (Gao *et al.* 2018). Rather interestingly, the same study on osteoblasts showed a significant decrease in the ratio of p-S6 at 1 nM and 1 pM ZOL when given every three days for two weeks (Gao *et al.* 2018). This suggests that inhibition of mTORC1 could be achieved in response to repeated doses of low concentration ZOL. Further experiments on hMSCs at lower doses of twice weekly ZOL are required to validate this theory. This work in this chapter somewhat contradicted that study as 1 µM ZOL given every three days to hMSCs for 12 days did not change levels of p-S6 (Figure 5.10). Alternatively, the repeated ZOL experiment in hMSCs in this chapter may have been underpowered to detect any significant changes in p-S6. Radioactive labelling of ZOL indicates a 10-1000-fold higher concentration of ZOL between skeletal and non-skeletal tissues in rats and dogs (Weiss *et al.* 2008). Given this, it is possible that many of the non-skeletal mouse tissues might fall closer to the 1 nM range of ZOL concentrations. This may mean that mTORC1 was inhibited in some of the mouse tissues in the healthspan experiment, but not others. Blotting of the mouse tissues from the healthspan experiment for the different mTOR markers (p-AKT, p-mTOR, p-S6 and p-P70S6K) would provide further evidence to support this theory.

The preferential inhibition of mTORC2 compared to mTORC1 could be important for understanding the outcome of the healthspan experiment. Potent inhibition of mTORC2 has been linked to negative features of healthspan in mice. For example, increased insulin resistance in mice (Lamming *et al.* 2012; Arriola Apelo *et al.* 2016). In addition, knocking out of RICTOR in mouse tissues such as the liver and hypothalamus has been linked to reduced lifespan (Lamming *et al.* 2014; Chellappa *et al.* 2019). On the other hand, mice heterozygous for AKT and RNA-i of AKT1 in *C.*

elegans increases lifespan (Nojima *et al.* 2013). In addition, the AKT inhibitor GSK690693 was capable of increasing lifespan and intestinal function with age in *Drosophila* (Cheng *et al.* 2022). Overall, the impact of loss of mTORC2 signalling on lifespan is currently unclear in the literature. In comparison, genetic interventions that lower mTORC1 signalling result in increased lifespan in mice (Selman *et al.* 2009; Zhang *et al.* 2017). Similarly, another study found an association between lower mTORC1 expression and longevity in different mammalian species (Mota-Martorell *et al.* 2020). Therefore, it may be better to maximise mTORC1 inhibition by ZOL in order to confer the greatest benefits to mouse survival and healthspan.

An interesting observation was the activation of mTOR markers between days 5-7 of the washing off ZOL experiment in hMSCs (Figure 5.8). This occurred at either Day 5 (for p-P70S6K and p-S6) or Day 7 (for p-AKT and p-mTOR). A connection could be made between this result and the increase in p-AKT observed during the ZOL time course experiment in kidney tissue (Figure 3.16). It is possible that similar mechanisms are at work. This could be due to the high levels of ZOL (around 30%-40% of total dose) that are removed via the kidney within 24 hours (Weiss *et al.* 2008). This may mimic the washing off experiment in the kidney tissue. One possible mechanism that could explain these results is by having a deeper look into the mechanisms by which ZOL may be inhibiting mTOR. ZOL blocks the mevalonate pathway by inhibiting the FPPS enzyme. The mevalonate pathway is required for the prenylation of GTPases such as RAS (Luckman *et al.* 1998). These are in turn needed for PI3K signalling, which is upstream of mTOR.

A recent study found that mTOR inhibition by deprivation with arginine or leucine *in vitro* resulted in a feedback mechanism by which both p-AKT and p-P70S6K are both activated in several cell types (Buel *et al.* 2022). They also found that knocking out of Rag-GTPase A/B produced a similar effect to arginine and leucine deprivation in stimulating mTOR activation. Therefore, hyperactivation of p-AKT and p-P70S6K by ZOL could be due to the influence of a loss of Rag-GTPases. Currently, there is no evidence in the literature to indicate that ZOL or BP treatment results in a reduction in Rag-GTPases. However, prenylation by the mevalonate pathway is required to produce other GTPases such as RAS (Luckman *et al.* 1998). This paper may also offer some explanation as to why the reactivation of mTOR doesn't occur sooner.

Further experiments conducted during that paper showed that application of an PI3K or AKT inhibitor prevented hyperactivation of p-AKT and p-P70S6K in response to leucine or arginine deprivation (Buel *et al.* 2022). Therefore, a single dose of ZOL may inhibit mTOR markers for a short period for around 3-4 days, consistent with the washing off experiment (Figure 5.8). Short term or repeated doses of ZOL may inhibit mTOR through a reduction in PI3K/AKT signalling due to reduced production of prenylated GTPases such as RAS. However, after 3-4 days of treatment this reduction in RAS may slowly start to revert to baseline. Following this, AKT inhibition could be lost. This in turn could trigger hyperactivation of mTOR markers due to a loss of Rag-GTPases by ZOL. Therefore, repeated doses of ZOL could prevent the hyperactivation of mTOR markers through continuous AKT inhibition. Although a major limitation to this proposed model is that this inhibition followed by inhibition/ reactivation in the literature occurs over the course of 6 hours, while in ZOL this occurs over the course of days. Nonetheless, there may well be unexpected feedback mechanisms that may explain the inhibition and hyperactivation of mTOR markers over time in response to ZOL.

During this investigation, it was not possible to verify that ZOL was blocking protein prenylation in hMSCs. This was achieved previously by blotting for unprenylated RAP1A (Misra *et al.* 2016). Unfortunately, this is because production of the unprenylated RAP1A antibody had been discontinued (Rap 1A, sc-1482, Santa Cruz). During this investigation, there was no suitable alternative antibody available on the market for measuring changes of protein prenylation. Inhibition of the mevalonate pathway was implied by the reversal of p-AKT inhibition by ZOL in response to FOH and GGOH supplementation (Figure 5.5). Although, it would have been preferable to have been able to more directly measure inhibition of the mevalonate pathway. Another limitation to this investigation was the small number of mTOR markers examined in hMSCs. Other markers of mTOR signalling that could be examined include 4E-BP1, ULK1, SGK and PKC (Alessi *et al.* 2009; Szwed *et al.* 2021). In conclusion this chapter has further shed light on how ZOL's ability to influence mTOR signalling, but there is still much that we do not understand about ZOL's inhibition of mTOR markers

Chapter 6 - General Discussion

During this study, ZOL was able to exhibit a modest effect on the mouse frailty in older mice (Figure 4.2). The remaining healthspan assays showed no significant change in response to ZOL treatment. There are many potential reasons as to why ZOL had such a small effect on healthy ageing. One such reason may be due to the premature termination of the experiment. Originally, the intention was to keep the mice to 24 months of age and to perform the final set of assays at this month. This is consistent with the healthy ageing pipeline for mice (Bellantuono *et al.* 2020). Future work should repeat this healthy ageing experiment, but the mice should be kept alive for longer. It may even be advisable to keep the mice for longer than 24 months. Previous work has shown that mice need to be 30 months old to measure changes in grid hanging caused by the mTOR inhibitor rapamycin (Ham *et al.* 2020). This may also be particularly useful for measuring how ZOL changes the survival of older mice, as during the last two months there was a notable increase in mortality in the PBS mice (Figure 4.10). Repeating the experiment and keeping the mice alive for longer may allow for detection of changes in survival in the ZOL treated mice. This may have also benefitted the rotarod test, which also did not reach significance by the final time point of the experiment (p=0.071) (Figure 4.4).

It may also be advisable to modify the experimental design in terms of when to perform certain assays during the mice's lifespan. An example of this would be NOR, which was not possible to perform at later time points as originally planned due to the blindness of the mice (Figure 4.8B). In a future iteration of the healthspan experiment, it may be advisable to perform this assay monthly from 18 months until the mice reach blindness. On the other hand, it is also possible that ZOL's effect on healthy ageing is very weak and requires a larger population of mice in order to detect changes in these assays. If that is the case then, this healthy ageing experiment is probably not worth repeating as other interventions more convincingly improve the healthy ageing of mice (Bitto *et al.* 2016; Martin-Montalvo *et al.* 2013). However, the effects of ZOL on healthspan later than 22 months should be examined before definitively arriving at this conclusion. In addition, both male and female mice should be tested during subsequent experiments. This is due to gender

differences in response to mTOR inhibitors with age, for example in terms of lifespan increase (Harrison *et al.* 2009; Miller *et al.* 2014; Strong *et al.* 2020). On a similar note, male mice undergo a more rapid deterioration in performance on the rotarod assay (Fischer *et al.* 2016). In order to determine if gender has any impact in ZOL's ability to confer benefits to mouse healthspan, the experiment could be repeated in both male and female mice. Such an experiment would allow for a more extensive assessment of whether ZOL can improve the healthy ageing of mice.

It may be possible to modify the frequency and/ or dose of ZOL to confer stronger effects on healthspan. In in order to understand why this maybe the case, it is necessary to examine ZOL's inhibition of markers of mTORC1 and mTORC2. ZOL appears to preferentially inhibit mTORC2 compared to mTORC1 when given repeatedly in hMSCs (Figure 5.10). There was a significant inhibition of p-AKT and p-mTOR signalling after repeated doses of ZOL every three days for 12 days in hMSCs. However, there was no significant change in p-P70S6K and p-S6 after the same time period. This suggests that mTORC1 inhibition is only transient in response to ZOL. This contradicts a previous study in the literature on osteoblasts, that showed that ZOL given every three days to osteoblasts increases the ratio p-S6/ total S6 after 14 days (Gao *et al.* 2018). Interestingly, the authors found that p-S6 was inhibited when given repeatedly at 1 nM and 1 pM for the same amount of time. In order to prevent reactivation of mTORC1, it might be better to administer ZOL at lower doses to confer a more consistent inhibition of mTORC1 to maximise the healthy ageing benefit. The repeated ZOL dose experiment in hMSCs should first be repeated, but with lower concentrations of the drug (1 nM and 1 pM) to see if a consistent p-S6 and p-P70S6K inhibition can be maintained.

Western blotting of p-S6 and p-P70S6K in the mouse tissues collected at the end of healthspan experiment should also shed some light on whether a lower dose may be warranted to continuously inhibit mTORC1 in a similar fashion as seen by others (Gao *et al.* 2018). This is because ZOL is found at concentrations 10-1000 times lower in non-skeletal tissues compared to in bone tissue (Weiss *et al.* 2008; Nikzad *et al.* 2013; Yousefnia *et al.* 2015). This may lead to mTORC1 being inhibited more effectively in certain tissues compared to others. Further iterations of the time course experiment on mTOR markers in response to lower concentrations of ZOL could

provide further evidence to support the use of a lower dose of ZOL to inhibit mTORC1. Another mouse healthspan experiment could then be performed using the original (125 µg/kg) and lower doses of ZOL to compare the different approaches.

There is some evidence in the literature to support the notion that a lower dose of ZOL is still effective in improving bone mineral density. ZOL is usually given to patients as a 5 mg infusion yearly to treat osteoporosis (Dhillon 2016). However, other studies in the literature have indicated that a lower dose of 1 mg is equally effective in improve bone mineral density at 12 months after infusion (Reid *et al.* 2002; Grey *et al.* 2017). Interestingly, one of the studies also found that a 0.25 mg infusion of ZOL given four times a year was equally as effective as a yearly infusion of 5 mg ZOL in improving bone mineral density in the lumbar spine and femoral neck (Reid *et al.* 2002). This implies that repeated doses of lower dose ZOL may still have a beneficial effect on the bone. However, the exact dose strength at which this effect is lost at lower doses is unknown and could be explored in future clinical trials. Many of the most common side effects of ZOL treatment are short term (Reid *et al.* 2010). This could be an issue if ZOL had to be given continuously to inhibit mTOR. Whether lower doses of ZOL can make these side effects less prevalent/ uncomfortable is currently unknown and could be explored in future clinical trials.

On a related note, it is currently unknown whether a less frequent ZOL injection to mice could give a similar healthspan improvement. ZOL can confer a beneficial effect on survival independent on fracture risk when given yearly to patients (Colón-Emeric *et al.* 2010). However, due to differences in bone turnover in mice and humans, it is unlikely that a yearly dose of ZOL would be as beneficial (Dresner Pollak *et al.* 1996; Melton *et al.* 1997; Shahnazari *et al.* 2012; Wishart *et al.* 1995). However, a monthly dose of ZOL is still capable of improving bone mineral density in C57BL/6J mice (Aref *et al.* 2016). Therefore, it would be interesting to see if similar benefits to the frailty index and survival could be seen with a less frequent dose of ZOL (e.g., with a monthly dose of ZOL). This may also allow for some distinction as to whether the frailty benefits seen in this study are due to p-AKT/ mTOR inhibition or whether there may other mechanisms involved such as improved bone strength or immune cell activation.

Another issue with the ZOL treatment during the mouse healthy ageing study might be that mTORC2 was inhibited too strongly. Chronic loss of mTORC2 has been linked to detrimental effects on mouse ageing. An example of this would be increased insulin resistance in mice (Lamming *et al.* 2012; Arriola Apelo *et al.* 2016). This is consistent with the increase in insulin resistance during chapter 4 seen at 18 months (Figure 4.7). Although this may not be a long-term issue for the healthspan of older mice as there was no longer any insulin resistance by 22 months. The importance of mTORC2 signalling has been further illustrated by knocking out the mTORC2 component RICTOR in certain tissues. This has been shown to adversely affect the lifespan of mice. For example, knocking out RICTOR in the hypothalamus reduces the lifespan of mice (Chellappa *et al.* 2019). Similarly, knocking out RICTOR in the liver of male, but not female mice resulted in a reduced lifespan (Lamming *et al.* 2014). On the other hand, the AKT inhibitor GSK690693 was capable of increasing lifespan and intestinal function with age in *Drosophila* (Cheng *et al.* 2022). In addition, mice heterozygous for AKT have increased lifespan (Nojima *et al.* 2013). During the same study RNA-i of AKT1 increased the lifespan of *C. elegans.* These studies suggest collectively that overly potent interference with AKT signalling can have detrimental effects on mouse ageing, but a partial inhibition of AKT signalling may have beneficial effects. On a similar note, intermittent administration of rapamycin avoids induction of insulin resistance (every 3-5 days), compared to daily doses of the drug in mice (Lamming *et al.* 2012; Arriola Apelo *et al.* 2016). In order to avoid inducing insulin resistance and any other detrimental effects of chronic mTORC2 inhibition in future studies, it may be advisable to administer ZOL less frequently in future healthspan experiments.

ZOL was found to have no significant effect on the mortality of mice at the time points examined (p=0.094) (Figure 4.10A). This contradicts a previous study on ZOL that found that ZOL treatment significantly improved the survival of *Drosophila* (Chen *et al.* 2021). ZOL is usually given as a yearly infusion to osteoporosis patients (Dhillon 2016). Despite this the effects of ZOL on survival are long lasting and are mainly facilitated through non-skeletal mechanisms (Colón-Emeric *et al.* 2010). While the effects of ZOL on improving survival in model organisms and patients are well documented, the exact mechanisms behind this improvement remain poorly understood.

One such mechanism by which this increase in survival could be achieved is through inhibition of the mTOR pathway, as discussed earlier. This study focussed on the activity of ZOL on a downstream marker of mTOR signalling as the basis for drug administration (Figures 3.2-3.20). During this investigation, it was determined that ZOL treatment is capable of inhibiting p-AKT at Day 3 post injection in the following mouse tissues: skeletal muscle, tibia, kidney, pancreas and spleen. In addition to this, ZOL's duration of action on p-AKT in mouse tissues was mirrored in hMSCs during the washing off experiment (Figure 5.8). These experiments suggest that inhibition of p-AKT is short in duration if a single dose of the drug is given. However, repeated doses of ZOL were able to inhibit p-AKT for 12 days when given every 3 days in hMSCs (Figure 5.10). This suggests that repeated doses of ZOL are required to inhibit p-AKT continuously. However, it is currently unknown for certain whether this is also the case for mouse tissues. It is also unknown whether this effect on p-AKT lasts for longer than 12 days. This question is particularly pertinent given that ZOL treatment during the healthspan experiment lasted for 11 months. In order to determine if ZOL is active after this time period, western blotting for p-AKT of the mouse tissues collected at the end of the mouse healthspan experiment should be performed. This should tell us whether p-AKT inhibition was active when ZOL is given for 11 months. It will also let us know whether ZOL is active on p-AKT in the tissues of older mice in a similar fashion to the younger mice in the time course experiments. It would be reassuring to know that p-AKT inhibition is achieved by ZOL in the tissues of older mice and that this effect is maintained after 11 months of treatment.

Another question that should be addressed in future work is whether ZOL is also capable of inhibiting other mTOR markers in mouse tissues (apart from p-AKT). During the experiments on hMSCs, ZOL was shown to be capable of inhibiting p-P70S6K, p-mTOR and p-S6 in addition to p-AKT (Figures 5.6). It should also be determined whether ZOL can inhibit these markers in mouse tissues during the healthspan experiment and in any future ZOL time course experiments. Western blotting for p-mTOR, p-S6 and p-P70S6K of the mouse tissues collected at the end of the mouse healthspan experiment should also be performed to examine this question. Given the lack of effect on repeated doses of ZOL on mTORC1 markers (Figure 5.10), it would be interesting to see if a similar effect could also be observed

in mouse tissues as well. If this was found to be the case, it would suggest that the effect on frailty and survival in mice (Figure 4.3 and 4.10) was not dependent on reduced mTORC1 signalling.

Another possibility that could be examined is that while ZOL only temporarily inhibits mTOR markers in response to a single dose, the downstream effects on the hallmarks of ageing such as DNA repair may be more long lasting. While it is currently known that ZOL can limit DNA damage in irradiated hMSCs (Misra *et al.* 2016), it is unknown how long this effect lasts for when the drug is removed. It may be advisable to repeat the ZOL washing off experiment, but this time do it on irradiated hMSCs and to stain cells for γH2AX to count DNA damage foci. If repair of DNA damage could be maintained for a long period of time in culture after removal of the drug, it may support less frequent doses of the drug for future healthy ageing studies in mice. It would also be interesting to see if the lower doses of ZOL are also capable of enhancing a similar DNA repair response in hMSCs to that of 1 μM ZOL. To this end, cells could be cultured in the presence or absence of 1 μM, 1nM or 1 pM ZOL. The cells could again be irradiated, stained for γH2AX and DNA damage foci could then be counted. This may also support the idea that lower doses of ZOL are equally effective in promoting ZOL's action as a geroprotector. This may then support further experiments in mouse tissues to see if a lower dose can inhibit mTORC1 and mTORC2 markers in mouse tissues more effectively. This in turn could lead to a recommendation of using this lower dose of ZOL in a repeat of the healthspan experiment in chapter 4, with the intent of maximising the healthspan outcome through more effective mTORC1 and mTORC2 inhibition.

Future work could also seek to shed further mechanistic light onto how ZOL can activate mTOR markers in certain circumstances. This may relate to work in the literature that showed a similar activation of mTOR markers in response to amino specific amino acid deprivation (Buel *et al.* 2022). Mechanistically, the authors of the paper on mTOR activation suspected that the activation was due to a loss of Rag-GTPases (Buel *et al.* 2022). Knocking out Rag A and Rag B produced a similar effect on activation of AKT and P70S6K compared to long term amino acid deprivation during that study. Given that ZOL is reduces the prenylation of other GTPases such as RAS, it is possible that a single dose of ZOL transiently activates

mTOR markers in the long term due to a reduction in the prenylation of Rag-GTPases. Continuous application of an AKT specific inhibitor prevented the reactivation of mTOR markers in the study on the mTOR marker activation found in the literature (Buel *et al.* 2022). This may explain why there was no significant activation of the mTOR markers in the repeated ZOL dose experiment (Figure 5.10) due to the consistent inhibition of p-AKT. In order to determine if this is the case, western blotting of Rag A and Rag B using a protein prenylation assay (Ali *et al.* 2015) could be performed in ZOL treated hMSCs to see if there is a loss of Rag prenylation. A repeat of the ZOL washing off experiment in hMSCs could be performed (Figure 5.8). Except, this time Rag A and Rag B could be knocked out as a separate condition. If there was no further reactivation of mTOR markers at days 5-7 with ZOL is RagA/B knockout cells, then this would implicate loss of Rag-GTPases in mTOR activation by ZOL.

It is already known that zoledronate can lower the amount of DNA damage present in later passage hMSCs and reduce markers of cellular senescence (Misra *et al.* 2016). However, it is currently unknown whether ZOL has any other effects on any of the other hallmarks of ageing (Figure 1.2). This is highly plausible given the central importance of mTOR signalling in regulating multiple hallmarks of ageing (section 1.4). This could be important as if a single dose of ZOL impacts hallmarks of ageing for longer periods of time longer than mTOR inhibition (Figure 5.8), this may support the idea that less frequent doses of the drug may deliver more optimal outcomes for survival and healthspan. In order to determine this, it is first necessary to identify hallmarks of ageing that are most likely to be impacted by ZOL treatment.

One such way in which zoledronate's inhibition of mTOR signalling could improve the healthy ageing of cells is through activation of autophagy. Indeed, some evidence in the literature supports the notion that this is the case. For example, ZOL induced autophagy *in vitro* in human umbilical vein endothelial cells and in carcinoma cells (Ge *et al.* 2014; Lu *et al.* 2016). However, it is currently unknown whether ZOL can induce autophagy in an ageing context. This could be examined by western blotting for proteins involved in autophagy such as LC3 in response to ZOL in hMSCs. Further experiments could look at autophagic flux (the degradative ability of autophagy) using a lysosomal fusion inhibitor such as bafilomycin A1.

If zoledronate improves autophagy in cells in an ageing context it may also be possible that ZOL could improve the mitochondrial function of cells by enhancing mitophagy. In order to assess this, one could co-stain for the autophagosome protein LC3 and a mitochondrial dye such as MitoTracker™ (Dolman *et al.* 2013). ZOL may impact mitochondrial dysfunction through other mechanisms such as increased translocation of FOXO3A into the nucleus (Misra *et al.* 2016). This process of increased FOXO3A activation has been shown in prior studies to improve features of mitochondrial function in several cell systems (Kops et al. 2002; Celestini et al. 2018). Levels of mitochondrial dysfunction could be assessed using the mitochondria specific ROS dye Mitosox™, to measure if ZOL treatment alters levels of superoxide generated in later passage hMSCs. Similarly, mitochondrial membrane potential could be assessed using microscopy and Rhodamine 123 dye. This should be assessed due to the drop in mitochondrial membrane potential seen in senescent cells (Cavazzoni *et al.* 1999; Passos *et al.* 2007).

Another way in which ZOL could improve the healthy ageing of cells by inhibiting mTOR is through reduced expression of SASP factors. Given that mTOR inhibitors have been shown to be senostatic by reducing the amount of SASP factors released by cells (Laberge *et al.* 2015; Herranz *et al.* 2015), this seems a distinctly possible mechanism by which ZOL could reduce the number of senescent cells present in culture. In order to determine if ZOL has effects on the SASP, a series of experiments could be performed. This could begin by looking at signalling pathways associated with the SASP such as NF-kB. This is important as NF-kB is a regulator of the SASP (Chien *et al.* 2011). For example, western blotting of the NF-kB component p-RelA from the nuclear fraction of protein lysates could be performed. This could then be used to compare the effects of ZOL treatment on p-RelA in late passage or irradiated hMSCs. It is also possible ZOL could alleviate the SASP through a reduction in DNA damage, as increased levels of DNA damage are also capable of inducing the SASP (Rodier et al. 2009). In order to determine levels of SASP components, hMSCs could be cultured in the presence or absence of ZOL until late passage. They could then be subjected to q-PCR to examine levels of MSC specific SASP components such as IL-6, IL-8 and MCP-1 (Gnani et al. 2019; Di et al. 2014). Overall, there are many potential cellular mechanisms by which ZOL could influence ageing that have yet to be sufficiently explored.

Chapter 7 - Conclusions

Previous studies have shown that ZOL can inhibit the downstream mTORC2 marker p-AKT in hMSCs and *Drosophila* (Misra *et al.* 2016; Chen *et al.* 2021). This study is the first to demonstrate that ZOL can inhibiting p-AKT as a marker of mTORC2 in a variety of mouse tissues during the first chapter of this thesis (Figures 3.2-3.20). The most common time point post injection that was found to inhibit p-AKT was found to be occurring at 3 Days post injection in the muscle, tibia, kidney, pancreas and spleen in mice. The effect of ZOL on p-AKT in non-skeletal mouse tissues was surprising given how previous studies had shown that these tissues retain ZOL at a far low concentration than in the bone (Weiss *et al.* 2008; Nikzad *et al.* 2013; Yousefnia *et al.* 2015). An inhibition of p-AKT was also found in the heart at Day 7 post injection and an activation of p-AKT was seen at Day 7 post injection in the kidney. An inhibition at Day 24 post injection was achieved in the brain. The short duration of the p-AKT inhibition was also surprising, given how ZOL administered to patients yearly has been shown to improve survival through non-skeletal effects (Colón-Emeric *et al.* 2010).

Zoledronate treatment had a very limited impact on improving the healthspan of mice at the time points examined. Most notably, there was a significant improvement in frailty score overall when mice were treated with ZOL compared to PBS mice (Figure 4.3). Furthermore, ZOL treatment did not significantly improve survival (p=0.09) (Figure 4.10A). Given the effects of ZOL on the survival of patients and *Drosophila* (Chen *et al.* 2021; Colón-Emeric *et al.* 2010), it is possible that a change in survival could have been detected if the mice had been kept alive for longer. The rotarod test may also have benefitted from keeping the mice alive for longer as this test had not yielded a significant change in response to ZOL treatment by 22 months (p=0.071) (Figure 4.4).

This study was also able to build on the initial insights into how ZOL inhibits mTOR in hMSCs. Firstly, it was able to verify previous findings that ZOL can inhibit a variety of mTOR markers in hMSCs such as p-AKT, p-mTOR and p-P70S6K in agreement with previous work (Figure 5.6) (Misra *et al.* 2016). Further to this, the study was able to show that ZOL can inhibit these mTOR markers at much lower concentrations of

ZOL than was previously believed to be possible. This may explain the effects of ZOL on p-AKT in mouse skeletal tissues in the first chapter of this thesis. This study has also been able to demonstrate that repeated dosage of ZOL is required to inhibit mTORC2 consistently in hMSCs. Treatment of hMSCs with a single dose of ZOL, followed by clearance of the drug from the cell media indicated that the drug was only active for 24 hours after washing off the drug (Figure 5.8). Meanwhile, repeated dosage of the drug every three days was able to continuously inhibit p-mTOR and p-AKT signalling (Figure 5.10). This was not found to be case for p-S6 and p-P70S6K. In combination these results suggest that prolonged mTORC2 inhibition by ZOL is best achieved by repeated doses of the drug. It also suggests that ZOL may inhibit mTORC2 preferentially compared to mTORC1 when given repeatedly. Overall, this study showed that ZOL was active on a mTOR marker in mice and allowed for a greater understanding of how mTOR inhibition is achieved *in vitro* by ZOL. While ZOL may not have conferred much benefit to the healthy ageing of mice, it is the belief of this researcher that better understanding of the biology of ageing will help older people to live more comfortable and independent lives.

References-

Acosta, J.C., Banito, A., Wuestefeld, T., Georgilis, A., Janich, P., Morton, J.P., Athineos, D., Kang, T.W., Lasitschka, F., Andrulis, M. and Pascual, G., 2013. A complex secretory program orchestrated by the inflammasome controls paracrine senescence. *Nature cell biology*, *15*(8), pp.978-990.

Acosta, J.C., O'Loghlen, A., Banito, A., Guijarro, M.V., Augert, A., Raguz, S., Fumagalli, M., Da Costa, M., Brown, C., Popov, N. and Takatsu, Y., 2008. Chemokine signaling via the CXCR2 receptor reinforces senescence. *cell*, *133*(6), pp.1006-1018.

Ahn, B., Pharaoh, G., Premkumar, P., Huseman, K., Ranjit, R., Kinter, M., Szweda, L., Kiss, T., Fulop, G., Tarantini, S. and Csiszar, A., 2018. Nrf2 deficiency exacerbates age-related contractile dysfunction and loss of skeletal muscle mass. *Redox biology*, *17*, p.47.

Aiello, G., Sabino, C., Pernici, D., Audano, M., Antonica, F., Gianesello, M., Ballabio, C., Quattrone, A., Mitro, N., Romanel, A. and Soldano, A., 2022. Transient rapamycin treatment during developmental stage extends lifespan in Mus musculus and Drosophila melanogaster. *EMBO reports*, *23*(9), p.e55299.

Alakangas, A., Selander, K., Mulari, M., Halleen, J., Lehenkari, P., Mönkkönen, J., Salo, J. and Väänänen, K., 2002. Alendronate disturbs vesicular trafficking in osteoclasts. *Calcified tissue international*, *70*(1), p.40.

Alessi, D.R., Pearce, L.R. and García-Martínez, J.M., 2009. New insights into mTOR signaling: mTORC2 and beyond. *Science signaling*, *2*(67), pp.pe27-pe27.

Ali, N., Jurczyluk, J., Shay, G., Tnimov, Z., Alexandrov, K., Munoz, M.A., Skinner, O.P., Pavlos, N.J. and Rogers, M.J., 2015. A highly sensitive prenylation assay reveals in vivo effects of bisphosphonate drug on the Rab prenylome of macrophages outside the skeleton. *Small GTPases*, *6*(4), pp.202-211.

Amor, C., Feucht, J., Leibold, J., Ho, Y.J., Zhu, C., Alonso-Curbelo, D., Mansilla-Soto, J., Boyer, J.A., Li, X., Giavridis, T. and Kulick, A., 2020. Senolytic CAR T cells reverse senescence-associated pathologies. *Nature*, *583*(7814), pp.127-132.

Anastasilakis, A.D., Polyzos, S.A., Makras, P., Sakellariou, G.T., Bisbinas, I., Gkiomisi, A., Delaroudis, S., Gerou, S., Ballaouri, I., Oikonomou, D. and Papapoulos, S.E., 2012. Acute phase response following intravenous zoledronate in postmenopausal women with low bone mass. *Bone*, *50*(5), pp.1130-1134.

Aref, M.W., McNerny, E.M., Brown, D., Jepsen, K.J. and Allen, M.R., 2016. Zoledronate treatment has different effects in mouse strains with contrasting baseline bone mechanical phenotypes. *Osteoporosis International*, *27*(12), pp.3637-3643.

Arias, E., Koga, H., Diaz, A., Mocholi, E., Patel, B. and Cuervo, A.M., 2015. Lysosomal mTORC2/PHLPP1/Akt regulate chaperone-mediated autophagy. *Molecular cell*, *59*(2), pp.270-284.

Armanios, M., Alder, J.K., Parry, E.M., Karim, B., Strong, M.A. and Greider, C.W., 2009. Short telomeres are sufficient to cause the degenerative defects associated with aging. *The American Journal of Human Genetics*, *85*(6), pp.823-832.

Arriola Apelo, S.I., Neuman, J.C., Baar, E.L., Syed, F.A., Cummings, N.E., Brar, H.K., Pumper, C.P., Kimple, M.E. and Lamming, D.W., 2016. Alternative rapamycin treatment regimens mitigate the impact of rapamycin on glucose homeostasis and the immune system. *Aging cell*, *15*(1), pp.28-38.

Baar, E.L., Carbajal, K.A., Ong, I.M. and Lamming, D.W., 2016. Sex-and tissue-specific changes in mTOR signaling with age in C57 BL/6J mice. *Aging Cell*, *15*(1), pp.155-166.

Bahrami-B, F., Ataie-Kachoie, P., Pourgholami, M.H. and Morris, D.L., 2014. p70 Ribosomal protein S6 kinase (Rps6kb1): an update. *Journal of clinical pathology*, *67*(12), pp.1019-1025.

Bahşi, R., Atmiş, V., Turgut, T., Mut Sürmeli, D., Coşarderelioğlu, Ç., Selvi Öztorun, H., Yalçin, A., Aras, S. and Varli, M., 2020. May zoledronic acid have negative effects on cognition and muscle performance?. *Irish Journal of Medical Science (1971-)*, *189*(1), pp.191-196.

Bai, J., Wang, Y., Wang, J., Zhai, J., He, F. and Zhu, G., 2020. Irradiation-induced senescence of bone marrow mesenchymal stem cells aggravates osteogenic

differentiation dysfunction via paracrine signaling. *American Journal of Physiology-Cell Physiology*, *318*(5), pp.C1005-C1017.

Baker, D.J., Wijshake, T., Tchkonia, T., LeBrasseur, N.K., Childs, B.G., Van De Sluis, B., Kirkland, J.L. and Van Deursen, J.M., 2011. Clearance of p16Ink4a-positive senescent cells delays ageing-associated disorders. *Nature*, *479*(7372), pp.232-236.

Barnett, K., Mercer, S.W., Norbury, M., Watt, G., Wyke, S. and Guthrie, B., 2012. Epidemiology of multimorbidity and implications for health care, research, and medical education: a cross-sectional study. *The Lancet*, *380*(9836), pp.37-43.#

Baxter, M.A., Wynn, R.F., Jowitt, S.N., Wraith, J.E., Fairbairn, L.J. and Bellantuono, I., 2004. Study of telomere length reveals rapid aging of human marrow stromal cells following in vitro expansion. *Stem cells*, *22*(5), pp.675-682.

Bellantuono, I., De Cabo, R., Ehninger, D., Di Germanio, C., Lawrie, A., Miller, J., Mitchell, S.J., Navas-Enamorado, I., Potter, P.K., Tchkonia, T. and Trejo, J.L., 2020. A toolbox for the longitudinal assessment of healthspan in aging mice. *Nature protocols*, *15*(2), pp.540-574.

Benice, T.S., Rizk, A., Kohama, S., Pfankuch, T. and Raber, J., 2006. Sex-differences in age-related cognitive decline in C57BL/6J mice associated with increased brain microtubule-associated protein 2 and synaptophysin immunoreactivity. *Neuroscience*, *137*(2), pp.413-423.

Bhatnagar, P., Wickramasinghe, K., Williams, J., Rayner, M. and Townsend, N., 2015. The epidemiology of cardiovascular disease in the UK 2014. *Heart*, *101*(15), pp.1182-1189.

Bitto, A., Ito, T.K., Pineda, V.V., LeTexier, N.J., Huang, H.Z., Sutlief, E., Tung, H., Vizzini, N., Chen, B., Smith, K. and Meza, D., 2016. Transient rapamycin treatment can increase lifespan and healthspan in middle-aged mice. *elife*, *5*, p.e16351.

Bjedov, I., Toivonen, J.M., Kerr, F., Slack, C., Jacobson, J., Foley, A. and Partridge, L., 2010. Mechanisms of life span extension by rapamycin in the fruit fly Drosophila melanogaster. *Cell metabolism*, *11*(1), pp.35-46.

Black, D.M., Delmas, P.D., Eastell, R., Reid, I.R., Boonen, S., Cauley, J.A., Cosman, F., Lakatos, P., Leung, P.C., Man, Z. and Mautalen, C., 2007. Once-yearly zoledronic acid for treatment of postmenopausal osteoporosis. *New England Journal of Medicine*, *356*(18), pp.1809-1822.

Blanch-Rubió, J., Soldevila-Domenech, N., Tío, L., Llorente-Onaindia, J., Ciria-Recasens, M., Polino, L., Gurt, A., de la Torre, R., Maldonado, R., Monfort, J. and Covidmar Study Group, 2020. Influence of anti-osteoporosis treatments on the incidence of COVID-19 in patients with non-inflammatory rheumatic conditions. *Aging (Albany NY)*, *12*(20), p.19923.

Bodnar, A.G., Ouellette, M., Frolkis, M., Holt, S.E., Chiu, C.P., Morin, G.B., Harley, C.B., Shay, J.W., Lichtsteiner, S. and Wright, W.E., 1998. Extension of life-span by introduction of telomerase into normal human cells. *science*, *279*(5349), pp.349-352.

Boonen, S., Sellmeyer, D.E., Lippuner, K., Orlov-Morozov, A., Abrams, K., Mesenbrink, P., Eriksen, E.F. and Miller, P.D., 2008. Renal safety of annual zoledronic acid infusions in osteoporotic postmenopausal women. *Kidney international*, *74*(5), pp.641-648.

Boulias, K. and Horvitz, H.R., 2012. The C. elegans microRNA mir-71 acts in neurons to promote germline-mediated longevity through regulation of DAF-16/FOXO. *Cell metabolism*, *15*(4), pp.439-450.

Buel, G.R., Dang, H.Q., Asara, J.M., Blenis, J. and Mutvei, A.P., 2022. Prolonged deprivation of arginine or leucine induces PI3K/Akt-dependent reactivation of mTORC1. *Journal of Biological Chemistry*, *298*(6).

Buhaescu, I. and Izzedine, H., 2007. Mevalonate pathway: a review of clinical and therapeutical implications. *Clinical biochemistry*, *40*(9-10), pp.575-584.

Calap-Quintana, P., Soriano, S., Llorens, J.V., Al-Ramahi, I., Botas, J., Moltó, M.D. and Martínez-Sebastián, M.J., 2015. TORC1 inhibition by rapamycin promotes antioxidant defences in a Drosophila model of Friedreich's ataxia. *PloS one*, *10*(7), p.e0132376.

Cambiaghi, M., Cursi, M., Magri, L., Castoldi, V., Comi, G., Minicucci, F., Galli, R. and Leocani, L., 2013. Behavioural and EEG effects of chronic rapamycin treatment in a mouse model of tuberous sclerosis complex. *Neuropharmacology*, *67*, pp.1-7.

Carano, A.S.J.P.H., Teitelbaum, S.L., Konsek, J.D., Schlesinger, P.H. and Blair, H.C., 1990. Bisphosphonates directly inhibit the bone resorption activity of isolated avian osteoclasts in vitro. *The Journal of clinical investigation*, *85*(2), pp.456-461.

Cavazzoni, M., Barogi, S., Baracca, A., Castelli, G.P. and Lenaz, G., 1999. The effect of aging and an oxidative stress on peroxide levels and the mitochondrial membrane potential in isolated rat hepatocytes. *FEBS letters*, *449*(1), pp.53-56.

Celestini, V., Tezil, T., Russo, L., Fasano, C., Sanese, P., Forte, G., Peserico, A., Lepore Signorile, M., Longo, G., De Rasmo, D. and Signorile, A., 2018. Uncoupling FoxO3A mitochondrial and nuclear functions in cancer cells undergoing metabolic stress and chemotherapy. *Cell death & disease*, *9*(2), pp.1-20.

Center, J.R., Lyles, K.W. and Bliuc, D., 2020. Bisphosphonates and lifespan. *Bone*, *141*, p.115566.

Chan, E.Y., Kir, S. and Tooze, S.A., 2007. siRNA screening of the kinome identifies ULK1 as a multidomain modulator of autophagy. *Journal of Biological Chemistry*, *282*(35), pp.25464-25474.

Chan, D.C., Yang, R.S., Ho, C.H., Tsai, Y.S., Wang, J.J. and Tsai, K.T., 2015. The use of alendronate is associated with a decreased incidence of type 2 diabetes mellitus—a population-based cohort study in Taiwan. *PloS one*, *10*(4), p.e0123279.

Chang, B.D., Broude, E.V., Dokmanovic, M., Zhu, H., Ruth, A., Xuan, Y., Kandel, E.S., Lausch, E., Christov, K. and Roninson, I.B., 1999. A senescence-like phenotype distinguishes tumor cells that undergo terminal proliferation arrest after exposure to anticancer agents. *Cancer research*, *59*(15), pp.3761-3767.

Chang, K.H., Chung, C.J., Lin, C.L., Sung, F.C., Wu, T.N. and Kao, C.H., 2014. Increased risk of dementia in patients with osteoporosis: a population-based retrospective cohort analysis. *Age*, *36*(2), pp.967-975.

Chellappa, K., Brinkman, J.A., Mukherjee, S., Morrison, M., Alotaibi, M.I., Carbajal, K.A., Alhadeff, A.L., Perron, I.J., Yao, R., Purdy, C.S. and DeFelice, D.M., 2019.

Hypothalamic mTORC2 is essential for metabolic health and longevity. *Aging cell*, *18*(5), p.e13014.

Chen, G., Wu, D.I., Guo, W., Cao, Y., Huang, D., Wang, H., Wang, T., Zhang, X., Chen, H., Yu, H. and Zhang, X., 2020. Clinical and immunological features of severe and moderate coronavirus disease 2019. *The Journal of clinical investigation*, *130*(5), pp.2620-2629.

Chen, T., Berenson, J., Vescio, R., Swift, R., Gilchick, A., Goodin, S., LoRusso, P., Ma, P., Ravera, C., Deckert, F. and Schran, H., 2002. Pharmacokinetics and pharmacodynamics of zoledronic acid in cancer patients with bone metastases. *The Journal of Clinical Pharmacology*, *42*(11), pp.1228-1236.

Chen, Y.R., Li, Y.H., Hsieh, T.C., Wang, C.M., Cheng, K.C., Wang, L., Lin, T.Y., Cheung, C.H.A., Wu, C.L. and Chiang, H., 2019. Aging-induced Akt activation involves in aging-related pathologies and Aβ-induced toxicity. *Aging cell*, *18*(4), p.e12989.

Chen, Z., Cordero, J., Alqarni, A.M., Slack, C., Zeidler, M.P. and Bellantuono, I., 2021. Zoledronate extends healthspan and survival via the mevalonate pathway in a FOXO-dependent manner. *Journals of Gerontology: Series A*.

Cheng, X., Xie, M., Luo, L., Tian, Y., Yu, G., Wu, Q., Fan, X., Yang, D., Mao, X., Gaur, U. and Yang, M., 2022. Inhibitor GSK690693 extends Drosophila lifespan via reduce AKT signaling pathway. *Mechanisms of Ageing and Development*, *202*, p.111633.

Chien, Y., Scuoppo, C., Wang, X., Fang, X., Balgley, B., Bolden, J.E., Premsrirut, P., Luo, W., Chicas, A., Lee, C.S. and Kogan, S.C., 2011. Control of the senescence-associated secretory phenotype by NF-κB promotes senescence and enhances chemosensitivity. *Genes & development*, *25*(20), pp.2125-2136.

Childs, B.G., Baker, D.J., Wijshake, T., Conover, C.A., Campisi, J. and Van Deursen, J.M., 2016. Senescent intimal foam cells are deleterious at all stages of atherosclerosis. *Science*, *354*(6311), pp.472-477.

Chkhotua, A.B., Gabusi, E., Altimari, A., D'Errico, A., Yakubovich, M., Vienken, J., Stefoni, S., Chieco, P., Yussim, A. and Grigioni, W.F., 2003. Increased expression of

p16 (INK4a) and p27 (Kip1) cyclin-dependent kinase inhibitor genes in aging human kidney and chronic allograft nephropathy. *American journal of kidney diseases*, *41*(6), pp.1303-1313.

Cleary, C., Linde, J.A.S., Hiscock, K.M., Hadas, I., Belmaker, R.H., Agam, G., Flaisher-Grinberg, S. and Einat, H., 2008. Antidepressive-like effects of rapamycin in animal models: Implications for mTOR inhibition as a new target for treatment of affective disorders. *Brain research bulletin*, *76*(5), pp.469-473.

Clegg, A., Young, J., Iliffe, S., Rikkert, M.O. and Rockwood, K., 2013. Frailty in elderly people. *The lancet*, *381*(9868), pp.752-762.

Colman, R.J., Beasley, T.M., Kemnitz, J.W., Johnson, S.C., Weindruch, R. and Anderson, R.M., 2014. Caloric restriction reduces age-related and all-cause mortality in rhesus monkeys. *Nature communications*, *5*(1), pp.1-5.

Coleman, R., Cameron, D., Dodwell, D., Bell, R., Wilson, C., Rathbone, E., Keane, M., Gil, M., Burkinshaw, R., Grieve, R. and Barrett-Lee, P., 2014. Adjuvant zoledronic acid in patients with early breast cancer: final efficacy analysis of the AZURE (BIG 01/04) randomised open-label phase 3 trial. *The lancet oncology*, *15*(9), pp.997-1006.

Colón-Emeric, C., Kuchibhatla, M., Pieper, C., Hawkes, W., Fredman, L., Magaziner, J., Zimmerman, S. and Lyles, K.W., 2003. The contribution of hip fracture to risk of subsequent fractures: data from two longitudinal studies. *Osteoporosis international*, *14*(11), pp.879-883.

Colón-Emeric, C.S., Mesenbrink, P., Lyles, K.W., Pieper, C.F., Boonen, S., Delmas, P., Eriksen, E.F. and Magaziner, J., 2010. Potential mediators of the mortality reduction with zoledronic acid after hip fracture. *Journal of Bone and Mineral Research*, *25*(1), pp.91-97.

Combemale, P., Sonzogni, L., Devic, C., Bencokova, Z., Ferlazzo, M.L., Granzotto, A., Burlet, S.F., Pinson, S., Amini-Adle, M., Al-Choboq, J. and Bodgi, L., 2022. Individual response to radiation of individuals with neurofibromatosis type I: Role of the ATM protein and influence of statins and bisphosphonates. *Molecular neurobiology*, *59*(1), pp.556-573.

Cong, L.N., Chen, H., Li, Y., Zhou, L., McGibbon, M.A., Taylor, S.I. and Quon, M.J., 1997. Physiological role of Akt in insulin-stimulated translocation of GLUT4 in transfected rat adipose cells. *Molecular endocrinology*, *11*(13), pp.1881-1890.

Coppé, J.P., Patil, C.K., Rodier, F., Sun, Y.U., Muñoz, D.P., Goldstein, J., Nelson, P.S., Desprez, P.Y. and Campisi, J., 2008. Senescence-associated secretory phenotypes reveal cell-nonautonomous functions of oncogenic RAS and the p53 tumor suppressor. *PLoS biology*, *6*(12), p.e301.

Coxon, F.P., Helfrich, M.H., Van't Hof, R., Sebti, S., Ralston, S.H., Hamilton, A. and Rogers, M.J., 2000. Protein geranylgeranylation is required for osteoclast formation, function, and survival: inhibition by bisphosphonates and GGTI-298. *Journal of Bone and Mineral Research*, *15*(8), pp.1467-1476.

Cui, H., Kong, Y. and Zhang, H., 2012. Oxidative stress, mitochondrial dysfunction, and aging. *Journal of signal transduction*, *2012*.

Dalle Carbonare, L., Valenti, M.T., Azzarello, G., Balducci, E., Crepaldi, G., Realdi, G., Vinante, O. and Giannini, S., 2005. Bisphosphonates decrease telomerase activity and hTERT expression in MCF-7 breast cancer cells. *Molecular and cellular endocrinology*, *240*(1-2), pp.23-31.

Daniali, L., Benetos, A., Susser, E., Kark, J.D., Labat, C., Kimura, M., Desai, K.K., Granick, M. and Aviv, A., 2013. Telomeres shorten at equivalent rates in somatic tissues of adults. *Nature communications*, *4*(1), pp.1-7.

Dash, P.K., Orsi, S.A. and Moore, A.N., 2006. Spatial memory formation and memory-enhancing effect of glucose involves activation of the tuberous sclerosis complex–mammalian target of rapamycin pathway. *Journal of Neuroscience*, *26*(31), pp.8048-8056.

Deblon, N., Bourgoin, L., Veyrat-Durebex, C., Peyrou, M., Vinciguerra, M., Caillon, A., Maeder, C., Fournier, M., Montet, X., Rohner-Jeanrenaud, F. and Foti, M., 2012. Chronic mTOR inhibition by rapamycin induces muscle insulin resistance despite weight loss in rats. *British journal of pharmacology*, *165*(7), pp.2325-2340.

Degli Esposti, L., Perrone, V., Sangiorgi, D., Andretta, M., Bartolini, F., Cavaliere, A., Ciaccia, A., Dell'orco, S., Grego, S., Salzano, S. and Ubertazzo, L., 2021. The Use of

Oral Amino-Bisphosphonates and Coronavirus Disease 2019 (COVID-19) Outcomes. *Journal of Bone and Mineral Research*, *36*(11), pp.2177-2183.

De Lange, T., 2005. Shelterin: the protein complex that shapes and safeguards human telomeres. *Genes & development*, *19*(18), pp.2100-2110.

Demontiero, O. and Duque, G., 2009. Once-yearly zoledronic acid in hip fracture prevention. *Clinical Interventions in Aging*, *4*, p.153.

Demontis, F. and Perrimon, N., 2010. FOXO/4E-BP signaling in Drosophila muscles regulates organism-wide proteostasis during aging. *Cell*, *143*(5), pp.813-825.

Denton, D. and Kumar, S., 2019. Autophagy-dependent cell death. *Cell Death & Differentiation*, *26*(4), pp.605-616.

Dhillon, S., 2016. Zoledronic acid (Reclast®, Aclasta®): a review in osteoporosis. *Drugs*, *76*(17), pp.1683-1697.

Di, G.H., Liu, Y., Lu, Y., Liu, J., Wu, C. and Duan, H.F., 2014. IL-6 secreted from senescent mesenchymal stem cells promotes proliferation and migration of breast cancer cells. *PloS one*, *9*(11), p.e113572.

Dodds, R.M., Granic, A., Davies, K., Kirkwood, T.B., Jagger, C. and Sayer, A.A., 2017. Prevalence and incidence of sarcopenia in the very old: findings from the Newcastle 85+ Study. *Journal of cachexia, sarcopenia and muscle*, *8*(2), pp.229-237.

Dolman, N.J., Chambers, K.M., Mandavilli, B., Batchelor, R.H. and Janes, M.S., 2013. Tools and techniques to measure mitophagy using fluorescence microscopy. *Autophagy*, *9*(11), pp.1653-1662.

Dominick, G., Bowman, J., Li, X., Miller, R.A. and Garcia, G.G., 2017. mTOR regulates the expression of DNA damage response enzymes in long-lived Snell dwarf, GHRKO, and PAPPA-KO mice. *Aging Cell*, *16*(1), pp.52-60.

Dresner-Pollak, R., Parker, R.A., Poku, M., Thompson, J., Seibel, M.J. and Greenspan, S.L., 1996. Biochemical markers of bone turnover reflect femoral bone loss in elderly women. *Calcified tissue international*, *59*(5), pp.328-333.

Driver, J.A., Djoussé, L., Logroscino, G., Gaziano, J.M. and Kurth, T., 2008. Incidence of cardiovascular disease and cancer in advanced age: prospective cohort study. *Bmj*, *337*.

Dunford, J.E., Thompson, K., Coxon, F.P., Luckman, S.P., Hahn, F.M., Poulter, C.D., Ebetino, F.H. and Rogers, M.J., 2001. Structure-activity relationships for inhibition of farnesyl diphosphate synthase in vitro and inhibition of bone resorption in vivo by nitrogen-containing bisphosphonates. *Journal of Pharmacology and Experimental Therapeutics*, *296*(2), pp.235-242.

Dunlop, E.A. and Tee, A.R., 2014, December. mTOR and autophagy: a dynamic relationship governed by nutrients and energy. In *Seminars in cell & developmental biology* (Vol. 36, pp. 121-129). Academic Press.

Ebert, R., Zeck, S., Krug, R., Meissner-Weigl, J., Schneider, D., Seefried, L., Eulert, J. and Jakob, F., 2009. Pulse treatment with zoledronic acid causes sustained commitment of bone marrow derived mesenchymal stem cells for osteogenic differentiation. *Bone*, *44*(5), pp.858-864.

Edwards, B.J., Sun, M., West, D.P., Guindani, M., Lin, Y.H., Lu, H., Hu, M., Barcenas, C., Bird, J., Feng, C. and Saraykar, S., 2016. Incidence of atypical femur fractures in cancer patients: the MD Anderson Cancer Center experience. *Journal of Bone and Mineral Research*, *31*(8), pp.1569-1576.

Ehrhardt, N., Cui, J., Dagdeviren, S., Saengnipanthkul, S., Goodridge, H.S., Kim, J.K., Lantier, L., Guo, X., Chen, Y.D.I., Raffel, L.J. and Buchanan, T.A., 2019. Adiposity-Independent Effects of Aging on Insulin Sensitivity and Clearance in Mice and Humans. *Obesity*, *27*(3), pp.434-443.

Eisenberg, T., Knauer, H., Schauer, A., Büttner, S., Ruckenstuhl, C., Carmona-Gutierrez, D., Ring, J., Schroeder, S., Magnes, C., Antonacci, L. and Fussi, H., 2009. Induction of autophagy by spermidine promotes longevity. *Nature cell biology*, *11*(11), pp.1305-1314.

Elstrom, R.L., Bauer, D.E., Buzzai, M., Karnauskas, R., Harris, M.H., Plas, D.R., Zhuang, H., Cinalli, R.M., Alavi, A., Rudin, C.M. and Thompson, C.B., 2004. Akt

stimulates aerobic glycolysis in cancer cells. *Cancer research*, *64*(11), pp.3892-3899.

Fahlström, A., Yu, Q. and Ulfhake, B., 2011. Behavioral changes in aging female C57BL/6 mice. *Neurobiology of aging*, *32*(10), pp.1868-1880.

Fanale, D., Amodeo, V., Bazan, V., Insalaco, L., Incorvaia, L., Barraco, N., Castiglia, M., Rizzo, S., Santini, D., Giordano, A. and Castorina, S., 2016. Can the microRNA expression profile help to identify novel targets for zoledronic acid in breast cancer?. *Oncotarget*, *7*(20), p.29321.

Fang, Y., Chen, B., Liu, Z., Gong, A.Y., Gunning, W.T., Ge, Y., Malhotra, D., Gohara, A.F., Dworkin, L.D. and Gong, R., 2022. Age-related GSK3 β overexpression drives podocyte senescence and glomerular aging. *Journal of Clinical Investigation*, *132*(4), p.e141848.

Farr, J.N., Xu, M., Weivoda, M.M., Monroe, D.G., Fraser, D.G., Onken, J.L., Negley, B.A., Sfeir, J.G., Ogrodnik, M.B., Hachfeld, C.M. and LeBrasseur, N.K., 2017. Targeting cellular senescence prevents age-related bone loss in mice. *Nature medicine*, *23*(9), pp.1072-1079.

Ferguson, N.M., Laydon, D., Nedjati-Gilani, G., Imai, N., Ainslie, K., Baguelin, M., Bhatia, S., Boonyasiri, A., Cucunubá, Z., Cuomo-Dannenburg, G. and Dighe, A., 2020. Impact of non-pharmaceutical interventions (NPIs) to reduce COVID-19 mortality and healthcare demand.

Fernandez-Capetillo, O., Chen, H.T., Celeste, A., Ward, I., Romanienko, P.J., Morales, J.C., Naka, K., Xia, Z., Camerini-Otero, R.D., Motoyama, N. and Carpenter, P.B., 2002. DNA damage-induced G2–M checkpoint activation by histone H2AX and 53BP1. *Nature cell biology*, *4*(12), pp.993-997.

Finkel, T., 2011. Signal transduction by reactive oxygen species. *Journal of Cell Biology*, *194*(1), pp.7-15.

Fischer, K.E., Hoffman, J.M., Sloane, L.B., Gelfond, J.A., Soto, V.Y., Richardson, A.G. and Austad, S.N., 2016. A cross-sectional study of male and female C57BL/6Nia mice suggests lifespan and healthspan are not necessarily correlated. *Aging (Albany NY)*, *8*(10), p.2370.

Fleisch, H. and Bisaz, S., 1962. Isolation from urine of pyrophosphate, a calcification inhibitor. *American Journal of Physiology-Legacy Content*, *203*(4), pp.671-675.

Fleisch, H., Graham, R., Russell, G. and Francis, M.D., 1969. Diphosphonates inhibit hydroxyapatite dissolution in vitro and bone resorption in tissue culture and in vivo. *Science*, *165*(3899), pp.1262-1264.

Fleisch, H. and Neuman, W.F., 1961. Mechanisms of calcification: role of collagen, polyphosphates, and phosphatase. *American Journal of Physiology-Legacy Content*, *200*(6), pp.1296-1300.

French, H.P., Galvin, R., Horgan, N.F. and Kenny, R.A., 2016. Prevalence and burden of osteoarthritis amongst older people in Ireland: findings from The Irish LongituDinal Study on Ageing (TILDA). *The European Journal of Public Health*, *26*(1), pp.192-198.

Frith, J.C., Mönkkönen, J., Auriola, S., Mönkkönen, H. and Rogers, M.J., 2001. The molecular mechanism of action of the antiresorptive and antiinflammatory drug clodronate: evidence for the formation in vivo of a metabolite that inhibits bone resorption and causes osteoclast and macrophage apoptosis. *Arthritis & Rheumatism: Official Journal of the American College of Rheumatology*, *44*(9), pp.2201-2210.

Fu, W. and Hall, M.N., 2020. Regulation of mTORC2 signaling. *Genes*, *11*(9), p.1045.

Gao, F., Liu, Y., Liu, M. and Zhu, L., 2018. Zoledronic acid regulates osteoblast differentiation via the mTORC1 signaling pathway. Int J Clin Exp Med, 11(5), pp.4585-4594.

Ge, X.Y., Yang, L.Q., Jiang, Y., Yang, W.W., Fu, J. and Li, S.L., 2014. Reactive oxygen species and autophagy associated apoptosis and limitation of clonogenic survival induced by zoledronic acid in salivary adenoid cystic carcinoma cell line SACC-83. *PLoS One*, *9*(6), p.e101207.

Gegechkori, N., Egorova, N., Mhango, G., Wisnivesky, J.P. and Lin, J.J., 2019. Bisphosphonate use and incident cardiovascular events among older breast cancer survivors. *The Breast*, *47*, pp.28-32.

Ghirlanda, G., Oradei, A., Manto, A., Lippa, S., Uccioli, L., Caputo, S., Greco, A.V. and Littarru, G.P., 1993. Evidence of plasma CoQ10-lowering effect by HMG-CoA reductase inhibitors: a double-blind, placebo-controlled study. *The Journal of Clinical Pharmacology*, *33*(3), pp.226-229.

Goldstein, J.L. and Brown, M.S., 1990. Regulation of the mevalonate pathway. *Nature*, *343*(6257), pp.425-430.

Gnani, D., Crippa, S., Della Volpe, L., Rossella, V., Conti, A., Lettera, E., Rivis, S., Ometti, M., Fraschini, G., Bernardo, M.E. and Di Micco, R., 2019. An early-senescence state in aged mesenchymal stromal cells contributes to hematopoietic stem and progenitor cell clonogenic impairment through the activation of a pro-inflammatory program. *Aging cell*, *18*(3), p.e12933.

Grbic, J.T., Landesberg, R., Lin, S.Q., Mesenbrink, P., Reid, I.R., Leung, P.C., Casas, N., Recknor, C.P., Hua, Y., Delmas, P.D. and Eriksen, E.F., 2008. Incidence of osteonecrosis of the jaw in women with postmenopausal osteoporosis in the health outcomes and reduced incidence with zoledronic acid once yearly pivotal fracture trial. *The Journal of the American dental association*, *139*(1), pp.32-40.

Green, J., Czanner, G., Reeves, G., Watson, J., Wise, L. and Beral, V., 2010. Oral bisphosphonates and risk of cancer of oesophagus, stomach, and colorectum: case-control analysis within a UK primary care cohort. *Bmj*, *341*.

Grey, A., Bolland, M.J., Horne, A., Mihov, B., Gamble, G. and Reid, I.R., 2017. Duration of antiresorptive activity of zoledronate in postmenopausal women with osteopenia: a randomized, controlled multidose trial. *CMAJ*, *189*(36), pp.E1130-E1136.

Grey, A., Bolland, M., Mihov, B., Wong, S., Horne, A., Gamble, G. and Reid, I.R., 2014. Duration of antiresorptive effects of low-dose zoledronate in osteopenic postmenopausal women: a randomized, placebo-controlled trial. *Journal of Bone and Mineral Research*, *29*(1), pp.166-172.

Griffith, J.D., Comeau, L., Rosenfield, S., Stansel, R.M., Bianchi, A., Moss, H. and De Lange, T., 1999. Mammalian telomeres end in a large duplex loop. *Cell*, *97*(4), pp.503-514.

Grote, C., Reinhardt, D., Zhang, M. and Wang, J., 2019. Regulatory mechanisms and clinical manifestations of musculoskeletal aging. *Journal of Orthopaedic Research®*, *37*(7), pp.1475-1488.

Guderyon, M.J., Chen, C., Bhattacharjee, A., Ge, G., Fernandez, R.A., Gelfond, J.A., Gorena, K.M., Cheng, C.J., Li, Y., Nelson, J.F. and Strong, R.J., 2020. Mobilization-based transplantation of young-donor hematopoietic stem cells extends lifespan in mice. *Aging cell*, *19*(3), p.e13110.

Hain, B.A., Jude, B., Xu, H., Smuin, D.M., Fox, E.J., Elfar, J.C. and Waning, D.L., 2020. Zoledronic acid improves muscle function in healthy mice treated with chemotherapy. *Journal of Bone and Mineral Research*, *35*(2), pp.368-381.

Ham, D.J., Börsch, A., Lin, S., Thürkauf, M., Weihrauch, M., Reinhard, J.R., Delezie, J., Battilana, F., Wang, X., Kaiser, M.S. and Guridi, M., 2020. The neuromuscular junction is a focal point of mTORC1 signaling in sarcopenia. *Nature communications*, *11*(1), pp.1-21.

Harley, C.B., Futcher, A.B. and Greider, C.W., 1990. Telomeres shorten during ageing of human fibroblasts. *Nature*, *345*(6274), pp.458-460.

Harman, D., 1972. The biologic clock: the mitochondria?. *Journal of the American Geriatrics Society*, *20*(4), pp.145-147.

Harrison, D.E., Strong, R., Sharp, Z.D., Nelson, J.F., Astle, C.M., Flurkey, K., Nadon, N.L., Wilkinson, J.E., Frenkel, K., Carter, C.S. and Pahor, M., 2009. Rapamycin fed late in life extends lifespan in genetically heterogeneous mice. *nature*, *460*(7253), pp.392-395.

Hayflick, L. and Moorhead, P.S., 1961. The serial cultivation of human diploid cell strains. *Experimental cell research*, *25*(3), pp.585-621.

Herranz, N., Gallage, S., Mellone, M., Wuestefeld, T., Klotz, S., Hanley, C.J., Raguz, S., Acosta, J.C., Innes, A.J., Banito, A. and Georgilis, A., 2015. mTOR regulates

MAPKAPK2 translation to control the senescence-associated secretory phenotype. Nature cell biology, 17(9), pp.1205-1217.

Hofman, A., Rocca, W.A., Brayne, C., Breteler, M.M.B., Clarke, M., Cooper, B., Copeland, J.R.M., Dartigues, J.F., Droux, A.D.S., Hagnell, O. and Heeren, T.J., 1991. The prevalence of dementia in Europe: a collaborative study of 1980–1990 findings. *International journal of epidemiology*, *20*(3), pp.736-748.

Holzenberger, M., Dupont, J., Ducos, B., Leneuve, P., Géloën, A., Even, P.C., Cervera, P. and Le Bouc, Y., 2003. IGF-1 receptor regulates lifespan and resistance to oxidative stress in mice. *Nature*, *421*(6919), pp.182-187.

Hresko, R.C. and Mueckler, M., 2005. mTOR· RICTOR is the Ser473 kinase for Akt/protein kinase B in 3T3-L1 adipocytes. *Journal of Biological Chemistry*, *280*(49), pp.40406-40416.

Huang, C.F., Shiao, M.S. and Mao, T.Y., 2021. Retrospective study of the effects of zoledronic acid on muscle mass in osteoporosis patients. *Drug Design, Development and Therapy*, *15*, p.3711.

Hue, T.F., Cummings, S.R., Cauley, J.A., Bauer, D.C., Ensrud, K.E., Barrett-Connor, E. and Black, D.M., 2014. Effect of bisphosphonate use on risk of postmenopausal breast cancer: results from the randomized clinical trials of alendronate and zoledronic acid. *JAMA internal medicine*, *174*(10), pp.1550-1557.

Iguchi, T., Miyakawa, Y., Saito, K., Nakabayashi, C., Nakanishi, M., Saya, H., Ikeda, Y. and Kizaki, M., 2007. Zoledronate-induced S phase arrest and apoptosis accompanied by DNA damage and activation of the ATM/Chk1/cdc25 pathway in human osteosarcoma cells. *International journal of oncology*, *31*(2), pp.285-291.

Iiboshi, Y., Papst, P.J., Kawasome, H., Hosoi, H., Abraham, R.T., Houghton, P.J. and Terada, N., 1999. Amino acid-dependent control of p70s6k: involvement of tRNA aminoacylation in the regulation. *Journal of Biological Chemistry*, *274*(2), pp.1092-1099.

Jacinto, E., Loewith, R., Schmidt, A., Lin, S., Rüegg, M.A., Hall, A. and Hall, M.N., 2004. Mammalian TOR complex 2 controls the actin cytoskeleton and is rapamycin insensitive. *Nature cell biology*, *6*(11), pp.1122-1128.

Jeon, O.H., Kim, C., Laberge, R.M., Demaria, M., Rathod, S., Vasserot, A.P., Chung, J.W., Kim, D.H., Poon, Y., David, N. and Baker, D.J., 2017. Local clearance of senescent cells attenuates the development of post-traumatic osteoarthritis and creates a pro-regenerative environment. *Nature medicine*, *23*(6), pp.775-781.

Jeyapalan, J.C., Ferreira, M., Sedivy, J.M. and Herbig, U., 2007. Accumulation of senescent cells in mitotic tissue of aging primates. *Mechanisms of ageing and development*, *128*(1), pp.36-44.

Jin, C., Li, J., Green, C.D., Yu, X., Tang, X., Han, D., Xian, B., Wang, D., Huang, X., Cao, X. and Yan, Z., 2011. Histone demethylase UTX-1 regulates C. elegans life span by targeting the insulin/IGF-1 signaling pathway. *Cell metabolism*, *14*(2), pp.161-172.

Junankar, S., Shay, G., Jurczyluk, J., Ali, N., Down, J., Pocock, N., Parker, A., Nguyen, A., Sun, S., Kashemirov, B. and McKenna, C.E., 2015. Real-Time Intravital Imaging Establishes Tumor-Associated Macrophages as the Extraskeletal Target of Bisphosphonate Action in Cancer Bisphosphonate Uptake by Tumor-Associated Macrophages. *Cancer discovery*, *5*(1), pp.35-42.

Jung, C.H., Ro, S.H., Cao, J., Otto, N.M. and Kim, D.H., 2010. mTOR regulation of autophagy. *FEBS letters*, *584*(7), pp.1287-1295.

Kajizono, M., Sada, H., Sugiura, Y., Soga, Y., Kitamura, Y., Matsuoka, J. and Sendo, T., 2015. Incidence and risk factors of osteonecrosis of the jaw in advanced cancer patients after treatment with zoledronic acid or denosumab: a retrospective cohort study. *Biological and Pharmaceutical Bulletin*, *38*(12), pp.1850-1855.

Kalyan, S., Huebbe, P., Esatbeyoglu, T., Niklowitz, P., Côté, H.C., Rimbach, G. and Kabelitz, D., 2014. Nitrogen-bisphosphonate therapy is linked to compromised coenzyme Q10 and vitamin E status in postmenopausal women. *The Journal of Clinical Endocrinology & Metabolism*, *99*(4), pp.1307-1313.

Kane, A.E., Hilmer, S.N., Boyer, D., Gavin, K., Nines, D., Howlett, S.E., de Cabo, R. and Mitchell, S.J., 2016. Impact of longevity interventions on a validated mouse clinical frailty index. *Journals of Gerontology Series A: Biomedical Sciences and Medical Sciences*, *71*(3), pp.333-339.

Kapitola, J., Zak, J., Lacinova, Z. and Justova, V., 2000. Effect of growth hormone and pamidronate on bone blood flow, bone mineral and IGF-I levels in the rat. *Physiological Research*, *49*, pp.S101-6.

Karlic, H., Thaler, R., Gerner, C., Grunt, T., Proestling, K., Haider, F. and Varga, F., 2015. Inhibition of the mevalonate pathway affects epigenetic regulation in cancer cells. *Cancer genetics*, *208*(5), pp.241-252.

Keller, K., Kane, A., Heinze-Milne, S., Grandy, S.A. and Howlett, S.E., 2019. Chronic treatment with the ACE inhibitor enalapril attenuates the development of frailty and differentially modifies pro-and anti-inflammatory cytokines in aging male and female C57BL/6 mice. *The Journals of Gerontology: Series A*, *74*(8), pp.1149-1157.

Kenyon, C., Chang, J., Gensch, E., Rudner, A. and Tabtiang, R., 1993. A C. elegans mutant that lives twice as long as wild type. *Nature*, *366*(6454), pp.461-464.

Kim, D.H., Rogers, J.R., Fulchino, L.A., Kim, C.A., Solomon, D.H. and Kim, S.C., 2015. Bisphosphonates and risk of cardiovascular events: a meta-analysis. *PloS one*, *10*(4), p.e0122646.

Kim, J., Kundu, M., Viollet, B. and Guan, K.L., 2011. AMPK and mTOR regulate autophagy through direct phosphorylation of Ulk1. *Nature cell biology*, *13*(2), pp.132-141.

Kim, R.H., Lee, R.S., Williams, D., Bae, S., Woo, J., Lieberman, M., Oh, J.E., Dong, Q., Shin, K.H., Kang, M.K. and Park, N.H., 2011. Bisphosphonates induce senescence in normal human oral keratinocytes. *Journal of dental research*, *90*(6), pp.810-816.

Kingston, A., Robinson, L., Booth, H., Knapp, M., Jagger, C. and MODEM project, 2018. Projections of multi-morbidity in the older population in England to 2035: estimates from the Population Ageing and Care Simulation (PACSim) model. *Age and ageing*, *47*(3), pp.374-380.

Klass, M.R., 1977. Aging in the nematode Caenorhabditis elegans: major biological and environmental factors influencing life span. *Mechanisms of ageing and development*, *6*, pp.413-429.

Kodali, M., Attaluri, S., Madhu, L.N., Shuai, B., Upadhya, R., Gonzalez, J.J., Rao, X. and Shetty, A.K., 2021. Metformin treatment in late middle age improves cognitive function with alleviation of microglial activation and enhancement of autophagy in the hippocampus. *Aging Cell*, *20*(2), p.e13277.

Kofman, A.E., McGraw, M.R. and Payne, C.J., 2012. Rapamycin increases oxidative stress response gene expression in adult stem cells. *Aging (Albany NY)*, *4*(4), p.279.

Kohno, N., Aogi, K., Minami, H., Nakamura, S., Asaga, T., Iino, Y., Watanabe, T., Goessl, C., Ohashi, Y. and Takashima, S., 2005. Zoledronic acid significantly reduces skeletal complications compared with placebo in Japanese women with bone metastases from breast cancer: a randomized, placebo-controlled trial. *Journal of Clinical Oncology*, *23*(15), pp.3314-3321.

Kops, G.J., Dansen, T.B., Polderman, P.E., Saarloos, I., Wirtz, K.W., Coffer, P.J., Huang, T.T., Bos, J.L., Medema, R.H. and Burgering, B.M., 2002. Forkhead transcription factor FOXO3a protects quiescent cells from oxidative stress. *Nature*, *419*(6904), pp.316-321.

Kranenburg, G., Bartstra, J.W., Weijmans, M., de Jong, P.A., Mali, W.P., Verhaar, H.J., Visseren, F.L. and Spiering, W., 2016. Bisphosphonates for cardiovascular risk reduction: a systematic review and meta-analysis. *Atherosclerosis*, *252*, pp.106-115.

Kremer, R., Gagnon, B., Meguerditchian, A.N., Nadeau, L. and Mayo, N., 2014. Effect of oral bisphosphonates for osteoporosis on development of skeletal metastases in women with breast cancer: results from a pharmaco-epidemiological study. *Journal of the National Cancer Institute*, *106*(11), p.dju264.

Kuiper, J.W.P., Forster, C., Sun, C., Peel, S. and Glogauer, M., 2012. Zoledronate and pamidronate depress neutrophil functions and survival in mice. *British journal of pharmacology*, *165*(2), pp.532-539.

Labbadia, J. and Morimoto, R.I., 2015. Repression of the heat shock response is a programmed event at the onset of reproduction. *Molecular cell*, *59*(4), pp.639-650.

Laberge, R.M., Sun, Y.U., Orjalo, A.V., Patil, C.K., Freund, A., Zhou, L., Curran, S.C., Davalos, A.R., Wilson-Edell, K.A., Liu, S.U. and Limbad, C., 2015. MTOR

regulates the pro-tumorigenic senescence-associated secretory phenotype by promoting IL1A translation. *Nature cell biology*, *17*(8), pp.1049-1061.

Lambert, A.J., Boysen, H.M., Buckingham, J.A., Yang, T., Podlutsky, A., Austad, S.N., Kunz, T.H., Buffenstein, R. and Brand, M.D., 2007. Low rates of hydrogen peroxide production by isolated heart mitochondria associate with long maximum lifespan in vertebrate homeotherms. *Aging cell*, *6*(5), pp.607-618.

Lamoureux, F., Baud'huin, M., Ory, B., Guiho, R., Zoubeidi, A., Gleave, M., Heymann, D. and Rédini, F., 2014. Clusterin inhibition using OGX-011 synergistically enhances zoledronic acid activity in osteosarcoma. *Oncotarget*, *5*(17), p.7805.

Lamming, D.W., Mihaylova, M.M., Katajisto, P., Baar, E.L., Yilmaz, O.H., Hutchins, A., Gultekin, Y., Gaither, R. and Sabatini, D.M., 2014. Depletion of Rictor, an essential protein component of m TORC 2, decreases male lifespan. *Aging cell*, *13*(5), pp.911-917.

Lamming, D.W., Ye, L., Astle, C.M., Baur, J.A., Sabatini, D.M. and Harrison, D.E., 2013. Young and old genetically heterogeneous HET 3 mice on a rapamycin diet are glucose intolerant but insulin sensitive. *Aging cell*, *12*(4), pp.712-718.

Lamming, D.W., Ye, L., Katajisto, P., Goncalves, M.D., Saitoh, M., Stevens, D.M., Davis, J.G., Salmon, A.B., Richardson, A., Ahima, R.S. and Guertin, D.A., 2012. Rapamycin-induced insulin resistance is mediated by mTORC2 loss and uncoupled from longevity. *science*, *335*(6076), pp.1638-1643.

Lan, Y.C., Chang, C.L., Sung, M.T., Yin, P.H., Hsu, C.C., Wang, K.C., Lee, H.C., Tseng, L.M. and Chi, C.W., 2013. Zoledronic acid-induced cytotoxicity through endoplasmic reticulum stress triggered REDD1-mTOR pathway in breast cancer cells. *Anticancer Research*, *33*(9), pp.3807-3814.

Lavasani, M., Robinson, A.R., Lu, A., Song, M., Feduska, J.M., Ahani, B., Tilstra, J.S., Feldman, C.H., Robbins, P.D., Niedernhofer, L.J. and Huard, J., 2012. Muscle-derived stem/progenitor cell dysfunction limits healthspan and lifespan in a murine progeria model. *Nature communications*, *3*(1), pp.1-12.

Lee, P., Ng, C., Slattery, A., Nair, P., Eisman, J.A. and Center, J.R., 2016. Preadmission bisphosphonate and mortality in critically ill patients. *The Journal of Clinical Endocrinology & Metabolism*, *101*(5), pp.1945-1953.

Lee, Y.K., Nho, J.H., Ha, Y.C. and Koo, K.H., 2012. Persistence with intravenous zoledronate in elderly patients with osteoporosis. *Osteoporosis International*, *23*(9), pp.2329-2333.

Leeson, G., Nanitashvili, N. AND Zaloznik, M. 2013. Future of an Ageing Population. Foresight Trends.: The Oxford Institute of Population Ageing.

Lehenkari, P.P., Kellinsalmi, M., Näpänkangas, J.P., Ylitalo, K.V., Mönkkönen, J., Rogers, M.J., Azhayev, A., Väänänen, H.K. and Hassinen, I.E., 2002. Further insight into mechanism of action of clodronate: inhibition of mitochondrial ADP/ATP translocase by a nonhydrolyzable, adenine-containing metabolite. *Molecular pharmacology*, *61*(5), pp.1255-1262.

Leiter, E.H., Premdas, F., Harrison, D.E. and Lipson, L.G., 1988. Aging and glucose homeostasis in C57BL/6J male mice. *The FASEB journal*, *2*(12), pp.2807-2811.

Leontieva, O.V., Demidenko, Z.N. and Blagosklonny, M.V., 2014. Contact inhibition and high cell density deactivate the mammalian target of rapamycin pathway, thus suppressing the senescence program. *Proceedings of the National Academy of Sciences*, *111*(24), pp.8832-8837.

López-Otín, C., Blasco, M.A., Partridge, L., Serrano, M. and Kroemer, G., 2013. The hallmarks of aging. *Cell*, *153*(6), pp.1194-1217.

Li, J., Zhu, J., Cao, B. and Mao, X., 2014. The mTOR signaling pathway is an emerging therapeutic target in multiple myeloma. *Current pharmaceutical design*, *20*(1), pp.125-135.

Li, L., Kim, E., Yuan, H., Inoki, K., Goraksha-Hicks, P., Schiesher, R.L., Neufeld, T.P. and Guan, K.L., 2010. Regulation of mTORC1 by the Rab and Arf GTPases. *Journal of Biological Chemistry*, *285*(26), pp.19705-19709.

Li, S. and Li, J.J., 2019. Zoledronic acid modulates human osteosarcoma cells proliferation via GSK-3β activation. *Neoplasma*, *66*(5), pp.766-775.

Lin, K., Dorman, J.B., Rodan, A. and Kenyon, C., 1997. daf-16: An HNF-3/forkhead family member that can function to double the life-span of Caenorhabditis elegans. *Science*, *278*(5341), pp.1319-1322.

Lipton, A., Zheng, M. and Seaman, J., 2003. Zoledronic acid delays the onset of skeletal-related events and progression of skeletal disease in patients with advanced renal cell carcinoma. *Cancer: Interdisciplinary International Journal of the American Cancer Society*, *98*(5), pp.962-969.

Liu, B., Wang, Z., Zhang, L., Ghosh, S., Zheng, H. and Zhou, Z., 2013. Depleting the methyltransferase Suv39h1 improves DNA repair and extends lifespan in a progeria mouse model. *Nature communications*, *4*(1), pp.1-12.

Liu, G., Rogers, J., Murphy, C.T. and Rongo, C., 2011. EGF signalling activates the ubiquitin proteasome system to modulate C. elegans lifespan. *The EMBO journal*, *30*(15), pp.2990-3003.

Lu, Y., Wang, Z., Han, W. and Li, H., 2016. Zoledronate induces autophagic cell death in human umbilical vein endothelial cells via Beclin-1 dependent pathway activation. *Molecular Medicine Reports*, *14*(5), pp.4747-4754.

Luckman, S.P., Hughes, D.E., Coxon, F.P., Russell, R.G.G. and Rogers, M.J., 1998. Nitrogen-containing bisphosphonates inhibit the mevalonate pathway and prevent post-translational prenylation of GTP-binding proteins, including Ras. *Journal of bone and mineral research*, *13*(4), pp.581-589.

Lühe, A., Künkele, K.P., Haiker, M., Schad, K., Zihlmann, C., Bauss, F., Suter, L. and Pfister, T., 2008. Preclinical evidence for nitrogen-containing bisphosphonate inhibition of farnesyl diphosphate (FPP) synthase in the kidney: implications for renal safety. *Toxicology in vitro*, *22*(4), pp.899-909.

Lyles, K.W., Colón-Emeric, C.S., Magaziner, J.S., Adachi, J.D., Pieper, C.F., Mautalen, C., Hyldstrup, L., Recknor, C., Nordsletten, L., Moore, K.A. and Lavecchia, C., 2007. Zoledronic acid and clinical fractures and mortality after hip fracture. *New England Journal of Medicine*, *357*(18), pp.1799-1809.

Maegawa, S., Hinkal, G., Kim, H.S., Shen, L., Zhang, L., Zhang, J., Zhang, N., Liang, S., Donehower, L.A. and Issa, J.P.J., 2010. Widespread and tissue specific age-related DNA methylation changes in mice. *Genome research*, *20*(3), pp.332-340.

Maleszewska, M., Mawer, J.S. and Tessarz, P., 2016. Histone modifications in ageing and lifespan regulation. *Current Molecular Biology Reports*, *2*(1), pp.26-35.

Manning, B.D. and Toker, A., 2017. AKT/PKB signaling: navigating the network. *Cell*, *169*(3), pp.381-405.

Marmentini, C., Soares, G.M., Bronczek, G.A., Piovan, S., Mareze-Costa, C.E., Carneiro, E.M., Boschero, A.C. and Kurauti, M.A., 2021. Aging Reduces Insulin Clearance in Mice. *Frontiers in endocrinology*, *12*, p.679492.

Martin-Montalvo, A., Mercken, E.M., Mitchell, S.J., Palacios, H.H., Mote, P.L., Scheibye-Knudsen, M., Gomes, A.P., Ward, T.M., Minor, R.K., Blouin, M.J. and Schwab, M., 2013. Metformin improves healthspan and lifespan in mice. *Nature communications*, *4*(1), pp.1-9.

Masarachia, P., Weinreb, M., Balena, R. and Rodan, G.A., 1996. Comparison of the distribution of 3H-alendronate and 3H-etidronate in rat and mouse bones. *Bone*, *19*(3), pp.281-290.

Mason, J.S., Wileman, T. and Chapman, T., 2018. Lifespan extension without fertility reduction following dietary addition of the autophagy activator Torin1 in Drosophila melanogaster. *PloS one*, *13*(1), p.e0190105.

Maures, T.J., Greer, E.L., Hauswirth, A.G. and Brunet, A., 2011. The H3K27 demethylase UTX-1 regulates C. elegans lifespan in a germline-independent, insulin-dependent manner. *Aging cell*, *10*(6), pp.980-990.

McCay, C.M., Crowell, M.F. and Maynard, L.A., 1935. The effect of retarded growth upon the length of life span and upon the ultimate body size: one figure. *The journal of Nutrition*, *10*(1), pp.63-79.

McConnell, B.B., Starborg, M., Brookes, S. and Peters, G., 1998. Inhibitors of cyclin-dependent kinases induce features of replicative senescence in early passage human diploid fibroblasts. *Current biology*, *8*(6), pp.351-354.

McGreevy, K.R., Tezanos, P., Ferreiro-Villar, I., Pallé, A., Moreno-Serrano, M., Esteve-Codina, A., Lamas-Toranzo, I., Bermejo-Álvarez, P., Fernández-Punzano, J., Martín-Montalvo, A. and Montalbán, R., 2019. Intergenerational transmission of the positive effects of physical exercise on brain and cognition. *Proceedings of the National Academy of Sciences*, *116*(20), pp.10103-10112.

Meier, R.P., Perneger, T.V., Stern, R., Rizzoli, R. and Peter, R.E., 2012. Increasing occurrence of atypical femoral fractures associated with bisphosphonate use. *Archives of Internal Medicine*, *172*(12), pp.930-936.

Melton III, L.J., Khosla, S., Atkinson, E.J., O'Fallon, W.M. and Riggs, B.L., 1997. Relationship of bone turnover to bone density and fractures. *Journal of Bone and Mineral Research*, *12*(7), pp.1083-1091.

Mendez-David, I., El-Ali, Z., Hen, R., Falissard, B., Corruble, E., Gardier, A.M., KERDINE-ROMER, S. and DAVID, D.J., 2013. A method for biomarker measurements in peripheral blood mononuclear cells isolated from anxious and depressed mice: β-arrestin 1 protein levels in depression and treatment. *Frontiers in pharmacology*, *4*, p.124.

Mendoza, M.C., Er, E.E. and Blenis, J., 2011. The Ras-ERK and PI3K-mTOR pathways: cross-talk and compensation. *Trends in biochemical sciences*, *36*(6), pp.320-328.

Michael, W.R., Kino, W.R. and Francis, M.D., 1971. Effectiveness of diphosphonates in preventing “osteoporosis” of disuse in the rat. *Clinical Orthopaedics and Related Research®*, *78*, pp.271-276.

Miller, R.A., Harrison, D.E., Astle, C.M., Fernandez, E., Flurkey, K., Han, M., Javors, M.A., Li, X., Nadon, N.L., Nelson, J.F. and Pletcher, S., 2014. Rapamycin-mediated lifespan increase in mice is dose and sex dependent and metabolically distinct from dietary restriction. *Aging cell*, *13*(3), pp.468-477.

Misra, J., Mohanty, S.T., Madan, S., Fernandes, J.A., Hal Ebetino, F., Russell, R.G.G. and Bellantuono, I., 2016. Zoledronate attenuates accumulation of DNA damage in mesenchymal stem cells and protects their function. *Stem cells*, *34*(3), pp.756-767.

Mizushima, N. and Yoshimori, T., 2007. How to interpret LC3 immunoblotting. *Autophagy*, *3*(6), pp.542-545.

Moloughney, J.G., Kim, P.K., Vega-Cotto, N.M., Wu, C.C., Zhang, S., Adlam, M., Lynch, T., Chou, P.C., Rabinowitz, J.D., Werlen, G. and Jacinto, E., 2016. mTORC2 responds to glutamine catabolite levels to modulate the hexosamine biosynthesis enzyme GFAT1. *Molecular cell*, *63*(5), pp.811-826.

Mönkkönen, J., Koponen, H.M. and Ylitalo, P., 1990. Comparison of the distribution of three bisphosphonates in mice. *Pharmacology & Toxicology*, *66*(4), pp.294-298.

Morgan, G.J., Davies, F.E., Gregory, W.M., Cocks, K., Bell, S.E., Szubert, A.J., Navarro-Coy, N., Drayson, M.T., Owen, R.G., Feyler, S. and Ashcroft, A.J., 2010. First-line treatment with zoledronic acid as compared with clodronic acid in multiple myeloma (MRC Myeloma IX): a randomised controlled trial. *The Lancet*, *376*(9757), pp.1989-1999.

Morrow, G., Samson, M., Michaud, S. and M. Tanguay, R., 2004. Overexpression of the small mitochondrial Hsp22 extends Drosophila life span and increases resistance to oxidative stress. *The FASEB journal*, *18*(3), pp.598-599.

Mota-Martorell, N., Jove, M., Pradas, I., Berdún, R., Sanchez, I., Naudi, A., Gari, E., Barja, G. and Pamplona, R., 2020. Gene expression and regulatory factors of the mechanistic target of rapamycin (mTOR) complex 1 predict mammalian longevity. *Geroscience*, *42*(4), pp.1157-1173.

Moussian, B., Schwarz, H., Bartoszewski, S. and Nüsslein-Volhard, C., 2005. Involvement of chitin in exoskeleton morphogenesis in Drosophila melanogaster. *Journal of morphology*, *264*(1), pp.117-130.

Munoz, M.A., Fletcher, E.K., Skinner, O.P., Jurczyluk, J., Kristianto, E., Hodson, M.P., Sun, S., Ebetino, F.H., Croucher, D.R., Hansbro, P.M. and Center, J.R., 2021. Bisphosphonate drugs have actions in the lung and inhibit the mevalonate pathway in alveolar macrophages. *Elife*, *10*, p.e72430.

Murga, M., Bunting, S., Montana, M.F., Soria, R., Mulero, F., Canamero, M., Lee, Y., McKinnon, P.J., Nussenzweig, A. and Fernandez-Capetillo, O., 2009. A mouse

model of ATR-Seckel shows embryonic replicative stress and accelerated aging. *Nature genetics*, *41*(8), pp.891-898.

Nakamura, K.I., Izumiyama-Shimomura, N., Takubo, K., Sawabe, M., Arai, T., Aoyagi, Y., Fujiwara, M., Tsuchiya, E., Kobayashi, Y., Kato, M. and Oshimura, M., 2002. Comparative analysis of telomere lengths and erosion with age in human epidermis and lingual epithelium. *Journal of Investigative Dermatology*, *119*(5), pp.1014-1019.

Nakamura, K.I., Kuramoto, K., Shibasaki, K., Shumiya, S. and Ohtsubo, K., 1992. Age-related incidence of spontaneous tumors in SPF C57BL/6 and BDF1 mice. *Experimental Animals*, *41*(3), pp.279-285.

Nancollas, G.H., Tang, R., Phipps, R.J., Henneman, Z., Gulde, S., Wu, W., Mangood, A., Russell, R.G.G. and Ebetino, F.H., 2006. Novel insights into actions of bisphosphonates on bone: differences in interactions with hydroxyapatite. *Bone*, *38*(5), pp.617-627.

Nelson, G., Wordsworth, J., Wang, C., Jurk, D., Lawless, C., Martin-Ruiz, C. and von Zglinicki, T., 2012. A senescent cell bystander effect: Senescence-induced senescence. *Aging cell*, *11*(2), pp.345-349.

Newcomb, P.A., Passarelli, M.N., Phipps, A.I., Anderson, G.L., Wactawski-Wende, J., Ho, G.Y., O'Sullivan, M.J. and Chlebowski, R.T., 2015. Oral bisphosphonate use and risk of postmenopausal endometrial cancer. *Journal of Clinical Oncology*, *33*(10), p.1186.

Nikzad, M., Jalilian, A.R., Shirvani-Arani, S., Bahrami-Samani, A. and Golchoubian, H., 2013. Production, quality control and pharmacokinetic studies of 177Lu–zoledronate for bone pain palliation therapy. *Journal of Radioanalytical and Nuclear Chemistry*, *298*(2), pp.1273-1281.

Noda, T. & Ohsumi, Y. 1998. Tor, a phosphatidylinositol kinase homologue, controls autophagy in yeast. *J Biol Chem,* 273**,** 3963-6.

Nojima, A., Yamashita, M., Yoshida, Y., Shimizu, I., Ichimiya, H., Kamimura, N., Kobayashi, Y., Ohta, S., Ishii, N. and Minamino, T., 2013. Haploinsufficiency of akt1 prolongs the lifespan of mice. *PloS one*, *8*(7), p.e69178.

Nuschke, A., Rodrigues, M., Stolz, D.B., Chu, C.T., Griffith, L. and Wells, A., 2014. Human mesenchymal stem cells/multipotent stromal cells consume accumulated autophagosomes early in differentiation. Stem cell research & therapy, 5(6), pp.1-14.

Ogburn, C.E., Carlberg, K., Ottinger, M.A., Holmes, D.J., Martin, G.M. and Austad, S.N., 2001. Exceptional cellular resistance to oxidative damage in long-lived birds requires active gene expression. *The Journals of Gerontology Series A: Biological Sciences and Medical Sciences*, *56*(11), pp.B468-B474.

Oh, Y.S., Seo, E.H., Lee, Y.S., Cho, S.C., Jung, H.S., Park, S.C. and Jun, H.S., 2016. Increase of calcium sensing receptor expression is related to compensatory insulin secretion during aging in mice. *PloS one*, *11*(7), p.e0159689.

Ohnuki, H., Izumi, K., Terada, M., Saito, T., Kato, H., Suzuki, A., Kawano, Y., Nozawa-Inoue, K., Takagi, R. and Maeda, T., 2012. Zoledronic acid induces S-phase arrest via a DNA damage response in normal human oral keratinocytes. *Archives of oral Biology*, *57*(7), pp.906-917.

O'Rourke, E.J., Kuballa, P., Xavier, R. and Ruvkun, G., 2013. ω-6 Polyunsaturated fatty acids extend life span through the activation of autophagy. *Genes & development*, *27*(4), pp.429-440.

Pang, W.W., Price, E.A., Sahoo, D., Beerman, I., Maloney, W.J., Rossi, D.J., Schrier, S.L. and Weissman, I.L., 2011. Human bone marrow hematopoietic stem cells are increased in frequency and myeloid-biased with age. *Proceedings of the National Academy of Sciences*, *108*(50), pp.20012-20017.

Passos, J.F., Saretzki, G., Ahmed, S., Nelson, G., Richter, T., Peters, H., Wappler, I., Birket, M.J., Harold, G., Schaeuble, K. and Birch-Machin, M.A., 2007. Mitochondrial dysfunction accounts for the stochastic heterogeneity in telomere-dependent senescence. *PLoS biology*, *5*(5), p.e110.

Pazianas, M., Abrahamsen, B., Eiken, P.A., Eastell, R. and Russell, R.G.G., 2012. Reduced colon cancer incidence and mortality in postmenopausal women treated

with an oral bisphosphonate—Danish National Register Based Cohort Study. *Osteoporosis international*, *23*(11), pp.2693-2701.

Peleg, S., Sananbenesi, F., Zovoilis, A., Burkhardt, S., Bahari-Javan, S., Agis-Balboa, R.C., Cota, P., Wittnam, J.L., Gogol-Doering, A., Opitz, L. and Salinas-Riester, G., 2010. Altered histone acetylation is associated with age-dependent memory impairment in mice. *science*, *328*(5979), pp.753-756.

Perifanis, V., Vyzantiadis, T., Tziomalos, K., Vakalopoulou, S., Garipidou, V., Athanassiou-Metaxa, M. and Harsoulis, F., 2007. Effect of zoledronic acid on markers of bone turnover and mineral density in osteoporotic patients with beta-thalassaemia. *Annals of hematology*, *86*(1), pp.23-30.

Powles, T., Paterson, A., McCloskey, E., Schein, P., Scheffler, B., Tidy, A., Ashley, S., Smith, I., Ottestad, L. and Kanis, J., 2006. Reduction in bone relapse and improved survival with oral clodronate for adjuvant treatment of operable breast cancer [ISRCTN83688026]. *Breast Cancer Research*, *8*(2), pp.1-7.

Qin, X., Jiang, B. and Zhang, Y., 2016. 4E-BP1, a multifactor regulated multifunctional protein. *Cell cycle*, *15*(6), pp.781-786.

Rabanal-Ruiz, Y., Otten, E.G. and Korolchuk, V.I., 2017. mTORC1 as the main gateway to autophagy. *Essays in biochemistry*, *61*(6), pp.565-584.

Ralston, S.H., Corral-Gudino, L., Cooper, C., Francis, R.M., Fraser, W.D., Gennari, L., Guanabens, N., Javaid, M.K., Layfield, R., O'Neill, T.W. and Russell, R.G.G., 2019. Diagnosis and management of Paget's disease of bone in adults: a clinical guideline. *Journal of Bone and Mineral Research*, *34*(4), pp.579-604.

Reid, I.R., Brown, J.P., Burckhardt, P., Horowitz, Z., Richardson, P., Trechsel, U., Widmer, A., Devogelaer, J.P., Kaufman, J.M., Jaeger, P. and Body, J.J., 2002. Intravenous zoledronic acid in postmenopausal women with low bone mineral density. *New England Journal of Medicine*, *346*(9), pp.653-661.

Reid, I.R., Gamble, G.D., Mesenbrink, P., Lakatos, P. and Black, D.M., 2010. Characterization of and risk factors for the acute-phase response after zoledronic acid. *The Journal of Clinical Endocrinology & Metabolism*, *95*(9), pp.4380-4387.

Reid, I.R., Horne, A.M., Mihov, B., Stewart, A., Garratt, E., Bastin, S. and Gamble, G.D., 2020. Effects of zoledronate on cancer, cardiac events, and mortality in osteopenic older women. *Journal of Bone and Mineral Research*, *35*(1), pp.20-27.

Reid, I.R., Horne, A.M., Mihov, B., Stewart, A., Garratt, E., Wong, S., Wiessing, K.R., Bolland, M.J., Bastin, S. and Gamble, G.D., 2018. Fracture prevention with zoledronate in older women with osteopenia. *New England Journal of Medicine*.

Reid, I.R., Horne, A.M., Mihov, B., Stewart, A., Bastin, S. and Gamble, G.D., 2021. Effect of zoledronate on lower respiratory infections in older women: secondary analysis of a randomized controlled trial. *Calcified Tissue International*, *109*(1), pp.12-16.

Reid, I.R., Miller, P., Lyles, K., Fraser, W., Brown, J.P., Saidi, Y., Mesenbrink, P., Su, G., Pak, J., Zelenakas, K. and Luchi, M., 2005. Comparison of a single infusion of zoledronic acid with risedronate for Paget's disease. *New England Journal of Medicine*, *353*(9), pp.898-908.

Rensing, N., Han, L. and Wong, M., 2015. Intermittent dosing of rapamycin maintains antiepileptogenic effects in a mouse model of tuberous sclerosis complex. *Epilepsia*, *56*(7), pp.1088-1097.

Richardson, N.E., Konon, E.N., Schuster, H.S., Mitchell, A.T., Boyle, C., Rodgers, A.C., Finke, M., Haider, L.R., Yu, D., Flores, V. and Pak, H.H., 2021. Lifelong restriction of dietary branched-chain amino acids has sex-specific benefits for frailty and life span in mice. *Nature Aging*, *1*(1), pp.73-86.

Richmond, J., Aharonoff, G.B., Zuckerman, J.D. and Koval, K.J., 2003. Mortality risk after hip fracture. *Journal of orthopaedic trauma*, *17*(1), pp.53-56.

Ripamonti, C.I., Maniezzo, M., Campa, T., Fagnoni, E., Brunelli, C., Saibene, G., Bareggi, C., Ascani, L. and Cislaghi, E., 2009. Decreased occurrence of osteonecrosis of the jaw after implementation of dental preventive measures in solid tumour patients with bone metastases treated with bisphosphonates. The experience of the National Cancer Institute of Milan. *Annals of Oncology*, *20*(1), pp.137-145.

Rockwood, K., Blodgett, J.M., Theou, O., Sun, M.H., Feridooni, H.A., Mitnitski, A., Rose, R.A., Godin, J., Gregson, E. and Howlett, A.S., 2017. A frailty index based on

deficit accumulation quantifies mortality risk in humans and in mice. *Scientific reports*, *7*(1), pp.1-10.

Rodier, F., Coppé, J.P., Patil, C.K., Hoeijmakers, W.A., Muñoz, D.P., Raza, S.R., Freund, A., Campeau, E., Davalos, A.R. and Campisi, J., 2009. Persistent DNA damage signalling triggers senescence-associated inflammatory cytokine secretion. *Nature cell biology*, *11*(8), pp.973-979.

Romanello, M., Bivi, N., Pines, A., Deganuto, M., Quadrifoglio, F., Moro, L. and Tell, G., 2006. Bisphosphonates activate nucleotide receptors signaling and induce the expression of Hsp90 in osteoblast-like cell lines. *Bone*, *39*(4), pp.739-753.

Roos, C.M., Zhang, B., Palmer, A.K., Ogrodnik, M.B., Pirtskhalava, T., Thalji, N.M., Hagler, M., Jurk, D., Smith, L.A., Casaclang-Verzosa, G. and Zhu, Y., 2016. Chronic senolytic treatment alleviates established vasomotor dysfunction in aged or atherosclerotic mice. *Aging cell*, *15*(5), pp.973-977.

Rosen, L.S., Gordon, D., Tchekmedyian, N.S., Yanagihara, R., Hirsh, V., Krzakowski, M., Pawlicki, M., De Souza, P., Zheng, M., Urbanowitz, G. and Reitsma, D., 2004. Long-term efficacy and safety of zoledronic acid in the treatment of skeletal metastases in patients with nonsmall cell lung carcinoma and other solid tumors: a randomized, phase III, double-blind, placebo-controlled trial. *Cancer*, *100*(12), pp.2613-2621.

Rosner, M., Fuchs, C., Siegel, N., Valli, A. and Hengstschläger, M., 2009. Functional interaction of mammalian target of rapamycin complexes in regulating mammalian cell size and cell cycle. *Human molecular genetics*, *18*(17), pp.3298-3310.

Rowlatt, C., Chesterman, F.C. and Sheriff, M.U., 1976. Lifespan, age changes and tumour incidence in an ageing C57BL mouse colony. *Laboratory animals*, *10*(4), pp.419-442.

Rudolph, K.L., Chang, S., Lee, H.W., Blasco, M., Gottlieb, G.J., Greider, C. and DePinho, R.A., 1999. Longevity, stress response, and cancer in aging telomerase-deficient mice. *Cell*, *96*(5), pp.701-712.

Russell, R.G.G., 2011. Bisphosphonates: the first 40 years. *Bone*, *49*(1), pp.2-19.

Ryu, D., Mouchiroud, L., Andreux, P.A., Katsyuba, E., Moullan, N., Nicolet-dit-Félix, A.A., Williams, E.G., Jha, P., Lo Sasso, G., Huzard, D. and Aebischer, P., 2016. Urolithin A induces mitophagy and prolongs lifespan in C. elegans and increases muscle function in rodents. *Nature medicine*, *22*(8), pp.879-888.

Saad, F., Gleason, D.M., Murray, R., Tchekmedyian, S., Venner, P., Lacombe, L., Chin, J.L., Vinholes, J.J., Goas, J.A. and Zheng, M., 2004. Long-term efficacy of zoledronic acid for the prevention of skeletal complications in patients with metastatic hormone-refractory prostate cancer. *Journal of the National Cancer Institute*, *96*(11), pp.879-882.

Sarbassov, D.D., Guertin, D.A., Ali, S.M. and Sabatini, D.M., 2005. Phosphorylation and regulation of Akt/PKB by the rictor-mTOR complex. *Science*, *307*(5712), pp.1098-1101.

Sambrook, P.N., Cameron, I.D., Chen, J.S., March, L.M., Simpson, J.M., Cumming, R.G. and Seibel, M.J., 2011. Oral bisphosphonates are associated with reduced mortality in frail older people: a prospective five-year study. *Osteoporosis international*, *22*(9), pp.2551-2556.

Schech, A.J., Kazi, A.A., Gilani, R.A. and Brodie, A.H., 2013. Zoledronic acid reverses the epithelial–mesenchymal transition and inhibits self-renewal of breast cancer cells through inactivation of NF-κB. *Molecular cancer therapeutics*, *12*(7), pp.1356-1366.

Schilcher, J., Koeppen, V., Aspenberg, P. and Michaelsson, K., 2014. Risk of atypical femoral fracture during and after bisphosphonate use. *New England Journal of Medicine*, *371*(10), pp.974-976.

Schneider, E.L., 1983. Infectious diseases in the elderly. *Annals of Internal Medicine*, *98*(3), pp.395-400.

Schulman, R.C., Moshier, E.L., Rho, L., Casey, M.F., Godbold, J.H., Zaidi, M. and Mechanick, J.I., 2016. Intravenous pamidronate is associated with reduced mortality in patients with chronic critical illness. *Endocrine Practice*, *22*(7), pp.799-808.

Sebti, S.M., 2005. Protein farnesylation: implications for normal physiology, malignant transformation, and cancer therapy. Cancer cell, 7(4), pp.297-300.

Sedelnikova, O.A., Horikawa, I., Zimonjic, D.B., Popescu, N.C., Bonner, W.M. and Barrett, J.C., 2004. Senescing human cells and ageing mice accumulate DNA lesions with unrepairable double-strand breaks. *Nature cell biology*, *6*(2), pp.168-170.

Selman, C., Tullet, J.M., Wieser, D., Irvine, E., Lingard, S.J., Choudhury, A.I., Claret, M., Al-Qassab, H., Carmignac, D., Ramadani, F. and Woods, A., 2009. Ribosomal protein S6 kinase 1 signaling regulates mammalian life span. *Science*, *326*(5949), pp.140-144.

Sengupta, S., Peterson, T.R. and Sabatini, D.M., 2010. Regulation of the mTOR complex 1 pathway by nutrients, growth factors, and stress. *Molecular cell*, *40*(2), pp.310-322.

Serrano, M., Lin, A.W., McCurrach, M.E., Beach, D. and Lowe, S.W., 1997. Oncogenic ras provokes premature cell senescence associated with accumulation of p53 and p16INK4a. *Cell*, *88*(5), pp.593-602.

Shahnazari, M., Dwyer, D., Chu, V., Asuncion, F., Stolina, M., Ominsky, M., Kostenuik, P. and Halloran, B., 2012. Bone turnover markers in peripheral blood and marrow plasma reflect trabecular bone loss but not endocortical expansion in aging mice. *Bone*, *50*(3), pp.628-637.

Shang, G.K., Han, L., Wang, Z.H., Liu, Y.P., Yan, S.B., Sai, W.W., Wang, D., Li, Y.H., Zhang, W. and Zhong, M., 2020. Sarcopenia is attenuated by TRB3 knockout in aging mice via the alleviation of atrophy and fibrosis of skeletal muscles. *Journal of cachexia, sarcopenia and muscle*, *11*(4), pp.1104-1120.

Sharma, N., Castorena, C.M. and Cartee, G.D., 2012. Tissue-specific responses of IGF-1/insulin and mTOR signaling in calorie restricted rats. *PloS one*, *7*(6).

Shay, J.W., Zou, Y., Hiyama, E. and Wright, W.E., 2001. Telomerase and cancer. *Human molecular genetics*, *10*(7), pp.677-685.

Shoji, H. and Miyakawa, T., 2019. Age-related behavioral changes from young to old age in male mice of a C57 BL/6J strain maintained under a genetic stability program. *Neuropsychopharmacology reports*, *39*(2), pp.100-118.

Sierra, F. and Kohanski, R., 2017. Geroscience and the trans-NIH geroscience interest group, GSIG. *Geroscience*, *39*(1), pp.1-5.

Sing, C.W., Kiel, D.P., Hubbard, R.B., Lau, W.C., Li, G.H., Kung, A.W., Wong, I.C. and Cheung, C.L., 2020. Nitrogen-containing bisphosphonates are associated with reduced risk of pneumonia in patients with hip fracture. *Journal of Bone and Mineral Research*, *35*(9), pp.1676-1684.

Sing, C.W., Wong, A.Y., Kiel, D.P., Cheung, E.Y., Lam, J.K., Cheung, T.T., Chan, E.W., Kung, A.W., Wong, I.C. and Cheung, C.L., 2018. Association of alendronate and risk of cardiovascular events in patients with hip fracture. *Journal of bone and mineral research*, *33*(8), pp.1422-1434.

Smith Jr, D.L., Mattison, J.A., Desmond, R.A., Gardner, J.P., Kimura, M., Roth, G.S., Ingram, D.K., Allison, D.B. and Aviv, A., 2011. Telomere dynamics in rhesus monkeys: no apparent effect of caloric restriction. *Journals of Gerontology Series A: Biomedical Sciences and Medical Sciences*, *66*(11), pp.1163-1168.

Smith, E.M. and Proud, C.G., 2008. cdc2–cyclin B regulates eEF2 kinase activity in a cell cycle-and amino acid-dependent manner. *The EMBO journal*, *27*(7), pp.1005-1016.

Smith, M.R., 2005. Zoledronic acid to prevent skeletal complications in cancer: corroborating the evidence. *Cancer treatment reviews*, *31*, pp.19-25.

Smith-Vikos, T. and Slack, F.J., 2012. MicroRNAs and their roles in aging. *Journal of cell science*, *125*(1), pp.7-17.

Stein, G.H., Drullinger, L.F., Soulard, A. and Dulić, V., 1999. Differential roles for cyclin-dependent kinase inhibitors p21 and p16 in the mechanisms of senescence and differentiation in human fibroblasts. *Molecular and cellular biology*, *19*(3), pp.2109-2117.

Strong, R., Miller, R.A., Bogue, M., Fernandez, E., Javors, M.A., Libert, S., Marinez, P.A., Murphy, M.P., Musi, N., Nelson, J.F. and Petrascheck, M., 2020. Rapamycin-mediated mouse lifespan extension: Late-life dosage regimes with sex-specific effects. *Aging Cell*, *19*(11), p.e13269.

Szwed, A., Kim, E. and Jacinto, E., 2021. Regulation and metabolic functions of mTORC1 and mTORC2. *Physiological reviews*, *101*(3), pp.1371-1426.

Tang, X., Zhang, Q., Shi, S., Yen, Y., Li, X., Zhang, Y., Zhou, K. and Le, A.D., 2010. Bisphosphonates suppress insulin-like growth factor 1-induced angiogenesis via the HIF-1α/VEGF signaling pathways in human breast cancer cells. *International journal of cancer*, *126*(1), pp.90-103.

Tatar, M., Kopelman, A., Epstein, D., Tu, M.P., Yin, C.M. and Garofalo, R., 2001. A mutant Drosophila insulin receptor homolog that extends life-span and impairs neuroendocrine function. *Science*, *292*(5514), pp.107-110.

Thompson, K., Rogers, M.J., Coxon, F.P. and Crockett, J.C., 2006. Cytosolic entry of bisphosphonate drugs requires acidification of vesicles after fluid-phase endocytosis. *Molecular pharmacology*, *69*(5), pp.1624-1632.

Tian, L., Chavez, M., Chang, G.S., Helton, N.M., Katerndahl, C.D., Miller, C.A. and Wartman, L.D., 2021. Kdm6a deficiency restricted to mouse hematopoietic cells causes an age-and sex-dependent myelodysplastic syndrome-like phenotype. *PloS one*, *16*(11), p.e0255706.

Tian, L., Yang, R., Wei, L., Liu, J., Yang, Y., Shao, F., Ma, W., Li, T., Wang, Y. and Guo, T., 2017. Prevalence of osteoporosis and related lifestyle and metabolic factors of postmenopausal women and elderly men: A cross-sectional study in Gansu province, Northwestern of China. *Medicine*, *96*(43).

Tomaru, U., Takahashi, S., Ishizu, A., Miyatake, Y., Gohda, A., Suzuki, S., Ono, A., Ohara, J., Baba, T., Murata, S. and Tanaka, K., 2012. Decreased proteasomal activity causes age-related phenotypes and promotes the development of metabolic abnormalities. *The American journal of pathology*, *180*(3), pp.963-972.

Toulis, K.A., Nirantharakumar, K., Ryan, R., Marshall, T. and Hemming, K., 2015. Bisphosphonates and glucose homeostasis: a population-based, retrospective cohort study. *The Journal of Clinical Endocrinology & Metabolism*, *100*(5), pp.1933-1940.

Trajkovic, K., Valdez, C., Ysselstein, D. and Krainc, D., 2019. Fluctuations in cell density alter protein markers of multiple cellular compartments, confounding experimental outcomes. *PloS one*, *14*(2), p.e0211727.

Toussaint, O., Medrano, E.E. and von Zglinicki, T., 2000. Cellular and molecular mechanisms of stress-induced premature senescence (SIPS) of human diploid fibroblasts and melanocytes. *Experimental gerontology*, *35*(8), pp.927-945.

Tsubaki, M., Takeda, T., Sakamoto, K., Shimaoka, H., Fujita, A., Itoh, T., Imano, M., Mashimo, K., Fujiwara, D., Sakaguchi, K. and Satou, T., 2015. Bisphosphonates and statins inhibit expression and secretion of MIP-1α via suppression of Ras/MEK/ERK/AML-1A and Ras/PI3K/Akt/AML-1A pathways. *American Journal of Cancer Research*, *5*(1), p.168.

Tsurumi, A. and Li, W., 2012. Global heterochromatin loss: a unifying theory of aging?. *Epigenetics*, *7*(7), pp.680-688.

Turturro, A., Witt, W.W., Lewis, S., Hass, B.S., Lipman, R.D. and Hart, R.W., 1999. Growth curves and survival characteristics of the animals used in the Biomarkers of Aging Program. *The Journals of Gerontology: Series A*, *54*(11), pp.B492-B501.

Ungvari, Z., Ridgway, I., Philipp, E.E., Campbell, C.M., McQuary, P., Chow, T., Coelho, M., Didier, E.S., Gelino, S., Holmbeck, M.A. and Kim, I., 2011. Extreme longevity is associated with increased resistance to oxidative stress in Arctica islandica, the longest-living non-colonial animal. *Journals of Gerontology Series A: Biomedical Sciences and Medical Sciences*, *66*(7), pp.741-750.

Valenti, M.T., Dalle Carbonare, L., Bertoldo, F., Donatelli, L. and Cascio, V.L., 2008. The effects on hTERT gene expression is an additional mechanism of amino-bisphosphonates in prostatic cancer cells. *European journal of pharmacology*, *580*(1-2), pp.36-42.

Vandone, A.M., Donadio, M., Mozzati, M., Ardine, M., Polimeni, M.A., Beatrice, S., Ciuffreda, L. and Scoletta, M., 2012. Impact of dental care in the prevention of bisphosphonate-associated osteonecrosis of the jaw: a single-center clinical experience. *Annals of Oncology*, *23*(1), pp.193-200.

Van Nguyen, T., Puebla-Osorio, N., Pang, H., Dujka, M.E. and Zhu, C., 2007. DNA damage-induced cellular senescence is sufficient to suppress tumorigenesis: a mouse model. *The Journal of experimental medicine*, *204*(6), pp.1453-1461.

Vermeij, W.P., Dollé, M.E.T., Reiling, E., Jaarsma, D., Payan-Gomez, C., Bombardieri, C.R., Wu, H., Roks, A.J.M., Botter, S.M., Van Der Eerden, B.C. and Youssef, S.A., 2016. Restricted diet delays accelerated ageing and genomic stress in DNA-repair-deficient mice. *Nature*, *537*(7620), pp.427-431.

Vestergaard, P., 2011. Risk of newly diagnosed type 2 diabetes is reduced in users of alendronate. *Calcified tissue international*, *89*(4), pp.265-270.

Von Zglinicki, T., 2002. Oxidative stress shortens telomeres. *Trends in biochemical sciences*, *27*(7), pp.339-344.

Walker, G.A. and Lithgow, G.J., 2003. Lifespan extension in C. elegans by a molecular chaperone dependent upon insulin-like signals. *Aging cell*, *2*(2), pp.131-139.

Wang, C., Jurk, D., Maddick, M., Nelson, G., Martin-Ruiz, C. and Von Zglinicki, T., 2009. DNA damage response and cellular senescence in tissues of aging mice. *Aging cell*, *8*(3), pp.311-323.

Wang, X., Li, W., Williams, M., Terada, N., Alessi, D.R. and Proud, C.G., 2001. Regulation of elongation factor 2 kinase by p90RSK1 and p70 S6 kinase. *The EMBO journal*, *20*(16), pp.4370-4379.

Warr, M.R., Binnewies, M., Flach, J., Reynaud, D., Garg, T., Malhotra, R., Debnath, J. and Passegué, E., 2013. FOXO3A directs a protective autophagy program in haematopoietic stem cells. *Nature*, *494*(7437), pp.323-327.

Weiss, H.M., Pfaar, U., Schweitzer, A., Wiegand, H., Skerjanec, A. and Schran, H., 2008. Biodistribution and plasma protein binding of zoledronic acid. *Drug metabolism and disposition*, *36*(10), pp.2043-2049.

Welton, J.L., Morgan, M.P., Martí, S., Stone, M.D., Moser, B., Sewell, A.K., Turton, J. and Eberl, M., 2013. Monocytes and γδ T cells control the acute-phase response to intravenous zoledronate: insights from a phase IV safety trial. *Journal of Bone and Mineral Research*, *28*(3), pp.464-471.

White, M.C., Holman, D.M., Boehm, J.E., Peipins, L.A., Grossman, M. and Henley, S.J., 2014. Age and cancer risk: a potentially modifiable relationship. *American journal of preventive medicine*, *46*(3), pp.S7-S15.

Whitehead, J.C., Hildebrand, B.A., Sun, M., Rockwood, M.R., Rose, R.A., Rockwood, K. and Howlett, S.E., 2014. A clinical frailty index in aging mice: comparisons with frailty index data in humans. *Journals of Gerontology Series A: Biomedical Sciences and Medical Sciences*, *69*(6), pp.621-632.

Wiley, C.D., Velarde, M.C., Lecot, P., Liu, S.U., Sarnoski, E.A., Freund, A., Shirakawa, K., Lim, H.W., Davis, S.S., Ramanathan, A. and Gerencser, A.A., 2016. Mitochondrial dysfunction induces senescence with a distinct secretory phenotype. *Cell metabolism*, *23*(2), pp.303-314.

Wimmer, M.E., Hernandez, P.J., Blackwell, J. and Abel, T., 2012. Aging impairs hippocampus-dependent long-term memory for object location in mice. *Neurobiology of aging*, *33*(9), pp.2220-2224.

Wishart, J.M., Need, A.O., Horowitz, M., Morris, H.A. and Nordin, B.E.C., 1995. Effect of age on bone density and bone turnover in men. *Clinical endocrinology*, *42*(2), pp.141-146.

Wolf, A.M., Rumpold, H., Tilg, H., Gastl, G., Gunsilius, E. and Wolf, D., 2006. The effect of zoledronic acid on the function and differentiation of myeloid cells. *Haematologica*, *91*(9), pp.1165-1171.

Wolfe, F., Bolster, M.B., O'Connor, C.M., Michaud, K., Lyles, K.W. and Colón-Emeric, C.S., 2013. Bisphosphonate use is associated with reduced risk of myocardial infarction in patients with rheumatoid arthritis. *Journal of Bone and Mineral Research*, *28*(5), pp.984-991.

Xu, M., Pirtskhalava, T., Farr, J.N., Weigand, B.M., Palmer, A.K., Weivoda, M.M., Inman, C.L., Ogrodnik, M.B., Hachfeld, C.M., Fraser, D.G. and Onken, J.L., 2018. Senolytics improve physical function and increase lifespan in old age. *Nature medicine*, *24*(8), pp.1246-1256.

Yang, W., Zhou, X. and Ma, T., 2019. Memory decline and behavioral inflexibility in aged mice are correlated with dysregulation of protein synthesis capacity. *Frontiers in Aging Neuroscience*, *11*, p.246.

Yang, X., Xu, X., Chen, J., Wang, Q., Wang, G., Ai, X., Wang, X. and Pan, J., 2020. Zoledronic acid regulates the synthesis and secretion of IL-1β through Histone methylation in macrophages. *Cell death discovery*, *6*(1), pp.1-14

Yoshikawa, T.T., 2000. Epidemiology and unique aspects of aging and infectious diseases. *Clinical Infectious Diseases*, *30*(6), pp.931-933.

Yousefnia, H., Zolghadri, S. and Jalilian, A.R., 2015. Absorbed dose assessment of 177Lu-zoledronate and 177Lu-EDTMP for human based on biodistribution data in rats. *Journal of Medical Physics/Association of Medical Physicists of India*, *40*(2), p.102.

Yousefzadeh, M.J., Zhao, J., Bukata, C., Wade, E.A., McGowan, S.J., Angelini, L.A., Bank, M.P., Gurkar, A.U., McGuckian, C.A., Calubag, M.F. and Kato, J.I., 2020. Tissue specificity of senescent cell accumulation during physiologic and accelerated aging of mice. *Aging cell*, *19*(3), p.e13094.

Zhang, F.L. and Casey, P.J., 1996. Protein prenylation: molecular mechanisms and functional consequences. *Annual review of biochemistry*, *65*(1), pp.241-269.

Zhang, H.M., Diaz, V., Walsh, M.E. and Zhang, Y., 2017. Moderate lifelong overexpression of tuberous sclerosis complex 1 (TSC1) improves health and survival in mice. *Scientific reports*, *7*(1), pp.1-14.

Zhang, J., Wang, R., Zhao, Y.L., Sun, X.H., Zhao, H.X., Tan, L., Chen, D.C. and Hai-Bin, X., 2012. Efficacy of intravenous zoledronic acid in the prevention and treatment of osteoporosis: A meta–analysis. *Asian Pacific journal of tropical medicine*, *5*(9), pp.743-748.

Zhang, Y., Bokov, A., Gelfond, J., Soto, V., Ikeno, Y., Hubbard, G., Diaz, V., Sloane, L., Maslin, K., Treaster, S. and Réndon, S., 2014. Rapamycin extends life and health in C57BL/6 mice. *Journals of Gerontology Series A: Biomedical Sciences and Medical Sciences*, *69*(2), pp.119-130.

Zhang, Y., Giacchetti, S., Parouchev, A., Hadadi, E., Li, X., Dallmann, R., Xandri-Monje, H., Portier, L., Adam, R., Lévi, F. and Dulong, S., 2018. Dosing time dependent in vitro pharmacodynamics of Everolimus despite a defective circadian clock. *Cell Cycle*, *17*(1), pp.33-42

Appendices-

Certificate of competition of the online SYSMIC statistics and programming course. This was completed during COVID lockdowns in which laboratory facilities were inaccessible (March 2020-July 2020).

SYS MIC

Certificate of Completion

This certifies that

Jeremy Richards

completed the SysMIC training module

An Introduction to Quantitative Biology

being commended with a distinction for their miniproject investigation.

issued by:

PW Lewis

on behalf of SysMIC

Issued: Feb 2021

This involved 120 hours of learning covering the following topics:

PROGRAMMING
- Programming using MATLAB
- Data analysis using R

NETWORKS
- Network theory and analysis
- Biochemical reaction networks
- Working with Petri nets

MODELLING
- Mathematics for biological modelling
- Modelling reactions and gene regulation
- Simulation and analysis of ODE models

STATISTICS
- Sample distributions & the central limit theorem
- Hypothesis testing
- Analysis of gene expression data

MINIPROJECT
- Completion of a modelling project

SysMIC.ac.uk

Online Training for the Bioscience Research Community

Use this QR code to access a digital version of this certificate
or visit http://sysmic.ac.uk/certificates/m1_completion_cert_j_richards_fd7a67